used in Secs. 95 and 107. We shall discuss their results for three cases, namely, nickel oxide (NiO), cuprous iodide, and potassium iodide. Although the last case does not involve transition metals, they consider it for comparative purposes.

In nickel oxide, which has sodium chloride structure and an oxygen excess, some metal-ion sites are vacant. De Boer and Verwey conclude that the electrons removed from the lattice with the positive ions are taken from two nickel ions alongside the vacancy, leaving two Ni^{+++} ions. These holes may be thermally freed making the crystal conducting.

Cuprous iodide has the zincblende structure and is a halogen excess semi-conductor. The workers conclude that in this case there are neutral iodine atoms at the iodine sites alongside the metal-ion vacancies. This case should be contrasted with that of cuprous oxide, discussed above, in which the hole is believed to reside on the positive ions. De Boer and Verwey estimate that in copper iodide the hole would be 1 ev less stable at a copper-ion site than at an iodine site.

Potassium iodide is also an excess halogen semi-conductor. The computational evidence indicates that there are positive-ion vacancies and neutral halogen atoms nearby, just as in copper iodide.

De Boer and Verwey also point out that the zone approximation is much less accurate for d-shell electrons than for electrons in s-p levels. It is probably true that the lowest level of the entire solid in a salt containing an odd number of d electrons per unit cell is separated from the higher levels by a large gap, even though the lowest levels should be quasi-continuous in the Bloch approximation. A case in point seems to be CoO which has the sodium chloride lattice with one cobalt ion per unit cell. Since this ion has seven d electrons, the salt should be a metallic conductor, according to the zone theory. Actually, it is not, a fact which shows that the ordinary rules for predicting metallic character cannot always be applied to d-electron groups.

E. MOLECULAR CRYSTALS

114. Survey.—There has been no explicit work on the electronic energy levels of molecular crystals. Apparently, it is safe to assume that the lower excited states may be treated by the methods of excitation waves to a high degree of accuracy. The widths of the excitation bands should be small, for the intermolecular forces are small. One consequence of this fact is that the spacing between the lower excitation bands should be nearly the same as the spacing between the electronic levels of the free molecules. In addition, there should be additional bands below the ionization continuum that correspond to the transfer of an electron from a molecule to one of its neighbors. The principles which determine all the levels should be enough like those which have been used success-

fully in connection with ionic crystals to require no further comment here. This subject probably could be developed considerably if experimental investigations of the absorption spectra of molecular crystals were carried out in the near ultraviolet and Schumann regions.

115. The Transition between the Solid Types.—In Chap. I, we attempted to show the interrelation between the solid types by means of Fig. 82. We may now discuss this diagram again, using our knowledge of the electronic states. The ideal metals, which are on the left, possess broad, incompletely filled bands when described by the zone approximation. They cannot be described adequately by the Heitler-London approximation, since the lowest energy levels of the entire solid are quasi-continuous.

As we move to the right in Fig. 82, the energy bands separate into filled and unfilled sets. This transition takes place gradually, being well advanced in metals such as calcium, bismuth, and graphite and complete in diamond and possibly boron. The separation of bands also occurs as we move from ideal substitutional alloys to ionic crystals. In this case, substances such as Mg_3Sb_2 occupy the intermediate positions that correspond to bismuth, and so forth, in the monatomic case. Ideal valence and ionic crystals may be described in terms of both the Heitler-London and the Bloch scheme. Neither is completely satisfactory when used alone, however, even for qualitative work, and the two approximations must be combined to form a complete picture. The atomic functions must be greatly perturbed in constructing the best Heitler-London functions for the lowest state of these solids. This is indicated by the fact that the best functions in valence crystals have directional properties and the best functions in ionic crystals are closely like the functions of free ions. In the energy-level diagram of the entire solid, a singlet separates from the quasi-continuous levels of metals as we move from left to right.

Passing still farther to the right, we come to molecular solids, which usually are described more satisfactorily by the Heitler-London approximation than by the Bloch approximation, since the Heitler-London functions are very nearly the same as those of the free molecular units. The lowest level of the entire solid is a discrete singlet, and the higher levels that lie below the ionization limit presumably are grouped into narrow excitation bands.

Semi-conductors are insulating crystals that have additional electronic states because they contain lattice defects or foreign atoms.

CHAPTER XIV

THE DYNAMICS OF NUCLEAR MOTION. PHASE CHANGES

116. The Adiabatic Approximation*.—We have treated the nuclear coordinates as parameters in practically all the preceding discussion because we were interested primarily in the stationary electronic states. We shall now examine the extent to which this procedure may be justified and shall discuss a scheme for treating electronic and nuclear motion together. This scheme was employed by Born and Oppenheimer[1] in connection with the stationary states of molecules and has been used subsequently in similar problems.[2]

The complete Hamiltonian operator, $\mathfrak{H}_c$, for a crystal is

$$\begin{aligned}\mathfrak{H}_c &= -\sum_i \frac{\hbar^2}{2m}\Delta_i - \sum_a \frac{\hbar^2}{M_a}\Delta_a + \frac{1}{2}{\sum_{i,j}}' \frac{e^2}{r_{ij}} + \\ &\qquad V_{ei}(x_1, \cdots, z_n, \xi_1, \cdots, \zeta_f) + V_{ii}(\xi_1, \cdots, \zeta_f) \\ &= H - \sum_a \frac{\hbar^2}{2M_a}\Delta_a. \end{aligned} \tag{1}$$

The indices $i, j, \ldots, n$ extend over all electrons, and the indices $a, b, \ldots, f$ extend over all ions. M_a is the mass of the ath ion, V_{ei} is the electron-ion interaction potential, V_{ii} is the interaction potential of the rigid ions, and H is the electronic Hamiltonian of Chap. VI, in which the nuclear kinetic-energy terms were neglected. In Chap. VI, V_{ei} was taken to have the form

$$\sum_{\substack{\text{lattice} \\ i}} V(\mathbf{r}_i).$$

Since the ions were regarded as being fixed, $V(\mathbf{r}_i)$ had the periodicity of the lattice. We must now include the dependence of V on the nuclear coordinates, since they will also be treated as dynamical variables.

[1] M. Born and J. R. Oppenheimer, *Ann. Physik*, **84**, 457 (1927).

[2] H. Pelzer and E. Wigner, *Z. physik. Chem.*, **15B**, 445 (1932); E. Wigner, *Z. physik. Chem.*, **19B**, 203 (1932); H. Eyring, *Jour. Chem. Phys.*, **3**, 107 *ff.* (1935) (*cf.* review article in *Chem. Rev.*, **17**, 65 (1935); L. Farkas and E. Wigner, *Trans. Faraday Soc.*, **32**, 708 (1936). A critique of this method as applied to problems in chemical reactions is given by E. Wigner, *Trans. Faraday Soc.*, **34**, 29 (1938); see also J. O. Hirschfelder and E. P. Wigner, *Jour. Chem. Phys.*, **7**, 616 (1939).

Although the exact characteristic functions Φ of $\mathfrak{H}_e$ usually are intricate functions of the x and the ξ, we shall attempt to use approximate solutions of the form

$$\Phi_{r\alpha}(x_1, \cdots, z_n, \xi_1, \cdots, \zeta_f) = \Psi_r(x_1, \cdots, z_n, \xi_1, \cdots, \zeta_f)\chi_{r\alpha}(\xi_1, \cdots, \zeta_f, t), \quad (2)$$

where Ψ_r is an electronic function of the type used in previous chapters, in which the ξ were regarded as parameters, and $\chi_{r\alpha}(\xi_1, \cdots, \zeta_f)$ is a function of the nuclear coordinates. This approximation is commonly called the adiabatic approximation, because at each instant the electronic distribution is taken to be the same as though the nuclear coordinates were at rest at the positions they have at this instant. This assumption obviously can be true only if the electrons move much more rapidly than the ions. We shall see presently that the accuracy of the approximation depends on the fact that ionic masses are great relative to the electron mass.

If the function (2) is substituted in the equation

$$\mathfrak{H}_e\Phi = -\frac{\hbar}{i}\frac{\partial\Phi}{\partial t} \quad (3)$$

and if it is recalled that

$$H\Psi_r(x_1, \cdots, z_n, \xi_1, \cdots, \zeta_f) = E_r(\xi_1, \cdots, \zeta_f)\Psi_r, \quad (4)$$

it is found that

$$-\sum_a \frac{\hbar^2}{2M_e}\chi_{r\alpha}\Delta_a\Psi_r - \sum_a \frac{\hbar^2}{M_a}\operatorname{grad}_a \Psi_r \cdot \operatorname{grad}_a \chi_{r\alpha} - \sum_a \frac{\hbar^2}{2M_e}\Psi_r\Delta_a\chi_{r\alpha} + E_r(\xi_1, \cdots, \zeta_f)\Psi_r\chi_{r\alpha} = -\frac{\hbar}{i}\Psi_r\frac{\partial\chi_{r\alpha}}{\partial t}. \quad (5)$$

Multiplying this by Ψ_r^* and integrating over the electronic coordinates, we obtain

$$\left[-\sum_a \frac{\hbar^2}{2M_a}\int \Psi_r^*\Delta_a\Psi_r d\tau(x_1, \cdots, z_n)\right]\chi_{r\alpha} - \sum_a\left[\frac{\hbar^2}{M_a}\left(\int \Psi_r^* \operatorname{grad}_a \Psi_r d\tau\right)\cdot \operatorname{grad}_a \chi_{r\alpha}\right] - \sum_a \frac{\hbar^2}{2M_a}\Delta_a\chi_{r\alpha} + E_r(\xi_1, \cdots, \zeta_f)\chi_{r\alpha} = -\frac{\hbar}{i}\frac{\partial\chi_{r\alpha}}{\partial t}. \quad (6)$$

It will now be shown that the first term may ordinarily be neglected for stationary-state problems. In order to do so, two extreme cases will be considered, namely, that in which the electrons are perfectly free and that in which they are completely bound.

The one-electron wave functions are of the form $e^{2\pi i\mathbf{k}\cdot\mathbf{r}}$ in the first case and hence are practically independent of nuclear coordinates. Thus, the first two terms in (6) are vanishingly small.

In the opposite case, we may, for simplicity, regard the wave function as though it were composed of one-electron functions of the type

$$f_a(x_i - \xi_a, y_i - \eta_a, z_i - \zeta_a). \tag{7}$$

Under this condition, we have the relation

$$\sum_a \operatorname{grad}_a \Psi = -\sum_i \operatorname{grad}_i \Psi; \tag{8}$$

hence, the first term in (6) is simply

$$\frac{m}{M}\sum_i \int \Psi_r^*\left(-\frac{\hbar^2}{2m}\Delta_i\right)\Psi_r d\tau \tag{9}$$

if it is assumed that there is only one type of ion. Since the quantity (9) is equal to m/M times the mean kinetic energy of the electrons, it is normally negligible because the ratio m/M is at most 1/1,840.

The second term also may be dropped in stationary-state problems, for Ψ can then be chosen as a real function. Hence,

$$\int \Psi^* \operatorname{grad}_a \Psi = \frac{1}{2}\operatorname{grad}_a \int |\Psi|^2 d\tau = \operatorname{grad}_a 1 = 0.$$

The final equation for χ_{ra} is

$$\sum_a -\frac{\hbar^2}{2M_a}\Delta_a\chi_{ra} + E_r(\xi_1, \cdots, \zeta_f)\chi_{ra} = -\frac{\hbar}{i}\frac{\partial\chi_{ra}}{\partial t}, \tag{10}$$

which has the form of a Schrödinger equation in which E_r is the effective nuclear potential function. This equation has stationary-state solutions of the form

$$\chi_{ra}(\xi_1, \cdots, \zeta_f, t) = \lambda_{ra}(\xi_1, \cdots, \zeta_f)e^{-\frac{i\mathfrak{E}_{ra}t}{\hbar}} \tag{11}$$

where λ_{ra} satisfies the equation

$$-\sum_a \frac{\hbar^2}{2M_a}\Delta_a\lambda_{ra} + E_r(\xi_1, \cdots, \zeta_r)\lambda_{ra} = \mathfrak{E}_{ra}\lambda_{ra} \tag{12}$$

and $\mathfrak{E}_{ra}$ is the constant total energy of the system. It is evident that $\mathfrak{E}_{ra}$ is the mean value of $\mathfrak{H}_e$ in the approximation in which the first two terms of (6) are negligible.

Although the mean value of $\mathfrak{H}_e$ for the function (2) is accurate to within terms of the order of m/M times the electronic kinetic energy

if Ψ and χ satisfy Eqs. (4), (11), and (12), it does not follow that all mean values are equally accurate,[1] for we know from the variational theorem that the energy is stationary for small variations in the wave functions. As we have seen in Sec. 39 the accuracy of the mean values of other quantities is usually of the order of magnitude $\sqrt{m/M}$.

117. A Qualitative Survey of the Theory of Phases.—Equation (12) of the preceding section, which is the equation for the stationary states of nuclear motion, is usually very difficult to solve accurately because $E_r(\xi_1, \cdots, \zeta_f)$ usually is an extremely intricate nonseparable function of the nuclear variables. This may be realized from the fact that this equation should yield a description of all types of phases of matter from solids to gases.

Let us consider the behavior of the function $E_0(\xi_1, \cdots, \zeta_f)$ that is associated with the lowest electronic wave function. This is the effective potential field in which the ions usually move. E_0 approaches a constant value corresponding to the normal energy of the constituent atoms when the atoms are separated by more than 10^{-6} cm, (*cf.* Fig. 1). As the nuclei are brought together, E_0 usually decreases to a certain minimum value and then increases again as the nuclei are crowded more closely. The depth of this absolute minimum relative to the value of E_0 for large separations is a measure of the cohesive energy of the solid. In addition to this absolute minimum there may be secondary minima corresponding to atomic configurations that may be metastable at very low temperatures. A part of the purpose of the next section is to examine the relative stability of the minima of this type that correspond to crystalline arrangements.

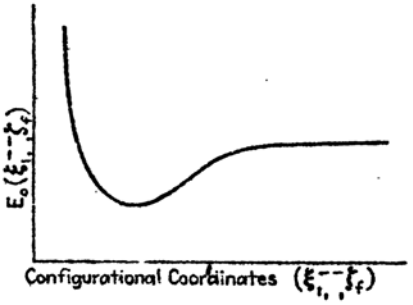

FIG. 1.—Schematic behavior of the electronic energy of the lowest state of the entire crystal as the interatomic distance is varied. For large separations E_0 approaches a constant, whereas it decreases and then increases again as the atoms are brought closer together.

If the coordinates of any atom or group of atoms are varied slightly when the system is at an equilibrium point, we may expect E_0 to increase. The change in E_0 is not the same for all directions of variation but depends upon the crystalline binding. Now, if we rearrange the atoms in any way that does not alter the crystal structure, the initial and final energies are the same. Since E_0 increases for changes near the equilibrium values, it follows that this function passes through a maximum

[1] The accuracy of the adiabatic approximation in special cases is discussed by H. Pelzer and E. Wigner and by E. Wigner (*cf.* footnote 2, p. 470).

during the rearrangement from one equilibrium distribution to another. The minimum value of this maximum for all possible rearrangement paths, that is, the height of the "saddle point" of E_0 in the potential barrier that separates the two minima, is called the "activation energy" for the rearrangement (*cf.* Fig. 2). Paths leading through this saddle point are the ones ordinarily followed when rearrangements take place thermally.[1]

We may now describe the stationary states of nuclear motion qualitatively, using these concepts. In the very lowest state, which is described by the wave function λ_{00}, the system is localized near the absolute minimum of $E_0(\xi_1, \cdots, \xi_f)$. The actual distribution of nuclei is given by the function $|\lambda_{00}|^2$, which will be described more fully in the next section. The energy parameter $\mathfrak{E}_{00}$, associated with the lowest state, is slightly greater than the minimum of E_0, the difference being the zero-point energy of the atoms. Since the probability distribution function decreases very rapidly in the regions where E_0 is greater than $\mathfrak{E}_{00}$, it follows that the individual atoms are statistically localized near their equilibrium positions as long as the energy per atom is less than the saddle point of the barrier surrounding the equilibrium position. There is a chance that a large part of the zero-point energy of the system may become localized in one atom, allowing it to move away; however, the likelihood of a large fluctuation usually is very small for the normal state as we shall see in the next section.

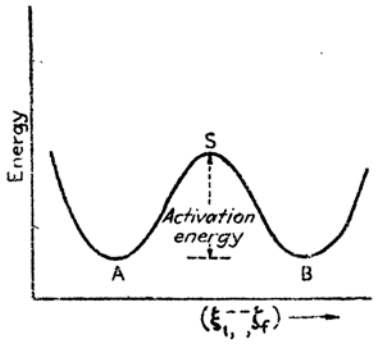

FIG. 2.—Schematic diagram showing the behavior of the energy of the system when the atoms are rearranged without changing the structure. *A* and *B* correspond to the minimum energy arrangements. During the rearrangement from *A* to *B* the energy increases, passes through a maximum, and decreases. The lowest maximum occurs at the saddle point *S* of the potential hill separating *A* and *B*. The height of *S* above *A* and *B* is the activation energy.

As we go to higher energy states, the probability of finding the entire system at regions away from the equilibrium position increases because there is a larger range of configuration space in which $\mathfrak{E}_{0\alpha} - E_0$ is positive. When the mean energy per atom becomes comparable with the height of the saddle point for a given rearrangement, this rearrangement may take place spontaneously with an appreciable probability. The very lowest states in which rearrangements occur appreciably are those in which the system is still crystalline and in which a small fraction of the atoms are diffusing about, whereas the higher states correspond to

[1] *Cf.* the survey article by H. Eyring, *Chem. Rev.*, **17**, 65 (1935).

liquid phases in which there is no lattice structure and in which atoms correlate their positions only with those of their nearer neighbors.[1] Thus the gradation of stationary states from the crystalline phase to the liquid phase is perfectly continuous. The phenomenon of melting, which ordinarily occurs abruptly with the absorption of heat, does not imply any discontinuity in the allowable energy states but is a process in which a range of possible states is jumped over for reasons that are described in Sec. 121. The states skipped during melting are those associated with glasses and supercooled liquids.

The states for which the total energy is greater than that of the system of free molecules correspond to the gaseous phase. In this phase each molecule has enough energy on the average to surmount the barriers holding the atoms of the solid or liquid phase together.

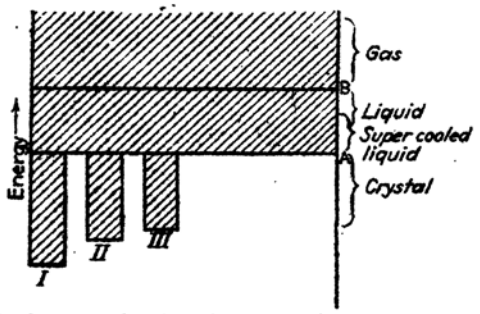

FIG. 3.—Schematic diagram showing the types of energy states of a system of atoms. I, II, and III represent relative minima of the $E_0(\xi_1, \cdots, \zeta_n)$ function that correspond to different allotropic phases. The energy states below A correspond to crystalline phases in which the atoms are vibrating. Long-distance order vanishes at A and the range of glasses, supercooled liquids, and liquids lies between A and B. The levels near A are usually skipped during melting. The gaseous phase lies above B.

When two or more different crystalline arrangements of the ξ correspond to relative minima of $E_0(\xi_1, \cdots, \zeta_f)$, only the lowest is thermodynamically stable at the absolute zero of temperature. The time required to bring about thermodynamical equilibrium may be very long, however, if the system gets caught in one of the higher minima at low temperature. For this reason, several different phases of a substance may be stable in a practical sense.

We may summarize this qualitative discussion by means of the energy-level diagram shown in Fig. 3. There usually are several types of stable states, labeled I, II, III, etc., which correspond to the different polymorphic forms. Above each of these is a range of energy, terminated by the line A, in which the system possesses lattice symmetry. The

[1] Evidence for this type of atomic correlation is given by X-ray analysis of liquids. See, for example, A. H. Compton and S. K. Allison, *X-rays in Theory and Experiment* (D. Van Nostrand Company, Inc., New York, 1935).

region above A, which is the domain of glasses or supercooled liquids, gradually blends into the less viscous liquid state. The states corresponding to energies near A usually are thermodynamically unstable at all temperatures. The line B, which marks the point at which the entire system is in the gaseous phase, depends upon the volume in which the system is kept. B actually may fall below A, in which case the solid sublimes before melting.

118. Low-energy States.—As stated in the last section, we shall assume that the relative minima of $E_0(\xi_1, \cdots, \zeta_f)$ occur for lattice arrangements of the nuclear coordinates. Let us consider a minimum of this type and describe the lattice in terms of the notation of Sec. 22, Chap. III. It will be assumed that the corner points of the unit cells are specified by the vectors

$$\mathbf{r}(p) = p_1\tau_1 + p_2\tau_2 + p_3\tau_3 \tag{1}$$

where the p_i are integers and the τ_i are the primitive translations. In place of the variables ξ_α, η_α, and ζ_α, we may introduce the variables

$$\mathbf{r}_\alpha(p_1,p_2,p_3) = \mathbf{r}(p_1,p_2,p_3) + \rho_\alpha \tag{2}$$

where the $\mathbf{r}_\alpha$ are the position vectors, relative to the origin of coordinates of the n atoms in the cell specified by p_1, p_2, p_3 and ρ_α is the position of these atoms relative to the corner point. In addition, we may introduce the variables

$$x_\alpha{}^i(p_1,p_2,p_3), \qquad (i = 1, 2, 3), \tag{3}$$

for the coordinates of the displacement of the αth atom from its equilibrium position.

If $E_0(\xi_1, \cdots, \zeta_f)$ is expanded in terms of the $x_\alpha{}^i(p)$, we need retain only the quadratic term in the first approximation. The problem of finding the stationary states then reduces to the normal coordinate problem that was discussed in Sec. 22, Chap. III. We know, from the results derived there, that the quadratic terms in E_0 may be reduced to the sum of squares by making the normal coordinate substitution

$$x_\alpha{}^i(p) = \frac{1}{\sqrt{NM_\alpha}} \sum_{t,\sigma} a_t(\sigma)\, \xi^i{}_{\alpha,t}(\sigma)\, e^{2\pi i\sigma\cdot\mathbf{r}_\alpha(p)} \tag{4}$$

where $a_t(\sigma)$ is the complex amplitude of the tth normal mode of wave number σ, and $\xi^i{}_{\alpha,t}(\sigma)$ is the complex direction vector of the displacement of the αth atom. If the $a_t(\sigma)$ are replaced by the real amplitudes

$$\left.\begin{aligned} \alpha_t(\sigma) &= \frac{a_t(\sigma) + a_t{}^*(\sigma)}{\sqrt{2}} \\ \text{and} \qquad \alpha_t(-\sigma) &= \frac{a_t(\sigma) - a_t{}^*(\sigma)}{\sqrt{2}i}, \end{aligned}\right\} \tag{5}$$

the normal form of E_0^g is

$$E_0^g = \tfrac{1}{2}\sum_{t,\sigma}' 4\pi^2\nu_t^2(\mathfrak{d})\alpha_t^2(\mathfrak{d}) \tag{6}$$

where $\mathfrak{d}$ is summed over an entire zone. There are $3nN$ $\alpha_t(\mathfrak{d})$ in all, for $\mathfrak{d}$ has N independent values and t has $3n$ values.

Since the kinetic energy T has the form

$$T = \tfrac{1}{2}\sum_{t,\sigma}' \dot{\alpha}_t^2(\mathfrak{d}) \tag{7}$$

when expressed in terms of the α, the Hamiltonian function of the system is

$$H = \tfrac{1}{2}\sum_{t,\sigma}' [p_t^2(\mathfrak{d}) + 4\pi\nu_t^2(\mathfrak{d})\alpha_t^2(\mathfrak{d})] \tag{8}$$

where $p_t(\mathfrak{d})$ is the momentum variable conjugate to $\alpha_t(\mathfrak{d})$. The corresponding quantum operator is

$$H = \frac{1}{2}\sum_{t,\sigma}' \left[-\hbar^2\frac{\partial^2}{\partial\alpha_t^2(\mathfrak{d})} + 4\pi^2\nu_t^2(\mathfrak{d})\alpha_t^2(\mathfrak{d}) \right], \tag{9}$$

which may be separated into operators for each normal coordinate. Hence, the stationary-state wave function has the form

$$\Lambda(\cdots, \alpha_t(\mathfrak{d}), \cdots) = \prod_{t,\sigma}' \lambda_{n(t,\sigma)}(\alpha_t(\mathfrak{d})) \tag{10}$$

where $\lambda_n(\alpha_t(\mathfrak{d}))$ satisfies the Schrödinger equation for a simple harmonic oscillator, namely,

$$-\frac{\hbar^2}{2}\frac{\partial^2\lambda_n}{\partial\alpha_t^2(\mathfrak{d})} + 2\pi^2\nu_t^2(\mathfrak{d})\alpha_t^2(\mathfrak{d})\lambda_n = \epsilon_n\lambda_n. \tag{11}$$

The total energy in the state (10) relative to the minimum of E_0 is

$$E(\cdots, n_t(\mathfrak{d}), \cdots) = \sum_{t,\sigma}' \epsilon_{n(t,\sigma)} = \sum_{t,\sigma}' [n(t,\mathfrak{d}) + \tfrac{1}{2}]h\nu_t(\mathfrak{d}). \tag{12}$$

Let us examine the properties of the lowest state. The normalized eigenfunctions of the wave equation (11) are

$$\lambda_0(\alpha_t(\mathfrak{d})) = \left(\frac{4\pi\nu}{h}\right)^{\frac{1}{4}} e^{-\frac{1}{2}\frac{4\pi^2\nu_t^2(\sigma)\alpha_t^2(\sigma)}{h\nu_t(\sigma)}} \tag{13}$$

so that

$$\Lambda_0 = Ce^{-\sum_{t,\sigma}'\frac{1}{2}\frac{4\pi^2\nu_t^2(\sigma)\alpha_t^2(\sigma)}{h\nu_t(\sigma)}}. \tag{14}$$

As an approximation, we may replace the exponent by

$$-\frac{1}{\hbar\bar{\nu}}\left[\sum_{t,\sigma}\frac{1}{2}4\pi^2\nu_t^2(\mathfrak{d})\alpha_t^2(\mathfrak{d})\right] = -\frac{E_\delta^2}{\hbar\bar{\nu}} \tag{15}$$

where E_δ^2 is the potential energy and $\bar{\nu}$ is a mean oscillator frequency, which is of the order of magnitude $k\Theta_D/h$, Θ_D being the characteristic temperature of the substance. The probability of finding the system in the volume element $\prod_{t,\sigma} d\alpha_t(\mathfrak{d})$ is

$$\left[\prod_{t,\sigma}\left(\frac{4\pi\nu_t(\mathfrak{d})}{h}\right)^{\frac{1}{2}}d\alpha_t(\mathfrak{d})\right]e^{-2\frac{E_\delta^2}{\hbar\bar{\nu}}}, \tag{16}$$

and the probability of finding E_δ^2 lying in the range from E to $E + dE$ is

$$C'e^{-\frac{2E}{\hbar\bar{\nu}}}E^{\frac{3N}{2}-1}dE \tag{17}$$

where C' is a constant. This function has a very steep maximum of width $\hbar\bar{\nu}$ at the value of E_0 satisfying the equation

$$E = \tfrac{3}{4}Nh\bar{\nu}.$$

The fluctuation in the position and energy of a single atom may be estimated by expressing Eq. (16) in terms of the atomic coordinates. If we keep all atoms except one fixed at their equilibrium positions, E depends on the displacement variable x of this atom as the function kx^2, where k is related to $\bar{\nu}$ in order of magnitude by the equation

$$k \cong 4\pi^2\bar{\nu}^2M$$

in which M is the atomic mass. Hence, the probability depends on x^2 through a factor of the form

$$e^{-\frac{4\pi^2\bar{\nu}M}{h}x^2}.$$

The half width of this distribution, namely, $(1/2\pi)\sqrt{h/\bar{\nu}M}$, is 10^{-9} cm for $\nu \cong 10^{14}$ sec and $M = 2 \times 10^{-24}$, the mass of hydrogen, a fact showing that the range of fluctuation ordinarily is small compared with interatomic distances.

119. Polymorphism.—When $E_0(\xi_1, \cdots, \zeta_f)$ has a relative minimum for two or more crystallographic phases, the thermodynamically stable one at the absolute zero of temperature is that having the lowest energy. Another arrangement may be more stable, however, at high temperatures. We may obtain a simple interpretation of this fact in the following way.

According to Boltzmann's theorem,[1] the relative probability of finding the αth modification in the energy state E_α at temperature T is

$$G(E_\alpha)e^{-\frac{E_\alpha}{kT}} = e^{-\frac{E_\alpha - TS(E_\alpha)}{kT}} \tag{1}$$

where $G(E_\alpha)$ is the degeneracy of the energy level E_α and $S = k \log G(E_\alpha)$ is the entropy associated with this level. The function (1) has an extremely steep maximum at the value of E_α satisfying the equation

$$\frac{dE_\alpha}{dS_\alpha} = T, \tag{2}$$

as may be proved by setting the derivative of (1) equal to zero. The sharpness of this peak may be appreciated from the fact that E_α is of the order of calories for an ordinary-sized crystal, whereas the fluctuations in E_α are of the order of kT, which is about 10^{-20} cal at ordinary temperatures. The condition (2) allows us to specify the equilibrium state of a given modification at any temperature very simply, for this state corresponds to the point on the $E(S)$ curve at which the slope is T (*cf.* Fig. 4). It should be observed, in passing, that the condition that the function (1) be a maximum is that the function $A(E) = E - TS(E)$ be a minimum. Since A is the thermodynamical free energy, this condition is identical with the thermodynamical condition for determining the stable state. The numerical value of A at any temperature is determined from the quantities in Fig. 4 by extrapolating the tangent line to the energy axis.

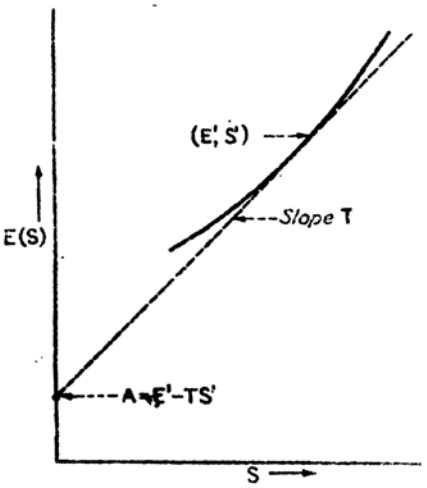

FIG. 4.—Schematic diagram showing the relationship between E, S, T, and A. The full line is the $E(S)$ curve as determined, for example, by solving the Schrödinger equation. The equilibrium state at temperature T is the state corresponding to the point (E', S') where the slope of $E(S)$ is T. The intercept of this tangent with the energy axis is the free energy. The specific heat at temperature T is related to the second derivative by the equation

$$C_V = \frac{\left(\frac{dE}{dS}\right)}{\left(\frac{d^2E}{dS^2}\right)}.$$

The relationship between E and S may be derived very easily when the lattice frequencies are all the same. In this case, the number of quanta available for distribution among the $3N$ degrees of freedom of the crystal is

[1] See the footnotes on statistical mechanics in Chaps. III and IV.

$$n = \frac{E - E'}{h\nu} \tag{3}$$

where E' is the energy of the lowest state and ν is the vibrational frequency of the modes. The degeneracy G of this state is the total number

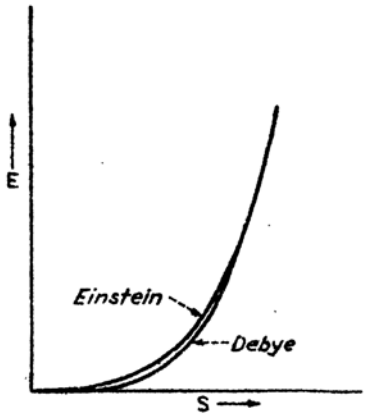

FIG. 5.—Schematic representation of the $E(S)$ curves for the lattice vibrations of a crystal. The Einstein curve rises more rapidly than the Debye curve because there are fewer ways of dividing E into quanta if the Einstein frequency distribution is used.

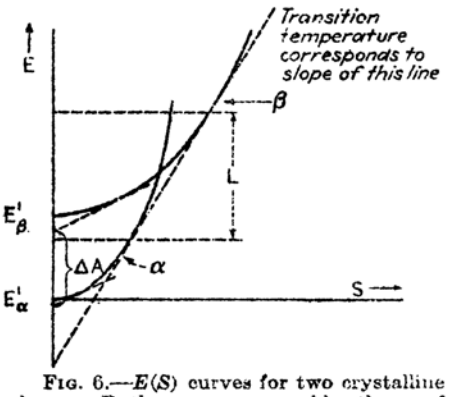

FIG. 6.—$E(S)$ curves for two crystalline phases. Both curves resemble those of Fig. 5; however, the curve rises more rapidly in the crystal having the higher vibrational frequency (the α phase in this case). Since the curves cross, they have a common tangent and a phase change will occur under equilibrium conditions at the temperature corresponding to the slope of the common tangent. The latent heat is the energy difference at the points of tangency, etc.

of ways in which these quanta may be distributed among the modes, namely,

$$G = \frac{(3N + n - 1)!}{(3N - 1)!\,n!}. \tag{4}$$

Hence, by the use of Stirling's approximation, we find

$$S = k \log G \cong k[(3N + n) \log (3N + n) - 3N \log 3N - n \log n]. \tag{5}$$

S and dE/dS are zero when $n = 0$ and S increases monatomically with E (*cf.* Fig. 5). The $E(S)$ curve rises more slowly for small values of S if the Debye distribution of frequencies is used. We may determine the value of E and S at any temperature T by employing the value of n that minimizes the free energy $E - TS$. Using E and S as determined by Eqs. (3) and (5), we find

$$n = 3N \frac{1}{e^{\frac{h\nu}{kT}} - 1}.$$

When E and S are computed from this, it is found that

$$A = E - TS = E' - 3NkT \log \frac{e^{\frac{h\nu}{kT}}}{e^{\frac{h\nu}{kT}} - 1}. \tag{6}$$

Let us consider two different crystallographic modifications α and β of a substance and determine the transition temperature for a case in which Eq. (5) may be used for both phases. The fundamental frequencies of the two phases will be designated by ν_α and ν_β, respectively. If it is assumed that E_β' is greater than E_α', so that the α phase is most stable at low temperatures, and that ν_α is greater than ν_β, the two $S(E)$ curves have the form shown in Fig. 6. Since $S_\alpha(E - E_\alpha')$ rises more slowly than $S_\beta(E - E_\beta')$, the two curves cross and have a common tangent line.

The ratio of the probabilities P_α and P_β of finding the system in either the first or the second phase at temperature T is

$$\begin{aligned} \frac{P_\alpha}{P_\beta} &= e^{-\frac{[E_\alpha(T) - TS_\alpha(T)] - [E_\beta(T) - TS_\beta(T)]}{kT}} \\ &= e^{-\frac{A_\alpha(T) - A_\beta(T)}{kT}} \end{aligned} \tag{7}$$

where A_α and A_β are the free energies of the two phases. The ratio (6) is either very great or very small except for a narrow temperature range in which A_α and A_β differ by a factor of order of magnitude kT. Thus, the transition temperature T' is given by the thermodynamical equation

$$A_\alpha(T') = A_\beta(T'). \tag{8}$$

It may be seen from the construction of Fig. 6 that this condition is satisfied at the temperature corresponding to the slope of the tangent line of the two $E(S)$ curves. The α phase is stable below this temperature, and the β phase is stable above; moreover, the heat of the transition is equal to the difference L between the energies of the two tangent points.

According to Eq. (6), the free energies of the two phases at temperature T are

$$\left.\begin{aligned} A_\alpha(T) &= E_\alpha' - 3NkT \log \frac{e^{\frac{h\nu_\alpha}{kT}}}{e^{\frac{h\nu_\alpha}{kT}} - 1} \\ A_\beta(T) &= E_\beta' - 3NkT \log \frac{e^{\frac{h\nu_\beta}{kT}}}{e^{\frac{h\nu_\beta}{kT}} - 1}. \end{aligned}\right\} \tag{9}$$

The difference of these free energies is

$$\Delta A_{\alpha\beta} = E_\alpha' - E_\beta' - 3NkT\left[\log e^{\frac{h(\nu_\alpha-\nu_\beta)}{kT}} - \log \frac{e^{\frac{h\nu_\alpha}{kT}}-1}{e^{\frac{h\nu_\beta}{kT}}-1}\right], \tag{10}$$

which is zero at the temperature defined by the equation

$$e^{-\frac{E_\alpha'-E_\beta'}{3NkT'}} = \frac{e^{-\frac{h\nu_\alpha}{kT'}}-1}{e^{-\frac{h\nu_\beta}{kT'}}-1}. \tag{11}$$

The necessary and sufficient condition that must be satisfied if this equation is to have a root is that ν_α should be greater than ν_β if E_β is greater than E_α'.

The condition replacing (11) when all the $3N$ frequencies are different is

$$e^{-\frac{E_\alpha'-E_\beta'}{kT}} = \frac{\prod^{\nu_\alpha}(e^{-\frac{h\nu_\alpha}{kT'}}-1)}{\prod^{\nu_\beta}(e^{-\frac{h\nu_\beta}{kT'}}-1)}, \tag{12}$$

as may be seen by using the expression

$$E_\alpha' + kT \log \prod^{\nu_\alpha}(1 - e^{-\frac{h\nu_\alpha}{kT}}) \tag{13}$$

for the free energy of a system of oscillators.[1] Equation (12) is difficult to solve directly even when there is a simple relation between frequency and the wave number. In practical work, it actually is simpler to compute numerically the free energies of the phases and to find the temperature at which these functions are equal. The specific heats of none of the phases for which transitions have been investigated thoroughly obey either the Einstein or the Debye law, however, so that there is no need for discussing these computations in detail. Instead, we shall discuss several actual cases. It should be mentioned at this point that the credit for the first intensive investigations of the thermal

[1] This expression may be derived from the partition functions discussed in Sec. 18, Chap. III, by the use of the relation

$$-kT \log f = A$$

connecting the free energy of a system and its total partition function. [See, for example, R. H. Fowler, *Statistical Mechanics* (Cambridge University Press, 1936).]

effects associated with allotropy is due to Nernst,[1] who used this subject as the cornerstone in establishing his heat theorem.

a. Tin.—The transition between black and white tin has been studied fairly completely and has practical interest because it is responsible for tin disease which may impair the protective coating of tinned metals. The low-temperature, or black, form has the diamond structure; the high-temperature form has a complex tetragonal lattice. The thermodynamical transition point was determined most accurately by Cohen and van Eijk[2] who measured the temperature at which the emf of an electrolytic cell in which the two electrodes are made of the different phases vanishes. This temperature is 292°K. The specific heats of

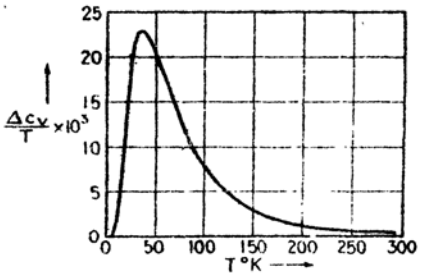

FIG. 7.—The $\Delta cv/T$ curve for gray and white tin. The specific heat of white tin is the larger and accounts for the phase change. The ordinates are cal/deg².

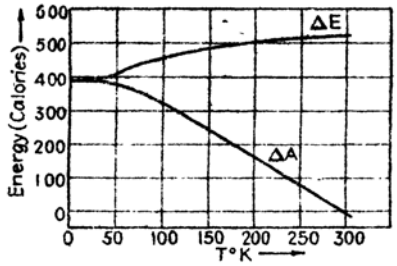

FIG. 8.—The ΔE and ΔA curves for gray and white tin. Below the transition temperature, A is smaller for the gray modification. The point at which ΔA becomes zero is the transition temperature.

both phases were measured by Lange[3] to within a few degrees of absolute zero; the difference of these specific heats divided by T is shown in Fig. 7. The specific-heat curves do not obey the Debye law closely, but they do approach $3R$ at high temperatures, showing that the oscillator model is probably accurate. The transition heat ΔE of the phase change was measured by Brönsted[4] and was found to be 535 cal at the transition temperature and 399 cal at absolute zero. The complete transition-heat curve is shown in Fig. 8. The corresponding free-energy curve ΔA, which may be determined by computing $\Delta E(T)$ and $\Delta S(T)$ from the empirical data under the condition that $S(T)$ vanish at absolute zero, is shown in the same figure. The same curve may be obtained from $\Delta E(T)$ alone by solving the Gibbs-Helmholtz equation

[1] W. NERNST, *The New Heat Theorem* (E. P. Dutton & Company, Inc., New York, 1926).

[2] E. COHEN and C. VAN EIJK, *Z. physik. Chem.*, **30A**, 601 (1899).

[3] F. LANGE, *Z. physik. Chem.*, **110A**, 360 (1924).

[4] J. N. BRÖNSTED, *Z. physik. Chem.*, 65, 744 (1909).

$$\Delta A = \Delta E - T\frac{\partial \Delta A}{\partial T}$$

under the third-law condition that $\partial \Delta A/\partial T$ be zero at absolute zero. ΔA crosses the axis at 295°, showing good agreement with Cohen and van Eijk's directly measured value.

b. Sulfur.—The transition of sulfur from rhombic to monoclinic form at 368.5°K was investigated by Nernst,[1] Brönsted,[2] and a number of other workers. It is worth mentioning that this transition is the first recorded case of allotropy.[3] The specific-heat curves deviate considerably from the Debye form, and their difference is shown in Fig. 9. The transition temperature as computed from the point at which ΔA vanishes is 370°K.

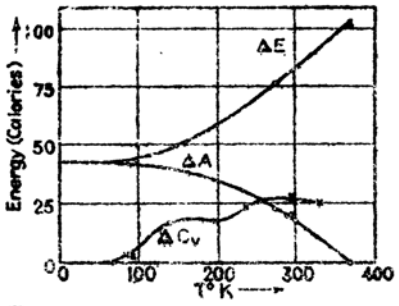

FIG. 9.—The ΔE, ΔA and ΔC_V curves for the two phases of sulfur.

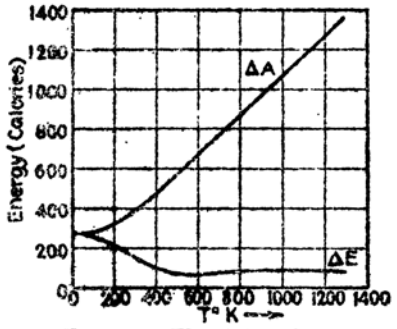

FIG. 10.—The ΔA and ΔE curves for diamond and graphite. The latter has the lower free energy at all temperatures at ordinary pressures.

c. Carbon.—Detailed measurements of the transition heat of the diamond-graphite phase change by Roth and Wallasch[4] show that graphite has the lower energy at ordinary temperatures and pressures. The difference, however, is only 160 ± 30 cal at room temperature. The lower curve of Fig. 10 shows the temperature dependence of this difference. Since the characteristic temperature of diamond is higher than that of graphite at ordinary pressures, it follows from the preceding discussion that graphite is more stable than diamond at all temperatures. The free-energy difference curve of Fig. 10 supports this conclusion, for it rises away from the value at absolute zero.

Simon[5] has made a thermodynamical estimate of the pressure dependence of the free-energy curve and has concluded that pressures in the

[1] NERNST, *op. cit.*
[2] J. N. BRÖNSTED, *Z. physik. Chem.*, **65**, 371 (1906).
[3] MITSCHERLICH, *Ann. Physik*, **83**, 328 (1852).
[4] ROTH and WALLASCH, *Ber. deut. Chem. Ges.*, **46**, 896 (1913).
[5] F. SIMON, *Handbuch der Physik*, Vol. X, p. 376 (Julius Springer, Berlin, 1926).

neighborhood of fifty thousand atmospheres would be needed to reverse the equilibrium at the high temperatures at which the rate of change is appreciable.

An outstanding exception to the rule that the amplitude of the zero-point oscillation is small compared with the interatomic distance seems to occur in one of the condensed phases of helium. The phase diagram of helium at low temperatures is shown[1] in Fig. 11. In the immediate vicinity of absolute zero, this substance forms a true solid if the pressure is above 25 atmospheres; however, at lower pressures, it forms two liquid phases, which are known as liquid helium I and liquid

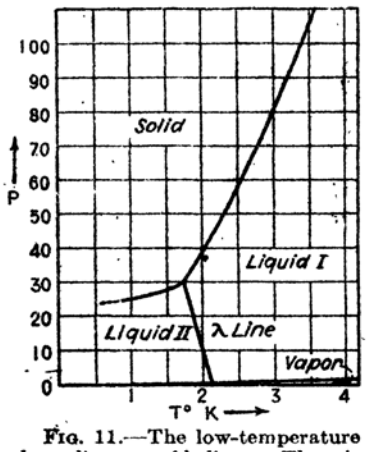

FIG. 11.—The low-temperature phase diagram of helium. There is no solid phase below 25 atmospheres. The ordinate is expressed in atmospheres.

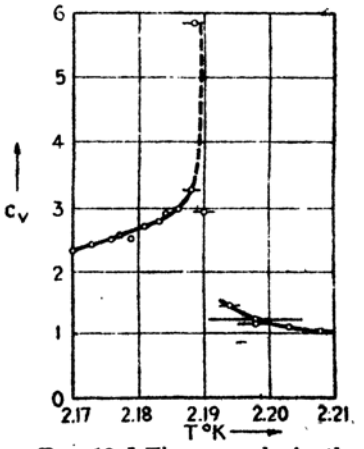

FIG. 12.—The anomaly in the specific heat of liquid helium at the λ-point. The ordinate is expressed in cal/gram-degree. (*After Keesom and Keesom.*)

helium II, and no ordinary type of solid. The density of the liquid phases is about 0.70 relative to that of the high pressure solid phase. The transition point between helium I and helium II, which is known as the λ point, is distinguished by several striking effects. Thus, it is found that the specific-heat curve[2] has the discontinuity shown in Fig. 12 and that the fluidity[3] and thermal conductivity increase very much in passing below the λ point. In addition, it is found[4] that liquid helium II exhibits the mechanical analogue of the thermoelectrical effects observed

[1] W. H. KEESOM and K. CLUSIUS, *Proc. Acad. Sci. Amsterdam*, **35**, 320 (1932); W. H. KEESOM and H. P. KEESOM, *Proc. Acad. Sci. Amsterdam*, **35**, 736 (1932).

[2] W. H. KEESOM and H. P. KEESOM, *Physica*, **2**, 557 (1935).

[3] W. H. KEESOM and H. P. KEESOM, *Physica*, **2**, 557 (1935); B. V. ROLLIN, *Physica*, **3**, 266 (1936); J. F. ALLEN, R. PEIERLS, and M. Z. UDDIN, *Nature*, **140**, 475 (1937).

[4] J. O. WILHELM, A. D. MISENER, and A. R. CLARK, *Proc. Roy. Soc.*, **151**, 342 (1935); E. F. BURTON, *Nature*, **135**, 265 (1935), **142**, 72 (1938).

in metals, for mechanical flow is induced as a result of temperature gradients.

Guided by the similarity of the specific-heat curve shown in Fig. 12 and the specific-heat curve observed during the transition between the ordered and disordered state in alloys such as β brass in which the components are present in equal numbers (*cf.* Fig. 43, Chap. I), Fröhlich[1] suggested that the two liquid helium phases represent ordered and disordered phases of a crystal. In particular, he suggested that the phases have the diamond structure (Fig. 4, Chap. I), which may be regarded as a body-centered cubic lattice in which half the atoms are replaced by vacancies, and that the disordering process consists in the interchange of atoms and vacancies. Thus, according to this picture, liquid helium I would correspond to the phase in which there is no long-distance order and liquid helium II would correspond to the partly ordered phase. There are, however, the following two objections to Fröhlich's model: (1) It should be expected that the liquid helium II phase would become more and more solidlike as the temperature is lowered and ordering increases, whereas it is actually found that the viscosity seems to become smaller and smaller. (2) London[2] showed, on the basis of the Slater-Kirkwood expression for the interaction energy of two helium atoms, that the diamond type of lattice is unstable relative to the interchange of vacancies and atoms, so that Fröhlich's ordering process is unlikely.

As a result of this work, London suggested that the amplitude of the zero-point oscillations in these liquid phases is so large that the atoms should be treated as though free in the same sense that the electrons in a metal are free. Since the helium atoms obey Einstein-Bose statistics instead of Fermi-Dirac statistics, London suggested that a qualitative insight into the properties of the two liquid helium phases might be obtained by treating them as a degenerate Bose-Einstein gas. The thermal and mechanical properties of a gas of this type may be obtained by methods analogous to those used in the Sommerfeld theory of metals, the function

$$f(\epsilon) = \frac{1}{Ae^{\frac{\epsilon}{kT}} - 1}$$

replacing the Fermi-Dirac function. It is found that the specific-heat curve of this gas has the singularity shown in Fig. 13 which begins when the particles start to condense in the lowest energy state. London suggested that this singularity corresponds to the λ point of liquid helium

[1] H. FRÖHLICH, *Physica*, **4**, 639 (1937).

[2] F. LONDON, *Nature*, **141**, 643 (1938), **142**, 612 (1938); *Phys Rev.*, **54**, 947 (1938).

and that the differences between the curves of Figs. 12 and 13 arise because the helium atoms interact and thus are not perfectly free. The temperature T_0 at which the singularity occurs in Fig. 13 would be 3.14°K for a perfect gas of helium atoms having the observed density of the liquids. This actually is fairly close to the observed λ point at 2.19°K. London has also shown that many of the unusual thermal and mechanical properties of liquid helium II can be given a qualitative explanation on the basis of his simple model.

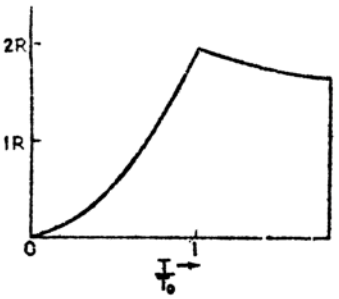

FIG. 13.—The molar heat of a Bose-Einstein gas near the degeneracy temperature T_0. The temperature T_0 is equal to

$$\frac{h^2}{2\pi Mk}\left(\frac{3n_0}{2.612}\right)^{2/3}$$

where M is the atomic mass and n_0 is the number of atoms per unit volume.

120. The Effect of Electronic Excitation on Phase Changes.—The Gibbs-Helmholtz equation, namely,

$$A = E + T\frac{\partial A}{\partial T}, \tag{1}$$

may be integrated and placed in the form

$$A = -T\int_0^T \frac{E}{T'^2}dT'. \tag{2}$$

which makes it possible to compute the free energy when the function $E(T)$ is known. Since

$$E(T') = E(0) + \int_0^{T'} C(T'')dT'' \tag{3}$$

where $C(T)$ is the molar heat,

$$A = E(0) + T\int_0^T \frac{1}{T'^2}\int_0^{T'} C(T'')dT''. \tag{4}$$

Thus, A may be computed from the molar heat. We may conclude from this equation that A is affected appreciably by a given part of a system only when this part contributes to the specific heat. Since the electrons do not contribute appreciably to the specific heat in simple metals and insulators, as is evidenced by their obedience to Dulong and Petit's law above the characteristic temperature, we may conclude that phase changes in these solids are not influenced by the electronic excitation which ordinarily occurs. This is not true of substances containing transition-element atoms, however, for the electronic specific heat usually is comparable with the $3R$ value at sufficiently high temperatures.

An important case in which the electronic excitation probably plays a role is afforded by iron. As we have seen in Sec. 2 the α or body-centered phase is stable at all temperatures in the range from 0°K to the melting point at 1803°K except for a region extending from 1174° to 1674°K in which the face-centered γ phase is stable. It is

possible to understand this behavior by using the information given by the specific-heat curves of Fig. 17, Chap. I. We may see from this figure that the γ phase has the lower characteristic temperature; hence, we may conclude from the discussion of the preceding section that it would be the stable phase at high temperatures if the free energy were determined by the lattice vibrations alone. Actually, the electronic specific heat of the α phase is larger than that of the γ phase at temperatures above 580°K, and this difference tends to compensate for the "advantage" the γ phase receives from the larger value of the vibrational specific heat below 200°C.

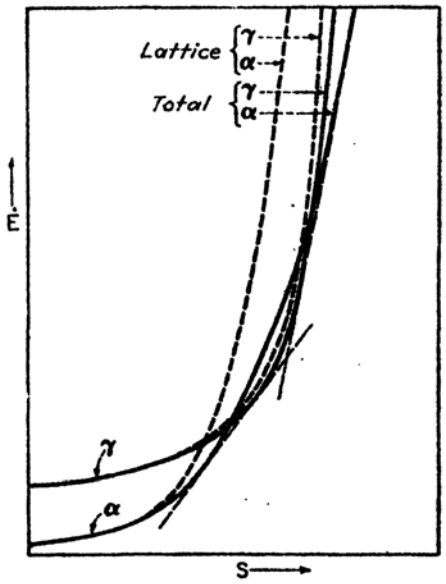

FIG. 14.—Probable behavior of the $E(S)$ curves of the α and γ phases of iron. The α curve is initially lower, but rises more rapidly because the characteristic temperature of the α phase is larger. At higher values of S, the larger electronic heat of the α phase reverses the curves.

The situation that probably exists is indicated schematically in Fig. 14 in which the dotted lines represent the contribution to the $E(S)$ curves of the two phases from lattice vibrations. If these were the actual curves, the γ phase would be stable at high temperatures. The electronic specific heat alters the curves and leads to the full lines. Since the electronic specific heat of the α phase is the larger at high temperatures, the $E(S)$ curve of this phase is altered most. We may conclude that the $E(S)$ curve for the γ phase crosses that for α twice in the manner shown, two tangent lines being thus produced.

If the electronic specific heats of α and γ iron were accurately measured,[1] it would be possible by the use of Eq. (4) to test the preceding picture by direct computations of the contributions to A.

Since cobalt has a similar reappearance of the low-temperature phase at high temperatures, we may conclude that Fig. 14 also applies to it.

121. Melting.—We shall not attempt to give a survey of the present status of the theory of liquids, for to do so would carry us too far afield, but we shall mention briefly the process of melting.[2]

[1] An analysis of the entire specific-heat curve of nickel that is based on the use of the low-temperature value has been given by E. C. Stoner, *Phil. Mag.*, **22**, 81 (1936).

[2] Survey articles on the theory of liquids are as follows: K. F. Herzfeld, *Jour.*

The quadratic approximation for the function $E_0(\xi_1, \cdots, \xi_f)$, which was discussed in Sec. 118, is not valid when the amplitude of atomic vibrations becomes comparable with the interatomic distances, because the potential well about any atom flattens in the directions in which there are saddle points (*cf.* Fig. 15), such as the saddle points corresponding to the interchange of two atoms. This flattening should cause the density of levels $G(E)$ to increase[1] more rapidly than for the quadratic approximation, so that the entropy may increase in the manner shown in Fig. 16. If the $S(E)$ curve has an inflection point, as in Fig. 16, the

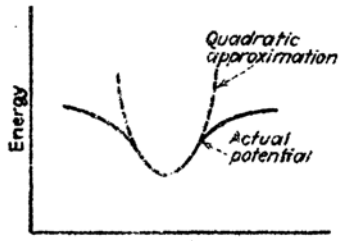

FIG. 15.—Schematic representation of the behavior of the atomic potential well. This deviates from the simple parabolic well assumed in the ordinary theory of specific heats, when the atomic displacements become large.

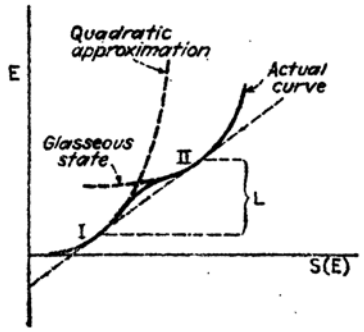

FIG. 16.—Schematic representation of the $E(S)$ curve for an actual solid (full line). The effect of anharmonic forces is to increase the entropy of higher energy states.

system jumps from the state I to the state II at a temperature T given by the slope of the line joining these two points. Below this temperature, the system is crystalline; above it, the system presumably is in the liquid state since this is the phase in which atomic rearrangements take place fairly freely, as is evidenced by the ability of liquids to flow. If ϵ is the height of the activation hill for the interchange of atoms, the number of atoms having enough energy to pass over this hill should vary with temperature in the manner

$$Ae^{-\frac{\epsilon}{kT}} \tag{1}$$

where A is nearly constant. Hence, the flowability, that is, the reciprocal of the viscosity, should vary with temperature as the quantity (1). The

Applied Phys., **8**, 319 (1937); H. Eyring and J. Hirschfelder, *Jour. Phys. Chem.*, **41**, 249 (1937); R. H. Ewell, *Jour. Applied Phys.*, **9**, 252 (1938); J. E. Lennard-Jones, *Physica*, **4**, 941 (1937); N. F. Mott and R. W. Gurney, *Reports on Physics Progress*, Vol. V (Cambridge University Press, 1939).

[1] A part of this increase may be regarded as a mixing entropy (*cf. ibid.*).

energy L (*cf.* Fig. 16), by which the system jumps during the transition, is the latent heat of fusion. It should be clear from the figure that this heat is connected with the change in entropy ΔS by the equation

$$\Delta S = \frac{L}{T}.$$

The states immediately below II, which are skipped during melting, describe supercooled liquids, whose flowability decreases with decreasing temperature and which become glasses at low temperatures. The $E(S)$ curve of such a glass may depart from the full curve of Fig. 15 (*cf.* the dotted section) when rearrangements no longer take place. Thus, the entropy may decrease rapidly, although the atomic arrangement is not crystalline and the energy is not so low as for a perfect crystal.

Mott[1] has used a simple model of the liquid state to compute a partition function, which he has employed successfully in relating some properties of the liquid and solid phases. He assumed that the liquid state is dynamically similar to a solid, inasmuch as the individual atoms are vibrating, and he assumed that the mean liquid vibrational frequency ν_l is lower than the mean solid frequency ν_s because the liquid is less rigid than the solid. He neglected the contribution to the partition function from the interchange of atoms so that the relationship between the solid and liquid phase in this model is essentially the same as that we have found for allotropic modifications. Thus, the partition functions for the liquid and solid phases are

$$\left.\begin{aligned} f_l &= e^{-\frac{E_l}{kT}}\left(\frac{e^{\frac{h\nu_l}{kT}}}{e^{\frac{h\nu_l}{kT}}-1}\right)^{3N}, \\ f_l &= e^{-\frac{E_s}{kT}}\left(\frac{e^{\frac{h\nu_s}{kT}}}{e^{\frac{h\nu_s}{kT}}-1}\right)^{3N}, \end{aligned}\right\} \tag{2}$$

where E_s is the lowest state of the crystal, E_l is the lowest state of the liquid, that is, the energy of the supercooled liquid at absolute zero, and N is the number of atoms. The condition for equilibrium at the melting temperature T_M is

$$\left(\frac{\nu_s}{\nu_l}\right)^3 = e^{\frac{E_l - E_s}{kT_M}}, \tag{3}$$

in which it is assumed that kT_M is much greater than $h\nu_s$. $E_l - E_s$ is very nearly equal to L, the latent heat of fusion, whence

[1] N. F. MOTT, *Proc. Roy. Soc.*, **146**, 465 (1934).

$$\left(\frac{\nu_s}{\nu_l}\right)^3 = e^{\frac{L}{RT_M}}, \tag{4}$$

which is Mott's relation.

Mott has tested this relation for metals by comparing the ratio ν_s/ν_l computed from (4) with the ratio derived from conductivity measurements. We shall discuss the connection between the electrical conductivity and the vibrational frequency of the lattice in the next chapter and shall find that

$$\frac{\sigma_l}{\sigma_s} = \frac{\nu_l^2}{\nu_s^2} \tag{5}$$

in simple cases. In other words, we have

$$\frac{\sigma_s}{\sigma_l} = e^{\frac{2L}{3RT_M}}. \tag{6}$$

The extent to which this equation is satisfied may be seen from Table LXXV. It is valid for the simpler metals, but it fails for the metals with

TABLE LXXV.—COMPARISON OF OBSERVED VALUES OF σ_s/σ_l WITH THOSE COMPUTED FROM MOTT'S RELATION (6) BY THE USE OF OBSERVED VALUES OF L AND T_M.

	σ_s/σ_l	
	Observed	Calculated
Li	1.68	1.84
Na	1.45	1.77
K	1.55	1.75
Rb	1.61	1.76
Cs	1.66	1.75
Cu	2.07	1.97
Ag	1.9	2.0
Au	2.28	2.22
Al	1.64	2.0
Cd	2.0	2.3
Pb	2.07	1.87
Sn	2.1	3
Tl	2.0	2.3
Zn	2.09	2.3
Hg	~4	2.23
Bi	0.43	5.0
Ga	0.58	4.5
Sb	0.67	5.6

unusual structures. This failure is explained in part by the fact that the relation (5) is not obeyed by the transition metals.

Equation (6) should apply to allotropic forms of a metal at the transition temperature in cases in which this temperature is much larger than the characteristic temperature of the two solids. There do not seem to be enough experimental data available to test the relation in any cases of this kind.

Herzfeld, Mayer, and Kane[1] have computed the free energies of the rare gas solids, relative to the free energies of the gaseous constituents, as functions of the lattice constants and have found that these solids would undergo a discontinuous expansion if they were superheated. In terms of a diagram of the type of Fig. 12, their results indicate that the first inflection point in the $E(S)$ curve of one of these solids occurs, not because the individual atomic potential wells are anharmonic, but because the curvature of the well decreases as the crystal expands. At the present time, it is not possible to say whether or not this effect makes an alteration of the qualitative picture of melting, presented above, necessary in all solids.

In the Debye approximation, the molar free energy of the solid may be written in the form

$$A(r) = E_0(r) + \tfrac{3}{2}N_A h\nu_m + A_D(\nu_m,T,r) \tag{7}$$

where $E_0(r)$ is the molar electronic energy, $\frac{3}{2}N_A h\nu_m$ is the zero-point vibrational energy, $A_D(\nu_m,T,r)$ is the free energy obtained from a Debye function, namely,

$$A = -T\int_0^T \frac{dT}{T^2}E_D(\nu_m,T), \tag{8}$$

and ν_m is the maximum frequency of the lattice. The energy $E_0(r)$ was expressed in terms of a van der Waals interaction term of the form

$$-\frac{C}{r^6} \tag{9}$$

and a repulsive term of the form

$$CBe^{-\frac{r}{\rho}}. \tag{10}$$

Thus,

$$E_0(r) = C\left\{-\frac{14.5}{r^6} + 12Be^{-\frac{r}{\rho}}\left[1 + \frac{1}{2}e^{-\frac{(\sqrt{2}-1)r}{\rho}} + \cdots\right]\right\} \tag{11}$$

[1] K. F. HERZFELD and MARIA G. MAYER, *Phys. Rev.*, **46**, 995 (1934); BROTHER GABRIEL KANE, *Jour. Chem. Phys.*, **7**, 603 (1939).

in which the factor 14.5 is the coefficient in the sum of terms (9) for a face-centered lattice and the coefficient of $12B$ is the sum of terms (10). In each case, ρ was given several values. For example, the values 0.345 Å and 0.209 Å were used in all cases. The first is the empirical value of Born and Mayer (see Chap. II), and the second is the value found by Bleick for neon. Corresponding values of C and B were then determined with the condition that (11) plus the zero-point energy should give the observed lattice constant and cohesive energy at low temperatures. The process of determining these constants actually involves a reiteration procedure; for ν_m, which occurs in the zero-point energy, was determined from the theoretical expressions for the elastic constants, which in turn involve C and B.

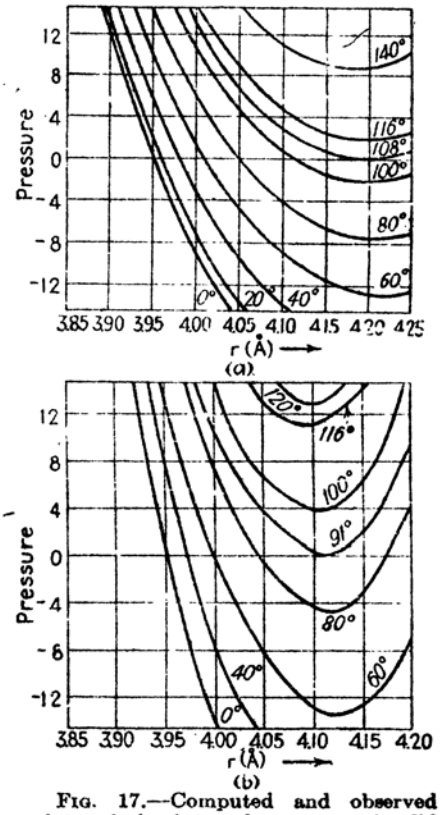

FIG. 17.—Computed and observed values of the internal pressure of solid krypton for several temperatures. *a* corresponds to the value 0.345Å of the repulsive parameter and *b* to the value 0.209Å. The minima that occur at high temperatures imply that the crystals become unstable. (*After Kane.*)

Figure 17 shows the computed and observed values of the internal pressure $-\partial A/\partial V$ of krypton for several temperatures near the observed melting temperature, namely, 116.0°K. The two sets of curves correspond to the values 0.345 and 0.209, respectively. The ordinary equilibrium volume is determined by the condition that $\partial A/\partial V$ vanish. The interesting feature of these curves is that those for temperatures above 108° and 91°K, respectively, are positive everywhere, which indicates that the body-centered crystal becomes unstable. This behavior is tied up with the fact that the elastic constants, and hence ν_m, decrease with increasing lattice constant and thus raise A_D. Thus, the free energy presumably could be decreased by rearranging the atoms into another phase, such as the liquid, and at the same time increasing the atomic volume. Since the solid phase becomes unstable even relative to the gaseous phase, it is natural to suggest that melting is forced by the disruption of the crystal.

122. Atomic Diffusion*.—Atomic diffusion has been studied with fair experimental accuracy[1] in a number of metals. The processes that have been treated are the diffusion of constituents in substitutional and interstitial alloys and the self-diffusion in those monatomic metals having radioactive isotopes.[2] Although the diffusion of atoms in insulating crystals has not been investigated so thoroughly as diffusion in metals, the general facts probably are very similar in the two cases.

It is usually assumed that diffusion in solids obeys the space-time diffusion equation

$$\frac{dc}{dt} = \text{div} D \text{ grad } c \tag{1}$$

where c is the concentration of the diffusing atoms and D is the diffusion coefficient, which usually depends on c. In order to translate D into an atomic constant in a simple case, let us assume that the distance between atomic planes in the direction of diffusion is δ and that the probability that an atom moves from one plane to the next in unit time is d. If n_1 is the number of diffusing atoms per unit area and n_2 is the number in the neighboring plane, the number per unit area that passes from plane 1 to plane 2 in unit time is

$$\frac{dN}{dt} = d(n_1 - n_2). \tag{2}$$

The quantity $n_1 - n_2$ is δ^2 times the concentration gradient in the direction normal to the plane, however, so that Eq. (2) is

$$\frac{dN}{dt} = \delta^2 d\mathbf{r}_1 \cdot \text{grad } c \tag{3}$$

where $\mathbf{r}_1$ is a unit vector normal to the plane. Equation (3) reduces to (1) if we set

$$D = d\delta^2. \tag{4}$$

This method of reasoning can be used to convert D into an atomic constant d, in more complex cases than the one treated here.

It is found experimentally that for fixed concentration D depends upon temperature in the manner

$$D = Ae^{-\frac{\epsilon}{kT}} \tag{5}$$

[1] See the review articles by R. F. MEHL, *Jour. Applied Phys.*, **8**, 174 (1937); R. M. Barrer, *Proc. Phys. Soc.* **52**, 58 (1940).

[2] The radioactive indicator method was first used by G. von Hevesy, W. Seith, and A. Keil (*cf. Z. physik. Chem.*, **37**, 528 (1931); *Z. Physik*, **79**, 197 (1932)).

where both A and ϵ are practically constant. Using equations of the type (4), we may translate A into an atomic constant. Thus, in the case in which (4) is valid, we may write

$$A = a\delta^2$$

where a is the "jumping frequency" for a given atom when kT becomes large compared with ϵ. It is also found experimentally[1] that these frequencies usually are of the order of 10^{13}. Figure 18 shows the dependence of log D on $1/T$ for the diffusion of gold in lead and illustrates a typical case in which Eq. (5) is valid. A number of values[2] of ϵ that are determined from the slopes of curves of this type are given in Table LXXVI.

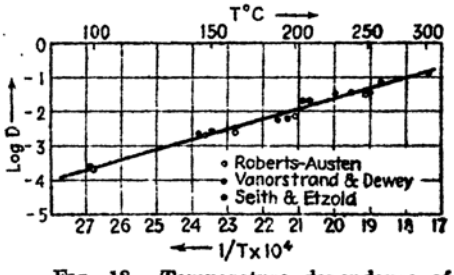

FIG. 18.—Temperature dependence of the diffusion coefficient of gold in lead. (*After Mehl.*)

There are three conceivable simple mechanisms for diffusion of atoms A in a solid AB, namely, the following:

1. Atoms A and B may interchange places, squeezing by one another in the normal lattice.

2. The A atoms may diffuse individually through interstices.

3. The diffusion may take place with the help of vacancies, the atoms moving only into vacant adjacent sites. It may be postulated that in this case the crystal with vacancies is thermodynamically more stable than one without vacancies.

The first mechanism has the disadvantage that if it were valid one might expect the activation energy for the process in which two atoms squeeze by one another to be very high, of the order of the cohesive energy, whereas the values in Table LXXVI are uniformly less than the cohesive energies. For this reason, this process is ordinarily ruled out.

[1] This fact was pointed out by S. Dushman and I. Langmuir, *Phys. Rev.*, **20**, 113 (1922), who suggested that an approximate value of a should be obtained from the relation $a = \epsilon/h$. Since ϵ is of the order of magnitude 10^{-14} erg, the values of a obtained in this way are of the order of magnitude 10^{13}.

[2] Most of these values are taken from footnote 1, p. 494. The values for self-diffusion in copper, gold, silver and bismuth have the following origin.

Cu: J. STEIGMAN, W. SHOCKLEY, and F. C. NIX, *Phys. Rev.*, **56**, 13 (1939).

Au: SAGRUBSKIJ, *Physik. Z. Sowj.*, **12**, 118 (1937); MCKAY, *Trans. Faraday Soc.*, **34**, 845 (1938).

Zn: F. BANKS, H. DAY and P. MILLER (see program Washington Meeting, Am. Phys. Soc., 1940).

Bi: W. SEITH and A. KEIL, *Z. Elektrochem.*, **39**, 538 (1933).

If it does occur, it is easy to understand why a is of the order of magnitude 10^{13}, for this is the magnitude of atomic vibrational frequencies.

The second process should require a smaller activation energy than the first only in crystals that have interstitial sites sufficiently large to accommodate the atoms A. Since the interstices of metals forming substitutional alloys usually are much smaller than the atomic size, it seems probable that this mechanism occurs only in interstitial alloys, such as iron carbide and nitride, and in semi-conductors, such as zinc oxide, that have interstitial atoms (*cf.* Sec. 112). We saw, in the case of zinc oxide, that the fraction of interstitial atoms f is governed by an equation of the type

$$f = n_{O_2}^{-\frac{1}{2}} B' e^{-\frac{\epsilon''}{kT}} \tag{6}$$

where n_{O_2} is the density of oxygen in the surrounding vapor and B' is a constant. If the probability that one of these atoms jumps is

$$\tilde{\nu}_i = \tilde{\nu}' e^{-\frac{\epsilon'}{kT}}, \tag{7}$$

TABLE LXXVI.—ACTIVATION ENERGIES FOR METALLIC DIFFUSION

Solvent	Solute	Activation energy, ev
Cu	Cu	2.5
	Zn (9.58%)	1.8
	Zn (29.08%)	1.8
	Sn (10%)	1.7
Zn	Zn	0.75
Pb	Pb	1.2
	Sn	1.04
	Tl	0.91
	Bi	0.81
	Cd	0.78
	Ag	0.66
	Au	0.57
Ag	Au	2.5
Au	Ag	3.0
Bi	Bi	⊥1.3 ∥6.1
Fe	C	1.6
	N	1.5

the atomic diffusion coefficient d should be

$$d = \bar{\nu}^i n_{0_2}^{-\frac{1}{3}} B' e^{-\frac{\epsilon' + \epsilon''}{kT}}. \tag{8}$$

In this case, both a and ϵ are composite quantities.

One should expect a much smaller value of the activation energy for the third process than for the two others in the case of substitutional alloys.[1] Since the number of vacancies should be less than the total number of atoms in this case, d should be a composite quantity as in Eq. (8). According to the discussion in Sec. 110, the fraction of vacancies f is given by the equation

$$f = e^{-\frac{\epsilon''}{kT}}$$

where ϵ'' is the energy required to remove an atom from an interior site to the surface. Hence,

$$d = \bar{\nu}_\infty^v e^{-\frac{\epsilon' + \epsilon''}{kT}} \tag{9}$$

where $\bar{\nu}_\infty^v e^{-\frac{\epsilon'}{kT}}$ is the probability per unit time that an atom and a vacancy on neighboring sites change places.

It is reasonable to suppose that the third mechanism occurs in substitutional alloys, but this supposition has not been conclusively demonstrated.

We may develop an equation for the jump frequency, using elementary principles of the theory of reaction rates. We shall treat the problem generally enough so that the results are applicable both to diffusing interstitial atoms and to diffusing vacancies although we shall refer to the diffusing particle as an interstitial atom.

As the atom moves from one equilibrium position to another, the energy of the system rises through a maximum at the saddle point of the barrier between minima. According to the theory of reaction rates, we may regard the jumping process as an act in which the system is thermally excited to the saddle point S through which it then passes. The probability per unit time $\bar{\nu}$ that this process occurs for a given atom is then equal to the rate at which atoms pass through S divided by the total number of interstitial atoms. For simplicity, we shall assume that the energy of the system depends only upon the three positional coordinates of the jumping atom; moreover, we shall assume that the potential is nearly constant for a short distance along the direction of flow

[1] Theoretical work of H. Huntington, in progress, indicates that the activation energy for interstitial diffusion in copper is about three times larger than that for the third process.

through the saddle point. The rate at which the atoms pass through S then is equal to the number of atoms per unit length of S times their mean velocity. As long as only a small fraction of the diffusing atoms are at the saddle point at any one time, the number of atoms n_s per unit length of S is equal to the total number of interstitial atoms n times the ratio of the partition function per unit length of S to the partition function of the interstitial atom at its equilibrium position.

We shall assume that the interstitial atom in an equilibrium position is at rest, for in this book this assumption is usually made in computing the number of interstitial atoms. It is incorrect, since the interstitial atom actually oscillates about an equilibrium position. The error made in this way, however, cancels in taking the product of n and the probability of finding an atom at S.

In addition, we shall assume that the forces acting on an atom in the saddle point are also harmonic in the two directions orthogonal to the direction of flow. If ν_s is the vibrational frequency, the partition function for these 2 degrees of freedom then is

$$f = \left(\frac{1}{1 - e^{-\frac{h\nu_s}{kT}}}\right)^2. \tag{10}$$

We shall be interested primarily in the case in which $h\nu_s$ is much smaller than kT. Then, f is

$$\left(\frac{kT}{h\nu_s}\right)^2. \tag{11}$$

The partition function per unit length in the direction of flow is equal to the partition function for a one-dimensional gas at a point where the potential energy is ϵ_s, where ϵ_s is the height of S above the equilibrium position. This function is

$$\frac{(2\pi MkT)^{\frac{1}{2}}}{h} e^{-\frac{\epsilon_s}{kT}}. \tag{12}$$

Hence, the complete partition function per unit length of the saddle point is

$$f_s = \frac{1}{\alpha}\left(\frac{kT}{h\nu_s}\right)^2 \frac{(2\pi MkT)^{\frac{1}{2}}}{h} e^{-\frac{\epsilon_s}{kT}}, \tag{13}$$

where α is the number of saddle points of height ϵ_s about a given equilibrium position. This number, which should depend upon crystal symmetry as well as upon the type of ions in the lattice, could be as large as forty-eight for a crystal with cubic symmetry.

The mean velocity with which the atoms pass through the saddle point is

$$\bar{v} = \frac{\int_0^\infty e^{-\frac{Mv^2}{2kT}} v dv}{\int_{-\infty}^\infty e^{-\frac{Mv^2}{2kT}} dv} = \left(\frac{kT}{2\pi M}\right)^{\frac{1}{2}}. \tag{14}$$

Hence, the jump frequency $\tilde{\nu}$ is

$$\tilde{\nu} = f_s \bar{v} = \frac{1}{h^3} \frac{(kT)^3}{\alpha \nu_s^2} e^{-\frac{e_i}{kT}}. \tag{15}$$

This equation has the form

$$\tilde{\nu} = \nu_\infty e^{-\frac{e_i}{kT}}$$

where

$$\nu_\infty = \frac{(kT)^3}{\alpha h^3 \nu_s^2}.$$

According to this result, the diffusion coefficient D has the form

$$D = d\delta^2 = \delta^2 \frac{n}{N} \frac{1}{\alpha h^3} \frac{(kT)^3}{\nu_s^2} e^{-\frac{e_i}{kT}}, \tag{16}$$

where n is the number of interstitial atoms or vacancies per unit volume and N is the total number of atoms per unit volume. This equation will be used in Sec. 132.

123. The Phase Boundaries of Alloys.—By applying the principle of minimum free energy, it is possible to derive the equations that determine the phase boundaries of alloys. Let us consider two binary alloy phases α and β of a pair of monatomic metals A and B. The necessary condition that the two phases be in thermodynamical equilibrium evidently is that the free energy of the entire system remain stationary if atoms are taken from one alloy to the other.

We shall assume that there are N_a A atoms and N_b B atoms in the entire system and that the total number N remains fixed when the atoms are taken from one alloy to the other. In addition, it will be assumed that there are n_a A atoms and n_b B atoms in the α phase. Thus, there are $(N_a - n_a)$ A atoms and $(N_b - n_b)$ B atoms in the β phase. The composition of the phases may then be specified by means of the fractions x_α and x_β of A atoms, which are, respectively,

$$x_\alpha = \frac{n_a}{n_a + n_b} \quad \text{and} \quad x_\beta = \frac{N_a - n_a}{N - n_a - n_b}. \tag{1}$$

Now, if $A_\alpha(x)$ is the free energy of a specimen of the α phase that contains N atoms of both types and has composition x and if $A_\beta(x)$ is the

same quantity for the β phase, the total free energy of the system is

$$A = \frac{n_a + n_b}{N} A_\alpha\left(\frac{n_a}{n_a + n_b}\right) + \frac{N - n_a - n_b}{N} A_\beta\left(\frac{N_a - n_a}{N - (n_a + n_b)}\right). \quad (2)$$

Thus, the conditions for equilibrium, which are

$$\frac{\partial A}{\partial n_a} = 0, \qquad \frac{\partial A}{\partial n_b} = 0, \quad (3)$$

lead to the equations

$$\begin{aligned} A_\alpha - A_\beta + (1 - x_\alpha)A_\alpha'(x_\alpha) - (1 - x_\beta)A_\beta'(x_\beta) &= 0, \\ A_\alpha - A_\beta - x_\alpha A_\alpha'(x_\alpha) + x_\beta A_\beta'(x_\beta) &= 0, \end{aligned} \quad (4)$$

in which $A' = \partial A/\partial x$. By subtracting these, we may derive the equation

$$A_\alpha'(x_\alpha) = A_\beta'(x_\beta), \quad (5)$$

which, when substituted in either equation, gives the additional relation

$$A_\alpha' = \frac{A_\alpha - A_\beta}{x_\alpha - x_\beta}. \quad (6)$$

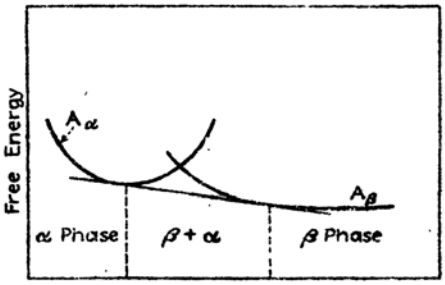

FIG. 19.—Schematic representation of the condition for determining the phase boundaries of alloys.

Equations (5) and (6) state that the boundaries of the α and β phases are determined by the points at which the slopes of the two free-energy curves are equal and have a common tangent (*cf.* Fig. 19). To the left of the point of tangency on the A_α curve, the α phase alone is stable, whereas to the right of the corresponding point on the A_β curve the β phase is stable.

Jones[1] has applied the relations (5) and (6) to the boundaries of the α and β brass types of phase of substitutional alloys that were discussed in Sec. 3. These phases are, respectively, face-centered and body-centered cubic and, as was seen in Sec. 102, are stable for a range of electron-atom ratios near the values for which the zones of the two lattices are filled to the points of highest level density. Jones assumed that all energies except the Fermi energy are practically the same for disordered specimens of the two phases so that the filling of the one-electron levels alone determines the relative energies at absolute zero of temperature. The $n(\epsilon)$ curves for the face-centered and body-centered lattices of the brass (Cu-Zn) system that are determined by the approximate methods

[1] H. JONES, *Proc. Phys. Soc.*, **49**, 243 (1937).

discussed in Sec. 65 are shown in Figs. 20*a* and *b*. The energy difference per atom of the two phases is shown in Fig. 20*c* as a function of the electron-atom ratio n_e. It should be observed that the $n(\epsilon)$ curves are identical to about 6 ev, which corresponds to an electron-atom ratio of about 0.95. The $n(\epsilon)$ curve for the face-centered lattice rises to a peak in the energy range just above this, so that this phase has a lower Fermi energy. The β phase then has its peak, and the relative energy curve changes sign. It is clear that when the composition corresponds to the intercept of the relative energy curve with the n_e axis, that is, when the electron-atom ratio n_e is 1.44, the system would be most stable if it consisted of a quantity of α phase having a lower value of n and a quantity of β phase having a higher value. On the other hand, if n_e is near 1.2, it would be necessary to raise the energy of the α phase a great deal in order to form a small quantity of β phase. Thus, we should expect the α phase to be stable at this point. The actual values of n_e at the phase boundary points, as determined from Eqs. (5) and (6) for the absolute zero of temperature by replacing the free energy by the energies computed from Fig. 20*a*, are

$$n_{e,\alpha} = 1.409,$$
$$n_{e,\beta} = 1.447.$$

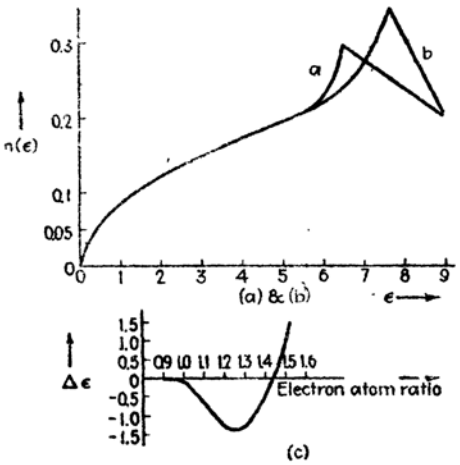

FIG. 20.—*a* and *b* are the $n(\epsilon)$ curves for the face-centered and body-centered structures, respectively. Curve *c* is the relative energy $\Delta\epsilon$ of the two phases as a function of the electron-atom ratio. The energy scales are in electron volts. (*After Jones.*)

As may be seen from Fig. 20*b*, these values lie very close to the point where the relative energy curve intercepts the axis.

Jones extended this work to higher temperature ranges by adding mixing entropy terms such as those considered in the theory of order and disorder. If a given disordered phase has n_a A atoms and n_b B atoms, its mixing entropy is

$$S = k \log \frac{(n_a + n_b)!}{n_a! n_b!}, \tag{7}$$

in which $(n_a + n_b)!/n_a!n_b!$ is the total number of ways of rearranging the A and B atoms among the $n_a + n_b$ sites. When this is expanded by means of Stirling's approximation, it becomes

$$S = -Nk[x \log x + (1 - x) \log (1 - x)] \tag{8}$$

where $N = n_a + n_b$ and x is defined by Eq. (1). Thus, if $E(x)$ is the energy of the N atoms as a function of x,

$$A(x) = E(x) + NkT[x \log x - (1 - x) \log (1 - x)]. \tag{9}$$

Using free-energy functions of this type and $E(x)$ curves obtained from the data of Fig. 20, Jones computed the phase boundaries of the α and β phases of the Cu-Zn and Cu-Al systems as functions of temperature. The observed and calculated curves are shown in Fig. 21. They agree as closely as one might expect in view of the simplifying assumptions made in this work.

Jones has applied similar computations to the liquidus and solidus curves of substitutional alloys, which are briefly described in Sec. 3,

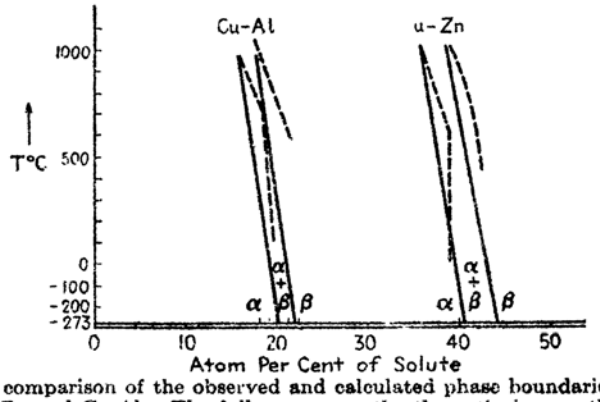

FIG. 21.—A comparison of the observed and calculated phase boundaries of the α and β phases of Cu-Zn and Cu-Al. The full curves are the theoretical ones; the broken lines are experimental. (*After Jones.*)

and has shown that the dependence of these curves upon composition may be adequately explained if the solid phases are assigned free-energy functions of type (9).

124. Order and Disorder in Alloys. *a. Experimental Discussion.*[1]—X-ray diffraction studies of substitutional alloys show in many cases that each type of atom is localized at a definite site in the unit cell, just as the constituents of ionic crystals are localized at definite positions. As the temperature is raised in these cases, the degree of order may decrease, even though the crystalline arrangement is maintained. This decrease is made evident by the fact that it is no longer possible to tell precisely which kind of atom occupies a given site. The order may decrease continuously, as in β brass, or it may undergo an abrupt change, as in Cu_3Au. These cases and others are discussed in Sec. 3, Chap. I. Alloys in which the order changes abruptly usually have an abrupt change in

[1] See the previous discussion in Sec. 3.

heat content at the transition temperature whereas those in which the change is continuous do not, although there may be a discontinuity in specific heat at the point at which all sites become equivalent.[1] The two types of phase change, characterized respectively by Cu_3Au and CuZn, are said to be of the first and second kinds.

Although two-component alloys have been investigated most widely, these are not the only substances in which order and disorder occur. Ketelaar[2] has found, for example, that silver and copper mercuric iodides (Ag_2HgI_4 and Cu_2HgI_4) show complex order and disorder changes which resemble closely those found in Cu_3Au. The low-temperature modifications have the tetragonal structure shown in Fig. 22 in which mercury atoms occupy the eight corners of a nearly cubic cell. The iodine atoms are distributed tetrahedrally about four of the eight corners, forming a face-centered lattice, and the silver or copper atoms are arranged at the centers of the four vertical faces. The iodine atoms do not change their relative positions as the temperature is raised. The metal atoms, however, make an abrupt change, becoming uniformly distributed over the eight corners and six face centers of the cube. It is evident that two of these fourteen sites must be vacant on the average. Hence, the disordering process involves silver atoms, mercury atoms, and vacancies in the ratio 2:1:1. The behavior of the ionic conductivity of Ag_2HgI_4 is shown in Fig. 23.

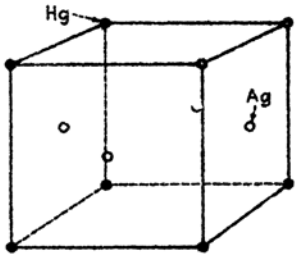

FIG. 22.—The positions of mercury and silver atoms in the ordered, low-temperature phase of Ag_2HgI_4. The iodine atoms, which are not shown, are distributed tetrahedrally about the Hg atoms. In the high-temperature phase the Hg atoms, the Ag atoms, and the vacancies at the centers of the top and bottom faces of the cube become mixed. The low-temperature form is slightly tetragonal; the high-temperature form is cubic.

b. Qualitative Principles.—We shall not devote space to a detailed treatment of the more advanced theories of order and disorder since discussions of these may be found in other writings;[3] however, we shall give a brief discussion of the principles involved and of the simpler theories.

It is clear that the disordered alloy has a higher entropy than the ordered one. If we neglect any difference in the vibrational entropy of the ordered and disordered state, we may estimate the maximum change in mixing entropy that accompanies disordering by computing the

[1] The discontinuous behavior of the elastic constants of Cu_3Au in the vicinity of the ordering temperature has been investigated by S. Siegel, *Phys. Rev.*, **57**, 537 (1940).

[2] J. A. A. KETELAAR, *Z. physik. Chem.*, **26B**, 327 (1934), **30B**, 53 (1935); *Z. Krist.*, **87**, 436 (1934).

[3] See the survey article by F. C. NIX and W. Shockley, *Rev. Modern Phys.*, **10**, 1 (1938).

number of arrangements associated with the completely ordered and disordered states. In the simplest system, namely, that in which there are two types of atom present in equal numbers N, the number of arrangements associated with the ordered state is unity because all atoms of a given type are equivalent. The number of arrangements in the completely disordered state is the number of ways of distributing N atoms among $2N$ sites, namely $(2N)!/(N!)^2$. Hence, the maximum increase in mixing entropy associated with disordering is

$$k \log \frac{(2N)!}{(N!)^2} \cong 2Nk \log 2. \tag{1}$$

A similar calculation may be made for any system.

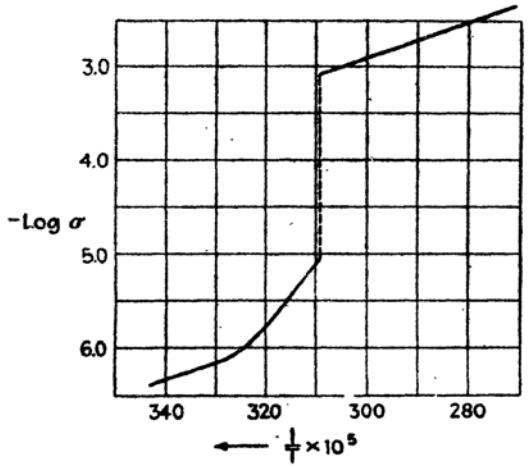

FIG. 23.—The conductivity of Ag_2HgI_4 near the transition temperature. σ is expressed in $ohm^{-1}\ cm^{-1}$. (*After Ketelaar.*)

The energy of the crystal presumably increases as we pass from the ordered to the disordered state, for otherwise the ordered state would not be stable at low temperatures. Hence, the energy versus entropy curve should rise with increasing disorder. Figure 24 shows two possible ways in which this curve may behave. In the first case, the $E(S)$ curve has an inflection point so that a tangent line may be drawn to two parts of the curve. Thus, the entropy, and hence the order, should show an abrupt change at the temperature equal to the slope of this tangent line, and there should be a latent heat, just as in melting. In the second case, the $E(S)$ curve has positive curvature so that there is no discontinuity in order.

The actual behavior of a solid is not necessarily determined by the $E(S)$ curve for disordering alone. It is possible that the vibrational

frequencies of the crystal may decrease in passing from the ordered to the disordered state; the disordered phase then has a higher vibrational entropy than the ordered one at corresponding temperatures. Thus, the ordered and disordered phases may behave like different allotropic phases, and the transition may occur abruptly even though the $E(S)$ curve for disordering alone would predict a gradual decrease of order. The theories of order and disorder that are discussed in the article referred to in footnote 3, page 503, do not yet interpret the experimental material in a quantitative way. The reason for this lack is, of course, that the complete entropy and energy changes which accompany disordering are very difficult to compute, just as are the changes of these quantities

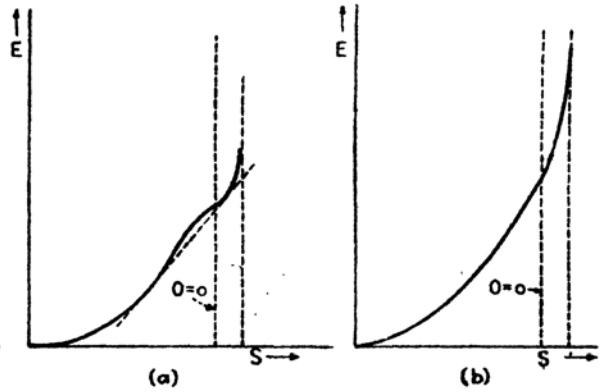

FIG. 24.—Two possible behaviors of the $E(S)$ curves for order-disorder changes. In case (a) there is an inflection point, whence long-distance order may appear and disappear abruptly with a latent heat. In the second case there is no inflection point and the transition is continuous. The curvature changes at the entropy corresponding to zero long-distance order ($O = 0$), so that there is a discontinuity in specific heat. The right-hand vertical line corresponds to the entropy for zero short-distance order in each case.

during melting. The results of this work, however, leave little doubt that the qualitative principles are now understood.

c. Definitions of Order.—There are two interesting types of order, namely, long-distance order, which measures the extent to which the positions of atoms in different cells of the lattice are correlated, and short-distance order, which measures the extent to which the positions of neighboring atoms are correlated. The first type of order is responsible for the Bragg reflection of X rays by lattices; the second is responsible for the diffraction rings of liquids and glasses. Following Bethe,[1] we may define these two types of order mathematically in the following way.

When long-distance order is discussed, the lattice may be divided into as many types of site as are occupied by different atoms in the completely ordered state. Thus, there are two types of site in β brass and in

[1] H. BETHE, *Proc. Roy. Soc.*, **150**, 552 (1935).

Cu_3Au, and there are three types in Ag_2HgI_4. In crystals in which two types of site are present in equal numbers, the long-distance order O is defined as the difference between the probability that an atom will occupy its own kind of site and the probability that the other kind of atom will occupy this site. Thus,

$$O = P_\alpha(A) - P_\alpha(B) \tag{2}$$

where $P_\alpha(A)$ is the probability that an A atom occupies its own site and $P_\alpha(B)$ is the probability that a B atom does. The four probabilities $P_\alpha(A)$, $P_\alpha(B)$, $P_\beta(B)$, $P_\beta(A)$ obviously satisfy the equations

$$\begin{aligned} P_\alpha(A) + P_\beta(A) &= 1, & P_\alpha(A) + P_\alpha(B) &= 1, \\ P_\alpha(B) + P_\beta(B) &= 1 & P_\beta(A) + P_\beta(B) &= 1, \end{aligned} \tag{3}$$

which shows that there is only one independent P. In the case of Cu_3Au in which there are three times as many A atoms as B atoms the long-distance order may be defined by the equation

$$O = P_\alpha(A) - 3P_\alpha(B). \tag{4}$$

The interrelations between the P are

$$\begin{aligned} P_\alpha(A) + P_\alpha(B) &= 1, & P_\beta(B) + P_\beta(A) &= 1, \\ P_\beta(B) + 3P_\alpha(B) &= 1, & P_\alpha(A) + \tfrac{1}{3}P_\beta(A) &= 1, \end{aligned} \tag{5}$$

so that again there is only one independent P. It is clear that the order parameters defined by Eqs. (2) and (4) are unity in the state of highest long-distance order and are zero when there is no long-distance order. This convenient fact is the principal reason for selecting these combinations of the P, for any one of them could serve as a measure of long-distance order.

Long-range order is not so easy to define in systems such as Ag_2HgI_4 that have three kinds of site, for there is then more than one independent P. Let us consider Ag_2HgI_4 as an example, designating the nine probabilities by

$$P_{A_\alpha}(\mathrm{Ag}), P_{A_\alpha}(\mathrm{Hg}), P_{A_\alpha}(V), \cdots, P_V(V)$$

where the subscripts refer to sites and V is the symbol for a vacancy. These probabilities are interrelated by the following six equations:

$$\left.\begin{aligned} P_{A_\alpha}(\mathrm{Ag}) + P_{A_\alpha}(\mathrm{Hg}) + P_{A_\alpha}(V) &= 1. \\ P_{H_\alpha}(\mathrm{Ag}) + P_{H_\alpha}(\mathrm{Hg}) + P_{H_\alpha}(V) &= 1. \\ P_V(\mathrm{Ag}) + P_V(\mathrm{Hg}) + P_V(V) &= 1. \end{aligned}\right\} \tag{6}$$

$$\left.\begin{aligned} P_{A_\alpha}(\mathrm{Ag}) + \tfrac{1}{3}P_{H_\alpha}(\mathrm{Ag}) + \tfrac{1}{2}P_V(\mathrm{Ag}) &= 1. \\ 2P_{A_\alpha}(\mathrm{Hg}) + P_{H_\alpha}(\mathrm{Hg}) + P_V(\mathrm{Hg}) &= 1. \\ 2P_{A_\alpha}(V) + P_{H_\alpha}(V) + P_V(V) &= 1. \end{aligned}\right\} \tag{7}$$

Only five of these equations are independent so that it is necessary to know four of the P before the average distribution of atoms in the unit cell can be given. Thus, it is not possible to express the degree of long-distance order in terms of a single parameter as it was in the preceding cases.

Short-distance order is also easy to define in two-component alloys. In the completely ordered state, a given kind of atom has a definite arrangement of atoms in the neighboring sites. We may specify the short-distance order in any state by giving the difference σ between the fraction of atoms in a shell surrounding a given atom that have the same arrangement as in the perfectly ordered state and the fraction of atoms that have not. The size of the cell may be varied to suit the case at hand. The quantity σ evidently is equal to unity in the completely ordered state and to zero in the completely random state.

The concept of long-distance order was introduced into the theory of order and disorder first because it is measured directly by ordinary X-ray diffraction data. Bethe[1] pointed out, however, that short-range order actually is a more fundamental quantity since the interatomic energy is determined primarily by it.

d. Elementary Theories of Order and Disorder.—The earliest theory of order and disorder was developed by Gorsky[2] and applied to two-component systems of the type AB. However, an equivalent theory developed later by Bragg and Williams[3] undoubtedly is responsible for the more recent interest in the subject. In these earlier theories, it was assumed that the long-distance order O existing at temperature T is determined by the energy V required to take an atom from an ordered position to a disordered one. This assumption is expressed by the equation

$$O = O(V,T). \tag{8}$$

It was also assumed that V is a function of the long-distance order so that there is a second relation

$$V = V(O,T). \tag{9}$$

The relations (8) and (9) are sufficient to determine O as a function of T alone.

Gorsky derived explicit forms for Eqs. (8) and (9) in the case of an alloy of composition AB. Since there are thermal fluctuations, there is a finite probability that each atom will leave its position, diffuse

[1] *Ibid.*

[2] W. GORSKY, *Z. Physik*, **50**, 64 (1928).

[3] W. L. BRAGG and E. J. WILLIAMS, *Proc. Roy. Soc.*, **145**, 699 (1934); **151**, 540 (1935).

through the lattice, and fall into a vacant site. Gorsky assumed that the probabilities per unit time of A and B atoms leaving their own sites are equal as are the probabilities that they will leave improper sites. We shall designate these probabilities by l_p and l_i, respectively. In addition, he assumed that the probabilities that the free atoms will fall into any vacant proper sites are equal, as are the probabilities that they will fall into improper sites. We shall designate these by f_p and f_i, respectively. If N is the total number of atoms of a given kind, n is the number of vacant sites, and α is the fraction of atoms on proper sites, the equilibrium equations for proper and improper sites are

$$\begin{aligned} N\alpha l_p &= n^2 f_p, \\ N(1-\alpha) l_i &= n^2 f_i. \end{aligned} \tag{10}$$

Solving these equations and using the relation

$$O = 2\alpha - 1, \tag{11}$$

we obtain

$$O = \frac{1 - (f_i l_p / f_p l_i)}{1 + (f_i l_p / f_p l_i)}. \tag{12}$$

Gorsky assumed that f_p and f_i are not strongly temperature-dependent and that they are nearly equal so that their ratio is practically unity. Since l_p and l_i are temperature-dependent, he assumed that their ratio is

$$\frac{l_p}{l_i} = \frac{e^{-\frac{\epsilon_p}{kT}}}{e^{-\frac{\epsilon_i}{kT}}}. \tag{13}$$

Using these relations, we find

$$O = \tanh \frac{\epsilon_p - \epsilon_i}{2kT}. \tag{14}$$

Evidently, $\epsilon_p - \epsilon_i$ is proportional to V, the energy required to remove an atom from an ordered site to a disordered one. Hence, (14) is

$$O = \tanh \frac{\beta V}{kT} \tag{15}$$

where β is a proportionality factor. This equation has the form (8).

Were V independent of O, O would decrease slowly with increasing temperature and would approach zero when T becomes infinite. It is clear that V must depend upon order, however, for there is no difference between proper and improper sites in the completely disordered state. Hence, Gorsky assumed that V varies linearly with O in the manner

$$V = V_0 O \tag{16}$$

where V_0 is a constant. This equation corresponds to (9).

The solution of Eqs. (15) and (16) is given by the equation

$$O = \tanh \frac{\beta V_0 O}{kT}. \tag{17}$$

This has two roots, namely, the root $O = 0$, which is independent of temperature, and a root which is unity when T is zero and zero when

$$T_c = \frac{\beta V_0}{2k} \tag{18}$$

and varies continuously in between (*cf.* Fig. 25). The relation described by the second root agrees qualitatively with that observed in β brass.

One obvious objection to the details of Gorsky's treatment is the fact that he assumes a questionable diffusion process in deriving Eq. (15).

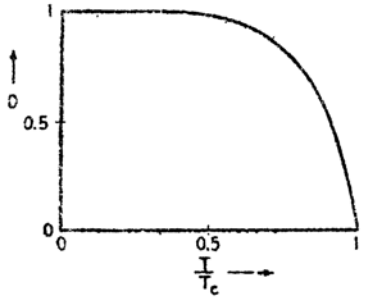

FIG. 25.—The $O(T)$ curve obtained from Gorsky's theory of order and disorder.

Bragg and Williams[1] modified the principles used in Gorsky's treatment and extended the field of application of the method. In earlier work, they introduced rate processes in order to derive equations equivalent to (15). Williams[2] subsequently showed that this procedure is not necessary and that the equations may be derived on the basis of statistical mechanics. We shall discuss their work from the later standpoint.

Let us consider a case in which there are n_a A atoms and a sites and n_b B atoms and b sites. Generalizing Eqs. (2) and (4), we may define the long-range order by the equation

$$\begin{aligned} O &= P_a(A) - \frac{n_a}{n_b} P_a(B) = P_a(A)\left(1 + \frac{n_a}{n_b}\right) - \frac{n_a}{n_b} \\ &= p\left(1 + \frac{x}{1-x}\right) - \frac{x}{1-x} = \frac{p-x}{1-x} \end{aligned} \tag{19}$$

where, for simplicity, we have replaced $P_a(A)$ by the symbol p, and $\frac{n_a}{n_a + n_b}$, the fraction of a sites, by x. Let us now compute the entropy associated with a given value of order. The $xN'p$ A atoms in the xN' a positions ($N' = n_a + n_b$) may be distributed in

$$n_1 = \frac{(xN')!}{(xN' - xN'p)!(xN'p)!} \tag{20}$$

[1] BRAGG and WILLIAMS, *op. cit.*

[2] E. J. WILLIAMS, *Proc. Roy. Soc.*, **152**, 231 (1935). See also R. H. FOWLER, *op. cit.*

independent ways, whereas the $(xN' - xN'p)$ A atoms in the $(N' - xN')$ b sites may be distributed in

$$n_2 = \frac{(N' - xN')!}{(N' - 2xN' + xN'p)!(xN' - xN'p)!} \tag{21}$$

ways. Since the total number of arrangements is the product of n_1 and n_2, the entropy[1] is

$$\begin{aligned} S &= k \log n_1 n_2 \\ &= C - N'k[x(1 - p) \log (1 - p) + xp \log p + \\ &\quad (1 - 2x + xp) \log (1 - 2x + xp) + (x - xp) \log (x - xp)] \end{aligned} \tag{22}$$

where C is independent of p.

The energy of the disordered state relative to the ordered one is

$$E = VN'x(1 - p) \tag{23}$$

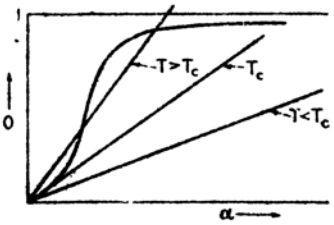

FIG. 26.—$O(\alpha)$ curve for $x = \frac{1}{4}$. As the temperature is raised from absolute zero the $\alpha = V/kT$ lines become tangent at the origin before the other intercept has reached the origin.

where $N'x(1 - p)$ is the number of atoms that have been moved from ordered to disordered positions. The value of p for which the free energy $E - TS$ computed from (22) and (23) is a minimum satisfies the equation

$$\log \frac{(1 - p)^2 x}{p(1 - 2x + xp)} = -\frac{V}{kT} \tag{24}$$

If we replace p by O, using Eq. (19) we obtain an equation connecting O and V, namely,

$$O = 1 - \frac{[4x(1 - x)(e^\alpha - 1) + 1]^{\frac{1}{2}} - 1}{2x(1 - x)(e^\alpha - 1)} \tag{25}$$

where $\alpha = V/kT$. This equation reduces to Gorsky's equation (15) when $x = \frac{1}{2}$, a fact showing that β should be $\frac{1}{4}$. The expansion of Eq. (25) in the neighborhood of $\alpha = 0$ is

$$O(\alpha) = x(1 - x)\alpha + \tfrac{1}{2}x(1 - x)(1 - 2x)^2\alpha^2 + \cdots. \tag{26}$$

Hence, S usually starts out with a finite slope and positive curvature, the exceptional case being $x = \frac{1}{2}$. If it is assumed that the relation (9) is

$$V = V_0 O,$$

as Gorsky did, the transition is of the first kind in all cases, except that in which $x = \frac{1}{2}$. This follows from the fact, illustrated in Fig. 26, that the

[1] In this computation, only the mixing entropy is considered. Actually, the change in vibrational entropy should be included as well.

$V(O)$ line becomes tangent to the $O(V)$ line at the origin before the other intercept approaches the origin when the $O(V)$ curve has positive curvature.

e. Bethe's Treatment of the Problem.—Bethe provided a new and important approach to the problem of order and disorder by pointing out that the ordering energy and entropy are determined primarily by the short-range order since neutral atoms interact with short-range forces. Thus, the equation of state may be determined by considering short-range order, and the long-distance order may be obtained as a by-product. In addition to recognizing this principle, Bethe developed an approximate method for computing the partition function of the system. Discussions of this and of subsequent theoretical work may be found in the review article listed in footnote 3, page 503.

125. Free Rotation in Crystals. *a. Experimental Survey.*—The specific-heat curves of molecular solids frequently show peaks resembling those observed during order-disorder transitions in alloys. Two interpretations of these peaks have been given in the theoretical development of the subject, namely, the hypothesis due to Pauling[1] that the peaks accompany the onset of free molecular rotation and the hypothesis due to Frenkel[2] that the molecules undergo only torsional oscillations both above and below the transition temperature and that they have less relative orientation above the transition than below. At least in the case of ammonium chloride, which has been investigated very thoroughly by Lawson,[3] the evidence seems to be in favor of Frenkel's hypothesis, as we shall see below. The observed cases may be classified as follows:

1. Nonpolar molecular crystals, such as CH_4, N_2, O_2.
2. Ammonium salts.
3. Polar molecular crystals.

We shall discuss these categorically.

1. *Nonpolar cases.*—Although carbon atoms of solid methane form a face-centered lattice below 89°K, there is no direct evidence concerning the position of the hydrogen atoms. The specific-heat curve possesses the changes, shown in Fig. 80, Chap. I, near 20°K, but these are not accompanied by the appearance of a latent heat. As the temperature is raised through this transition region, the molar volume increases abruptly from 30.57 to 36.65 cm^3. There is no other obvious change in crystal structure during the transition. It is assumed, however, that the hydrogen atoms are localized below the transition temperature and are not localized above it.

[1] L. PAULING, *Phys. Rev.*, **36**, 430 (1930).
[2] J. FRENKEL, *Acta Physicochemica*, **3**, 23 (1935).
[3] A. W. LAWSON, *Phys. Rev.*, **57**, 417 (1940).

Solid oxygen and nitrogen seem to possess similar transitions at 23.7° and 35.4°K, respectively. The experimental work indicates that there are large hysteresis effects associated with the transition in these cases, so that the results are not so definite as for methane.

2. *Ammonium salts.*—A number of ionic crystals that contain the NH_4 radical, such as the ammonium halides, ammonium sulfate, and ammonium nitrate, have specific-heat curves that show anomalies similar to those observed in methane. The curve for ammonium chloride is shown in Fig. 69 of Chap. I. As a result of a very careful set of experiments, Lawson has shown in this case that the specific heat at fixed volume does not exhibit nearly so high a peak as the specific heat at constant pressure and that C_V is $9R$ above the transition temperature, corresponding to torsional oscillations of the molecules rather than free rotation. Thus his results support Frenkel's hypothesis rather than Pauling's in this case. It seems likely that Frenkel's picture is also valid in the other ammonium salts and probably in solids of polar molecules, but it does not appear safe to draw conclusions concerning other cases.

3. *Polar molecular crystals.*—Many crystals that are composed of polar molecules, such as solid hydrogen chloride, hydrogen iodide, and hydrogen sulfide, behave in a way similar to the substances already mentioned and yet show important differences. For example, hydrogen chloride forms a cubic crystal above 98.8°K in which the chlorine nuclei are localized in a face-centered cubic lattice. Since this fact clearly means that the molecules are not parallel, we may safely assume that they are more randomly oriented. The lattice changes abruptly to a tetragonal face-centered form at 98.8°K with the appearance of a latent heat. We may conclude that the molecules have higher relative orientation in the low-temperature form of the substance. Apparently, the intermolecular forces and lattice frequencies are sufficiently different in the two states that the crystal behaves as though it were undergoing an allotropic phase change.

Hydrogen bromide and iodide behave more nearly like nonpolar crystals since they do not exhibit a latent heat during the transition; however, their specific-heat curves have very large discontinuities.

b. Pauling's Theory and Fowler's Extension.—Pauling's hypothesis was treated in a semiquantitative manner by Fowler. Since this work resembles that on order and disorder discussed in the previous section, we shall discuss it briefly. Pauling assumed that the potential energy of a molecule in a lattice depends upon its angular orientation relative to the crystallographic axes. Let us consider a lattice of nonpolar diatomic molecules and specify the position of a molecule relative to the orientation for minimum energy by a polar angle θ and an azimuthal angle ϕ. When ϕ is fixed, we may expect that the energy varies with

θ in the manner shown in Fig. 27, the direction $\theta = \pi$ being equivalent to $\theta = 0$. If V_0 is large enough, the lowest energy levels of the molecule E_i correspond to states of oscillation about the equilibrium orientation so that the molecules should not rotate at very low temperatures. They should rotate, however, at sufficiently high temperatures. Pauling realized that the height of the potential-energy curve depends upon the amount of rotation of the other molecules, for otherwise the specific-heat curve would not be discontinuous.

It is clear that the principles embodied in Pauling's picture of the onset of free rotation are the same as those used to explain the order-disorder transitions in alloys. This was first pointed out by Fowler[1] who applied the equivalent of a Bragg-Williams approximation to Pauling's theory in the case of a lattice of polar diatomic molecules. He assumed that the aligning potential may be expressed in the form

$$V = -V_0 \cos \theta \tag{1}$$

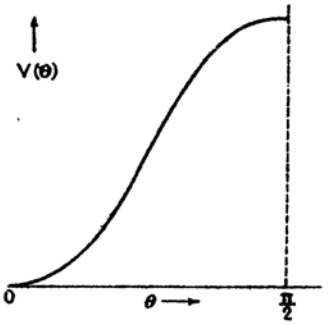

FIG. 27.—The variation of $V(\theta)$ as a function of θ for a non-polar diatomic molecule. The equilibrium position is $\theta = 0$.

and that there are enough negative energy levels to justify the use of classical mechanics when one is computing the partition function near the transition temperature. The partition function then is

$$\begin{aligned} f(T) &= \frac{1}{h^2}\int e^{\frac{-\frac{1}{2I}\left(p_\theta^2+\frac{p_\varphi^2}{\sin^2\theta}\right)+V_0\cos\theta}{kT}} dp_\theta dp_\varphi \sin\theta d\theta d\varphi \\ &= \frac{2I}{h^2}\frac{k^2T^2}{V_0}\sinh\frac{V_0}{kT}. \end{aligned} \tag{2}$$

Thus the specific heat is

$$C_V = Nk\left[2 - \left(\frac{V_0}{kT\sinh\frac{V_0}{kT}}\right)^2\right]. \tag{3}$$

Now, V_0 should depend upon temperature because it is affected by the prevailing degree of rotation, which is a temperature-dependent quantity. In a treatment of the present problem that is closely patterned after the Bragg and Williams treatment of order and disorder, the degree of rotation R would be defined in a physically reasonable way; it would

[1] R. H. FOWLER, *Proc. Roy. Soc.*, **149**, 1 (1935); see also *Statistical Mechanics* Cambridge University Press, 1936).

then be assumed that V_0 depends upon this variable in some explicit manner. This equation and Eq. (2) would then be analogous to Eqs. (8) and (9) of the preceding section and would lead to a relation between the degree of rotation and temperature. In this scheme, different types of transition could be treated by varying the relation between V_0 and the degree of rotation. Instead, Fowler used a fixed relation between V_0 and R and treated different transition-types by taking different definitions of R. We shall discuss two of his cases.

In the first case, he defined the nonrotating molecules as those satisfying the relation

$$\frac{1}{2I}\left(p_\theta^2 + \frac{p_\varphi^2}{\sin^2\theta}\right) < \beta V_0 \tag{4}$$

where β is an adjustable parameter. The molecules specified by Eq. (4) evidently have kinetic energy less than βW for any angular orientation. The fraction R of molecules that are rotating is then given by the equation

$$R = \frac{f_0}{f} \tag{5}$$

where f is the partition function (2) and

$$\begin{aligned} f_0 &= \frac{2\pi}{h^2}\int_0^\pi e^{\frac{V_0\cos\theta}{kT}} \int_{(p_\theta^2 + p_\varphi^2/\sin^2\theta) > 2I\beta V_0} e^{-\frac{p_\theta^2 + p_\varphi^2/\sin^2\theta}{2IkT}} dp_\theta dp_\varphi \\ &= \frac{2IkT}{h^2}\frac{kT}{V_0} e^{-\frac{\beta V_0}{kT}} \sinh\frac{V_0}{kT}. \end{aligned} \tag{6}$$

Thus,

$$R = e^{-\frac{\beta V_0}{kT}} \tag{7}$$

For simplicity, the dependence of V_0 on R was taken as

$$V_0 = V_0'(1 - R) \tag{8}$$

where V_0' is a constant. Equations (7) and (8) determine the relation between R and temperature. It is easily seen that R is unity at

$$T_c = \frac{\beta V_0}{k}$$

and that

$$R = 1 - \frac{2T}{T_c}\left(1 - \frac{T}{T_c}\right)$$

near the transition point. The specific heat below T_c is

$$C_v = Nk\left(2 - \frac{x^2}{\sinh^2 x}\right) + N_0 V_0 \frac{dR}{dT}\left(\frac{\cosh x \sinh x - x}{\sinh^2 x}\right)$$

where

$$x = \frac{V_0(1 - R)}{kT},$$

and is Nk above T_c. Moreover, the specific heat is continuous at T in this case, although it has the maximum shown in Fig. 28 below T_c.

Fowler was able to alter the definition of order in such a way as to obtain a more abrupt change. If it is assumed that the nonrotating

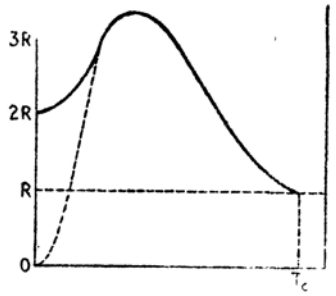

FIG. 28.—The type of molar heat curve obtained from Eq. (3). Above T_c the value is R, as for diatomic molecules. The full line corresponds to the classical case treated by Fowler. The broken line represents the effect of quantum mechanical modification.

molecules satisfy the relation

$$\frac{1}{2I}\left(p_\theta^2 + \frac{p_\varphi^2}{\sin^2\theta}\right) < \frac{V_0}{2}(1 + \cos\theta)$$

instead of the relation (4), it is found that

$$1 - R = \tanh\frac{V_0}{2kT},$$

which is analogous to Gorsky's equation of the preceding section. When coupled with Eq. (7), this relation leads to a discontinuous specific-heat curve, as in the case of alloys. It is possible to obtain transitions of the first kind in a similar way.

Note: The topics of nucleation and rates of simple phase changes in solids, which we have omitted for reasons of space, should properly be included in this chapter. A discussion of these topics that is in accord with the presentation of the preceding sections has been given by R. Becker, *Ann. Physik*, **32**, 128 (1938). Becker shows that many of the facts concerning the rates of simple phase changes may be explained semiquantitatively on the assumption that the energy of the surfaces of misfit between the new and the old phase is such that only relatively large nuclei are stable.

CHAPTER XV

THEORY OF CONDUCTIVITY

In the present chapter, we shall be interested in three types of conductivity, namely, metallic conductivity, ionic conductivity, and photoconductivity. The first of these was discussed in Chap. IV on the basis of the free-electron gas model and will be redeveloped in the first part of this chapter following a method that was first used by Houston and Bloch. The two other topics will be discussed in subsequent parts of the chapter.

A. METALLIC CONDUCTIVITY

126. Summary of Older Equations.—The Lorentz-Sommerfeld theory of metallic conduction is based upon Boltzmann's equation of state

$$\mathbf{v} \cdot \text{grad}_r f + \mathbf{a} \cdot \text{grad}_v f = b - a \tag{1}$$

where $\mathbf{v}$ is the electronic velocity, $\mathbf{a}$ is the electronic acceleration,

$$\text{grad}_r = \mathbf{i}\frac{\partial}{\partial x} + \mathbf{j}\frac{\partial}{\partial y} + \mathbf{k}\frac{\partial}{\partial z},$$

$$\text{grad}_v = \mathbf{i}\frac{\partial}{\partial v_x} + \mathbf{j}\frac{\partial}{\partial v_y} + \mathbf{k}\frac{\partial}{\partial v_z},$$

f is the statistical distribution function, which gives the number of particles per unit volume having velocity v_x, v_y, v_z, and a and b are collision terms. This equation was derived in Sec. 31 and was solved on the assumption that f has the form

$$f = f_0 + v_x\chi(v) \tag{1a}$$

where f_0 is the distribution function in the absence of a field and χ is an undetermined function that is small compared with f_0. In addition, the quantity $b - a$, which gives the difference between the numbers of particles entering and leaving a unit volume of phase space because of collisions, was computed on the assumption that the electrons make elastic collisions with the ions of the lattice. It was found to have the value

$$b - a = -\frac{v_x v\chi(v)}{l_0} \tag{2}$$

where l_0 is the mean free path, which is assumed to be independent of

velocity. If f_0 is the Maxwell-Boltzmann distribution function

$$Ae^{-\frac{\epsilon}{kT}}$$

where A is a constant, the conductivity σ_M is

$$\sigma_M = \frac{4}{3}\frac{n_f l_0 e^2}{\sqrt{2\pi m^* kT}} \tag{3}$$

where n_f is the number of free electrons per unit volume, etc. [*cf.* Eq. (5), Sec. 36]. Since the mean velocity $\bar{v}_M$ in Maxwell-Boltzmann statistics is

$$4\sqrt{\frac{kT}{2\pi m^*}}, \tag{4}$$

Eq. (3) may be placed in the form

$$\sigma_M = \frac{n_f l_0 e^2 \bar{v}_M}{3kT}. \tag{5}$$

On the other hand, if f_0 is the Fermi-Dirac distribution function

$$A'\frac{1}{e^{\frac{\epsilon-\epsilon_0'}{kT}}+1}$$

σ_F is

$$\sigma_F = \frac{n_0 l(\epsilon_0') e^2}{m^* v(\epsilon_0')} \tag{6}$$

[*cf.* Eq. (13), Sec. 32], where $v(\epsilon_0')$ is the velocity of the electrons at the top of the filled band.

Equation (3) gives the proper order of magnitude for the conductivity at room temperature if l_0 is taken as the interatomic distance and if n_f is the total number of electrons per unit volume. The temperature dependence is wrong, however, for the observed conductivity varies as $1/T$ near room temperature.

Equation (6) is incorrect if l_0 is given the same value as in the preceding case because $v(\epsilon_0')$ is between ten and one hundred times larger than $\sqrt{kT/m^*}$, if m^* is the electronic mass. Moreover, the temperature dependence is also wrong. In order to justify the use of this equation, which is more reasonable than (3) since electrons actually obey the Pauli principle, it is necessary to assume that l is temperature-dependent and at room temperature is between ten and one hundred times larger than the interatomic distance. It must also be assumed that l approaches infinity at low temperatures in order to explain the observed increase in conductivity with decreasing temperature (*cf.* Fig. 3). This type of temperature dependence would imply, however, that the assumptions going into the derivation of Eq. (2) are also in error.

Houston[1] and Bloch[2] reopened the problem of metallic conductivity by investigating the way in which electrons interact with a crystal lattice on the basis of quantum mechanics. We shall discuss this work and subsequent refinements in the next section. It will be seen that inelastic electron-lattice collisions are of primary importance in determining the resistance; however, the amount of energy given to the lattice by the electrons is small, so that Sommerfeld's equation (6) is not badly in error.

127. The Collisions between Electrons and Lattice Vibrations in Monovalent Metals[A].—Houston[1] first pointed out that the mean free path of an electron in a perfect nonoscillating lattice should be infinite. This is very easy to see in the Bloch scheme; for then the one-electron functions have the form

$$\psi_{\mathbf{k}} = \chi_{\mathbf{k}} e^{2\pi i \mathbf{k}\cdot\mathbf{r}},$$

and the velocity of the electron in a given state is

$$\mathbf{v} = \text{grad}_{\mathbf{k}}\, \epsilon(\mathbf{k})/h.$$

In the absence of any perturbation, an electron should continue in this state indefinitely.

An ordinary metal does not satisfy these ideal conditions for two reasons: (1) Its lattice is undergoing thermal oscillations, and (2) it usually contains imperfections, such as impurities and lattice defects. Both these effects may scatter electrons and thus make the mean free path finite.

The temperature oscillations should decrease with decreasing temperature and become very small at absolute zero. This fact provides a satisfactory qualitative explanation of the great rise in conductivity at low temperatures. The imperfections, on the other hand, should not be affected appreciably by decreasing temperature and should account for the residual resistance at low temperatures. Moreover, since the imperfections should depend upon the previous history of a specimen, we should expect the residual resistance to vary from specimen to specimen, as is observed.

From a wave standpoint, we may say that the atoms of a perfect lattice scatter electrons coherently, that is, in a manner that resembles the Laue diffraction of X rays. Hence, before an electron can be scattered in a perfect lattice it must occupy a level at the boundary of a zone, and the level to which it can jump must be vacant. These conditions are not ordinarily satisfied by an appreciable fraction of the conduction electrons. We shall see below that the scattering due to thermal vibrations may be regarded as the analogous coherent scattering by a lattice

[1] W. V. HOUSTON, *Z. Physik*, **48**, 449 (1928); *Phys. Rev.*, **34**, 279 (1929).
[2] F. BLOCH, *Z. Physik*, **52**, 555 (1928); **59**, 208 (1930).

which is periodically deformed by a vibrational wave, the distorted crystal behaving like a grating with a grating constant equal to the wave length of the lattice wave. Since this type of scattering is also limited by Laue conditions, a given vibrational mode can deflect a given electron only through definite angles. It is generally assumed that the temperature-independent scattering which gives rise to residual resistance is essentially incoherent, that is, that the scattering centers are arranged so haphazardly that they may be treated as though independent of one another. We shall discuss this in more detail in Sec. 130.

We shall devote the rest of this section to a quantitative discussion of the scattering of electrons by lattice vibrations. All quantitative treatments of this topic have been simplified by means of the assumption that the electronic energy depends only upon $k = \sqrt{k_x^2 + k_y^2 + k_z^2}$, the scalar wave number. This condition is closely satisfied in the monovalent metals, and thus the discussion of the present section should apply most nearly to them.

The differences between the various treatments of the problem of electron scattering lie in the different assumptions that have been made regarding the interaction between the electrons and the lattice. Let us consider a simple monatomic metal containing N atoms and designate the equilibrium positions of the atoms by the variables

$$\mathbf{r}(p) = p_1\mathbf{v}_1 + p_2\mathbf{v}_2 + p_3\mathbf{v}_3 \tag{1}$$

where the p are integers and the $\mathbf{v}$ are primitive translations. We shall designate the displacement of this atom from its equilibrium position by $\mathbf{R}(p)$. In the quadratic approximation, $\mathbf{R}$ may be expressed in the form

$$\mathbf{R}(p) = \frac{1}{\sqrt{N}} \sum_{t,\sigma} \frac{a_t(\sigma)}{\sqrt{M}} \xi_t(\sigma) e^{2\pi i \sigma \cdot \mathbf{r}(p)} \tag{2}$$

[*cf.* Eq. (4), Sec. 118], where the a are the complex amplitudes and the ξ are the unit polarization vectors of the normal modes, the σ are the wave-number vectors, which extend over the N values in a single zone, and M is the atomic mass. Since each atom is a center of symmetry in our simple lattice and $\mathbf{R}(p)$ is real, the ξ are real vectors and

$$a_t(\sigma) = a_t(-\sigma).$$

As we have seen in Sec. 22 it is convenient to define real amplitudes $\alpha_t(\sigma)$ in terms of the a by means of the equations

$$\left.\begin{aligned} \alpha_t(\sigma) &= \frac{a_t(\sigma) + a_t^*(\sigma)}{\sqrt{2}}, \\ \alpha_t(-\sigma) &= \frac{a_t(\sigma) - a_t^*(\sigma)}{\sqrt{2}i}. \end{aligned}\right\} \tag{3}$$

a. The Perturbing Potential.—In the earliest work on the quantum theory of conductivity by Bloch,[1] Brillouin[2] and Bethe,[3] it was assumed, for convenience, that as the ions move the electronic charge is deformed in such a way that the potential of an electron at the point $\mathbf{r}'$ in the deformed lattice is the same as that at the point $\mathbf{r}$ in the undeformed one. Here $\mathbf{r}$ and $\mathbf{r}'$ are connected by the equation

$$\mathbf{r}' = \mathbf{r} + \mathbf{R}(\mathbf{r}) \tag{4}$$

where $\mathbf{R}(\mathbf{r})$ is obtained from Eq. (2) by replacing $\mathbf{r}(p)$ by $\mathbf{r}$. Thus,

$$V_d(\mathbf{r} + \mathbf{R}(\mathbf{r})) = V_n(r) \tag{5}$$

in which V_n is the potential in the undeformed lattice and V_d is the perturbed potential. In first approximation the perturbing potential $\delta V(\mathbf{r})$ is

$$\delta V = V_d(\mathbf{r}) - V_n(\mathbf{r}) = -\mathbf{R} \cdot \text{grad } V_n(\mathbf{r}). \tag{6}$$

Nordheim[4] objected to this assumption because he believed that the important part of the field is that near the ions which moves almost unchanged as the nuclei oscillate. For this reason, he suggested that the perturbing potential should be obtained by treating the lattice as though it were a system of rigid oscillating atoms. In this case,

$$V(\mathbf{r}) = \sum_p v(\mathbf{r} - [\mathbf{r}(p) + \mathbf{R}(p)])$$

where v is the potential of an atom. Thus, the perturbing potential then is

$$\delta V(\mathbf{r}) = -\sum_p \mathbf{R}(p) \cdot \text{grad } v(\mathbf{r} - \mathbf{R}(p)). \tag{7}$$

The most satisfactory discussion of the potential has been given by Bardeen[5] who obtained it by a self-consistent field method. His result, which should be valid for the monovalent metals, is more nearly like Bloch's than like Nordheim's, the reason being that the volume of space near the ions in which the atomic potential $v(\mathbf{r})$ is large is so small that the "rigid" part of the field actually can be neglected. We shall not discuss the derivation of Bardeen's results in full mathematical detail but refer the reader to the original paper. His final equation for the matrix components $\delta V_{\mathbf{k},\mathbf{k}'}$ of the perturbing potential connecting

[1] BLOCH, *op. cit.*
[2] L. BRILLOUIN, *Quantenstatistik* (Julius Springer, Berlin, 1931).
[3] H. BETHE, *Handbuch der Physik* XXIV/2 (1933).
[4] L. NORDHEIM, *Ann. Physik*, **9**, 607 (1931).
[5] J. BARDEEN, *Phys. Rev.*, **52**, 688 (1937).

the states of electronic wave number $\mathbf{k}$ and $\mathbf{k}'$ is

$$\delta V_{\mathbf{k},\mathbf{k}'} = \sum_{i,\sigma,\alpha} D_i(\mathfrak{d} + \mathbf{K}_\alpha)\alpha_i(\mathfrak{d}) \cos \gamma_i(\mathfrak{d})\delta(\mathbf{k}', \mathbf{k} + \mathfrak{d} + \mathbf{K}_\alpha) \tag{8}$$

in which the $\mathbf{K}_\alpha$ are principal vectors in the reciprocal lattice, $D_i(\mathfrak{d} + \mathbf{K}_\alpha)$ is a function of $|\mathfrak{d} + \mathbf{K}_\alpha|$ alone, and $\cos \gamma_i(\mathfrak{d})$ is the angle between $\mathfrak{d}$ and $\xi_i(\mathfrak{d})$.

We shall now discuss the manner in which the resistivity is related to the matrix components of the perturbing potential in the general one-electron case as well as that in which Eq. (8) is valid.

b. The Selection Rules for Electronic Collisions.—It was seen in Sec. 43 that the probability $P_{\alpha\beta}$ that a perturbed system will change from a state of energy E_α to a state of energy E_β in time t is

$$P_{\alpha\beta} = \left(\frac{t}{\hbar}\right)^2 |V_{\alpha\beta}|^2 \frac{\sin^2 x}{x^2} \tag{9}$$

where

$$x = \frac{(E_\alpha - E_\beta)t}{2\hbar} \tag{10}$$

and $V_{\alpha\beta}$ is the matrix component of the perturbing potential connecting the two states:

$$V_{\alpha\beta} = \int \Phi_\beta^* V \Phi_\alpha d\tau. \tag{11}$$

For sufficiently long times, we may replace $\frac{\sin^2 x}{x^2}$ by

$$\frac{2\pi\hbar}{t}\delta(E_\alpha - E_\beta)$$

so that

$$P_{\alpha\beta} = \frac{2\pi t}{\hbar}|V_{\alpha\beta}|^2\delta(E_\alpha - E_\beta). \tag{12}$$

We shall apply these results to the problem of conductivity, regarding the entire crystal as a single system. The unperturbed wave functions of this system have the form [*cf.* Eqs. (2) and (11), Sec. 116]

$$\Phi_{r,\alpha}(x_1, \cdots, z_n, \xi_1, \cdots, \zeta_f) = \Psi_r(x_1, \cdots, z_n)\Lambda_{r\alpha}(\xi_1, \cdots, \zeta_f)$$

where Ψ_r is the electronic wave function and $\Lambda_{r\alpha}$ is the nuclear-coordinate wave function. In the present case, in which the harmonic approximation is employed, the wave functions $\Lambda_{r\alpha}$ are

$$\Lambda(\alpha) = \prod_{\sigma,i}^{\sigma,i} \lambda_{n_i(\sigma)}(\alpha_i(\mathfrak{d})). \tag{13}$$

The α appearing in this equation are defined by Eqs. (3), and the λ satisfy the harmonic-oscillator equation

$$-\frac{\hbar^2}{2}\frac{\partial^2\lambda_n}{\partial\alpha_i^2(\mathfrak{s})} + 2\pi^2\nu_i^2(\mathfrak{s})\alpha_i^2(\mathfrak{s})\lambda_n = \epsilon_{n_i}(\mathfrak{s})\lambda_{n_i}(\mathfrak{s}) \tag{14}$$

where

$$\epsilon_{n_i(\nu)} = [n_i(\mathfrak{s}) + \tfrac{1}{2}]\hbar\nu_i(\mathfrak{s}). \tag{14a}$$

It is assumed, of course, that the electronic wave function is a determinant of Bloch functions. Hence, the entire state of the system may be specified by the electronic wave numbers $\mathbf{k}$, the electronic-spin quantum numbers, and the vibrational quantum numbers of the lattice. Since Bardeen's perturbation potential discussed in part *a* is the sum of identical one-electron terms that are independent of spin, those matrix components connecting states in which spin quantum numbers differ, or in which more than one wave-number vector is different, vanish. The nonvanishing components connect states for which the changing wave number satisfies the condition[1]

$$\mathbf{k}' = \mathbf{k} + \mathfrak{s} + \mathbf{K}_\sigma \tag{15}$$

where $\mathbf{k}$ is its initial value and $\mathbf{k}'$ its final value [*cf.* Eq. (8)]. We must now find the matrix components of the quantity in the right-hand side of Eq. (8) for the nuclear-coordinate wave functions. This term involves the nuclear coordinates $\alpha_i(\mathfrak{s})$ through the function

$$\alpha_i(\mathfrak{s})\cos\gamma_i(\mathfrak{s}) \tag{16}$$

which appears as a coefficient of $D_i(\mathfrak{s} + \mathbf{K}_\sigma)$ in Eq. (8). The matrix components of (16) vanish for all states except those in which $n_i(\mathfrak{s})$ differs by an integer, because $\Lambda(\alpha)$ is a product of one-dimensional harmonic-oscillator functions. The nonvanishing components of (16) are

$$[\alpha_i(\mathfrak{s})\cos\gamma_i(\mathfrak{s})]_{n,n'} = \sqrt{\frac{n+1}{2}\frac{\hbar}{2\pi\nu_i(\mathfrak{s})}}\delta(n', n+1)\cos\gamma_i(\mathfrak{s}) + \sqrt{\frac{n}{2}\frac{\hbar}{2\pi\nu_i(\mathfrak{s})}}\delta(n', n-1)\cos\gamma_i(\mathfrak{s}). \tag{17}$$

We may summarize these results by saying that an electron may change its quantum number from $\mathbf{k}$ to $\mathbf{k}'$ in a single collision, where $\mathbf{k}$ and $\mathbf{k}'$ satisfy Eq. (15). This change must also satisfy the Pauli principle; that is, the state $\mathbf{k}'$ must be unoccupied. At the same time, one and only one of the three modes of vibration of given $\mathfrak{s}$ may change its vibrational quantum number by unity. This quantum number may

[1] This relationship is essentially Laue's equation for the diffraction of a wave of wave number $\mathbf{k}$ by a lattice having lattice constant $1/|\sigma|$.

decrease only if the initial value is 1 or greater than 1, that is, if the mode is initially in an excited state. Since energy must be conserved during this collision according to Eq. (12), $\mathbf{k}'$ and $\mathfrak{d}$ must satisfy one of the relations

$$\left.\begin{aligned}\epsilon(\mathbf{k}') &= \epsilon(\mathbf{k} \pm (\mathfrak{d} + \mathbf{K}_a)) + h\nu_t(\mathfrak{d}),\\ \epsilon(\mathbf{k}') &= \epsilon(\mathbf{k} \pm (\mathfrak{d} + \mathbf{K}_a)) - h\nu_t(\mathfrak{d})\end{aligned}\right\} \tag{18}$$

It should be mentioned here that Peierls[1] was the first person to point out that values of $\mathbf{K}_a$ different from zero should be considered in the preceding equations. As we shall see below, these additional terms make an appreciable contribution to the resistivity.

The matrix component for a given change of state of the system is obtained by choosing the components of (8) for one of the three vibrational modes of given $\mathfrak{d}$ and by using Eq. (17). When this matrix component is substituted in Eq. (12), we obtain the probability for the process

$$\begin{aligned}\mathbf{k} &\to \mathbf{k}',\\ n_t(\mathfrak{d}) &\to n_t(\mathfrak{d}) \pm 1,\end{aligned} \tag{19}$$

all other quantum numbers remaining fixed. The total probability that an electron of given $\mathbf{k}$ is scattered in given time when the vibrational system is initially in the state specified by a given set of vibrational quantum numbers is obtained by summing the probability for an individual process over all values of $\mathfrak{d}$, $\mathbf{K}_a$, and t with the different alternatives in sign.

For the purposes of the following discussion, we shall write the square of the matrix element of the perturbing potential connecting the electronic states $\mathbf{k}$ and $\mathbf{k} + \mathfrak{d} + \mathbf{K}_a$ and the vibrational states $n_t(\mathfrak{d})$ and $n_t(\mathfrak{d}) + 1$ or $n_t(\mathfrak{d}) - 1$ in the form

$$A_t(\mathbf{k}, \mathfrak{d} + \mathbf{K}_a) \cdot \begin{cases} n_t(\mathfrak{d}) + 1 \\ n_t(\mathfrak{d}) \end{cases} \tag{20}$$

where

$$A_t(\mathbf{k}, \mathfrak{d} + \mathbf{K}_a) = |D_t(\mathfrak{d} + \mathbf{K}_a)|^2 \frac{\hbar}{4\pi\nu_t(\mathfrak{d})} \cos^2 \gamma_t(\mathfrak{d}). \tag{21}$$

c. The Computation of $b - a$ for Temperatures above the Characteristic Temperature.—According to Eq. (9) and the preceding results, the total probability $P(\mathbf{k}, \mathfrak{d} + \mathbf{K}_a)$ that an electron in state $\mathbf{k}$ shall make a transition to another state $\mathbf{k} + \mathfrak{d} + \mathbf{K}_a$ is

$$P(\mathbf{k}, \mathfrak{d} + \mathbf{K}_a) = \sum_t A_t(\mathbf{k}, \mathfrak{d} + \mathbf{K}_a)\{[n_t(\mathfrak{d}) + 1]\omega(\epsilon(\mathbf{k}') - \epsilon(\mathbf{k}) - h\nu_t(\mathfrak{d})) + n_t(\mathfrak{d})\omega(\epsilon(\mathbf{k}') - \epsilon(\mathbf{k}) + h\nu_t(\mathfrak{d}))\} \tag{22}$$

[1] R. PEIERLS, *Ann. Physik*, 12, 154 (1932).

where

$$\omega(\epsilon) = \frac{4 \sin^2 \frac{\epsilon t}{2\hbar}}{\epsilon^2} \tag{23}$$

and

$$\mathbf{k}' = \mathbf{k} + \boldsymbol{\delta} + \mathbf{K}_a.$$

It is assumed at this point that the state $\mathbf{k}'$ is unoccupied. We may conveniently note that $h\nu_t(\boldsymbol{\delta})$ is small compared with $\epsilon(\mathbf{k})$ or $\epsilon(\mathbf{k}')$ for the electrons near the top of the filled region since $k\Theta_D$, which corresponds to the maximum value of $h\nu_t(\boldsymbol{\delta})$, is less than 0.05 ev for most metals, whereas $\epsilon(k_0)$ is at least 1 ev for all metals. This means that the electronic energy is very nearly conserved during the collisions discussed in this part of the present section. Hence, as a practical approximation, we shall replace the ω in (22) by $\omega(\epsilon(\mathbf{k}') - \epsilon(\mathbf{k}))$. As will be seen below, this approximation is justifiable as long as T is appreciably larger than Θ_D. With this simplification, $P(\mathbf{k}, \boldsymbol{\delta} + \mathbf{K}_a)$ becomes

$$\begin{aligned} P(\mathbf{k}, \boldsymbol{\delta} + \mathbf{K}_a) &= \sum_t A_t(\mathbf{k}, \boldsymbol{\delta} + \mathbf{K}_a)[2n_t(\boldsymbol{\delta}) + 1]\omega(\epsilon(\mathbf{k}') - \epsilon(\mathbf{k})) \\ &\equiv B(\mathbf{k},\mathbf{k} + \boldsymbol{\delta} + \mathbf{K}_a)\omega(\epsilon(\mathbf{k}') - \epsilon(\mathbf{k})). \end{aligned} \tag{22a}$$

In a practical problem in which we know only that a metal is at temperature T, we are not able to give the $n_t(\boldsymbol{\delta})$ in this equation particular integer values. Instead, we can know only the average values, which we shall assume are given by the equation

$$n_t(\boldsymbol{\delta}) = \frac{1}{e^{\frac{h\nu_t(\sigma)}{kT}} - 1}$$

(*cf.* Sec. 18).

It was remarked above that Eq. (22*a*) gives the transition probability only when the state $\mathbf{k}'$ is unoccupied. If $f(\mathbf{k}')$ is the probability that this state is occupied, the probability that it is not occupied is $[1 - f(\mathbf{k}')]$. Under equilibrium conditions in the absence of an external field, we may assume that f has the value

$$f_0(\mathbf{k}) = \frac{1}{e^{\frac{\epsilon(\mathbf{k}) - \epsilon_0}{kT}} + 1}, \tag{24}$$

corresponding to Fermi-Dirac statistics.

We may now compute the collision terms in Boltzmann's equation for statistical equilibrium. The total number of electrons per unit volume leaving a unit volume in $\mathbf{k}$ space per unit time because of collisions is

$$a = \frac{d}{dt}\int f(\mathbf{k})B(\mathbf{k},\mathbf{k}')\omega(\epsilon(\mathbf{k}) - \epsilon(\mathbf{k}'))[1 - f(\mathbf{k}')]\rho(\mathbf{k}')d\tau(\mathbf{k}')$$

where $\rho(\mathbf{k}')$ is the density of levels at the point $\mathbf{k}'$ and the integration extends over those points in wave-number space for which the selection rules are satisfied. Similarly, the number of electrons per unit volume entering the unit volume of $\mathbf{k}$ space because of collisions is

$$b = \frac{d}{dt}\int f(\mathbf{k}')B(\mathbf{k},\mathbf{k}')\omega(\epsilon(\mathbf{k}) - \epsilon(\mathbf{k}'))[1 - f(\mathbf{k})]\rho(\mathbf{k}')d\tau(\mathbf{k}').$$

Hence, $b - a$ is

$$b - a = \frac{d}{dt}\int B(\mathbf{k},\mathbf{k}')\omega(\epsilon(\mathbf{k}') - \epsilon(\mathbf{k}))\{f(\mathbf{k}')[1 - f(\mathbf{k})] - f(\mathbf{k})[1 - f(\mathbf{k}')]\}\rho(\mathbf{k}')d\tau(\mathbf{k}'). \quad (25)$$

This evidently vanishes when $f(\mathbf{k})$ has the form of Eq. (24). In the case in which there is an electrical field, we shall assume that f has the form

$$f(\mathbf{k}) = f_0(\mathbf{k}) + k_x g(\mathbf{k}) \quad (26)$$

where $g(\mathbf{k})$ is a small function that depends only upon $\epsilon(\mathbf{k})$. This assumption evidently is equivalent to that of Eq. (1a), Sec. 126. If (26) is substituted in Eq. (25) and only first-order terms are kept, it is found that

$$b - a = \frac{d}{dt}\int B(\mathbf{k},\mathbf{k}')\omega(\epsilon(\mathbf{k}) - \epsilon(\mathbf{k}'))[k_x' g(\mathbf{k}') - k_x g(\mathbf{k})]\rho(\mathbf{k}')d\tau(\mathbf{k}'). \quad (27)$$

We shall now integrate this under the assumption that

$$\epsilon(\mathbf{k}) = \frac{\hbar^2\mathbf{k}^2}{2m}$$

and that, when $|\mathbf{k}| = |\mathbf{k}'|$, $B(\mathbf{k},\mathbf{k}')$ depends only upon $|\mathbf{k}|$ and the angle θ between $\mathbf{k}$ and $\mathbf{k}'$. Then, $\rho(\mathbf{k}')$ is a constant equal to $2V$, and

$$\begin{aligned} d\tau(\mathbf{k}') &= k'^2 dk' \sin\theta d\theta d\varphi \\ &= \left(\frac{dk'}{d\epsilon'}\right)' {}^2 d\epsilon(k') \sin\theta d\theta d\varphi \end{aligned}$$

where θ and φ are the polar angles of the vector $\mathbf{k}'$ measured relative to $\mathbf{k}$. Making use of the relations

$$\int_{-a}^{a} F(\epsilon)\omega(\epsilon)d\epsilon \cong \frac{2\pi t}{\hbar}F(0), \quad (28)$$

for $at >> \hbar\pi$ and

$$\int_0^{2\pi} (k_x - k_x')d\varphi = 2\pi k_x(1 - \cos\theta),$$

we find

$$b - a = -\left(\frac{dk}{d\epsilon}\right) Vk^2 k_x g(\epsilon) \frac{8\pi^2}{h} \int_0^{\pi} B(\mathbf{k},\mathbf{k}')(1 - \cos\theta) \sin\theta d\theta$$

where the integration extends over θ.

Comparing this equation with the corresponding equation for Sommerfeld's theory [*cf.* Eq. (2), Sec. 126], namely,

$$b - a = -\frac{v_x v\chi(v)}{l},$$

we may conclude by analogy that the mean free path l is

$$\frac{1}{l(k)} = 16\pi^3 \left(\frac{dk}{d\epsilon}\right)^2 Vk^2 \int_0^{\pi} B(\mathbf{k},\mathbf{k}')(1 - \cos\theta) \sin\theta d\theta \tag{29}$$

since $v_x\chi(v)$ is replaced by $k_x g(\epsilon)$ in the present problem and since

$$= \frac{1}{h}\frac{d\epsilon}{dk}.$$

Before this result can be substituted in Eq. (6) of the preceding section for the conductivity, it must be shown that $k_x g$ and $v_x\chi$ have the same form. In order to do so, we must solve Boltzmann's equation

$$\left(\frac{\partial f}{\partial t}\right)_{\text{drift}} = b - a.$$

In the Lorentz-Sommerfeld case, the solution of this is (*cf.* Sec. 31)

$$v_x\chi = e\mathsf{E}_x l \frac{v_x}{v}\frac{\partial f_0}{\partial v_x}. \tag{30}$$

Now, in the present case,

$$\left(\frac{\partial f}{\partial t}\right)_{\text{drift}} = -\frac{e\mathsf{E}_x}{h}\frac{\partial f}{\partial \epsilon}\frac{\partial \epsilon}{\partial k_x} - \frac{1}{h}\frac{\partial \epsilon}{\partial k_x}\frac{\partial f}{\partial x}. \tag{31}$$

We may assume that f is independent of x and may retain only the first part of (26) in the remaining term in (31). We obtain

$$\left(\frac{\partial f}{\partial t}\right)_{\text{drift}} = -\frac{e\mathsf{E}_x}{h}\frac{\partial f_0}{\partial \epsilon}\frac{\partial \epsilon}{\partial k_x}. \tag{32}$$

Thus, the equation to be solved is

$$e\mathsf{E}_x v_x \frac{\partial f_0}{\partial \epsilon} = \frac{g}{l}\frac{k_x}{h}\left(\frac{d\epsilon}{dk}\right)$$

where l is given by Eq. (29). The solution of this is

$$k_z g = e\mathcal{E}_z l \frac{v_z}{v} \frac{\partial f_0}{\partial \epsilon}, \tag{33}$$

which is identical with Eq. (30); hence, we may use the value of $l(k)$ given by Eq. (29) in all the equations of the Lorentz-Sommerfeld theory. Thus, the conductivity is

$$\sigma = \frac{e^2 n_0 l(k_0)}{m v(k_0)}. \tag{34}$$

It is sometimes convenient to write Eq. (34) in the form

$$\rho = \frac{1}{\sigma} = \frac{m v(k_0)}{e^2 n_0} \frac{1}{l(k_0)} \tag{35}$$

where ρ is the resistivity. When coupled with Eq. (29), this form shows clearly the way in which the resistivity depends upon the matrix components of the perturbing potential.

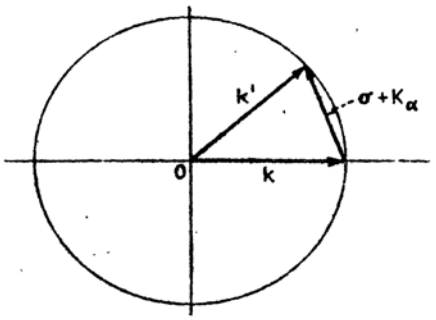

FIG. 1.—The relationship between $\mathbf{k}$, $\mathbf{k}'$ and $\sigma + \mathbf{K}_\alpha$. The center of the circle is at the origin of $\mathbf{k}$ space and the radius of the circle is $|\mathbf{k}| = |\mathbf{k}'|$. The values over which $\sigma + \mathbf{K}_\alpha$ is integrated are given by the chords that connect $\mathbf{k}$ and $\mathbf{k}'$.

d. The Numerical Computation of the High-temperature Conductivity.—We shall now outline the way in which Bardeen computed $1/l$. According to the equations of parts *b* and *c*

$$B(\mathbf{k},\mathbf{k}') = \sum_t |D_t(\mathfrak{d} + \mathbf{K}_\alpha)|^2 \frac{\hbar}{4\pi\nu_t(\mathfrak{d})} \cos^2 \gamma_t(\mathfrak{d})[2n_t(\mathfrak{d}) + 1]. \tag{36}$$

This must be substituted in Eq. (29), and the result must be integrated over θ. Before this can be done, it is necessary to investigate the dependence of $\mathfrak{d}$ and $\mathbf{K}_\alpha$ upon θ. The relations between $\mathbf{k}$, $\mathbf{k}'$, $\mathfrak{d}$, and $\mathbf{K}_\alpha$ are given by the equations

$$\left.\begin{aligned} \mathbf{k}' - \mathbf{k} &= \mathfrak{d} + \mathbf{K}_\alpha, \\ \mathbf{k}'^2 = \mathbf{k}^2 &= |\mathbf{k} + \mathfrak{d} + \mathbf{K}_\alpha|^2, \end{aligned}\right\} \tag{37}$$

which show that the allowed values of $\mathfrak{d} + \mathbf{K}_\alpha$ are the chords of a sphere of radius $|\mathbf{k}|$ that pass through the point $\mathbf{k}$ (*cf.* Fig. 1). Moreover, each allowed value of $\mathfrak{d} + \mathbf{K}_\alpha$ satisfies this relation only once. The relation between $|\mathfrak{d} + \mathbf{k}_\alpha|$ and θ, the angle between $\mathbf{k}$ and $\mathbf{k}'$, may be found by use of elementary geometry and is

$$|\mathfrak{d} + \mathbf{K}_\alpha| = 2k \sin \frac{\theta}{2}. \tag{38}$$

Hence, all the terms of $B(\mathbf{k},\mathbf{k}')$ except $\frac{\cos^2 \gamma_t(\mathfrak{d})}{4\pi\nu_t(\mathfrak{d})}$ and $[2n_t(\mathfrak{d}) + 1]$ depend upon θ alone. A part of the complication arising from the additional terms may be removed by assuming that

$$\nu_t(\mathfrak{d}) = c\sigma$$

where c is independent of t and $\mathfrak{d}$. This relation is not rigorous since the velocity of vibrational waves usually depends upon wave number even in an isotropic solid. With this assumption, we may make use of the relation

$$\Sigma \cos^2 \gamma_t(\mathfrak{d}) = 1,$$

which is valid because the three directions of polarization of lattice waves are orthogonal. We are then left only with the complication that part of the coefficients in the terms of B depend upon $|\mathfrak{d} + \mathbf{K}_\alpha|$ and part depend upon $|\mathfrak{d}|$. As long as $\mathfrak{d} + \mathbf{K}_\alpha$ lies in the first zone, $\mathbf{K}_\alpha$ is zero, so that these terms depend only upon $|\mathfrak{d}|$. Bardeen has pointed out that $|\mathfrak{d}|$ is very near to its maximum in the monovalent metals when $\mathbf{K}_\alpha$ is not zero. This fact can be made evident by observing that in monovalent metals the circle of radius $2k_0$ in $\mathfrak{d} + \mathbf{K}_\alpha$ space, which determines the allowed values of $\mathfrak{d} + \mathbf{K}_\alpha$, usually is not close to points $\mathbf{K}_\alpha$ other than the origin. Hence, we may replace $\nu_t(\mathfrak{d})$ by $c\sigma_m$ in those terms of $B(\mathbf{k},\mathbf{k}')$ for which $\mathbf{K}_\alpha \neq 0$. This assumption evidently decreases the theoretical resistivity to some extent.

As a further simplification, it may be assumed that the first zone of wave-number space is a sphere of radius

$$\sigma_m = 2^{\frac{1}{2}}k_0.$$

The vector $|\mathfrak{d} + \mathbf{K}_\alpha|$ extends outside this sphere whenever

$$\sin\frac{\theta}{2} > \frac{2^{\frac{1}{2}}}{2} = \frac{1}{2^{\frac{1}{2}}}$$

or whenever $\theta > 79°$.

Finally, it will be assumed that the temperature is so high that

$$n_t = \frac{1}{e^{\frac{h\nu_t}{kT}} - 1}$$

may be replaced by $kT/h\nu_t$.

With these assumptions, we have

$$B(\mathbf{k},\mathbf{k}') = \frac{2kT}{9c^2NM}G(u)^2, \tag{39a}$$

when $\sin \theta/2 < 2^{-\frac{1}{2}}$, and

$$B(\mathbf{k},\mathbf{k}') = \frac{2kT}{9c^2NM}\frac{4k_0^2u^2}{\sigma_m^2}G(u)^2, \tag{39b}$$

when $\sin \theta/2 > 2^{-\frac{1}{2}}$, where

$$u = \sin\frac{\theta}{2}$$

and $G(u)$ is a somewhat intricate function that may be derived in a straightforward manner from the coefficients $D_l(\mathfrak{o} + \mathbf{K}_\alpha)$ in Eq. (8). It should be observed that the value of $B(\mathbf{k},\mathbf{k}')$ for which $\sin \theta/2$ is less than $2^{-\frac{1}{2}}$ joins continuously with that for which $\sin \theta/2$ is greater than $2^{-\frac{1}{2}}$, since

$$\frac{4k_0^2 2^{-1}}{\sigma_m^2} = 1.$$

The function $G(u)^2$, which determines the angular distribution of scattering, decreases from a relative value of 1 to a value of about 0.1 in the range extending from $\theta = 0$ to $\theta = \pi$, as is shown in Fig. 2. Hence, collisions in which the electron is scattered in the forward direction are most probable.

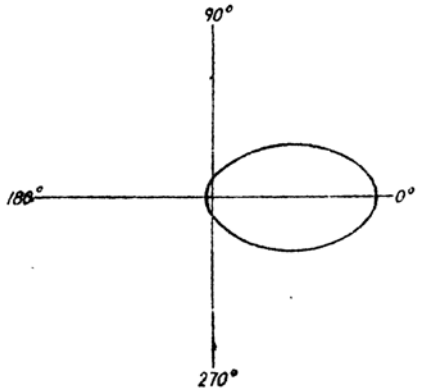

FIG. 2.—A relative plot of $G(u)^2$ as a function of the polar angle θ.

Substituting the foregoing value of $B(\mathbf{k},\mathbf{k}')$ in Eq. (29), we obtain

$$\frac{1}{l(k)} = \frac{32\pi^3kT}{9c^2NM}\left(\frac{dk}{d\epsilon}\right)^2_{k=k_0} k_0^2 \cdot 2^{-\frac{1}{2}}C^2 \tag{40}$$

where C^2 is defined by the equation

$$C^2 = 2^{\frac{1}{2}}\left[\int_0^{2^{-\frac{1}{2}}} G(u)^2u^2du + \int_{2^{-\frac{1}{2}}}^1 G(u)^2\frac{4k_0^2u^2}{\sigma_m^2}u^2du\right]. \tag{41}$$

Hence, if we use the relation $\Theta_D = hc\sigma_m/k$ the conductivity is

$$\sigma = \frac{4e^2k_0}{h^3\pi}\left(\frac{d\epsilon}{dk}\right)^2_{k=k_0}\left(\frac{Mk\Theta_D^2}{T}\right)\frac{1}{C^2}. \tag{42}$$

It should be observed that the effect of the relatively large value of $G(u)$ in the direction of forward scattering is partly compensated by the coefficients of this function in the integrands of (41). Actually the second integral represents about 40 per cent of C^2. A list of computed and observed values of the conductivity of a number of monovalent

metals is given in Table LXXVII. The important simplifying assumptions made in deriving these values are that the electrons are perfectly free and that the lattice potential at the surface of the equivalent sphere (see Chap. X) is equal to $\epsilon(0)$. These assumptions are most closely satisfied by sodium, for which the agreement between observed and calculated values is best. The theoretical values usually are larger

TABLE LXXVII.—COMPARISON OF OBSERVED AND CALCULATED VALUES OF THE CONDUCTIVITY OF SEVERAL MONOVALENT METALS AT 0°C

[These values are taken from the review article by J. Bardeen, *Jour. Applied Phys.*, 11, 88 (1940). In 10^4 ohm-cm]

Metal	Observed	Calculated
Li	11.8	28
Na	23.4	23
K	16.4	20
Rb	8.6	33
Ca	5.3	22
Cu	64	174
Ag	66	143
Au	49	142

than the measured ones, a fact showing that the computed values of $1/l$ should be larger. Bardeen estimates that about 10 or 15 per cent of the difference is due to the fact that ν is replaced by ν_m in the terms of B for which $\mathbf{K}_a$ is not zero.

e. Other Computations.—Other workers have obtained results comparable with Bardeen's on the basis of somewhat different assumptions. We mentioned, for example, Bloch's assumption of deformable ions and Nordheim's assumption of rigid ions in part *a*. The first of these leads to an equation similar to (42) in which the constant C is given by an expression different from (41) which involves the electronic potential in the undeformed lattice. Peterson and Nordheim[1] have used the potential function for sodium, determined by the methods discussed in Chap. X, to compute Bloch's C and have found that this value leads to a conductivity about three times smaller than the experimental value given in Table LXXVII. This fact indicates that the actual fluctuations in potential are less than those given by the deformable atom picture, so that scattering is less. The rigid-ion picture is not very well founded, as we saw in part *a*, and has not actually been used as the basis for a quantitative computation.

Peterson and Nordheim have proposed another method for determining the electron scattering in metals that is simpler, although less accurate

[1] E. L. PETERSON and L. W. NORDHEIM, *Phys Rev.*, 51, 355 (1937).

than Bardeen's. They assume that the electronic wave functions have the form

$$\chi_0 e^{2\pi i \mathbf{\delta}\cdot\mathbf{r}}.$$

where $|\chi_0|^2$ varies inversely as the change in atomic volume, when the lattice is perturbed by a vibrational wave of wave number δ. They then expand the perturbed wave function in terms of the unperturbed functions and compute the matrix components of the perturbing potential from the coefficients. The value of the square of these components is

$$(\delta V)^2_{k,k+\sigma} = \frac{\pi^2 h^4 \delta^6}{4m^2}|a_t(\delta)|^2,$$

which may be used to compute $1/l$ in a way similar to that discussed in the preceding section. Peterson and Nordheim neglect the terms for which $\mathbf{K}_\alpha \neq 0$, and obtain

$$\frac{C}{\epsilon_0} = 0.84$$

for all metals. Although this result agrees within about 10 per cent with values of the same quantity computed by Bardeen, Bardeen points out that the neglect of terms for which $\mathbf{K}_\alpha \neq 0$ is a serious omission, for if they were included, the value of C/ϵ_0' would be increased by a factor of the order 2.

Mott and Jones[1] have developed another simplified method for treating the resistivity at high temperatures. They compute the probability that an electron is scattered in a single polyhedron on the assumption that the fluctuations of potential within a given polyhedron may be handled as though independent of the fluctuations in other cells The total scattering probability is then determined by adding the contributions from each cell. This approximation is equivalent to assuming that the atoms have individual oscillation frequencies, as in the Einstein theory of specific heats, and is roughly valid as long as T is appreciably larger than the characteristic temperature. Since the scattering depends upon the square of the atomic amplitude, which varies as $\sqrt{T}$, the ordinary linear temperature dependence of resistance is obtained very simply in this theory.

f. Low Temperature.—The first extensive investigation of the low-temporature conductivity was carried through by Bloch.[2] His work follows closely the procedure presented above for high temperature,

[1] N. F. MOTT and H. JONES, *The Theory of the Properties of Metals and Alloys* (Oxford University Press, New York, 1936).

[2] F. BLOCH, *Z. Physik*, **59**, 208 (1930).

although he made the additional simplifying assumptions that the scattering is isotropic and that the term for which $\mathbf{K}_\alpha$ is not zero may be neglected. On the whole, his computation, which will not be presented here, is more intricate because the assumption that

$$\omega(\epsilon(\mathbf{k}') - \epsilon(\mathbf{k}) \pm h\nu) = \omega(\epsilon(\mathbf{k}') - \epsilon(\mathbf{k}))$$

may not be made at low temperatures. Bardeen has corrected Bloch's results to conform to the use of his own interaction potential. This means, in principle, that he repeated the computation of parts *a* to *c* on the assumption that T is less than Θ_D. The results show that the ratio of the high-temperature conductivity σ_2 to the low-temperature conductivity σ_1 is

$$\frac{\sigma_2}{\sigma_1} = 497.6\left(\frac{\epsilon_0'}{C}\right)^2\left(\frac{T_1}{\Theta_D}\right)^4\frac{T_1}{T_2} \tag{43}$$

where $T_1 << \Theta_D << T_2$. In other words, the results predict that the low-temperature conductivity should vary as T^{-5}. This temperature dependence was also found by Bloch who derived the relation

$$\frac{\sigma_2}{\sigma_1} = 497.6\left(\frac{T_1}{\Theta_D}\right)^4\frac{T_1}{T_2} \tag{44}$$

in place of (43).

The physical origin of this T^{-5} law may be understood in the following way. If we schematize the collision process by saying that the electrons make collisions with the quanta of lattice vibrations, the mean free path should contain a factor $1/T^3$ because the density of quanta varies as T^3 when T is well below the characteristic temperature. In addition, the collisions become less effective as the temperature decreases, for only the lattice waves of smaller wave number are excited. In fact, the mean wave number $\bar{\sigma}$ is of the order of magnitude kT/hc at temperature T, where c is the acoustical velocity. Consider an electron that is traveling in the direction of the field and has wave number $\mathbf{k}$. After a collision, its wave number is $\mathbf{k} + \boldsymbol{\sigma}$, where $\boldsymbol{\sigma}$ is the wave number of the quantum with which it has collided. Since $\boldsymbol{\sigma}$ ranges over a sphere, the component of momentum in the direction of the field is not changed on the average by a factor of the order of magnitude $\bar{\sigma}/k$; instead, the change is of the order of magnitude $\bar{\sigma}^2/k^2$. Thus, the number of collisions required to stop the electron is of the order of magnitude $k^2/\bar{\sigma}^2$, which varies as $1/T^2$, whence the effective mean free path for stopping varies as

$$\frac{1}{(T^3 \cdot T^2)} = \frac{1}{T^5}.$$

If the atoms scattered the electrons independently at low temperatures,

as Mott and Jones in their simplified theory assumed that they do at high temperatures, the density of quanta would decrease as $e^{-\frac{h\nu}{kT}}$ with decreasing temperature, where ν is a constant, and the resistance would decrease much more rapidly than T^5.

In this connection, Peierls[1] has raised the objection to the low-temperature theory that thermal equilibrium is assumed without adequate proof. He points out that in the Bloch-Bardeen type of treatment the electrons make only small-angle collisions at low temperatures, at least in the monovalent metals, in which the top of the filled region is not near a zone boundary, and that the number of low-frequency quanta excited may not correspond to equilibrium. This objection has not yet been fully cleared.

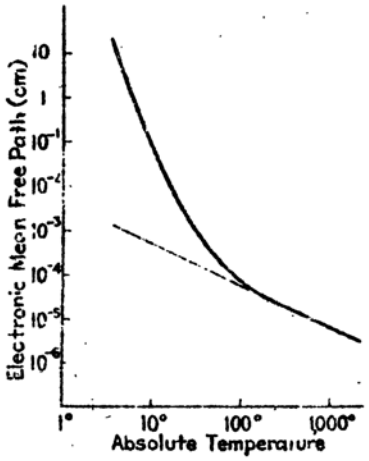

FIG. 3.—The electronic mean free path in silver as determined by equating the expression (6) of Sec. 126 for the theoretical conductivity to Grüneisen's empirical function for silver.

Extensive experimental work of Grüneisen[2] shows that the T^{1-5} law is closely obeyed at low temperatures. It is not possible to distinguish between Eqs. (43) and (44), however, because the characteristic temperature cannot be fixed closely enough. Grüneisen has also found empirically that the reciprocal of the conductivity of many simple metals is given closely over a wide temperature range by the function

$$\frac{1}{\sigma} = AG(T) = AT^5 \int_0^{\frac{\Theta}{T}} \frac{x^5 dx}{(e^x - 1)(1 - e^{-x})} \tag{45}$$

if the constants A and Θ are properly chosen (*cf.* Fig. 3). Usually, Θ is close to the characteristic temperature of the substance. At high temperatures, this function approaches the value $AT/4$; at low temperatures, it approaches the value $124.4AT^5$. Thus, according to this empirical relation, the ratio of the high-temperature conductivity to the low-temperature conductivity is the same as Bloch's relation (44).

It is probably well to bear in mind that the basis of the T^{1-5} law is intimately connected with the validity of Debye's T^3 law for specific heats. Since the apparent experimental verification of the latter at temperatures above 10°K is open to the criticisms discussed in Secs. 20

[1] R. PEIERLS, *Ann. Physik*, **4**, 121 (1930).
[2] E. GRÜNEISEN, *Ann. Physik*, **16**, 530 (1933).

and 23, the experimental test of the T^{-5} law is not so significant as it seems at first sight.

g. Critique of the High-temperature Treatment of Conductivity.—Kretschmann[1] has pointed out that, in the preceding treatments of the theory of conductivity, the electronic states are described as though their energy were accurately defined to well within the limits of the changes in energy occurring during transitions. Since these changes are of the order of magnitude $h\nu_m$, where ν_m is the maximum Debye frequency, he suggests this description can be accurate only if the perturbing effect of the lattice vibrations is much less than $h\nu_m$. The effect of the lattice is measured by the mean time between collisions, namely, $\tau = l/v$ where l is the mean free path and v is the mean velocity. At room temperature, $l \sim 10^{-5}$ cm in a good conductor and $v \sim 10^7$ cm/sec so that $\tau \sim 10^{-12}$ sec. Hence, the condition that should be satisfied, if the perturbing effects are small compared with $h\nu_m$, is that

$$\frac{h}{\tau} << h\nu_m$$

or

$$\nu_m >> \frac{1}{\tau} \sim 10^{12}. \tag{46}$$

Actually, the lattice frequencies are also of the order of magnitude 10^{12} sec^{-1}.

Peierls[2] has suggested in this connection that Kretschmann's criticism would be accurate only if the delta-function approximation of Eq. (12) had to be employed from the start. Actually, we have been able to use the form (9) of the perturbation equation until reaching Eq. (29) because the matrix component $|V_{\alpha\beta}|^2$ in (9) is a slowly varying function of the variable ϵ. The condition under which the relation (29) is valid is that the integrand should vary slowly within the range of ϵ in which $\omega(\epsilon)$ has its peak. Since the g in (27), which are expressed in terms of the Fermi-Dirac distribution function, vary within a range kT near the edge of the filled region, it follows that we must have

$$\frac{h}{kT} < t < \tau \tag{47}$$

instead of (46). This is slightly less restrictive than Kretschmann's condition, although room temperature is a borderline temperature even for good conductors.

[1] E. KRETSCHMANN, *Z. Physik*, **87**, 518 (1934); **88**, 786 (1934).
[2] R. PEIERLS, *Z. Physik*, **88**, 786 (1934); *Helvetica Phys. Acta*, **7** (Sup.), 24 (1934).

h. The Effect of Electronic Coupling.—Houston[1] has suggested that the effects of electrostatic coupling between electrons which are disregarded in using wave functions constructed of one-electron functions may appreciably alter the quantitative values of the computed conductivity. He has pointed out, for example, that because of this coupling collisions may occur in which two or more electrons change their wave-number vectors at the same time. The wave-number vectors of individual electrons need not obey Eq. (15) in such collisions since this equation is replaced by one concerning the behavior of the total wave-number vectors of all electrons. In view of the excellent results Bardeen obtained for the theoretical conductivity in the case of sodium, it seems unlikely that Houston's conclusions are important in the case of the simpler metals at ordinary temperatures; however, they are possibly important at low temperatures for establishing thermal equilibrium.

128. Other Simple Metals.—We should not expect the equations developed in the preceding section to apply quantitatively to divalent metals in which the distribution of levels near the top of the filled band is different from that for perfectly free electrons as Manning's results show (Sec. 99). In agreement with this, it is observed that the resistivity of these metals is about four times larger than the resistivity of the monovalent metals preceding them in the periodic chart, even though the former have twice as many electrons and nearly the same lattice parameters and characteristic temperatures as the latter. The increase in resistivity may be understood qualitatively from the fact that the effective number of free electrons, that is, the number in the energy range of width kT near the top of the band, is smaller in the divalent metals than in the monovalent metals, for these electrons alone transport the current. No quantitative computations of the resistivity have been carried out.

Jones[2] has pointed out that the principle that accounts for the comparatively high resistivity of the divalent metals should also apply to those metals, such as bismuth, which lie between ideal metallic and valence types, since they also have nearly filled zones.

129. The Temperature-dependent Resistivity of the Transition-element Metals.—The resistivity of transition-element metals, such as iron, cobalt, and nickel, usually is higher than that of the simpler metals, such as copper, following them in the periodic chart and having nearly the same lattice parameters. We have seen in Chap. XIII that the transition metals differ from the simpler metals by having unfilled d levels with the same energy as the lowest unoccupied s-p levels. Since the s-p levels in transition-element metals are very nearly the same as those

[1] W. V. HOUSTON, *Phys. Rev.*, **55**, 1255 (1939).

[2] H. JONES *Proc. Roy. Soc.*, **147**, 396 (1934). See also Mott and Jones, *op. cit.*

in the simple metals which follow, the resistivity arising from transitions of the conduction electrons between s-p levels should be nearly alike in the two cases. Mott[1] was the first to suggest that the s-p electrons are principally responsible for the current in transition metals and that the additional transitions from s-p levels to the unfilled d levels accounts for most of the additional resistivity. As proof of the first of these suggestions, it is usually pointed out that the conductivity of any single band of electrons may be placed in the form

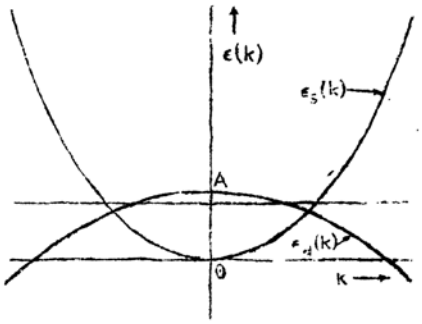

FIG. 4.—The relative positions of the s and d levels in the transition metals [*cf.* Eqs. (1) and (2)]. The dotted line represents the top of the filled region.

$$\sigma = \frac{n_0 e^2}{m^*}\tau \tag{1}$$

[*cf.* Eq. (6), Sec. 126] where

$$\tau = l/v(\epsilon_0')$$

is the collision time and m^* is the effective mass of the electrons in the band. Since m^* for d-shell electrons is much larger than the electronic mass, it is assumed that (1) is small in comparison with the conductivity of the s-p electrons. Mott developed a simple mathematical theory of the scattering of s-p electrons arising from transitions to the d band; however, Wilson[2] has since given a more extensive treatment, which we shall discuss here.

Wilson assumed that the energy states in both the s-p bands and the d bands may be treated with the Bloch approximation and that the energy in each band is a quadratic function of the wave number in the reduced-zone scheme. The $\epsilon(\mathbf{k})$ curves for the two overlapping bands then appear as in Fig. 4. We shall select the zero of energy so that the energy $\epsilon_s(\mathbf{k})$ of the s-p electrons is

$$\epsilon_s(\mathbf{k}) = \frac{E^2}{2m_s}\mathbf{k}^2 \tag{2}$$

and the energy $\epsilon_d(\mathbf{k})$ of the d levels is

$$\epsilon_d(\mathbf{k}) = A - \frac{\hbar^2}{2m_d}\mathbf{k}^2 \tag{3}$$

where m_s and m_d are the effective electron masses in the two bands.

In the one-electron approximation, the selection rules for transitions from the s-p band to the d band should be the same as those derived in

[1] N. F. MOTT, *Proc. Phys. Soc.*, **47**, 57, (1935); *Proc. Roy Soc.*, **153**, 699 (1936), **156**, 368 (1936).

[2] A. H. WILSON, *Proc. Roy Soc.*, **167**, 530 (1938).

Sec. 127 for transitions between levels of the s-p band, namely,

$$\mathbf{k}' - \mathbf{k} = \mathfrak{d} + \mathbf{K}_\alpha, \tag{4}$$

$$\epsilon(\mathbf{k}') = \epsilon(\mathbf{k}) \pm h\nu_t(\mathfrak{d}), \tag{5}$$

where $\mathbf{k}$ is the wave number of the initial state, $\mathbf{k}'$ is that of the final state, $\mathfrak{d}$ is the wave number of the vibrational mode causing the transition, and $\mathbf{K}_\alpha$ is a principal vector in the inverse lattice.

We may treat separately the contributions to the resistivity from the collisions in which the s-p electrons jump to s-p levels and those in which they jump to d levels, since we are dealing with a one-electron approximation. The first contribution was discussed in Sec. 127 for the monovalent metals. The result for the present case should differ from the result found there only in the fact that k_0 should be replaced by a value appropriate for the s-p levels in the transition metals. Since there is 0.6 free electron per atom in nickel, for example, we have

$$k_0 = \left(\frac{3}{8\pi} 0.6 n_0\right)^{\frac{1}{3}} \tag{6}$$

where n_0 is the number of atoms per unit volume. If this is substituted in the equations of Sec. 127, it is found that the resistivity increases by a factor $(0.6)^{-\frac{1}{3}}$ compared with the resistivity for a monovalent metal.

Wilson developed an expression for the additional resistivity that is valid for both high and low temperatures, using simplifying assumptions which will now be outlined. Let us assume that the lattice frequencies are distributed according to the Debye theory and that the longitudinal and transverse modes have the same value of $\nu(\mathfrak{d})$. The probability for a transition in time t to a vacant state in the s-p band from one in the d band then is

$$\alpha_d(\mathbf{k},\mathbf{k}')\frac{\hbar}{2\pi\nu(\mathfrak{d})} \cdot \begin{cases} [n(\mathfrak{d}) + 1]\omega(\epsilon_d(\mathbf{k}') - \epsilon_s(\mathbf{k}) - h\nu(\mathfrak{d})) & (7a) \\ n(\mathfrak{d})\omega(\epsilon_d(\mathbf{k}') - \epsilon_s(\mathbf{k}) + h\nu(\mathfrak{d})) & (7b) \end{cases}$$

where α_d is a function of $\mathbf{k}$ and $\mathbf{k}'$ that is equivalent to $2\pi\nu_t(\mathfrak{d})/\hbar$ times the quantity $A_t(\mathbf{k},\mathbf{k}')$ appearing in Eq. (20), Sec. 127. Case (7a) corresponds to a collision in which the vibrational mode of wave number $\mathfrak{d}$ gains a quantum, and (7b) to one in which it loses a quantum. The probabilities for the reverse transitions are

$$\alpha_d(\mathbf{k},\mathbf{k}')\frac{\hbar}{2\pi\nu(\mathfrak{d})} \cdot \begin{cases} n(\mathfrak{d})\omega(\epsilon_d(\mathbf{k}') - \epsilon_s(\mathbf{k}) - h\nu(\mathfrak{d})) \\ [n(\mathfrak{d}) + 1]\omega(\epsilon_d(\mathbf{k}') - \epsilon_s(\mathbf{k}) + h\nu(\mathfrak{d})) \end{cases} \tag{8}$$

As we remarked in part c, Sec. 127, the approximation

$$\omega(\epsilon_d(\mathbf{k}') - \epsilon_s(\mathbf{k}) \pm h\nu(\mathfrak{d})) \cong \omega(\epsilon_d(\mathbf{k}') - \epsilon_s(\mathbf{k}))$$

may be employed at high temperatures but not at low temperatures. If we designate the electronic distribution functions for the levels of the s and d bands by f_s and f_d, we obtain the following expression for the contribution to the collision terms from the s-p to d transitions:

$$b - a = \frac{d}{dt}\int \alpha_{\sigma}\frac{\hbar}{2\pi\nu(\sigma)}\Big(\{[n(\sigma)+1]f_s(1-f_d) - n(\sigma)f_d(1-f_s)\}$$
$$\omega(\epsilon_d(\mathbf{k}') - \epsilon_s(\mathbf{k}) - h\nu(\sigma)) + \{n(\sigma)f_s(1-f_d) - [n(\sigma)+1]f_d(1-f_s)\}$$
$$\omega(\epsilon_d(\mathbf{k}') - \epsilon_s(\mathbf{k}) + h\nu(\sigma))\Big)\rho(\mathbf{k}')d\tau(\mathbf{k}') \quad (9)$$

where the integration extends over the values of $\mathbf{k}'$ satisfying Eq. (4). Wilson integrated this under the following assumptions.

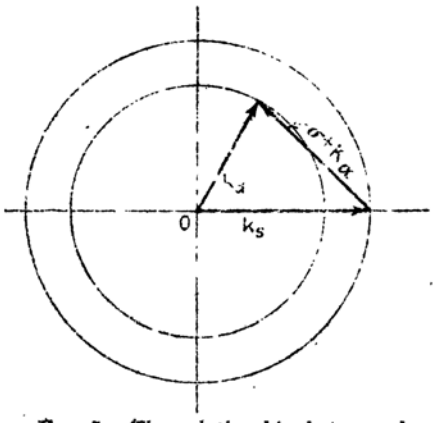

FIG. 5.—The relationship between k_{os}, k_{od} and $\sigma + \mathbf{K}_\alpha$ in the case of the transition metal. The outer circle is the boundary of the filled region in the s-p band, whereas the inner circle is the boundary in the d band, (*cf.* Fig. 3). These circles usually should not coincide. The vector $\sigma + \mathbf{K}_\alpha$ joins $\mathbf{k}_d$ and $\mathbf{k}_s$, so that its minimum value is

$$|\mathbf{k}_{os}| - |\mathbf{k}_{od}|.$$

a. α_d is a constant. This is equivalent to assuming isotropic scattering.

b. f_s and f_d may be placed in the form

$$\left.\begin{aligned} f_s &= f_{0,s} + k_x g_s(\epsilon_s(\mathbf{k})), \\ f_d &= f_{0,d} + k_x g_d(\epsilon_d(\mathbf{k})), \end{aligned}\right\} \quad (10)$$

where $f_{0,s}$ and $f_{0,d}$ are the Fermi-Dirac distribution functions for the field free problem and the g are comparatively small functions.

c. The functions g in (10) have the form

$$g(\epsilon) = C(\epsilon)\frac{\partial f}{\partial \epsilon}.$$

This functional form was also assumed in the cases discussed in Sec. 127.

d. The values of $n(\sigma)$ are given by the equation

$$n(\sigma) = \frac{1}{e^{\frac{h\nu(\sigma)}{kT}} - 1}$$

As in Sec. 127, it is convenient to integrate over the values of the vector $\sigma + \mathbf{K}_\alpha$ instead of the values of $\mathbf{k}$; there is, however, an important difference between the present and preceding cases. In the preceding case, the values of $\sigma + \mathbf{K}_\alpha$ ranged over a sphere of radius k_0 that passed through the origin (*cf.* Fig. 1). Hence, the range of $|\sigma + \mathbf{K}_\alpha|$ extended from zero to $2k_0$. In the present case, however, the values k_0 and k_{01}

of the wave number of the electrons at the limit of the filled regions in the s and d zones should usually be different, so that the vectors $\mathbf{\delta} + \mathbf{K}_\alpha$ should range over a sphere of radius k_{0d} that is centered at a point k_{0s} (*cf.* Fig. 5). This sphere evidently will not pass through the origin, unless by accident. Since the lowest value of $|\mathbf{\delta} + \mathbf{K}_\alpha|$ in the integration is $|k_{0s} - k_{0d}|$, the vibrational modes of longest wave length usually do not play a role in scattering electrons between the s-p and d bands. Only these modes are active at sufficiently low temperatures, however, whence the resistance arising from the s-p- to d-band transitions should drop to zero at low temperatures much more rapidly than the resistance arising from s-p- to s-p-band jumps.

Wilson's result for the resistivity arising from the s-p- to d-band transitions at temperature T is

$$\rho = \frac{2m_s m_d}{n_0 e^2 \epsilon_0'^{\frac{1}{2}}} P_{sd} \left(\frac{T}{\Theta_D}\right)^3 \int_{\frac{\Theta'}{T}}^{\frac{\Theta_D}{T}} \frac{z^3 dz}{(e^z - 1)(1 - e^{-z})} \tag{11}$$

where Θ_D is the characteristic temperature,

$$\epsilon_0' = \frac{h^2}{2m_s} k_{0s}^2,$$

$$P_{sd} = \left(\frac{3}{4\pi}\right)^{\frac{1}{3}} \frac{3\pi^2 \epsilon_0'^2}{\sqrt{2} m_s^{\frac{1}{2}} M a k \Theta_D},$$

and $k\Theta'$ is the energy of the lowest vibrational frequency that scatters electrons between the s-p and d bands, that is,

$$k\Theta' = h|k_{0s} - k_{0d}|c$$

where c is the velocity of the elastic waves. The a in the denominator of P_{sd} is the lattice parameter.

At high temperatures, Eq (11) approaches the value

$$\rho \cong \frac{m_s m_d}{n_0 e^2 \epsilon_0'^{\frac{1}{2}}} \left(\frac{T}{\Theta_D}\right) P_{sd} \left(1 - \frac{\Theta'^2}{\Theta_D^2}\right)$$

which has the linear temperature-dependence characteristic of the transitions within the s-p band. At low temperatures, however, Eq. (11) approaches zero as

$$e^{-\frac{\Theta'}{T}}.$$

The only extensive measurement of low-temperature resistance seems to be for platinum, which does not show the anomaly one would expect if an appreciable part of its resistivity were described by Eq. (11).

Oe Haas and de Boer,[1] who made the measurements, found that the resistivity ρ can be fitted by the function

$$\rho = CG\left(\frac{\Theta_D}{T}\right) + 1.5 \cdot 10^{-6}\rho_0 T^2 \tag{12}$$

where ρ_0 is the room-temperature resistivity, and G is a Grüneisen function [*cf.* Eq. (45), Sec. 127]. An interpretation of the term in T^2 is given below. There are several reasonable explanations of the fact that a part of the resistance does not obey Eq. (11). (*a*) It is possible that Θ' is accidentally very small for platinum and that the experiments are not accurate enough to distinguish between a contribution to the resistivity of the form $G(\Theta/T)$ and one of the form of Eq. (11) with $\Theta' = 0$. (*b*) It is possible that the *d*-shell electrons should not be treated by the Bloch theory, so that the selection rule (4) is not applicable in the present case. (*c*) It is possible that the *s*-*p*- to *d*-band transitions actually are negligibly small and that the resistance may be explained by extension of the theory of Sec. 127. (*d*) It is possible that the $\epsilon(\mathbf{k})$ relation for the *d* electrons is so different from the free-electron relation (3) that there are many directions in $\mathbf{k}$ space for which $\mathbf{k}_{0s}$ and $\mathbf{k}_{0d}$ are equal. In this case, the very long lattice waves would always play a role, and the *d*-shell resistivity would not decrease so rapidly as an exponential function with decreasing temperature. This problem can be settled only on the basis of more extensive work.

Baber[2] has interpreted the term in Eq. (12) that varies as T^2 in terms of an enhancement of the transitions between *s*-*p* levels due to the presence of the holes in the *d* band. If the holes were rigidly fixed, they would behave like impurity atoms and would give rise to a temperature-independent scattering. If the band approximation may be used, however, the holes are also able to move and should also be scattered. Since they must obey the Pauli principle during these transitions and since the way in which the levels are occupied is temperature-dependent, the resistivity turns out to be temperature-dependent. Baber assumed that the interaction potential of an electron and a hole has the form[3]

$$V(r) = \frac{e^2}{r}e^{-qr}$$

and showed that the observed T^2 term in platinum may be derived by the use of reasonable numerical values of q.

[1] W. J. DE HAAS and J. H. DE BOER, *Physica*, **1**, 609 (1934).
[2] W. G. BABER, *Proc. Roy. Soc.*, **158**, 383 (1937).
[3] The reason for using this potential is discussed in the next section.

130. Residual Resistance. The Resistivity of Alloys*.—Nordheim[1] was the first to point out that the residual resistance of nonsuperconducting metals probably is due to the scattering of electrons by lattice imperfections such as impurity atoms and flaws. This qualitative explanation agrees very well with the fact that the residual resistance of a specimen depends upon its previous history. If Q_i is the cross section for scattering by a given kind of imperfection, such as an impurity atom, and n_i is the density of imperfections, the mean free path l_i for scattering by these imperfections is given by the equation

$$\frac{1}{l_i} = n_i Q_i. \tag{1}$$

Thus, according to Eq. (6), Sec. 126, the residual resistance ρ_i due to this type of imperfection is

$$\rho_i = \frac{mv(\epsilon_0')}{n_0 e^2} n_i Q_i, \tag{2}$$

which is temperature-independent. If Q_i is about 10^{-17}cm^2, which is a customary atomic cross section, and if n is 10^{18} cm^{-3}, which is the concentration of impurities in a reasonably pure specimen of metal, l_i is of the order 0.1 cm. The mean free path for the scattering due to lattice vibrations, which was discussed in the previous sections, approaches this value at temperatures near 15°K in a good conductor such as silver.

In a sense, a disordered alloy may be viewed as a metal in which the impurity content is very high. Hence, if Nordheim's picture is correct, it should be possible to compute the contribution to the resistance of alloys from the disordered atoms by a method similar to that used above in estimating the residual resistance. We shall discuss this resistance on the basis of a procedure developed by Nordheim.

It is known from the discussion of Sec. 127 that the quantities determining the resistance are the squares of the matrix components of potential connecting electronic states. We shall assume for simplicity that the potential V may be written as the sum of potential terms arising from each atom:

$$V = \sum_p v_p(\mathbf{r} - \mathbf{r}(p)) \tag{3}$$

where $v_p(\mathbf{r} - \mathbf{r}(p))$ is the potential of the atom at the position $\mathbf{r}(p)$. We shall also assume that v_p is zero outside the pth cell. The matrix components of V then are

$$V_{\mathbf{k},\mathbf{k}'} = \sum_p \int \psi_{\mathbf{k}}^* v_p \psi_{\mathbf{k}'} d\tau. \tag{4}$$

[1] NORDHEIM, *op. cit.*

The integrand in the pth term in this series is finite only in the pth cell; moreover, the origin of each integrand may be shifted in such a way that it falls at $\mathbf{r}(p)$. Thus, the series may be written in the form

$$V_{\mathbf{k},\mathbf{k}'} = \sum_p e^{2\pi i(\mathbf{k}'-\mathbf{k})\cdot\mathbf{r}(p)} f_{p,\mathbf{k}\mathbf{k}'} \tag{5}$$

where

$$f_{p,\mathbf{k}\mathbf{k}'} = \int \psi_{\mathbf{k}}^*(\mathbf{r}) v_p(\mathbf{r}) \psi_{\mathbf{k}'}(\mathbf{r}) d\tau, \tag{6}$$

in which the integration extends over the cell centered at $\mathbf{r} = 0$. We shall retain the index p because v_p varies from cell to cell if there is more than one kind of ion present. The square of the absolute value of (5) is

$$|V_{\mathbf{k},\mathbf{k}'}|^2 = \sum_{q,p} e^{2\pi i(\mathbf{k}'-\mathbf{k})\cdot[\mathbf{r}(q)-\mathbf{r}(p)]} f^*_{p,\mathbf{k}\mathbf{k}'} f_{q,\mathbf{k}\mathbf{k}'}. \tag{7}$$

Let us suppose that there are s kinds of atom in the alloy and that the fraction of the ith kind is p_i. Then, the mean value of $f_{p,\mathbf{k}\mathbf{k}'}$ is

$$\overline{f_{\mathbf{k}\mathbf{k}'}} = \sum_{i=1} p_i f_{i,\mathbf{k}\mathbf{k}'} \tag{8}$$

where $f_{i,\mathbf{k}\mathbf{k}'}$ is the value of the integral (6) for the ith kind of atom. If we use this mean value of $f_{p,\mathbf{k}\mathbf{k}'}$ in place of the $f_{p,\mathbf{k}\mathbf{k}'}$ in Eq. (5), the sum vanishes since

$$\sum_{p,q} e^{2\pi i(\mathbf{k}'-\mathbf{k})\cdot[\mathbf{r}(q)-\mathbf{r}(p)]}$$

is zero, if $\mathbf{k}' - \mathbf{k}$ is not a principal vector in the reciprocal lattice. This result is not surprising, for the case in which $f_{p,\mathbf{k}\mathbf{k}}$ is independent of p is that of a perfect lattice, in which electrons are scattered only as a result of Bragg reflection or thermal oscillations. With this in mind, Nordheim assumed that the contribution to the effective squared matrix component from the pth atom is the difference of $|f_{p,\mathbf{k}\mathbf{k}}|^2$ and the square of the mean value $|\overline{f_{\mathbf{k}\mathbf{k}'}}|^2$. Although this difference is negative for an atom for which $|f_{p,\mathbf{k}\mathbf{k}'}|^2$ is less than average, the square of the total effective matrix component, namely,

$$|V_{\mathbf{k},\mathbf{k}'}|^2_{\text{eff}} = n(\overline{|f_{p,\mathbf{k}\mathbf{k}'}|^2} - |\overline{f_{\mathbf{k}\mathbf{k}'}}|^2), \tag{9}$$

is positive. Here,

$$\overline{|f_{r\,\mathbf{k}\mathbf{k}'}|^2} = \sum_i p_i |f_{i\,\mathbf{k}\mathbf{k}'}|^2, \tag{10}$$

and n is the total number of atoms. The use of Eq. (9) is equivalent to

assuming that the part of the atomic scattering that is greater or less than the average is incoherent. This evidently can be true only if the alloy has no secondary long-distance order, such as can occur in β brass.

Let us consider a case in which the alloy contains two kinds of atom, A and B, and designate the fraction of A atoms by x. For simplicity we shall consider a unit volume. The value of the quantity (9) then is

$$nx(1 - x)(f_{a,\mathbf{kk}'} - f_{b,\mathbf{kk}'})^2. \tag{11}$$

This function, which is the analogue of the function $B(\mathbf{k}, \delta + \mathbf{K}_s)$ appearing in the theory of lattice vibrational scattering, leads to the equation

$$\frac{1}{l_x} = 16\pi^3\left(\frac{dk}{d\epsilon}\right)_0^2 k_0^2 nx(1 - x)\int_0^\pi (f_{a\,\mathbf{kk}'} - f_{b\,\mathbf{kk}'})^2(1 - \cos\theta)\sin\theta d\theta \tag{12}$$

if we assume that (11) depends only upon θ. If, in addition, we assume that the scattering is isotropic and that $(dk/d\epsilon)_0 = m/h^2k_0$, we obtain

$$\frac{1}{l_x} = \frac{32\pi^3m^2}{h^4}nx(1 - x)(f_{a,\mathbf{kk}'} - f_{b,\mathbf{kk}'})^2.$$

We shall place this equation in the form

$$\frac{1}{l} = nx(1 - x)Q \tag{13}$$

where the quantity

$$Q = \frac{32\pi^3m^2}{h^4}(f_{a,\mathbf{kk}'} - f_{b,\mathbf{kk}'})^2$$

is the atomic cross section.

The resistivity ρ_x', that is associated with this type of scattering, then is

$$\rho_x' = \frac{mv(\epsilon_0')}{e^2}Q'x(1 - x) = \frac{h}{2e^2}\left(\frac{3n}{\pi}\right)^{\frac{1}{3}}Q'x(1 - x). \tag{14}$$

Thus, Nordheim's theory predicts that the temperature-independent part of the resistivity of a disordered solid solution should vary with concentration as $x(x - 1)$. This prediction has been checked in the silver-gold system. It is found that the experimental values of the additional resistivity can be fitted closely by Eq. (14) with

$$Q' = 0.635 \quad 10^{-16}\ \text{cm}^2.$$

Computed and observed values of ρ_x' are listed in Table LXXVIII.

As we mentioned previously, Eq (14) is not valid in a range of concentration in which the alloy has an ordered phase for then more of the scattering is coherent than is assumed in using Eq. (9). Suppose,

for example, that the lattice sites of the two-component alloy can be divided into two sets, namely, a sites, which are occupied by A atoms alone in the perfectly ordered alloy, and b sites, which are occupied by B atoms alone in the same phase. The a sites and the b sites may then be regarded as independent lattices when the temperature-independent resistivity is computed. We know from our previous result that the incoherent scattering is zero when each kind of site is occupied by only one type of atom. Hence, the Nordheim type of resistivity of the perfectly ordered lattice is zero. In a partly ordered state in which there are some B atoms in a sites and some A atoms in b sites and in which there still is a difference between a and b sites, the scattering by the atoms in the two lattices may be computed separately by the use of Eq. (9), the mean values $\overline{f_{a,kk'}}$ and $\overline{f_{b,kk'}}$ evidently being the appropriate matrix components to use in each case. When the long-distance order vanishes, the a and b sites become identical and Eq. (14) is again valid.

TABLE LXXVIII

x	0.01	0.025	0.316	0.629
ρ_x' (obs) $\times 10^6$	0.35	0.86	7.3	8.2
ρ_x' (calc) $\times 10^6$	0.35	0.88	7.6	8.2

The topic of the resistivity in disordered and ordered alloys has been considered in a high degree of detail on the basis of the Bragg-Williams theory by Muto,[1] who found that the resistivity arising from disordering should depend on the long-distance order parameter O in accordance with the equation

$$\rho_0 = A + BO + CO^2$$

in which A, B, and C are temperature-dependent. Muto has shown that this relation is in reasonable agreement with experiment in several interesting cases.

Mott[2] has used an extended form of Nordheim's theory to discuss the resistivity of substitutional alloys of copper (*cf.* Figs. 45 and 49, Chap. I). Let us suppose that an atom having $Z + 1$ electrons outside closed shells is placed in a monovalent metal. In the immediate vicinity of the foreign atom and outside its closed shells, we may expect the potential to be larger than that at the corresponding position near the monovalent atom by an amount

$$\frac{Ze^2}{r}$$

[1] T. MUTO, *Sci. Papers, Inst. Phys. Chem. Res.*, **30**, 99 (1936); **31**, 153 (1937).
[2] N. F. MOTT, *Proc. Cambridge Phil. Soc.*, **32**, 281, 1936.

where r is the distance from the nucleus. The valence electrons will swarm around the more highly charged ion preferentially, however, so that we may expect the difference in potential to vanish for large values of r. Mott assumed that the actual difference varies as

$$\frac{Ze^2}{r}e^{-qr} \tag{15}$$

where q is a constant, $1/q$ being the mean radius of the swarm of valence electrons. The function (15) evidently is an explicit form for the part of the atomic potential that gives rise to incoherent scattering in Nordheim's theory. Using this function and assuming that the electrons are nearly free, Mott found that the increase in resistance per atom per cent of the foreign atom is

$$\rho_0 = \frac{v}{100}\left(\frac{Ze^2}{mv^2}\right)^2\left[\log\left(1+\frac{1}{y}\right) - \frac{1}{(1+y)}\right] \tag{16}$$

where

$$y = \frac{q^2h^2}{16\pi^2mv^2}$$

and v is the electron velocity. This result explains qualitatively the curves shown in Fig. 49, Chap. I. If the foreign atom is a nontransition atom and if the atomic radii are nearly the same, as is true for the atoms that form good solid solutions when mixed, we should expect q to be a constant so that ρ_0 should increase as Z^2. It may be seen that the two curves in Fig. 49 are very nearly parabolic on the positive side of the origin. The value of $1/q$ in this case is of the order of magnitude 0.3 Å. The points obtained by adding transition metals to copper and silver also lie very nearly on parabolas, suggesting that the potential (15) may be used for negative values of Z, which correspond to the number of holes in the transition-element atoms relative to the monovalent atoms.

131. Superconductivity.—Superconductivity, which was discussed very briefly in Chap. I, has developed theoretically in two directions. (1) There has been a phenomenological development in which the observed properties of superconductors are discussed in terms of the functions of thermodynamics and of Maxwell's equations. (2) There has been a very rudimentary treatment in terms of the electron theory of solids.

The first development, which is surveyed extensively in a tract by London,[1] leads to the conclusion that, in addition to having a high electrical conductivity, a superconductor is a medium in which the

[1] F. LONDON, *Une conception nouvelle de la supra-conductabilité, actualités scientifiques et industrielles* (Hermann et Cie., Paris, 1937).

magnetic flux is zero, a fact implying a very large diamagnetism. Moreover, the entropy associated with the superconducting state is abnormally low compared with the entropy of a metal in its normal state. Although the unique magnetic characteristics of superconductors are not so spectacular as the electrical properties, their theoretical significance is no less important. The reader is referred to London's article for a detailed discussion of this type of work.

The development along the lines of the electron theory of solids is due principally to Slater[1] and is still in only the most qualitative stage. Slater has suggested that the levels of the entire metal (see Secs. 66 and 98) become discrete, or at least possess extremely low density, at the bottom of the spectrum. In essence, the levels in this region are to be regarded as the residues of the excitation states that occur in the atomic approximation when the atoms of the metal are widely separated. Because of the strong perturbations, however, they cannot be described in terms of ordinary exciton theory Instead, Slater would regard them as possessing extremely intricate wave functions corresponding to a blend of many exciton states, so that the electrons in a comparatively large region of the metal are intimately correlated. Thus, in a schematic way, Slater regards the metal, when in one of these lower states, as an aggregate of very large molecular units extending over one hundred or more atomic distances and having discrete levels that are very finely spaced, but not so finely spaced as they would be if the units were as large as the entire specimen of metal. Being large compared with ordinary molecules, these units should have a large diamagnetism, and Slater suggests that their properties are basically those of a superconductor; hence, he would regard the low-lying low-density levels of the entire metal as the superconducting states. The system can occupy these levels only at temperatures near absolute zero since they have very low statistical weights and are favored only by their low energy. For the reasons discussed in Chap. XIV, we may expect the system to jump to states of higher energy and higher entropy at temperatures above absolute zero, the transition taking the form of one of the three possible types of phase change. The most probable high-entropy states are, of course, those described in the band approximation, in which the metal has normal properties. Presumably, these states differ from the low-entropy ones principally in the fact that the pseudomolecular structure responsible for superconductivity has melted; that is, the electronic motions are no longer correlated over many atomic distances, but only over a few, as in the approximations developed in preceding chapters. The precise form of the change from the superconducting to the ordinary state depends upon the density of levels of the entire solid in the region

[1] J. C. SLATER, *Phys. Rev.*, **51**, 195 (1937); **52**, 214 (1937).

between the two types of level, and the theory has not developed to a point where this may be predicted. Experiment shows that the phase change is of the second kind, in which there is a discontinuity in specific heat, but no latent heat.

The difficulties that stand in the way of a quantitative test of any electronic theory of superconductivity obviously arise from the difficulties of handling wave functions for the entire solid in a degree of approximation sufficiently high to include states of the type discussed by Slater. There seems little likelihood that these difficulties will be surmounted in the immediate future.

B. IONIC CONDUCTIVITY

132. General Principles.—It is believed at present that the ionic conductivity of solids is closely connected with the type of lattice imperfections that occur in pure semi-conductors. This idea was first suggested by Frenkel[1] and has been substantiated by subsequent work, the most thorough investigation of the possible types of lattice defect having been made by Schottky and Wagner.[2] We shall begin by discussing their work.

Let us consider a crystal of composition MX, such as a monovalent metal halide or an alkaline-earth oxide or sulfide. If the crystal is entirely perfect in its equilibrium state, a volume ionic conductivity is found only if positive or negative ions leave their normal sites and wander in the lattice because of the influence of the field. In this case, the crystal lattice would develop imperfections as an effect of the field. It is evident, however, that a very large field would be required to dislodge an ion from its normal position, for the potential energy of an ion varies by an amount of the order of magnitude of 1 volt in an interatomic distance. Thus, a field of millions of volts per centimeter would be required to induce a current. Hence, it is necessary to assume that the ions carrying the volume ionic current are wandering before the field is applied and that the field simply disturbs the statistical distribution of motion.

There are two ways in which ions may move through the crystal (*cf.* Fig. 6). (1) They may move through interstitial positions which are unoccupied in the perfect crystal. (2) They may move by jumping into vacant sites. In the second case, it is common to say that the vacancies move through the lattice and carry the current. Specific examples of crystals in which these types of conductivity occur are discussed below.

[1] J. FRENKEL, *Z. Physik*, 35, 652 (1926).

[2] C. WAGNER and W. SCHOTTKY, *Z. physik. Chem.*, **B11**, 163 (1930). C. WAGNER, *Z. physik. Chem.*, Bodenstein Fest., 177 (1931); **B22**, 181 *ff.* (1933).

In order to derive an equation for the conductivity of the interstitial ions or the vacancies, we shall employ the same model of the flow process that was used in the derivation of the equation for the jump frequency of diffusing atoms in Sec. 122. According to this work, the probability per unit time that the interstitial atom or the vacancy will jump in one of the α directions, in which there is a saddle point of height ϵ_s, is

$$\tilde{\nu} = \frac{1}{\alpha} \frac{(kT)^3}{h^3 \nu_s^2} e^{-\frac{\epsilon_s}{kT}} \tag{1}$$

in the absence of an electrostatic field. Here, ν_s is the vibration frequency in the two directions in the saddle point that are normal to the direction of flow. We shall treat a simple model in which there are six saddle points of energy ϵ_s, which lie along the six axial directions relative to

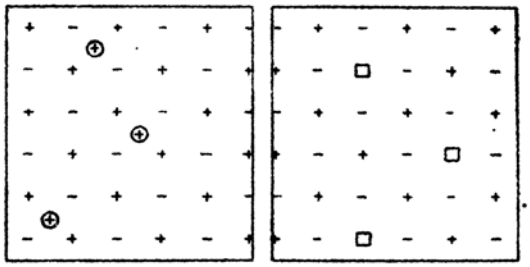

(a) (b)

FIG. 6.—Schematic representation of the two modes of ionic motion. In (a) the interstitial ions ⊕ diffuse through the interstitial sites. In (b) the ions move via the vacancies □.

the equilibrium point. Let us now assume that there is an electrostatic field of intensity E in the x direction. The saddle point lying in the direction of the field relative to a given equilibrium position is lowered by an amount $Ee\delta/2$ where $\delta/2$ is the distance between the equilibrium position and the saddle point and e is the charge on the ion or vacancy. Hence, the jump frequency for this barrier is changed to

$$\tilde{\nu}_E{}^+ = \frac{1}{\alpha} \frac{(kT)^3}{h^3 \nu_s^2} e^{-\frac{\epsilon_s}{kT}} e^{\frac{Ee\delta}{2kT}}. \tag{2}$$

The saddle point in the opposite direction is raised by the same amount so that the jump frequency in the backward direction is

$$\tilde{\nu}_E{}^- = \frac{1}{\alpha} \frac{(kT)^3}{h^3 \nu_s^2} e^{-\frac{\epsilon_s}{kT}} e^{-\frac{Ee\delta}{2kT}}. \tag{3}$$

Thus, the excess probability for jumping in the field direction is

$$\tilde{\nu}_E = \tilde{\nu}_E{}^+ - \tilde{\nu}_E{}^- = \tilde{\nu}\, 2 \sinh \frac{Ee\delta}{2kT}. \tag{4}$$

We shall be interested in fields so weak that $E e\delta << kT$, in which case

$$\bar{\nu}_p = \bar{\nu}\frac{E e\delta}{kT}. \tag{5}$$

Since the electrical polarization associated with each favorable jump is $e\delta$, the current i per unit area is

$$i = n\bar{\nu}\frac{E e^2\delta^2}{kT} \tag{6}$$

where n is the number of interstitial ions or vacancies per unit volume. Thus, the contribution σ to the conductivity from this flow is

$$\sigma = n\bar{\nu}\frac{e^2\delta^2}{kT}. \tag{7}$$

The conductivity and ionic mobility are related by the equation

$$\sigma = ne\mu \tag{8}$$

whence

$$\mu = \bar{\nu}\frac{e\delta^2}{kT}. \tag{9}$$

Equation (7) may be compared with the similar equation derived by Lorentz on the basis of a free-particle model, namely,

$$\sigma = n_f\frac{e^2\bar{v}l}{3kT} \tag{10}$$

[cf. Eq. (5), Sec. 126.] Here, $\bar{v} = 4\sqrt{kT/2\pi M}$, l is the mean free path, and n_f is the density of free ions. Equations (7) and (10) are formally equivalent if we make the correspondence

$$l \sim \delta, \qquad \frac{n_f\bar{v}}{3} \sim n\bar{\nu}\delta.$$

If more than one kind of interstitial ion or vacancy is present in the lattice, the total ionic conductivity may be obtained by adding together the contributions of type (7) from each kind of ion.

The temperature dependence of n in Eq. (7) is determined by the particular way in which the lattice defects occur. We have discussed two types of defect in Sec. 110, namely, those which occur in the alkali halides and those which occur in zinc oxide and zinc sulfide. In the first case, it is believed that the metal-ion lattice and the halogen-ion lattice have equal numbers of vacancies so that the number of vacancies of a given kind is

$$n = Ne^{-\frac{\epsilon''}{2kT}} \tag{11}$$

when the crystal is in thermal equilibrium. Here, ϵ'' is the energy required to take an alkali-metal ion and a halogen ion from the interior to the surface of the crystal, and N is the total number of ions of a given kind. In the second case, it is believed that oxygen and sulfur atoms, respectively, evaporate and the excess metal atoms diffuse into the interstices of the crystal. The number of interstitial atoms in this case is

$$n = N_{O_i}^{-\frac{1}{2}} B' e^{-\frac{\epsilon''}{kT}} \tag{12}$$

where ϵ'' is the energy required to produce an interstitial zinc atom and an oxygen atom, the latter being bound to another to form a molecule in the vapor phase These two cases do not exhaust the possible types. Schottky and Wagner have pointed out that there are in all the following three independent types.

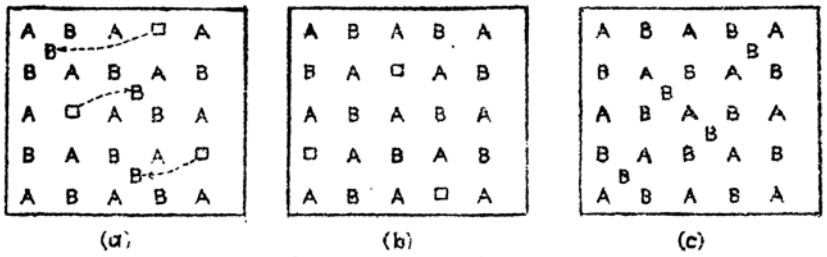

FIG. 7.—The three types of lattice defects. In (*a*) some of the *B* atoms have moved to interstitial places leaving vacancies. (*b*) *B* atoms have evaporated leaving vacancies in the lattice. There are no interstitial atoms. In the alkali halides there are equal numbers of *A* and *B* vacancies. An excess of one type or the other may be obtained, however, by heating the crystal in an appropriate vapor. (*c*) A fraction of the *A* atoms have evaporated from the surface leaving an excess of *B* atoms which diffuse into interstitial positions.

I (*cf.* Fig. 7*a*). There are interstitial M or X ions (or atoms) and there are in each of these cases an equal number of vacant M or X sites, respectively. If $n\epsilon$ is the energy required to rempve n ions of a given kind to form n vacancies and n interstitial ions and if $-2kTn \log (n/N)$ is the entropy gained in doing so, the equilibrium value of n/N is

$$\frac{n}{N} = e^{-\frac{\epsilon}{2kT}} \tag{13}$$

where N is the total number of ions of the given kind.

IIa (*cf.* Fig. 7*b*). Some M or X atoms evaporate, leaving an equal number of vacancies in M or X sites. Since the evaporating atoms must be neutral, there is an excess or a deficit of electrons in these two cases. These electrons or holes should reside near the vacancies in the lowest energy state. This case is similar to I, the difference being that there are no interstitial atoms in the lattice in the present case

II*b*. We may classify separately the case in which the positive and negative ions leave in equal numbers. This ordinarily occurs in the alkali halides, for which the equilibrium value of n is given by an equation of the type (11).

III (*cf.* Fig. 7*c*). A fraction of one of the constituents may evaporate, leaving an excess of the other in interstitial sites. Zinc oxide and zinc sulfide, which were mentioned above, belong to this class.

We might expect that the deviations of type I and III, which involve interstitial atoms, should occur primarily in lattices that have large interstitial spaces, such as the zincblende and wurtzite structures, which have low coordination numbers.

Jost[1] has investigated the relative probability of case I and case II*b* for crystals having the sodium chloride structure, in which the interstitial spaces are comparatively small. If the values of n and ϵ'' in the two cases are distinguished by subscripts I and II, we have from Eqs. (11) and (13)

$$\frac{n_{\mathrm{I}}}{n_{\mathrm{II}}} = \frac{e^{-\frac{\epsilon_{\mathrm{I}}''}{2kT}}}{e^{-\frac{\epsilon_{\mathrm{II}}''}{2kT}}} = e^{-\frac{\epsilon_{\mathrm{I}}''-\epsilon_{\mathrm{II}}''}{2kT}}. \tag{14}$$

Let us compute the difference $\epsilon_{\mathrm{I}}'' - \epsilon_{\mathrm{II}}''$ on the assumption that the interionic distances near a vacancy or near an interstitial ion are the same as for a perfect crystal. For simplicity, it may be assumed that the repulsive potential between ions varies as b/r^n where $n \sim 9$. The energy of an ion in a normal site then is (Sec. 11)

$$\epsilon = -1.746\frac{e^2}{a_0}\left(1 - \frac{1}{n}\right), \tag{15}$$

and the energy necessary to remove both a positive and a negative ion completely from the lattice is twice the negative of this. If, however, the ions are brought only to the surface, the energy should be -2ϵ minus the energy required to remove a positive and a negative ion from the surface, which is just the heat of sublimation per molecule. Hence, in the present approximation,

$$\epsilon_{\mathrm{II}}'' = -\epsilon. \tag{16}$$

The electrostatic energy of an interstitial ion in an undistorted sodium chloride lattice is zero because the relationship between the distribution of positive and negative ions is a symmetrical one. The distance between

[1] W. Jost, *Jour. Chem. Phys.*, **1**, 466 (1933); *Z. physik. Chem.*, **A169**, 129 (1934); *Physik. Z.*, **36**, 757 (1935). See also *Diffusion und chemische Reactiones in festen Stoffen* (J. Steinkopf: Leipzig, 1937).

the center of the interstitial-ion site and the centers of the neighboring ions is $a\sqrt{3}/2$, whence the repulsive energy for the interstitial atom is

$$\epsilon_r \sim 1.74\frac{e^2}{na}\left(\frac{2}{\sqrt{3}}\right)^n\frac{2}{3}$$

where the factor $\frac{2}{3}$ enters because there are only four neighboring halogen ions instead of six, as for an ordinary ion. Hence,

$$\epsilon_{\mathrm{I}}'' = -\epsilon + \epsilon_r,$$

and

$$\epsilon_{\mathrm{I}}'' - \epsilon_{\mathrm{II}}'' = \epsilon_r. \tag{17}$$

This difference is of the order of magnitude 1 ev for the alkali halides so that

$$\frac{n_{\mathrm{I}}}{n_{\mathrm{II}}} \sim e^{-\frac{5,700}{T}}$$

Thus, case II*b* is much more probable than case I under the assumptions made above.

It is clear, however, that these assumptions must be seriously in error, for the magnitude of $\epsilon_{\mathrm{II}}/2$ as given by Eq. (16) is about 3.7 ev for sodium chloride. According to Eq. (7), the activation energy for ionic conductivity should be at least as large as this, whereas the observed value[1] is only 1.90 ev. A reasonable explanation of this discrepancy is that the atoms or ions around vacancies and interstitial atoms become displaced from their normal positions in the undeformed lattice and thus lower the energy of the lattice. The source of the additional energy is not hard to find. If an ion of charge e is removed from a site, the region about the vacancy is left with an excess charge $-e$. This charge should polarize the surrounding lattice and the energy of the equilibrium state should be lower than that of the undeformed lattice by the polarization energy; moreover an interstitial ion should polarize the lattice in a similar way. If the charges occupied a spherical domain of radius r and if the medium were continuous and had a static-field dielectric constant κ_s, the polarization energy would be

$$= -\frac{e^2}{2r}\left(1 - \frac{1}{\kappa_s}\right). \tag{18}$$

The energy actually should be computed with the use of a more detailed atomic picture; however, we shall use Eq. (18) for an order-of-magnitude estimate. For vacancies, it will be assumed that r is equal to the mean ionic radius, that is, to $a/2$, and for interstitial ions it will be assumed

[1] W. LEHFELDT, *Z. Physik*, **85**, 717 (1933).

that r is equal to half the distance between the center of an interstitial site and the nearest ion site, namely, $a\sqrt{3}/4$. The energy required to produce an interstitial ion in case I then is

$$\epsilon_{\mathrm{I}}'' = -\epsilon + \frac{e^2}{a}\left[\frac{1.74}{n}\left(\frac{2}{\sqrt{3}}\right)^n \frac{2}{3} - \left(1 - \frac{1}{\kappa_s}\right)\frac{2}{\sqrt{3}} - \left(1 - \frac{1}{\kappa_s}\right)\right], \quad (19)$$

and the energy required to produce a vacancy in each lattice is

$$\epsilon_{\mathrm{II}}'' = -\epsilon - \frac{2e^2}{a}\left(1 - \frac{1}{\kappa_s}\right). \quad (20)$$

When the static dielectric constants of the alkali halides, which are of the order of magnitude 6, are used in these equations, the value of the additional negative terms in (19) are comparable with ϵ and reduce ϵ_{II}'' to values that are much more nearly in accord with the experimental activation energies. The difference between Eqs. (19) and (20) is

$$\epsilon_{\mathrm{I}}'' - \epsilon_{\mathrm{II}}'' \cong \frac{1.74e^2}{2a}\left[0.54 - 0.18\left(1 - \frac{1}{\kappa_s}\right)\right]. \quad (21)$$

The negative term reduces the difference to a value somewhat below that of Eq. (17) but does not reduce it enough to change the previous conclusion that the ratio (14) is very small. Jost and Nehlep[1] have made a more accurate estimate of $\epsilon_{\mathrm{I}}'' - \epsilon_{\mathrm{II}}''$ by taking into account the actual displacements of nearest ions. They find the value $0.40(1.74e^2/2a)$ for the extreme case in which κ_s is infinite. Since the difference should be larger than this in actual cases, we may conclude that deviations of type I do not occur in the crystals having sodium chloride structure for which only the electrostatic and repulsive terms of the Born theory are important. This includes practically all the alkali halides and probably the oxides and sulfides of beryllium, magnesium, and calcium.[2]

We saw in Chap. II that the van der Waals energy plays an important role in the halides of metals such as silver and thallium which have newly filled d shells. Jost and Nehlep have investigated the cohesive energy of interstitial metal ions in crystals of this type and have found that the contribution to $\epsilon_{\mathrm{I}}'' - \epsilon_{\mathrm{II}}''$ from the van der Waals term may reasonably reverse the sign of this difference. Thus, they find that in silver bromide, which has the sodium chloride structure, the correction to $\epsilon_{\mathrm{I}}'' - \epsilon_{\mathrm{II}}''$ should be

[1] W. JOST and G. NEHLEP, *Z. physik. Chem.*, **B32**, 1 (1936).

[2] A careful analysis of the contributions to the activation energy for electrolytic conductivity in sodium chloride has also been given by N. F. Mott and M. J. Littleton, *Trans Faraday Soc.*, **34**, 485 (1938).

$$-1.0\left(\frac{1.74e^2}{2a}\right),$$

which is sufficient to reverse the sign of (21). Although this result is not yet conclusive, it does show that case I is a possibility in some salts having sodium chloride structure.

Let us now discuss the ionic conductivity of the alkali halides on the assumption that they belong to class IIa. The number of vacancies of each kind then is $Ne^{-\frac{\epsilon''}{kT}}$, and the equation for the total ionic conductivity may be placed in the form

$$\sigma = N\frac{e^2\delta^2}{kT}e^{-\frac{\epsilon''}{2kT}}(\tilde{\nu}_+ + \tilde{\nu}_-) \tag{22}$$

where $\tilde{\nu}_+$ and $\tilde{\nu}_-$ are the jump frequencies for the two types of vacancy. The distance δ between neighboring like ions is the same in the two cases. In sodium chloride, the vacancies undoubtedly diffuse in the twelve (110) directions instead of in the six (100) directions as assumed in deriving (22). This fact does not impair the use of Eqs. (1) and (22) for an order-of-magnitude estimate of ν_s. According to Eq. (22) the ratio of the transport numbers of the two ions is determined by the ratio of the two terms in parenthesis. Tubandt's measurements on the transport numbers of the ions in NaCl show that the sodium-ion vacancies carry about 92 per cent of the current at 580°C. For this reason, we shall neglect $\tilde{\nu}_-$ in Eq. (22) for this substance. The equation may then be placed in the form

$$\sigma = Ae^{-\frac{\epsilon}{kT}} \tag{23}$$

where

$$\left.\begin{aligned} A &= N\frac{e^2\delta^2}{kT}\frac{1}{\alpha}\frac{(kT)^3}{h^3\nu_s^2}, \\ \epsilon &= \frac{\epsilon''}{2} + \epsilon_s. \end{aligned}\right\} \tag{24}$$

Lehfeldt's measured value of A (*cf.* Fig. 66, Chap. I) is 10^6 ohm^{-1} cm^{-1}. If we assume that

$$\begin{aligned} \delta &= 2.8 \times 10^{-8} \text{ cm}, \\ kT &= 1.0 \times 10^{-13}, \\ N &= 2.24 \times 10^{22}, \end{aligned}$$

and solve for $1/\nu_s^2$, we find

$$\nu_s^2 \sim \frac{17 \times 10^{22}}{\alpha}, \tag{25}$$

or $\nu_s \sim 10^{11}$. This value, which is surprisingly low, implies that the saddle point is very flat in the direction at right angles to the direction of flow. It is possible, however, that the assumption made in deriving Eq. (7), namely, that the potential energy is determined by the position of the ion or vacancy alone, is far from correct and that many ions should be taken into account in computing the jump frequency of a vacancy. It is also possible, as has been suggested by Jost,[1] that ϵ is not temperature-independent but contains a linear term of the type qT. In this event, as in the case of thermionic emission, the measured value A^* of the intercept of the logarithmic plot would be a composite quantity of the form

$$A^* = Ae^{-\frac{q}{k}}$$

in which A is the computed constant (24). Jost has shown that the exponential factor in this equation may reasonably be of the order of magnitude 1,000.

At lower temperatures, the measured conductivities deviate from Eq. (23) in a way that depends upon the previous history of the crystal (*cf.* Fig. 66) This change may be described by saying that ϵ decreases with decreasing temperature. It is possible that the rate at which the equilibrium value of n is attained becomes so slow at temperatures below a temperature T' that the value of n for this temperature is retained. In this case, the temperature dependence of σ would be determined by ϵ_s alone. The slope of the low-temperature part of Lehfeldt's log σ versus $1/T$ plots for the alkali halides is usually about one-third that of the high-temperature part. Hence, if the preceding interpretation of this change is correct, this value shows that

$$\epsilon_s \sim \frac{1}{3}\left(\frac{\epsilon''}{2} + \epsilon_s\right)$$

or

$$\frac{\epsilon''}{2} \sim \frac{2}{3}\epsilon_s \tag{26}$$

where ϵ is the high-temperature activation energy.

An alternative interpretation of the difference in slope of the low- and high-temperature portions of the curve is that the low-temperature conductivity arises from a very small number of ions that are situated at surfaces of internal cracks of the crystal and are more free to move than the ions in ordinary sites. It does not cem to be possible to decide between these alternatives at the present time.

[1] W. JOST, *Z. physik. Chem.*, A169, 129 (1934).

If Eq. (26) may be used, the ratio r of the number of vacancies to the total number of ions may be computed from the equation

$$r = e^{-\frac{\epsilon''}{2kT}} \cong e^{-\frac{2}{3}\frac{\epsilon}{kT}}.$$

Using the value $\epsilon = 1.90$ for sodium chloride, we find that $r \sim 10^{-6}$ at the melting point.

As we have seen above, it is not possible to say definitely in which category silver chloride and silver bromide may be placed, although Jost and Nehlep's computations indicate that they belong to class I. If the ratio of vacancies to normal atoms were large enough, it would be possible to distinguish between case I and case II*b* by a comparison of the measured density and the density computed from X-ray data by assuming that there are no vacancies. In case I, the two should agree since there is one interstitial ion for each vacancy. In case II*b*, however, the computed density should be larger than the measured one by a factor $(1 - r)^{-1}$ where r is the ratio of the number of vacancies to the number of normal ions. If we examine Fig. 66, Chap. I, we may see that the high-temperature slope is about twice the low-temperature value for silver chloride and silver bromide. Hence, in place of Eq. (26) we have

$$\epsilon'' = \epsilon. \tag{27}$$

For silver bromide, the value of r at the melting point computed[1] in this way is

$$r = e^{-\frac{\epsilon}{2kT}} = 10^{-2.8}. \tag{28}$$

The experimental accuracy of density and lattice constant measurements is not large enough[2] to detect the difference in densities that would arise from this value of r in case II*b*. Wagner and Koch,[3] however, have used an ingenious indirect method, involving conductivity measurements, to determine the number of lattice defects in AgBr at various temperatures. Their method is based on the fact that the number of holes in AgBr may be increased by adding fixed quantities of $PbBr_2$. The lead salt forms a perfect solid solution when present in small concentrations. Since the lead ion is divalent, each ion added replaces two silver ions; hence, one vacancy is produced in the silver-ion lattice for each dissolved lead ion. The conductivity per vacancy may be determined from an investigation of the increase in conductivity as lead is

[1] F. SEITZ, *Phys. Rev.*, **54**, 1111 (1938); **56**, 1063 (1939).

[2] Density measurements have been made by C. Wagner and J. Beyer, *Z. physik. Chem.*, **B32**, 113 (1936). See *ibid.* for the reason why the conclusions drawn by these workers are not trustworthy.

[3] E. KOCH and C. WAGNER, *Z. physik. Chem.*, **B38**, 295 (1938).

added, and the result may then be used to determine the number of vacancies in the pure crystal. Table LXXIX gives a comparison of the fraction of vacancies determined in this way with the fraction determined from Eq. (27). The computed values are off by a factor 5, a discrepancy that is not surprising in view of the simplifying assumptions used in the theoretical computation.

TABLE LXXIX.—COMPARISON OF THE FRACTION OF VACANT SITES IN SILVER BROMIDE AT VARIOUS TEMPERATURES AS DETERMINED BY EQ. (27) AND BY THE METHOD OF KOCH AND WAGNER

T, °C	r (theor.) $\cdot 10^3$	r (exp.) $\cdot 10^3$
300	0.71	4.0
250	0.36	1.8
210	0.18	0.76

If we compare Eq. (7) with Eq. (16) of Sec. 122 for the diffusion coefficient, namely,

$$D = \frac{n}{N}\bar{\nu}\delta^2,$$

we obtain the important relation

$$\sigma = N\frac{e^2}{kT}D. \tag{29}$$

This relation has been checked by von Hevesy and Seith[1] for PbI_2, in which the conductivity of Pb^{++} is known. They determined the diffusion coefficient of radioactive lead in single crystals of PbI_2 and compared this value with that computed from Tubandt's measured values of σ by means of relation (29). The two agree, within experimental error, in the temperature range from 255° to 290°C.

Von Hevesy and Seith have also measured the rate of diffusion of radioactive lead in $PbCl_2$. The positive-ion transport number is immeasurably small in this case, but by use of Eq. (29) they obtained the equation

$$\sigma(\text{ohm}^{-1}\,\text{cm}^{-1}) = 9.78 \cdot 10^{-4} e^{-\frac{4{,}180}{T}} + 1.15 \cdot 10^{5} e^{-\frac{15{,}000}{T}}$$

for the total conductivity. The first term is the chlorine-ion conductivity which was measured directly; the second term is the positive-ion conductivity which was computed by means of (29). The types of lattice defect that occur in $PbCl_2$ have not been determined, and so it is not

[1] G. VON HEVESY and W. SEITH, *Z. Physik*, **56**, 790 (1929); **57**, 869 (1929).

yet possible to give an interpretation of the large difference in the coefficients in this equation.

C. PHOTOCONDUCTIVITY

133. The Mean Free Path of Free Electrons in Ionic Crystals.—The semiempirical computations of the mean free path of free electrons in semi-conductors that were discussed in Part B of Chap. IV indicate that at room temperature the path is of the order of an interatomic distance, and is usually less than the mean free path of an electron in a metal. This result is not surprising, for the metal lattice is nearly at complete equilibrium when the conduction electrons move through it, whereas the ionic crystal is under stress.

We shall consider the simplified model of a crystal that is practically isotropic and shall discuss the scattering by the vibrational modes of frequency ν. If the kinetic energy ϵ of the free electron is greater than $h\nu$, the electron may lose energy to the lattice as well as gain it. It follows from the discussion of Sec. 127 that the probabilities that these processes will occur in unit time ar of the form

$$\left.\begin{matrix} A_\nu(\epsilon)(n_\nu + 1), \\ A_\nu(\epsilon)n_\nu, \end{matrix}\right\} \tag{1}$$

respectively, where in the isotropic case $A_\nu(\epsilon)$ is dependent only upon the electronic energy, and n_ν is the mean vibrational quantum number per oscillator, that is,

$$n_\nu = \frac{1}{e^{\frac{h\nu}{kT}} - 1}. \tag{2}$$

Thus, the total probability per unit time that the electron will be scattered by a lattice vibration of frequency ν is

$$P_\nu = A_\nu(\epsilon)(2n_\nu + 1) \qquad (\epsilon > h\nu). \tag{3}$$

In the case in which the electronic energy is less than $h\nu$, the electron cannot lose energy to the lattice so that

$$P_\nu = A_\nu(\epsilon)n_\nu \qquad (\epsilon < h\nu). \tag{4}$$

Thus, an electron having energy greater than $h\nu$ is scattered by the waves of frequency ν even at absolute zero of temperature, whereas one having energy less than ν is not. The total probability of scattering may be obtained by summing expressions of the type (3) and (4) over all lattice frequencies. We may expect that the terms for which $\nu < \epsilon/h$ will lead to a finite mean free path even at absolute zero.

We shall not discuss the computation of the function $A(\epsilon)$ in complete detail[1] but shall give a simplified discussion, due to Seeger and Teller,[2] of the case in which $n_r = 0$. This result may then be used to estimate the mean free path.

If it is assumed that a free electron in an ionic crystal is scattered isotropically by inelastic collisions in which it loses energy and that the average energy lost per collision is $h\nu_m$ where ν_m is the vibrational frequency of the optically active mode, the mean free path l and the energy loss per unit distance dW/dS should be related by the equation

$$h\nu_m = l\frac{dW}{dS}. \tag{5}$$

We shall use this equation to compute l after computing dW/dS by the method employed by Seeger and Teller. The equation evidently is valid only if the collisions are nearly isotropic. This condition is satisfied for electrons having energies not too large in comparison with $h\nu_m$ since the changes in velocity resulting from individual collisions then are comparable with the initial velocity. It is not satisfied, however, when the electronic energy is very large compared with $h\nu_m$, for then the collisions are predominantly through small angles, as in the case of electrons in metals.

An electron that is passing through an ionic crystal ordinarily moves so quickly, even when it has thermal energy, that the ions do not have time to come to complete equilibrium under the force of the electron. This fact is, of course, the basis of the Franck-Condon principle. For this reason, we shall assume that only that part of the polarization of the crystal arising from the electronic displacement is induced by the moving electron. The dielectric constant associated with this polarization is simply n^2, where n is the refractive index extrapolated for infinite wave length. The electrostatic field strength at a distance r from the electron then is

$$E = -\frac{e}{n^2r^2}\mathbf{r}_1 \tag{6}$$

where $\mathbf{r}_1$ is a unit vector in the radial direction. Seeger and Teller use

[1] A discussion based entirely upon quantum mechanical perturbation methods may be found in the following papers: H. Fröhlich, *Proc. Roy. Soc.*, **160**, 230 (1937); H. Fröhlich and N. F. Mott, *Proc. Roy. Soc.*, **171**, 496 (1939). This discussion is more complete than the one in the present volume in the sense that temperature dependence is included; however, as Seeger and Teller point out, it is unreliable in the range of energy in which the mean free path is least because the mean time between collisions is of the order of magnitude 10^{-15} sec (see part *g*, Sec. 127). See also *Phys. Rev.*, **56**, 349 (1939).

[2] R. J. SEEGER and E. TELLER, *Phys. Rev.*, **54**, 515 (1938). See also *Phys. Rev.*, **56**, 352 (1939).

a slightly different constant for the coefficient of e/r^2, but the simple value $1/n^2$ is at least as accurate as theirs, in the writer's opinion.

Let us suppose that an electron moving with velocity v passes at distance b from an ion having charge Ze. The force f normal to the direction of the electron velocity at time t is

$$f = \frac{1}{n^2} \frac{Ze^2}{b^2 + v^2t^2} \frac{b}{\sqrt{b^2 + v^2t^2}}, \tag{7}$$

in which the origin of t is chosen as the time of closest approach. The total impulse p transferred to the ion by the electron is the time integral of (7), namely,

$$p = \frac{2}{n^2} \frac{Ze^2}{vb}, \tag{8}$$

which is equivalent to the energy

$$\bar{\epsilon} = \frac{p^2}{2M} = \frac{2}{n^4} \frac{Z^2e^2}{Mb^2v^2}$$

where M is the ionic mass. Thus, the amount of energy that the electron loses to those ions lying within a cylindrical shell of radius b and thickness db in traveling unit distance is

$$\delta\left(\frac{dW}{dS}\right) = \bar{\epsilon} \frac{\pi b db}{d^3}, \tag{9}$$

in which d is the distance between like ions. If the lattice is of the type, such as sodium chloride, that is symmetrical in two types of ion, the total differential energy loss then is the sum of terms of type (9) for both types of ion. Setting

$$\frac{1}{\mu} = \frac{1}{M_1} + \frac{1}{M_2}$$

where M_1 and M_2 are the masses of the two kinds of ion, we may write this sum in the form

$$\delta\left(\frac{dW}{dS}\right) = \frac{2}{n^4} \frac{Z^2e^4}{\mu b^2v^2} \frac{\pi b db}{d^3}. \tag{10}$$

It may seem from Eq. (10) that $\delta(dW/dS)$ decreases as $1/b$, which shows that the *total* effect of distant ions is much greater than that of the ions through which the electron passes. Hence, we may integrate Eq. (10) with reasonable accuracy by treating the solid as though continuous. Thus,

$$\frac{dW}{dS} \cong \int \frac{2\pi Z^2 e^4}{n^4 \mu b^2 v^2} \frac{db}{b}, \tag{11}$$

in which the limits are yet to be specified.

We shall assume that the time τ during which the distance between the electron and ion is of the order of magnitude b may be taken as $2b/v$. In order that Eq. (11) shall be valid, this must be short compared

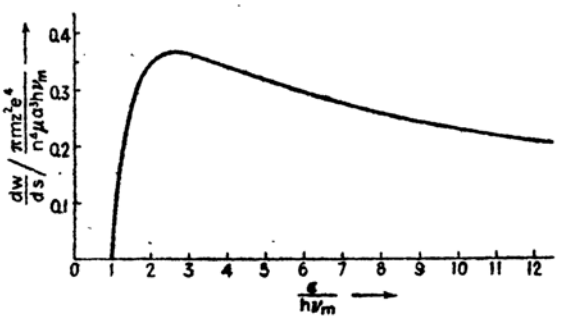

FIG. 8.—The semiclassical excitation function.

with the oscillational time of the optically active frequency, for otherwise the work done by the force averages to zero. Hence, we must have

$$\frac{2b}{v} < \frac{1}{2\pi\nu_m},$$

which gives as the upper limit of integration

$$b_{\max} = \frac{v}{4\pi\nu_m}.$$

As a lower limit, Seeger and Teller take the de Broglie wave length of the electron divided by 2π:

$$b_{\min} = \frac{\lambda}{2\pi} = \frac{h}{2\pi mv}.$$

Using these limits in Eq. (11), we find

$$\frac{dW}{dS} = \frac{2\pi Z^2 e^4}{n^4 \mu a^3 v^2} \log\left(\frac{mv^2/2}{h\nu_m}\right) \equiv \frac{\pi m Z^2 e^4}{n^4 \mu a^3} \frac{1}{\epsilon} \log \frac{\epsilon}{h\nu_m}, \tag{12}$$

where $\epsilon = mv^2/2$. This function, which is shown in Fig. 8, has the maximum value

$$\left(\frac{dW}{dS}\right)_{\max} = 0.37 \frac{\pi m Z^2 e^4}{n^4 \mu a^3 h\nu_m} \tag{13}$$

when $\epsilon = 2.7 h\nu_m$.

Combining Eqs. (1) and (10), we obtain

$$l = \frac{h\nu_m}{dW/dS} = \frac{n^4\mu a^2 h\nu_m}{\pi m Z^2 e^4} \frac{\epsilon}{\log \epsilon/h\nu_m}. \tag{14}$$

The minimum values of l, corresponding to $\epsilon = 2.7h\nu_m$, are listed in Table LXXX for several alkali halides.

TABLE LXXX.—THE MEAN FREE PATHS OF ELECTRONS IN IONIC CRYSTALS

	n^2	$l_{\min} \cdot 10^8$ cm	$E_B \cdot 10^{-5}$, volts/cm	
			Calculated	Observed, room temperature
LiF	1.93	4.74	15.4	31
NaCl	2.19	5.0	4.7	15
KCl	2.19	4.0	4.8	10
KI	2.40	6.4	2.0	5.7
RbBr	2.40	7.4	1.6	6.3
RbI	2.85	12.9	0.81	4.9

These results obviously should apply only at the absolute zero of temperature and then only very approximately in the low-energy range where $\epsilon \sim h\nu_m$, for it has been assumed that the crystal possesses a single lattice vibrational frequency whereas actual crystals possess a continuous range of frequencies extending from zero to ν_m. Thus the actual dW/dS curve for absolute zero should not drop sharply to the axis at $\epsilon = h\nu_m$ but should continue smoothly to the origin.

Von Hippel[1] has suggested that dielectric breakdown in insulators occurs when the electrostatic field becomes so strong that on the average a free electron in the lattice can gain more energy from the field between collisions than it loses as a result of collisions. If E_B is the breakdown field, von Hippel's condition is

$$E_B l_{\min} = h\nu_m. \tag{15}$$

By use of Eq. (1), this may be transformed to the form

$$E_B = \left(\frac{dW}{dS}\right)_{\max} \tag{16}$$

[1] A. VON HIPPEL, *Jour. Applied Phys.*, **8**, 815 (1937). Discussions of this and other theories of dielectric breakdown may be found in the following papers: H. Fröhlich, *Proc. Roy. Soc.*, **160**, 230 (1937), **172**, 94 (1939). W. Franz, *Z. Physik*, **113**, 607 (1939); Seeger and Teller, *op. cit.*; R. C. Buehl and A. von Hippel, *Phys. Rev.*, **56**, 941 (1939).

The results[1] that are obtained are shown in Table LXXX and are compared with von Hippel's measured values. The computed ones all are smaller than the observed ones. Seeger and Teller suggest that a part of this discrepancy may be due to the use of the actual electronic mass m in Eq. (11) instead of the effective mass for the interior of the crystal. Actually, it seems unlikely that the semiclassical computation of the mean free path is sufficiently trustworthy to merit accurate comparison with experimental results even if (15) is the correct condition for breakdown.

According to the discussion in the earlier part of this section, we should expect the mean free path to decrease with increasing temperature because the n_i in Eqs. (3) and (4) increase with increasing temperature. Thus, the breakdown strength of crystals should increase with increasing temperature if Eq. (15) is valid. Buehl and von Hippel[2] have observed that the dielectric strength of the alkali halides is decreased by cooling from room temperature to liquid-air temperature; however, the observed decrease is much more rapid than is to be expected from Eq. (15). It seems likely, at the present time, that the simple theory of dielectric breakdown needs important revision.[3]

Reasoning from his inability to detect a measurable Hall effect in photoconducting specimens of sodium chloride, potassium chloride, and potassium bromide crystals, Evans[4] has concluded that the mean free path in these crystals at room temperature is less than $4.5 \cdot 10^{-3}$ cm. The Hall effect is easily observable in zinc oxide and zinc sulfide (Sec. 37), and corresponds to mean free paths of 10^{-7} cm. The origin of the difference in properties of these two types of salt remains to be investigated.

134. Photoconductivity in Colored Alkali Halide Crystals.[5]—In this section and the next, we shall discuss the present status of the theory of photoconductivity. The most extensive interpretive work has been done on the photoconductivity of alkali halide crystals that contain F centers. As we have seen in Sec. 111, the properties of these crystals may be explained most reasonably by assuming that they contain more halogen-ion vacancies than alkali-metal-ion vacancies and that the

[1] These values differ somewhat from Seeger and Teller's because of differences in the form of Eq. (6).

[2] BUEHL and VON HIPPEL, *op. cit.*

[3] In an attempt to explain the observed temperature dependence, H. B. Sampson and the writer have pointed out that the primary excitation process of the free electrons is the production of excitons, rather than secondary electrons as is ordinarily assumed. Unless the excitons are dissociated by either the field or temperature, breakdown cannot occur. (To be published shortly.)

[4] J. EVANS, *Phys. Rev.*, **57**, 47 (1940).

[5] See the articles by R. W. Pohl surveying the experimental work, *Proc. Phys. Soc.*, **49** (1937); *Physik. Z.*, **39**, 36 (1938).

excess halogen vacancies are occupied by electrons. In addition to the alkali halides, we shall discuss photoconductivity in zinc sulfide and silver halide crystals.

Let us begin by considering the photoconductivity of colored sodium chloride. The other colored alkali halides behave in an essentially

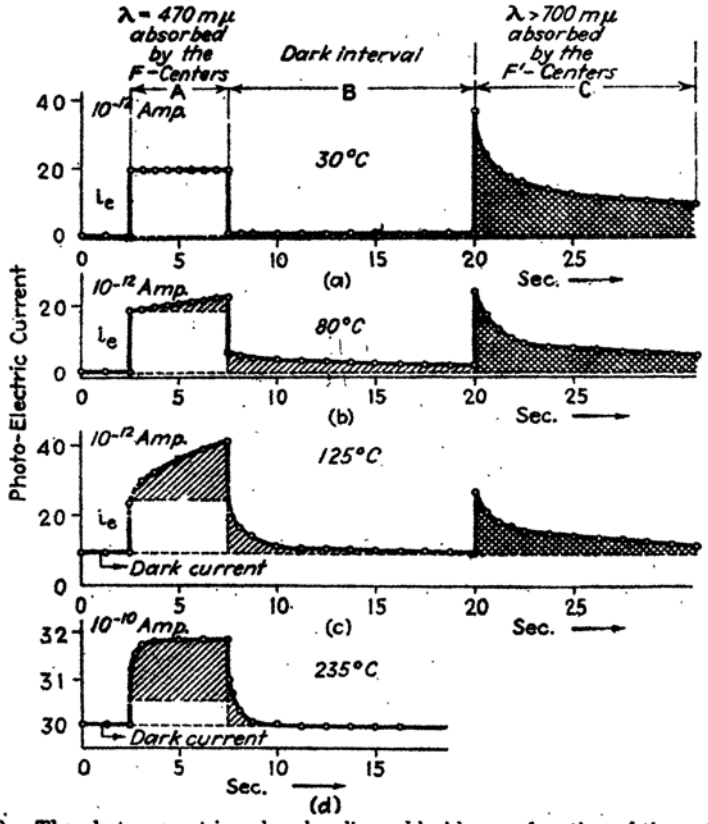

FIG. 9.—The photocurrent in colored sodium chloride as a function of time at different temperatures. During the interval *A* the crystal was irradiated with light in the *F*-center absorption band. During *B* the crystal was in the dark, and during *C* it was irradiated with infrared light. In (*a*) the crystal was at 30°C and only a primary current is observed during *A*; that is, the current varies abruptly when the light is turned on or off. Further current may be induced by infrared radiation *after* illumination with light in the *F* band. In (*b*) the temperature was 80°C and the current continued to rise after illumination began and did not drop to zero when the light was turned off. This secondary current is larger in cases (*c*) and (*d*). (*After Hilsch and Pohl.*)

similar way. At temperatures below 30°C, the photoconductivity begins abruptly when the crystal is exposed to light in the *F*-center absorption band, remains constant during a constant exposure that does not endure for too long a time, and drops abruptly to zero when the light is cut off (*cf.* Fig. 9*a*). A photocurrent that behaves in this way is said to be a

primary current. Its properties may be explained[1] in terms of the following simple assumptions:

a. A fraction η of the absorbed light quanta free electrons, which wander about the lattice with thermal velocities.

b. In the presence of an electrostatic field of intensity E, the electrons drift in the direction of the field with mean velocity μE where μ is the mobility, which is temperature-dependent.

c. The electrons that do not reach the electrodes eventually become trapped. If λ is the mean distance traveled before trapping takes place, the mean distance ω an electron drifts in the direction of the field is

$$\omega = \mu E \frac{\lambda}{\bar{v}} \tag{1}$$

where $\bar{v}$ is the mean velocity of random motion. We shall call ω the displacement distance.

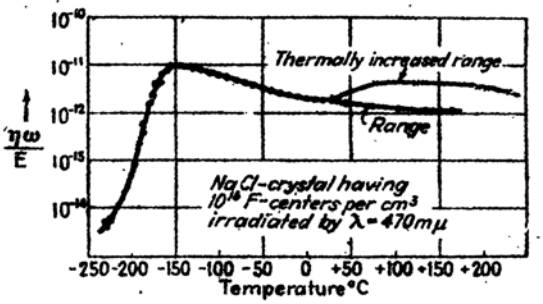

FIG. 10.—The function $\eta\omega/E$ as a function of temperature for sodium chloride with *F*-centers. It should be noted that the photocurrent drops sharply below −150°C. The units of the ordinate scale are meter²/volt. (*After Pohl.*)

If I is the intensity of the absorbed radiation per unit distance between electrodes, the measured current i should be

$$i = \eta \frac{I}{h\nu} e\omega, \tag{2}$$

according to these assumptions, where $h\nu$ is the energy of the absorbed light quanta. Since ω is proportional to E and η is presumably independent of field intensity, the quantity

$$\frac{ih\nu}{EeI} = \frac{\omega}{\eta E} \tag{3}$$

should be independent of E. This actually is found to be the case in the primary-current range. Figure 10 shows the temperature depend-

[1] *Ibid.*

ence of the measured value of (3) for sodium chloride.[1] It should be observed that $\eta\omega/E$ varies relatively slowly from 25° down to −150°C and then drops very rapidly, indicating that either η or ω decreases very rapidly near the absolute zero of temperature. A similar drop in photosensitivity has also been observed in potassium chloride.

Mott[2] has given an explanation of this decrease in terms of a decrease in the quantum yield η. If an F center corresponds to the lowest stable state of an electron and a vacancy in the halogen-ion lattice, the electrostatic field in which the electron moves should vary as $-e^2/n^2r^2$ at large distances from the vacancy. Hence, the electron should have more than one discrete level beneath the ionization continuum. By analogy with a hydrogen atom, or an alkali-metal atom, the lowest state of the system should be an s-like state and the strongest absorption band should correspond to the transition from this state to the lowest, discrete, p-like state, which Mott postulated is the F absorption band. Since the electron is bound in the p state, the crystal should not become photoconducting unless the electrons are thermally excited to the ionization continuum. Hence, there should be no photoconductivity at the absolute zero of temperature. If A is the relative probability that the electron jumps from the p state to the ground state in unit time without becoming free and if B is the relative probability that it becomes free in the same time, the quantum yield should be

$$\eta = \frac{B}{A+B} = \frac{1}{1+(A/B)}. \tag{4}$$

Mott assumes that A has the value 10^8 sec^{-1} and that B has the form

$$B = \nu e^{-\frac{\epsilon}{kT}} \tag{5}$$

where ν is of the order of magnitude of an atomic oscillational frequency 10^{13} sec^{-1} and ϵ is the energy required to ionize an electron in the excited state. Under these conditions,

$$\eta = \frac{1}{1+10^{-5}e^{\frac{\epsilon}{kT}}}. \tag{6}$$

The condition, which must be satisfied if this is to begin dropping to zero at 100°K, is that ϵ should be of the order of magnitude 0.61 ev.

Indirect evidence shows that the trapping centers are other F centers. As the crystal is illuminated[3] with light in the F absorption band in the

[1] G. GLASER and W. LEHFELDT, *Nachr. Kgl. Ges. Wiss. Göttingen*, **2**, 91 (1936).
[2] N. F. MOTT, *Proc. Phys. Soc.*, **50**, 196 (1938).
[3] Z. GYULAI, *Z. Physik*, **33**, 251 (1925); R. HILSCH and R. W. POHL, *Z. Physik*, **66**, 721 (1931).

region of temperature in which the primary photocurrent is observed, the F band gradually disappears and a new band appears on the long wave-length side of the F band. This new band, which is called the F' absorption band, ordinarily overlaps partly with the F band (*cf.* Fig. 11). Evidently, the F' band corresponds to the absorption of light by the centers that are formed by the trapped electrons. Measurements[1] on the displacement distance per unit field strength, ω/E, show that this quantity is inversely proportional to the concentration of F centers (*cf.* Fig. 12). This result suggests that the F centers act as trapping points for the free electrons and that an F' center consists of a

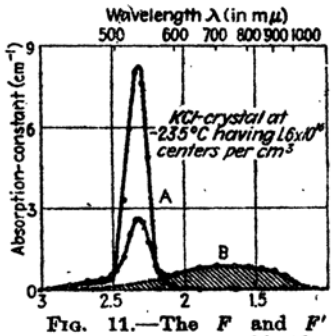

FIG. 11.—The F and F' bands of potassium chloride. A is the F band as it occurs before illumination with light in this band. After illumination, the intensity of the F band decreases and the F' band B occurs. The unit of wave length is 10^{-7} cm. The unit of ordinate scale is cm^{-1}. (*After Pohl.*)

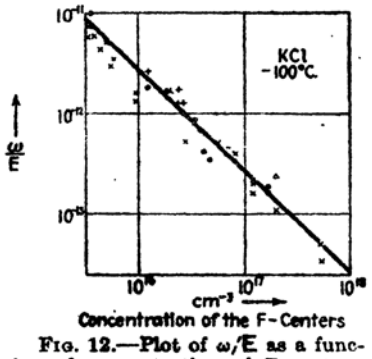

FIG. 12.—Plot of ω/E as a function of concentration of F centers. Since ω/E is the displacement distance per unit field intensity it follows that the mean free path for trapping is dependent upon the concentration of F centers. The ordinates are expressed in units of meter²/volt. (*After Pohl.*)

vacancy plus two electrons. If this interpretation is correct, two F centers should be destroyed for each F' center formed. Pohl and his collaborators have found evidence showing that this condition actually is satisfied.

It is also found that the crystal containing F' centers becomes photoconducting when it is illuminated with light in the F' band. This shows that the electrons in F' centers may be freed by optical excitation, just as may those in an F band.

From the curve of Fig. 12, we may estimate the ratio of the mean free path l for scattering of free electrons and the cross section σ for capture of a free electron by an F center. Let us assume that η is unity at $-100°C$ for potassium chloride. According to Eq. (1),

[1] G. GLASER, *Nachr. Kgl. Ges. Wiss. Göttingen*, **3**, 31 (1937).

$$\frac{\omega}{E} = \mu\frac{\lambda}{\bar{v}}. \tag{7}$$

The mobility μ is related to the conductivity σ by the equation

$$\sigma = ne\mu \tag{8}$$

where n is the number of free electrons per unit volume. Since

$$\sigma = \frac{ne^2\bar{v}l}{3kT}, \tag{9}$$

according to classical theory [*cf.* Eq. (5) Sec. 126], we have

$$\mu = \frac{1}{3}\frac{e\bar{v}l}{kT}. \tag{10}$$

The mean distance λ for capture and the capture cross section Q are related to the density δ of capturing centers by the equation

$$\frac{1}{\lambda Q} = \delta. \tag{11}$$

Using Eqs. (7), (10), and (11), we obtain

$$\frac{\omega}{E} = \frac{1}{3}\frac{e}{kT}\delta\frac{l}{Q}$$

or

$$\frac{l}{Q} = 3\frac{\omega}{E}\delta\frac{kT}{e}. \tag{12}$$

If we employ the experimental values of ω/E and δ that are given in Fig. 12 and assume $Q \sim 10^{-16}$ cm^2, we find

$$l \sim 5 \cdot 10^{-9} \text{ cm}.$$

Although this estimated value is about one-tenth as large as the value computed in Sec. 138, it does not seem safe to draw any conclusions about the validity of the preceding equations from the discrepancy.

When a sodium chloride crystal that contains F' centers, which have been formed by illuminating the colored crystal in the F band, is heated above room temperature, the F' centers disappear[1] and are replaced by F centers. Hence, the trapped electrons may be thermally released and should be able to move farther than the displacement distance ω at high temperatures. This expectation is supported by the appearance of a secondary photocurrent above room temperature. It is found[2] that the

[1] GYULAI, *op. cit.*; HILSCH and POHL, *op. cit.*

[2] B. GUDDEN and R. W. POHL, *Z. Physik*, **31**, 651 (1925); W. THIELE, *Ann. Physik*, **25**, 561 (1936).

photocurrent continues to rise after illumination begins and approaches a saturation value. The rate at which this value is attained is greater at higher temperatures (*cf.* Fig. 9). In addition, the current does not disappear completely when the light is removed. Instead, it decreases abruptly by an amount equal to the initial rise and then gradually dies out. In Fig. 10, the double sets of points above 25°C correspond, respectively, to the initial and saturation photocurrents.

A complete mathematical treatment of the problem of secondary currents has not yet been developed. It seems likely, however, that the following three qualitative principles determine the behavior of the secondary current in all photoconductors, as well as in colored sodium chloride.

1. Electrons that are trapped after being released by light may be freed thermally at sufficiently high temperatures and may continue to drift toward the anode. This contribution i_s to the secondary current should not rise to a saturation value instantly if the electrons are trapped for a measurable time τ. Suppose that the electrons are optically freed at a rate n per unit time, so that the number in the crystal at the end of time t is nt. After being initially freed, the electrons move a distance ω and become trapped, giving rise to the primary current. If the probability that one of the nt trapped electrons is released in unit time is $1/\tau$, the total number released per unit time is nt/τ. If it is assumed that they move a distance ω and are again trapped, the secondary current as a function of time is

$$i_s = \frac{nt}{\tau} e\omega. \tag{13}$$

Deviations from this linear rise occur as soon as the electrons begin arriving at the anode at a rate comparable with the rate at which they are optically freed. The greatest possible value of i_s for uniform illumination between electrodes that are a distance d apart is $nde/2$ since each freed electron moves a mean distance $d/2$.

2. Additional electrons may enter the crystal from the cathode and move through the crystal to the anode. This flow from the cathode is induced by the space charge fields set up in the crystal by the displacement of the electrons in the primary current and in i_s. Either field emission from the cathode or an inherent dark electronic conductivity may serve to introduce the electrons into the crystal. We shall call this contribution to the current i_{II}. Since the space charge field should vary with time, immediately after illumination, i_{II} should also be a function of time. It may be difficult to separate i_{II} from i_s for this reason. The limiting value of the total photocurrent for long periods of illumination is determined by the dependence of i_{II} on the field strength near the

cathode; for if a sufficiently large space charge accumulates, the optically freed electrons will not be able to reach the cathode.

3. The migrating electrons may become permanently trapped to form anew the centers that were originally ionized by light quanta. In the alkali halides, this means that F centers may be formed by the recombination of freed electrons and halogen-ion vacancies. In a true equilibrium state, the rate at which this process occurs is equal to the rate at which the centers are ionized by light.

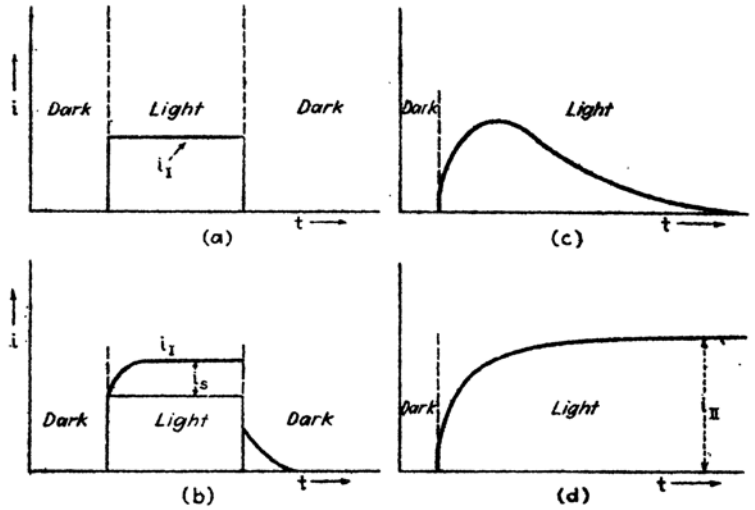

FIG. 13.—Schematic representation of the behavior of primary and secondary photocurrents. In (*a*) there is only a primary current i_I which corresponds to electrons actually released by light. These electrons ultimately become trapped. In (*b*), which is at a higher temperature, there is an additional current i_s corresponding to the flow of the thermally released trapped electrons. (*c*) corresponds to a case in which charge cannot pass from the cathode into the crystal. Polarization eventually reduces the current to zero in spite of continuous illumination. In (*d*) a current i_{II} flows from the cathode in the equilibrium state. All cases intermediate between (*c*) and (*d*) are possible.

Several different possible cases are illustrated schematically in Figs. 13*a* to *d*. In the first, there is only the primary current which rises and falls abruptly with changes in illumination. This current could not exist indefinitely if no charges entered the crystal to neutralize space charge. In Fig. 13*b*, we have the primary current and the secondary current i_s, which we have assumed reaches its saturation value. If there are no electrons flowing from the cathode, the primary current and the secondary current i_s eventually fall to zero because of polarization (Fig. 13*c*). The cathode current i_{II} prevents this drop and makes the final current finite. If i_{II} is large, the total current need not have a maximum (Fig. 13*d*), whereas if i_{II} is small, the current may rise to a peak and then fall asymptotically to a finite value.

Only the primary current flows in colored sodium chloride below 25°C. Since there is no direct evidence that electrons enter the crystal from the cathode between this temperature and 230°C, it is possible that only the primary current and i_s coexist in this range. Above 230°C, the electrons bound in F centers are freed thermally, and the current i_{II} undoubtedly occurs. The three components of current have not been separated experimentally, however.

Hilsch and Pohl[1] have treated a particular case of the general problem, namely, the case in which τ is so short that the primary current and i_s are inseparable and the rate at which electrons are trapped by ionized centers (effect 3) is negligible. They find that the total steady-state electronic current i is related to the effective primary current i_p by the equation

$$i = \frac{1}{1 - \gamma} i_p$$

where γ is the fraction of the dark conductivity before illumination that is due to electrons. If σ_e and σ_i are the electronic and ionic dark conductivities,

$$\gamma = \frac{\sigma_e}{\sigma_i + \sigma_e}.$$

They did not consider the transition current before the steady state is reached.

135. Photoconductivity of Zinc Sulfide and of the Silver Halides.[2]—Gudden and Pohl[3] have also made measurements on the photoconductivity of natural single crystals and artificially prepared powders of zinc sulfide that can be interpreted along the lines discussed in the preceding section. Although the impurity content of the single crystals is not discussed, we shall assume that the composition of crystals and powders is similar, since the photoconducting properties of both are nearly alike. The photoconducting powders are usually prepared by heating pure zinc sulfide either alone or in the presence of small quantities of salts of other metals, such as copper, manganese, or silver. It is believed (*cf.* Sec. 112) that small quantities of neutral metal atoms enter interstitial positions in the lattice as a result of the heating process and provide centers that may be ionized by the conductivity-inducing radiation in the near ultraviolet. The position of the spectral sensitivity curve is dependent upon the kinds of interstitial atom present, but it usually has its maximum near 3650Å and has a small tail in the blue region of the visible spectrum. Many of the photoconducting zinc sulfides, such as the pure heated

[1] R. HILSCH and R. W. POHL, *Z. Physik*, **103**, 55 (1937).

[2] Review of experiments: F. C. NIX, *Rev. Modern Phys.*, **4**, 723 (1932).

[3] B. GUDDEN and R. W. POHL, *Z. Physik*, **2**, 181, 361 (1920); **3**, 98 (1920); **4**, 206 (1921); **5**, 176 (1921); **6**, 248 (1921); **17**, 331 (1923); *Physik. Z.*, **23**, 417 (1922).

material and those activated by means of copper, silver, or manganese, luminesce brightly when excited with radiation lying in the region in which photoconductivity occurs. We shall discuss the correlation of these two effects below.

It is found that the photocurrents in the zinc sulfides are primary for electrostatic fields below 6,000 volts/cm. The primary current saturates, however, in sufficiently thin crystals; for example, Fig. 14 shows the saturation obtained for a crystal about 1 mm thick. When the maximum current is reached, one electron arrives at the anode for each light quantum that is absorbed, which indicates that the displacement distance ω is greater than the distance between electrodes. If, in

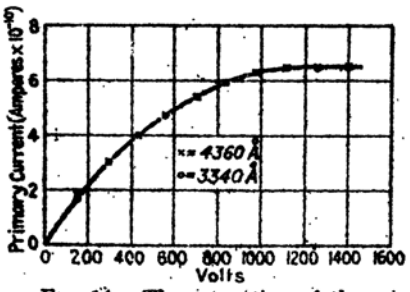

FIG. 14.—The saturation of the primary photocurrent with voltage in zinc sulfide. Saturation occurs when each electron flows to the cathode. (*After Hilsch and Pohl.*)

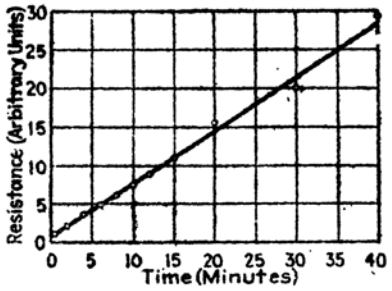

FIG. 15.—The resistance of a specimen of zinc sulfide as a function of time. The specimen had previously been irradiated with ultraviolet light. It was then placed in liquid air and irradiated with infrared radiation, starting at time zero. (*After Reimann.*)

Eq. (12) of the preceding section, we set ω equal to the thickness of the crystal for the value of E at which the current is half the saturation value and if we set l equal to 10^{-5} cm and Q equal to 10^{-16} cm^2, we find

$$\delta \sim 3 \cdot 10^{13}.$$

This implies that the density of trapping centers is very low compared with the density of interstitial atoms, which usually is about 10^{18} cm^{-3}. Moreover, since the shape of the saturation current is independent of light intensity, we cannot conclude that the trapping centers are the ionized centers. No satisfactory explanation of the trapping has yet been given.[1]

[1] In recent experiments based on a study of the decay of luminescence, R. P. Johnson, *Jour. Optical Soc.*, **29**, 387 (1939), has shown that there are at least two types of trapping center. One of these binds the electrons more tightly than the others and probably is the trapping center that is important for room-temperature photoconductivity. The other probably would also be important at lower temperatures.

The trapped electrons may be temporarily released either by heating the crystal to sufficiently high temperatures or by illuminating it with infrared light at any temperature. This freeing is made evident by the appearance of conductivity. Hence, if a crystal that has previously been illuminated with ultraviolet light is continuously illuminated with infrared light or is kept sufficiently warm, the electrons that are continuously being freed from the trapping centers should eventually recombine with the ionized interstitial atoms and the conductivity should gradually decrease. If we assume that the rate at which n ionized electrons and n ionized atoms recombine is proportional to the product of the number of each, we obtain the equation[1]

$$\frac{dn}{dt} = -\alpha n^2, \tag{1}$$

which has the integral

$$\frac{1}{n} = \alpha t + \frac{1}{n_0} \tag{2}$$

where n_0 is the number of photoelectrons at time $t = 0$. Under these conditions, the resistivity of the crystal that is illuminated with infrared light should increase linearly with time. A relationship of this type has been observed by Reimann[2] (*cf.* Fig. 15) on a specimen of zinc sulfide that was kept at liquid-air temperature and was continuously illuminated with infrared light after an initial excitation with ultraviolet light.

According to Eqs. (1) and (2), the rate at which electrons and interstitial ions recombine is given by the equation

$$\frac{dn}{dt} = -\frac{\alpha n_0^2}{(n_0\alpha t + 1)^2}. \tag{3}$$

If light quanta of frequency ν were emitted during this recombination, the intensity $I(t)$ at time t would be

$$I(t) = h\nu\frac{dn}{dt} = -\frac{h\nu\alpha n_0^2}{(n_0\alpha t + 1)^2} = \frac{I(0)}{(\beta t + 1)^2} \tag{4}$$

where

$$\beta = n_0\alpha.$$

It is found experimentally that the luminescence of zinc sulfide decays very nearly in accordance with this equation at times not too near the initial time of excitation. This fact provides a possible explanation of the

[1] This discussion is valid only when there is a single trapping center. It has been generalized by Johnson, *op. cit.*

[2] A. L. REIMANN, *Nature*, **140**, 501 (1937).

luminescence of the salts. A more definite correlation between luminescence and recombination would be provided by simultaneous measurements of the decay of conductivity and of luminescence when a previously excited crystal is illum ated with infrared radiation or is warmed.

Currents higher than the saturation values of Fig. 13 may be obtained at room temperature by continuously illuminating the crystal with ultraviolet light while maintaining high electrostatic field intensity. Figure 16 shows the way in which the total charge removed from the crystal, as a function of time, deviates from linearity at different field

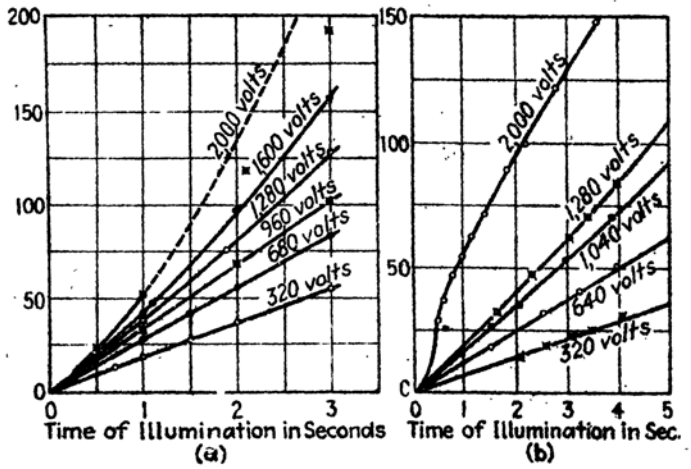

FIG. 16.—The total charge conducted by a specimen of zinc sulfide that was continually illuminated with ultraviolet light as a function of time. At high field intensities the current rises above the saturation value of the primary current that is shown in Fig. 14. The scale of ordinates is such that 100 units equal 7.2×10^{-11} coulomb. (*After Hilsch and Pohl.*)

strengths. These secondary currents, like those in the colored halides, have not been studied quantitatively.

Photoconductivity that is qualitatively similar to that observed in zinc sulfide has been found in many other natural and artificial crystals. Most notable among these are selenium and the silver halides. The first of these is used in the photovoltaic cell and has been studied extensively for practical work. The results, however, are not very useful for interpretive work.

The photoconductivity of the similar salts, AgCl and AgBr, has been investigated by Hilsch and Pohl,[1] Toy and Harrison,[2] and Lehfeldt,[3] the work of the last of these investigators being the most extensive. The spectral sensitivity curves for stimulating conductivity extend

[1] R. HILSCH and R. W. POHL, *Z. Physik*, **64**, 606 (1930).
[2] F. C. TOY and G. B. HARRISON, *Proc. Roy. Soc.*, **127**, 613 (1930).
[3] LEHFELDT, *Nachr. Kgl. Ges. Wiss. Göttingen*, **1**, 170 (1935).

throughout the visible and into the near ultraviolet region of the spectrum, have peaks in the blue, and lie close to, if not actually in, the tail of the fundamental absorption band. Lehfeldt has found that in the range from room temperature to liquid-air temperature the quantum yield of photoelectrons is close to unity for all absorbed light.

It has often been suggested that electrons are freed with quantum yield unity throughout the fundamental absorption region, and that photoconductivity is observed in the tail of this region and not in its center only, because the reflection coefficient becomes large in the center. According to present view concerning the excited states of perfect insulating crystals (Chap. XII), the observed photoconductivity arises from impurities or lattice defects, at least in the case of the alkali halides.

As we saw in Sec. 132, Jost and Nehlep have given theoretical evidence that the lattice defects in silver halides are interstitial silver ions. Thus, it is possible that the source of photoelectrons is either the interstitial silver ion, if the ion carries an electron with it, or the negative ions near the vacancy, if the interstitial ion does not take an electron. Mott[1] has shown, however, that it is not unreasonable to suppose that photoelectrons are produced in these salts by thermal decomposition of excitons formed by absorption in the fundamental band.

Note: The theory of contact rectification of the type occurring in galena and copper oxide rectifiers has not been discussed in this chapter, in which it would naturally belong. This subject has passed through a gradual development and the most recent treatment, which seems to correlate most of the known facts, is that given by N. F. Mott, *Proc. Roy. Soc.*, **171**, 27, 281 (1939).

[1] N. F. MOTT, *Proc. Roy. Soc.*, **167**, 384 (1938).

CHAPTER XVI

THE MAGNETIC PROPERTIES OF SOLIDS

136. Introduction.—It was seen in Chap. I that there are three main classes of solids as far as magnetic properties are concerned, namely, diamagnetic, paramagnetic, and ferromagnetic substances. Practically all simple insulators and about half the simple metals are diamagnetic, whereas all other insulators and metals, except for a few ferromagnetic substances, are paramagnetic. The ferromagnetic materials become paramagnetic when heated to sufficiently high temperatures, a fact showing that paramagnetism and ferromagnetism are intimately connected.

Diamagnetism is related to changes in the orbital motion of electrons that occur when atomic systems are placed in a magnetic field. It may be recalled that the current induced in a closed electrical circuit by a magnetic field is always in such a direction as to tend to keep the total flux unchanged. Thus, the circuit has, in effect, a negative susceptibility. This effect is retained even in systems of charges that must be treated by quantum mechanics and is responsible for diamagnetism. Paramagnetism, on the other hand, is related to the tendency of a permanent magnet to align itself in a magnetic field in such a way that its dipole moment is parallel to the field. In atomic systems, the permanent moment is the magnetic moment associated with electron spin in the simplest cases, but it may also be the permanent moment of an unfilled atomic shell that arises from a combination of spin and orbital motion. If a system is more stable when the atomic dipoles are parallel, the system is ferromagnetic at low temperatures. Ferromagnetism disappears at high temperatures for a reason similar to that for which solids melt, namely, because the nonferromagnetic state is more disordered and has a higher entropy than the ferromagnetic one. The moment-aligning forces in ferromagnetic substances are not the magnetic forces between dipoles but have electrostatic origin, as we shall see in Sec. 143.

137. The Hamiltonian Operator in a Magnetic Field.—According to the results of Sec. 42, the Hamiltonian operator for any system of electrons in an external electromagnetic field is

$$H = \sum_i \frac{1}{2m}\left(\mathbf{p}_i + \frac{e}{c}\mathbf{A}_i\right)^2 + V - \sum_i e\,\varphi_i + \sum_i \frac{e}{mc}\mathbf{s}_i \cdot \operatorname{curl} \mathbf{A}_i \qquad (1)$$

where $\mathbf{p}_i$ is the momentum operator for the ith electron, φ and A are the scalar and vector potentials of the external field, V is the internal electrostatic potential of the electronic system, and $-e\boldsymbol{\sigma}_i/mc$ is the spin magnetic moment of the ith electron.[1] If the external field is uniform and of intensity H, we may choose A as

$$\mathsf{A} = \tfrac{1}{2}\mathsf{H} \times \mathbf{r}. \tag{2}$$

For convenience, we shall take H to lie in the z direction. Under these conditions,

$$H = \sum\left[-\frac{\hbar^2}{2m}\Delta_i + \frac{\mathsf{H}_z e}{2mc}\frac{\hbar}{i}\left(x_i\frac{\partial}{\partial y_i} - y_i\frac{\partial}{\partial x_i}\right) + \frac{\mathsf{H}_z^2 e^2}{8mc^2}(x_i^2 + y_i^2)\right] + V + \sum_i \frac{e}{mc}\mathsf{H}_z\sigma_{z_i}. \tag{3}$$

The operator

$$\sum_i \frac{\hbar}{i}\left(x_i\frac{\partial}{\partial y_i} - y_i\frac{\partial}{\partial x_i}\right) = \sum_i m_{z_i} \tag{4}$$

is the z component of the total angular momentum operator (*cf.* Sec. 40). If the two terms containing H_z to the first power are combined, they reduce to

$$\mathsf{H}_z\frac{e}{2mc}\sum_i (m_{z_i} + 2\sigma_{z_i}), \tag{5}$$

in which the negative of the coefficient of H_z is the z component of the total magnetic moment arising from both orbital motion and spin. This term accounts for the weak-field Zeeman effect in free atoms since its matrix components are usually much larger than those of the quadratic term

$$\frac{\mathsf{H}_z^2 e^2}{8mc^2}\sum_i (x_i^2 + y_i^2). \tag{6}$$

We may discuss the contributions to the total energy from the terms (5) and (6) separately for the inner-shell electrons and for the valence electrons. Some of the properties of the first type of electron, which may be treated like the electrons in free atoms or ions, will be presented in this section. These results can be applied to all the electrons in those ionic crystals whose constituent ions behave as if they were nearly free.

[1] The interaction between the field and the magnetic moments of the electrons, not considered in Sec. 42, is also included in this Hamiltonian.

We shall devote other sections to the valence electrons of other substances that require separate consideration.

Although the z component of the total angular momentum operator is a constant of motion for a free atom, the z component of magnetic moment usually is not, because of the factor 2 that appears as a coefficient of σ_{z_i} in (5). There is one important exceptional case, however, namely, that of Russell-Saunders coupling,[1] in which the spin-orbit interaction terms are small. This case occurs commonly among the atoms on the left-hand side of the periodic chart. We shall list the operators that are constants of motion in this case. The conventional form of the eigenvalues of each operator are also given.

a. The square of the total angular momentum

$$\Big[\sum_i (\mathbf{m}_i + \mathbf{s}_i)\Big]^2; \qquad \hbar^2 J(J+1). \tag{7}$$

b. The square of the orbital angular momentum

$$\Big[\sum_i \mathbf{m}_i\Big]^2; \qquad \hbar^2 L(L+1). \tag{8}$$

c. The square of the spin angular momentum

$$\Big[\sum_i \mathbf{s}_i\Big]^2; \qquad \hbar^2 S(S+1). \tag{9}$$

d. The z component of the total angular momentum

$$\sum_i (m_{z_i} + \sigma_{z_i}); \qquad \hbar J_z. \tag{10}$$

e. The z component of the total orbital angular momentum

$$\sum_i m_{z_i}; \qquad \hbar M_z. \tag{11}$$

f. The z component of the total spin angular momentum

$$\sum_i \sigma_{z_i}; \qquad \hbar S_z. \tag{12}$$

In the preceding equations, the quantum numbers L and M_z are allowed only integer values, whereas the quantum numbers J, S, and J_z are integers in atoms having an even number of electrons and are half integers in atoms having an odd number of electrons. The levels of

[1] *Cf.* E. U. CONDON and G. H. SHORTLEY, *The Theory of Atomic Spectra* (Cambridge University Press, 1935); G. HERZBERG, *Atomic Spectra* (Prentice-Hall, Inc., New York, 1937).

given J are $(2J + 1)$-fold degenerate and the different degenerate states may be specified by the $2J + 1$ values of J_z that range from J to $-J$ in integer steps. In an ideal case of Russell-Saunders coupling, the levels group themselves into widely separated sets, called multiplets, which are specified by given values of L and S (*cf.* Fig. 1). The different levels in each multiplet are in turn specified by values of J that range by integer steps from the value $L + S$ to the value $|L - S|$. The separation of levels in the same multiplet, which is determined by a small interaction between spin and orbital motion that does not appear in Eq. (1), is given by the simple equation

$$E_{J+1} - E_J = \alpha(J + 1)$$

where α is a constant for a given multiplet.

In terms of these quantum numbers, the eigenvalues of the magnetic term (5) are

$$H_z\beta\left[1 + \frac{J(J+1) + S(S+1) - L(L+1)}{2J(J+1)}\right]J_z \tag{13}$$

where

$$\beta = \frac{e\hbar}{2mc}$$

is the Bohr magneton. We shall be interested in this result principally for the discussion of the magnetic effects of inner shells of the atoms in solids. Since J, L, and S are all zero for completely closed shells, the contribution to (5) arising from these shells is zero; however, they do contribute to the term (6). On the other hand, the quantum numbers usually are not zero for the unfilled inner shells of the transition-element atoms or of the rare earth atoms. Hence, the term (5) is important in these cases. It is easy to see that (6) is unimportant whenever the expression (13) is not zero, for if the coefficient of $H_z\beta$ in (13) is of the order of unity and if the mean value of $(x_i^2 + y_i^2)$ in (7) is of the order of magnitude a_0^2, the ratio of (6) to (5) is

$$H_z\frac{\hbar^3}{6ce^3m^2}$$

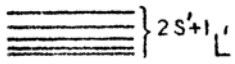

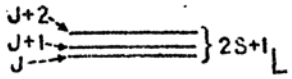

FIG. 1.—The distribution of multiplets in Russell-Saunders coupling. The distance between the multiplets, that is, between the groups of levels of given J, are large compared with the inner multiplet separations.

which is of the order of magnitude $H_z \cdot 10^{-10}$ in cgs units. This is completely negligible for ordinary magnetic field strengths.

We shall now examine the connection between the energy states and the magnetic susceptibility of an atomic system. The susceptibility χ is, by definition, the ratio of the magnetic polarization per unit volume M and the magnetic field H; that is,

$$\mathsf{M} = \chi \cdot \mathsf{H}. \tag{14}$$

In the general case in which M and H are not in the same direction, χ is a tensor. We shall restrict the present discussion to the case in which χ is a constant. If the external magnetic field is changed by an increment $\Delta\mathsf{H}$, the change in energy of a system that is in the energy state E' and has a magnetic polarization per unit volume M is

$$\frac{\Delta E'}{V} = -\mathsf{M} \cdot \Delta\mathsf{H} = -\chi\mathsf{H} \cdot \Delta\mathsf{H}. \tag{15}$$

Hence, if H' is the scalar value of the magnetic field,

$$\chi = -\frac{1}{V\mathsf{H}'}\frac{\partial E'}{\partial \mathsf{H}'}. \tag{16}$$

If the system is at the absolute zero of temperature, E' is the lowest energy state E_0. Thus, in this case,

$$\chi = -\frac{1}{V\mathsf{H}'}\frac{\partial E_0}{\partial \mathsf{H}'}. \tag{17}$$

On the other hand, if the system is at a finite temperature T, the mean value of $\partial E'/\partial \mathsf{H}'$ is

$$\frac{\sum_i (\partial E_i/\partial \mathsf{H}') e^{-\frac{E_i}{kT}}}{\sum_i e^{-\frac{E_i}{kT}}} = -kT\frac{\partial \log f}{\partial \mathsf{H}'} \tag{18}$$

where

$$f = \sum_i e^{-\frac{E_i}{kT}} \tag{19}$$

is the partition function of the system. Hence,

$$\chi = \frac{kT}{V\mathsf{H}'}\frac{\partial}{\partial \mathsf{H}'}\log f. \tag{20}$$

Since $-kT \log f$ is also the free energy A of the system, (20) may be written in the form

$$\chi = -\frac{1}{\mathsf{H}'V}\frac{\partial A}{\partial \mathsf{H}'}, \tag{20a}$$

which is a generalization of (17).

Let us apply Eq. (20) to a simple system consisting of N independent atoms. We shall assume that the inner-multiplet spacing is so large compared with kT that all atoms are in the lowest $2J + 1$ states of a multiplet, which are degenerate in the absence of a field. This model applies to an ionic or molecular crystal in which some ions or atoms have incompleted inner shells so perfectly screened that they are the same as in a free atom. If we use Eq. (13) for the splitting of the lowest level, the partition function is

$$f = \left[\sum_{M_z=-J}^{J} e^{-\frac{\mathsf{H}_z\beta g(J,L,S)M_z}{kT}}\right]^N \tag{21}$$

where

$$g = \left[1 + \frac{J(J+1) + S(S+1) - L(L+1)}{2J(J+1)}\right] \tag{22}$$

is the Landé g factor. Summing the series, we find

$$f = \left[\frac{\sinh\,(J+\tfrac{1}{2})\alpha}{\sinh\,\alpha/2}\right]^N \tag{23}$$

where

$$\alpha = \frac{\mathsf{H}_z\beta g}{kT}. \tag{24}$$

Thus, the susceptibility is

$$\chi = \frac{N}{V}\frac{\beta g J}{\mathsf{H}_z}B_J(\alpha), \tag{25}$$

in which

$$B_J(\alpha) = \frac{(J+\tfrac{1}{2})\coth\,(J+\tfrac{1}{2})\alpha - \tfrac{1}{2}\coth\,\alpha/2}{J} \tag{26}$$

is the Brillouin function.[1] Values of B_J for several values of J are shown in Fig. 2. Since $B_J(\alpha)$ approaches unity for large values of α, the limiting value of M is $N\beta gJ/V$ when $\beta\mathsf{H}_z$ is much larger than kT, which corresponds to complete alignment of the magnetic moment parallel to the magnetic field. For small values of α, B_J varies linearly with α so that, when $\beta\mathsf{H}_z$ is much smaller than kT, the magnetic polarization is

$$\mathsf{M}(\mathsf{H}) = \frac{N}{V}\frac{\beta^2 g^2 J(J+1)}{3kT}\mathsf{H}, \tag{27}$$

and the susceptibility is

$$\chi = \frac{N}{V}\frac{\beta^2 g^2 J(J+1)}{3kT}. \tag{28}$$

[1] L. BRILLOUIN, *Jour. phys.*, **8**, 74 (1927).

Equation (28) was first derived by Langevin[1] for the case of classical mechanics, in which $\beta g\sqrt{J(J+1)}$ is replaced by the permanent atomic magnetic moment.

If the atom has a closed-shell structure, so that J is zero, (28) vanishes and the susceptibility should be determined by the quadratic energy term (6). Since closed shells are spherically symmetrical, the matrix component of $\sum_i (x_i^2 + y_i^2)$ for the lowest state is

$$\tfrac{2}{3}n\overline{r^2} \tag{29}$$

where n is the total number of electrons in the atom and $\overline{r^2}$ is the mean

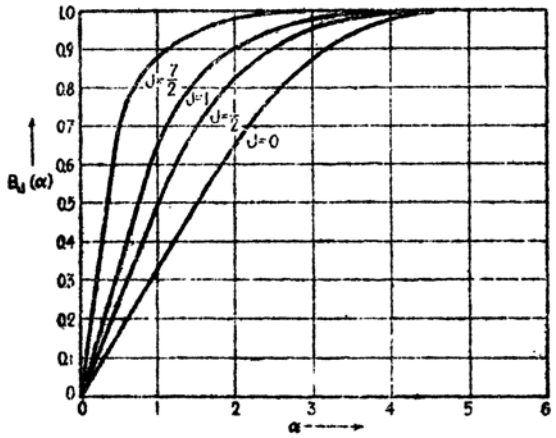

FIG. 2.—Values of $B_J(\alpha)$ for the values $J = 0, \frac{1}{2}, 1$, and $\frac{7}{2}$.

value of r^2 for any electron. Thus, the magnetic energy per unit volume of a group of N atoms of this type is

$$\frac{H_z^2 e^2}{12mc^2}\frac{Nn}{V}\overline{r^2}, \tag{30}$$

and their susceptibility is

$$-\frac{Nn}{V}\frac{e^2}{6mc^2}\overline{r^2}, \tag{31}$$

which corresponds to diamagnetism.

We have seen in the previous chapters that simple ionic crystals behave as though they were composed of spherically symmetric closed-shell ions of the constituent atoms. If there are N_α/V ions of the αth type per unit volume of this crystal, the diamagnetic susceptibility is

[1] P. LANGEVIN, *Jour. phys.*, **4**, 678 (1905).

$$\chi = -\frac{e^2}{6mc^2}\sum\frac{N_\alpha n_\alpha}{V}\overline{r_\alpha^2} \tag{32}$$

where n_α and $\overline{r_\alpha^2}$ are, respectively, the number of electrons on the αth ion and the mean value of r^2 for this ion. Equation (32) may also be used to compute the diamagnetic contribution to the susceptibility from the closed shells of any solid. A discussion of the methods of computing the diamagnetic susceptibilities of various closed-shell ions and tables of numerical values of these susceptibilities may be found in Chap. VIII of Van Vleck's book.[1]

138. The Orbital Diamagnetism of Free Electrons*.—A theorem of classical mechanics[2] states that a system of charges that are confined in a fixed volume but are otherwise free has zero magnetic susceptibility. If the system is not confined, each constituent charge is induced to move in a helical path and the total magnetic flux is decreased. The charges striking the wall, however, have their paths changed in such a way that their magnetic field nullifies the field of the rest. This result may be understood on the basis of the following formal argument. In classical mechanics, a magnetic field alters the direction of motion of a charge but does not change its speed. Hence, the distribution of energy states and, as a result, the partition function of a system of charges that is at equilibrium are unaltered by the magnetic field. According to Eq. (20) of the preceding section this means that the susceptibility is zero. The fact that the charges are confined assures us that the system is in equilibrium.

Landau[3] first pointed out that this theorem is not valid in quantum mechanics because the distribution of energy levels is altered by a magnetic field in the new scheme. This may be demonstrated as follows. The Schrödinger equation for a free electron in a magnetic field, as derived from the Hamiltonian (3) of the preceding section, is

$$-\frac{\hbar^2}{2m}\Delta\psi + \frac{\mathsf{H}_z e}{2mc}\frac{\hbar}{i}\left(x\frac{\partial}{\partial y} - y\frac{\partial}{\partial x}\right)\psi + \frac{\mathsf{H}_z^2 e^2}{8mc^2}(x^2 + y^2)\psi = \epsilon\psi, \tag{1}$$

in which it is assumed that the field is in the z direction. The spin term is neglected in the present section. If we make the transformation

$$\psi = \varphi(x,y,z)e^{i\frac{\mathsf{H}_z e}{2c}\frac{xy}{\hbar}}, \tag{2}$$

Eq. (1) reduces to

$$-\frac{\hbar^2}{2m}\Delta\varphi + \frac{\mathsf{H}_z e}{mc}\frac{\hbar}{i}x\frac{\partial\varphi}{\partial y} + \frac{\mathsf{H}_z^2 e^2}{2mc^2}x^2\varphi = \epsilon\varphi, \tag{3}$$

[1] J. H. VAN VLECK, *The Theory of Electric and Magnetic Susceptibilities* (Oxford University Press, New York, 1932).

[2] *Cf. ibid.*

[3] L. LANDAU, *Z. Physik*, **64**, 629 (1930).

which does not explicitly contain y or z. This equation may be further simplified by means of the substitution

$$\varphi(x,y,z) = \lambda(x)e^{2\pi i(k_y y + k_z z)}, \tag{4}$$

for it then becomes

$$-\frac{\hbar^2}{2m}\frac{d^2\lambda}{dx^2} + \left[\frac{1}{2m}\left(hk_y + \mathsf{H}_z\frac{e}{c}x\right)^2 + \frac{h^2k_z^2}{2m}\right]\lambda = \epsilon\lambda, \tag{5}$$

which is identical with the equation for a simple one-dimensional oscillator that is centered about the position

$$x' = -\frac{ch}{e\mathsf{H}_z}k_y \tag{6}$$

and has the natural frequency

$$\nu = \frac{1}{2\pi}\frac{\mathsf{H}_z e}{mc}. \tag{7}$$

Hence, the allowed values of ϵ are

$$\epsilon = \frac{h^2k_z^2}{2m} + \frac{\mathsf{H}_z he}{2\pi mc}\left(n + \frac{1}{2}\right), \tag{8}$$

where n is restricted to integer values.

The form of the total wave function, namely,

$$\psi_{n,k_y,k_z} = e^{2\pi i\left(\frac{\mathsf{H}_z e}{2ch}xy + k_y y\right)}\lambda(x)e^{2\pi i k_z z}, \tag{9}$$

shows that the motion in the z direction is the same as for a free particle having a component of momentum hk_z along this axis. Thus if L_z is the length of the container in the z direction, the number of states that have a fixed value of n and k_y and values of k_z lying in any range Δk_z is

$$N_{\Delta z} = \Delta k_z L_z. \tag{10}$$

The contribution to the total energy from the other two degrees of freedom is (8) minus $h^2k_z^2/2m$, or

$$\epsilon' = \frac{\mathsf{H}_z he}{2\pi mc}\left(n + \frac{1}{2}\right). \tag{11}$$

Each of the discrete levels of this two-dimensional system is highly degenerate. This degeneracy may be estimated in the following way. The parameter k_y in Eq. (8) is analogous to a y component of wave number so that the number of values of k_y in an allowed range Δk_y is

$$N_{\Delta k_y} = \Delta k_y L_y$$

by analogy with Eq. (10). The allowed range of k_y, however, is not unlimited as is that of k_x, for the point x' defined by Eq. (6), which is the center of gravity of the electron position in the x direction, should lie within the container. Thus, if the width of the box in the x direction is L_x, the total number of allowed values of k_y is

$$N_n = \frac{e\mathsf{H}_z}{ch} L_x L_y, \tag{12}$$

which is also the number of states of given ϵ'.

The distance $\Delta\epsilon'$ between successive values of the two-dimensional energy parameter is $\mathsf{H}_z he/2\pi mc$, according to Eq. (11). Hence, the

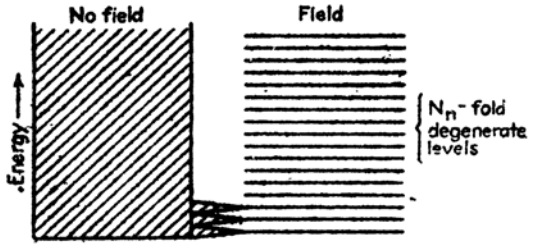

FIG. 3.—Schematic representation of the coalescence of levels of the two-dimensional system in a magnetic field. In effect, bundles of N_n levels of the continuum for perfectly free electrons combine to form discrete levels. The center of gravity of the bundle remains unchanged.

density of the states of the two-dimensional system is

$$\frac{N_n}{\Delta\epsilon'} = 2\pi m \frac{L_x L_y}{h^2}. \tag{13}$$

This is independent of H_z and is the same as the density of levels for a free particle in two dimensions. Thus, the magnetic field does not change the average density of levels although it does alter the detailed distribution.

We may obtain a qualitative picture of Landau's diamagnetism for a system obeying classical statistics from a discussion of the energy levels of the two-dimensional system. The quasi-continuous energy levels of the field-free system become discrete in the presence of the field. In effect, groups of N_n levels coalesce to form each member of the discrete set of levels (11) as is shown in Fig. 3. The individual groups coalesce about their center of gravity; that is, the quasi-continuous set from 0 to $\mathsf{H}_z he/2\pi mc$ coalesce to $\mathsf{H}_z he/4\pi mc$, and so forth. Now, in the absence of a magnetic field the lower levels of any group are preferentially filled if Boltzmann statistics are used. Hence, the mean energy of electrons in a group is less than the energy at the center point. Since all the particles have the energy of the single level into which the group coalesces

in the presence of a magnetic field, the mean energy of the electrons is raised. Thus, the system is diamagnetic. This effect is much smaller if the particles obey Fermi-Dirac statistics and if the system is degenerate, for then only the few electrons at the top of the filled region have their mean energy altered by the field. There is a diamagnetic term, however, even in this case, as will be shown below.

We shall now compute the value of the susceptibility of the three-dimensional model for both classical and Fermi-Dirac statistics. In the classical case, the partition function for a single particle is

$$\left.\begin{aligned} f &= \int_{-\infty}^{\infty} L_z dk_z \left\{ \sum_{n=0}^{\infty} \frac{eH_z L_x L_y}{ch} e^{-\frac{\frac{h^2k_z^2}{2m} + H_z\beta(2n+1)}{kT}} \right\} \\ &= \frac{VeH_z}{ch} \sqrt{\frac{2\pi mkT}{h^2}} \sum_{n=0}^{\infty} e^{-\frac{H_z\beta(2n+1)}{kT}} \\ &= \frac{VeH_z}{ch^2} \sqrt{2\pi mkT} \frac{1}{2 \sinh (H_z\beta/kT)} \end{aligned}\right\} \tag{14}$$

where $V = L_x L_y L_z$. For normal field intensities, the susceptibility determined from this partition function by means of Eq. (20) of the preceding section is

$$\chi = -\frac{1}{3} \frac{N}{V} \frac{\beta^2}{kT} \tag{15}$$

where N is the total number of particles.

For Fermi-Dirac statistics, the partition function f of a particle is given by the equation[1]

$$\log f = 2 \sum_{n=0}^{\infty} \int_{-\infty}^{\infty} \frac{eH_z V}{ch} dk_z \log \{1 + e^{\alpha - \frac{\frac{h^2k_z^2}{2m} + H_z\beta(2n+1)}{kT}}\}.$$

Since α is very large for a degenerate gas, we may replace the logarithm in the integrand by

$$\alpha - \frac{\left[\frac{h^2k_z^2}{2m} + H_z\beta(2n+1)\right]}{kT}$$

and evaluate the summations only for those values of n and k_z for which this quantity is positive. This procedure is equivalent to assuming that the major part of the contributien to diamagnetism arises from the

[1] See, for example, R. H. Fowler, *Statistical Mechanics* (Cambridge University Press, 1937). The quantity α is equal to ϵ_0'/kT, as in Sec. 26.

electrons in the completely filled part of the Fermi distribution. The integration over k_z then takes place between the limits

$$\pm\frac{1}{h}(2mkT)^{\frac{1}{2}}\left[\alpha - \frac{H_z\beta(2n+1)}{kT}\right]^{\frac{1}{2}} \tag{16}$$

and leads to the result

$$\sum_n \frac{2eH_zV}{ch^2}\frac{4}{3}(2mkT)^{\frac{1}{2}}\left[\alpha - \frac{H_z\beta(2n+1)}{kT}\right]^{\frac{3}{2}}. \tag{17}$$

The summation over n extends from zero to $kT\alpha/2H_z\beta$ and may be obtained by use of the approximate equation

$$\sum_0^N F(n) \cong \int_{-\frac{1}{2}}^{N+\frac{1}{2}} F(n)dn - \tfrac{1}{24}\left[F'(n)\right]_{-\frac{1}{2}}^{N+\frac{1}{2}}. \tag{18}$$

The result is

$$\left[N\frac{h^2}{5m}\left(\frac{3N}{8\pi V}\right)^{\frac{2}{3}} - \frac{2\pi mV\beta^2}{3h^2}\left(\frac{3N}{\pi V}\right)^{\frac{1}{3}}H_z^2\right]\frac{1}{kT}, \tag{19}$$

in which the two terms arise, respectively, from the two terms of (18). The first term is independent of H_z, so that the second is entirely responsible for the magnetism of the system. The susceptibility determined from it is

$$\chi = -\frac{4\pi m\beta^2}{3h^2}\left(\frac{3N}{\pi V}\right)^{\frac{1}{3}}. \tag{20}$$

It is easy to see from the form of Eq. (17) that the summation over n would vanish in the approximation of Eq. (18) if it were carried out before the integration rather than after it. This shows that the diamagnetic term (20) is a three-dimensional effect and is related to a redistribution of electrons near the top of the filled band among different levels. The reason for the redistribution is illustrated schematically in Fig. 4, which represents a plane in wave-number space that is normal to the z axis. The circle is the limit of the occupied region. In the absence of a field, the allowable values of wave number are uniformly distributed, whereas, in the presence of a field H_z, the group of levels lying in the cylindrical shell parallel to the z axis associated with a range

$$\Delta\epsilon' = \frac{H_zhe}{2\pi mc}$$

coalesce to form levels going with a single value of n. Some of the levels near the boundary of the circle that were previously occupied now lie

outside the circle. Others that previously were unoccupied now lie inside. Although the electrons move from the first set of levels to the second, the mean free energy remains larger than the value in the absence of a field by the second term in the brackets of Eq. (19).

Peierls[1] has pointed out that Eq. (18) is valid only when the condition

$$|F(m) - F(m-1)| << F(m) \quad (21)$$

is satisfied for all values of m, which implies that $H_z\beta << kT$.[2] This condition is not satisfied for sufficiently low temperatures and high field strengths. Thus, $kT/H_z\beta$ is of the order unity for $T \sim 10°K$ and $H_z \sim 10$ kilogauss. Under these conditions, the susceptibility must be computed by using different approximational methods.

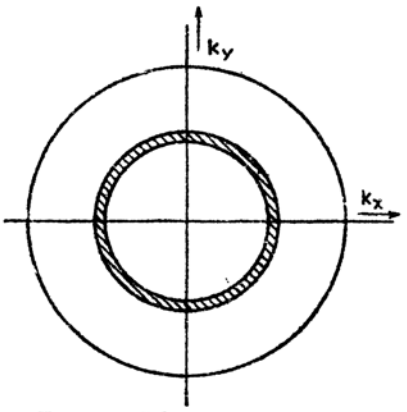

FIG. 4.—Schematic representation of the behavior of the electronic levels in the three-dimensional case. The diagram represents a cross section of wave-number space normal to the z axis, the field being in the z direction. The outer circle is the limit of the filled region. In the presence of a field the group of levels contained in the shaded cylindrical tube parallel to the z axis coalesce to form levels associated with a single value of n. Some of the levels of given k_z are raised and an equal number are lowered. This is unimportant for the electrons well inside the filled region, since the mean energy is unchanged. On the other hand, the effect is important for the electrons near the surface of the filled region and their mean energy is raised.

Suppose that we have a two-dimensional system of free particles at absolute zero of temperature and that the energy levels, in the presence of a field, are determined by Eq. (11), namely,

$$\epsilon' = H_z\beta(2n + 1).$$

When the degeneracy $eH_zL_xL_y/ch$ becomes greater than N, the total number of particles, all particles occupy the state for which $n = 0$ and the total energy is

$$E = NH_z\beta, \quad (22)$$

which corresponds to a constant magnetic moment and zero susceptibility. As H_z is lowered, E decreases until the degeneracy becomes less than N, whereupon some of the electrons begin filling levels for which n is unity. The energy then increases with decreasing field intensity, so that the system becomes paramagnetic when

$$H_z = \frac{chN}{eL_xL_y}.$$

[1] R. PEIERLS, *Z. Physik*, **80**, 763 (1933); **81**, 186 (1933).

[2] Otherwise it is possible that $\alpha - \frac{H_z\beta(2n+1)}{kT}$ may be accidentally zero for $n = n'$ and very large for $n = n' + 1$.

It is easy to see that the general expression for the total energy is

$$\left.\begin{aligned} E(n) &= g\beta H_z^2\{1 + 3 + \cdots + [2(n-1)+1]\} + \\ &\qquad (N - ngH_z)H_z\beta(2n+1) \\ &= NH_z\beta(2n+1) - gH_z^2\beta n(n+1) \end{aligned}\right\} \quad (23)$$

when

$$\frac{N}{n+1} < gH_z < \frac{N}{n} \quad (24)$$

where

$$g = \frac{e}{ch} L_x L_y.$$

The magnetic moment for fields in the range (24) is

$$M = -\frac{\partial E(n)}{\partial H_z} = -N\beta(2n+1) + 2gH_z\beta n(n+1),$$

which is equal to $N\beta$ when $gH_z = N/n$ and is $-N\beta$ when

$$gH_z = \frac{N}{(n+1)}.$$

Thus, the moment abruptly changes sign at frequent intervals as the

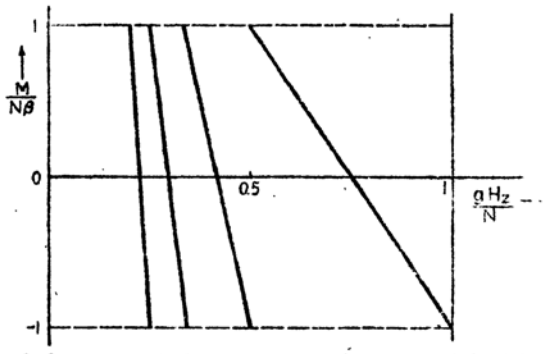

FIG. 5.—Behavior of the magnetic intensity as a function of field intensity at absolute temperature in the two-dimensional case.

field is lowered, the discontinuities occurring at points for which gH_z is equal to N/n. This behavior is shown in Fig. 5.

The three-dimensional spectrum is not discrete, so that discontinuous changes in sign do not occur. Peierls[1] has shown, however, that oscillations in sign still occur. By a direct extension of the preceding work, he obtained the equation

$$-\frac{M}{V} = \frac{e^3}{\pi^2\hbar^3c^3}\frac{\epsilon_0'^3}{\beta^2}\sigma\left(\frac{\beta H_z}{kT}, \frac{\epsilon_0'}{kT}\right) \quad (25)$$

[1] R. PEIERLS, *Z. Physik*, **81**, 186 (1933).

for the magnetic moment per unit volume. Values of σ, determined by direct computation, are shown in Fig. 6. Variations similar to this have been observed in bismuth and will be discussed in the next section.

139. The Orbital Diamagnetism of Quasi-bound Electrons*.—Peierls[1] has extended the theory of the diamagnetism of valence electrons to include the case in which the electrons are nearly bound. It turns out in this case that there are three contributions to the susceptibility, namely, one that is identical with the susceptibility of atomic electrons, given by Eq. (31), Sec. 137, another that is a generalization of Eq. (20) of the previous section for perfectly free electrons, and a third that has no analogue in either the free or the bound models. Although

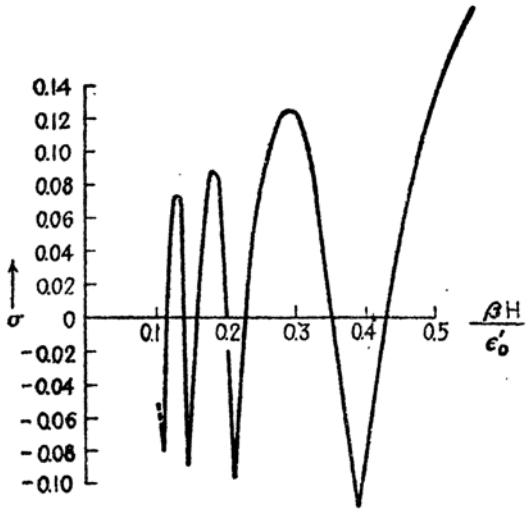

FIG. 6.—The function σ in Eq. (25) for the absolute zero of temperature.

Peierls's treatment of the problem, which is presented here, is valid only for nearly-bound electrons, Wilson[2] has shown that the second term also occurs for nearly free electrons and is a measure of the susceptibility accompanying the type of free-electron motion found in metals. As we shall see, this term may be used to explain the unusually large diamagnetism of bismuth and the γ phases.

Consider a set of weakly interacting atoms that are centered at the lattice positions $\mathbf{r}(n)$ given by the equation

$$\mathbf{r}(n) = n_1\boldsymbol{\tau}_1 + n_2\boldsymbol{\tau}_2 + n_3\boldsymbol{\tau}_3, \tag{1}$$

in which the $\boldsymbol{\tau}$ are primitive translations for a simple cubic lattice having lattice constant d. If the interaction forces are neglected, the Schröd-

[1] *Ibid.*

[2] A. H. WILSON, *The Theory of Metals* (Cambridge University Press, 1936).

inger equation for the electron on the nth atom is

$$-\frac{\hbar^2}{2m}\Delta\varphi_n(\mathbf{r}-\mathbf{r}(n))+\left\{V(\mathbf{r}-\mathbf{r}(n))-\frac{ie\hbar}{2mc}H_z\left(x\frac{\partial}{\partial y}-y\frac{\partial}{\partial x}\right)+\frac{e^2H_z^2}{8mc^2}(x^2+y^2)\right\}\varphi_n=\epsilon\varphi_n, \quad (2)$$

in which φ_n and V are the atomic wave function and potential, respectively. This equation is different for each atom because the zero of the vector potential has been chosen to be the origin of coordinates. We may reduce the equations to a standard form by the transformation

$$\varphi_n = e^{-2\pi i\alpha\mathbf{r}(n)\cdot(\mathbf{r}\times\mathbf{H})}\psi(\mathbf{r}-\mathbf{r}(n)) \quad (3)$$

where $\alpha = e/2hc$. The equation satisfied by ψ, namely,

$$-\frac{\hbar^2}{2m}\Delta\psi(\mathbf{r}-\mathbf{r}(n))+\left\{V(\mathbf{r}-\mathbf{r}(n))-\frac{ie\hbar}{2mc}H_z\left((x-n_xd)\frac{\partial}{\partial y}-(y-n_yd)\frac{\partial}{\partial x}\right)+\frac{e^2H_z^2}{8mc^2}[(x-n_xd)^2+(y-n_yd)^2]\right\}\psi=\epsilon\psi, \quad (4)$$

is the same as the equation for $\varphi_0(\mathbf{r}-\mathbf{r}(n))$. Hence,

$$\varphi_n = e^{-2\pi i\alpha\mathbf{r}(n)\cdot(\mathbf{r}\times\mathbf{H})}\varphi_0(\mathbf{r}-\mathbf{r}(n)). \quad (5)$$

This result shows that the energy $\epsilon(H_z)$ of each of the unperturbed functions is the same, namely,

$$\epsilon(H_z) = \epsilon_0 + \chi_a\frac{H_z^2}{2}, \quad (6)$$

where ϵ_0 is the energy in the absence of a field and χ_a is the atomic diamagnetic susceptibility:

$$\chi_a = \frac{e^2}{8mc^2}\int|\varphi|^2(x^2+y^2)d\tau \quad (7)$$

[*cf.* Eq. (30), Sec. 137]. This is the first of the three contributions to the total susceptibility that were mentioned in the opening paragraph.

Equation (5) may be placed in another convenient form by employing the displacement operator $e^{-a\frac{\partial}{\partial x}}$, which has the property[1]

$$e^{-a\frac{\partial}{\partial x}}f(x) = f(x-a). \quad (8)$$

[1] This property of the operator $e^{-a\frac{\partial}{\partial x}}$ may easily be demonstrated by expanding it as a power series in terms of the exponent, and comparing the result of the operation of the operator on a function with Taylor's series.

Using this operator, we may write φ_n in the form

$$\varphi_0(\mathbf{r} - \mathbf{r}(n)) = e^{-\frac{i}{\hbar}\mathbf{r}(n)\cdot\mathbf{p}}\varphi_0(\mathbf{r}) \tag{9}$$

where

$$\mathbf{p} = \frac{\hbar}{i}\,\mathrm{grad}.$$

Thus, Eq. (5) becomes

$$\varphi_n = e^{-2\pi i\mathbf{r}(n)\cdot\mathbf{P}}\varphi_0, \tag{10}$$

in which

$$\mathbf{P} = \left(\frac{\mathbf{p}}{h} + \alpha\mathbf{r} \times \mathsf{H}\right). \tag{11}$$

We shall now consider interatomic perturbation terms on the assumption that the Hamiltonian operator for an electron near the nth atom is

$$H' = -\frac{\hbar^2}{2m}\Delta + \sum_m V(\mathbf{r} - [\mathbf{r}(n) - \mathbf{r}(m)]) - \frac{ie\hbar}{2mc}\mathsf{H}_z\left(x\frac{\partial}{\partial y} - y\frac{\partial}{\partial x}\right) + \frac{e^2\mathsf{H}_z^2}{8mc^2}(x^2 + y^2). \tag{12}$$

This is the same as the Hamiltonian operator in Eq. (2) except for the term

$$\sum_m{}' V(\mathbf{r} - [\mathbf{r}(n) - \mathbf{r}(m)]). \tag{13}$$

If we assume that the perturbed eigenfunction ψ may be expressed in the form

$$\psi = \sum_m{}' a_m\varphi_m, \tag{14}$$

the eigenvalue equations for the a_m are

$$\epsilon' a_m = \sum_l{}' u_{ml}a_l \tag{15}$$

where ϵ' is the eigenvalue of the perturbed system and

$$u_{ml} = \int \varphi_m{}^* H' \varphi_l d\tau = \int \varphi_0{}^* e^{2\pi i\mathbf{r}(n)\cdot\mathbf{P}} H' e^{-2\pi i\mathbf{r}(l)\cdot\mathbf{P}}\varphi_0 d\tau. \tag{16}$$

Peierls proved that the off-diagonal matrix elements (16) are matrix components of the operator

$$E = \epsilon(\mathsf{H}) + \sum_l{}' A(l)e^{2\pi i\mathbf{r}(l)\cdot\mathbf{K}} \tag{17}$$

where

$$A(l) = \int \varphi_l^* \Big\{ \sum_q{}' V(\mathbf{r} - \mathbf{r}(q)) \Big\} \varphi_0 d\tau \tag{18}$$

and

$$\mathbf{K} = \mathbf{P} - \frac{e}{hc}(\mathbf{r}_0 \times \mathbf{H}), \tag{19}$$

in which $\mathbf{r}_0$ is by definition the matrix satisfying the relation

$$\mathbf{r}_0 \cdot \varphi_n = \mathbf{r}(n)\varphi_n.$$

In the presence of a magnetic field, $A(l)$ involves the field intensities through the function φ_n^*. This fact may be made explicit by writing φ_n^* in the form (10) with the help of Eq. (11). In the absence of a magnetic field,

$$\mathbf{K} = \frac{1}{2\pi i} \operatorname{grad}, \tag{20}$$

and the eigenvalues of $\mathbf{K}$ are the wave-number vectors $\mathbf{k}$. Hence, in this case the eigenvalues of E are

$$\epsilon(\mathbf{k}) = \epsilon_0 + \sum_l A_0(l) e^{2\pi i \mathbf{k} \cdot \mathbf{r}(l)} \tag{21}$$

where A_0 is the value of A when $\mathbf{H} = 0$. This result was previously derived in Sec. 65 by more direct means.

Using Eq. (17) Peierls computed the total partition function for the perturbed system by a method that will not be discussed here. The result is

$$\log f = \int \left\{ g\left(\epsilon(\mathbf{k}) + \frac{(\chi_a + \epsilon_1)\mathbf{H}_z^2}{2} \right) + \frac{\mathbf{H}_z^2 \alpha^2}{24\pi^2} \left[\frac{\partial^2 \epsilon}{\partial k_x^2} \cdot \frac{\partial^2 \epsilon}{\partial k_y^2} - \left(\frac{\partial^2 \epsilon}{\partial k_x \partial k_y} \right)^2 \right] g''(\epsilon_0'(\mathbf{k})) \right\} d\tau \tag{22}$$

where

$$\left.\begin{aligned} g(\epsilon) &= \log\left(1 + e^{\frac{\epsilon_0' - \epsilon}{kT}}\right), \\ \epsilon_1(\mathbf{k}) &= -\frac{\alpha^2}{\mathbf{H}_z^2} \sum_l \left(e^{2\pi i \mathbf{k} \cdot \mathbf{r}(l)} \int \varphi_0(\mathbf{r} - \mathbf{r}(l)) \cdot [\mathbf{r}(l) \cdot (\mathbf{r} \times \mathbf{H})]^2 \right. \\ &\qquad \left. \Big\{ \sum_n{}' V(\mathbf{r} - \mathbf{r}(n)) \Big\} \varphi_0 d\tau \right), \end{aligned}\right\} \tag{23}$$

and the integration extends over all wave-number space. It should be observed that ϵ_1 is independent of $\mathbf{H}_z$. If the first integrand in (22) is

expanded to terms in H_z^2, it leads to the result

$$\int\left[g(\epsilon)+\frac{\mathsf{H}_z^2}{2}(\chi_a+\epsilon_1)g'(\epsilon)\right]d\tau(\mathbf{k}), \tag{24}$$

in which the integral involving the first term is the partition function in the absence of a field. Since χ_a is a constant, the remaining terms may be placed in the form

$$\frac{\mathsf{H}_z^2}{2}\left[-\frac{N\chi_a}{kT}+\int\epsilon_1 g'(\epsilon)d\tau(\mathbf{k})\right]. \tag{25}$$

Thus, if we include the second term in the integrand of (22), we see that there are three contributions to the susceptibility, namely,

$$\chi_1=-\frac{N}{V}\chi_a, \tag{26}$$

$$\chi_2=\frac{kT}{V}\int\epsilon_1 g'(\epsilon(\mathbf{k}))d\tau, \tag{27}$$

$$\chi_3=\frac{kT}{12\pi^2}\frac{\alpha^2}{V}\int\left[\frac{\partial^2\epsilon}{\partial k_z^2}\frac{\partial^2\epsilon}{\partial k_y^2}-\left(\frac{\partial^2\epsilon}{\partial k_x\partial k_y}\right)^2\right]g''(\epsilon)d\tau(\mathbf{k}). \tag{28}$$

χ_a should be the same order of magnitude as the atomic susceptibility of gases, namely,

$$\frac{e^2}{6mc^2}\overline{r^2},$$

and should lead to a diamagnetic susceptibility of the order of 10^{-7}. A simple estimate of χ_2 shows that it is related to χ_1 in order of magnitude by the equation

$$\chi_2\sim\frac{m}{m^*}\chi_1$$

where m is the true electronic mass and m^* is the effective mass of the electrons in the filled region. Thus, χ_2 would be negligible in the limiting case of very narrow bands.[1]

The factor $g''(\epsilon)$ in the integrand of (28) is

$$\frac{1}{kT}\frac{\partial}{\partial\epsilon}\left(\frac{1}{e^{\frac{\epsilon-\epsilon'}{kT}}+1}\right)=\frac{1}{kT}\frac{\partial f}{\partial\epsilon}$$

where f is the Fermi function. This derivative has a sharp peak at the point $\epsilon=\epsilon_0'$ and satisfies the relation [see Eq. (29), Sec. 26]

$$\int\alpha(\epsilon)\frac{\partial f}{\partial\epsilon}d\epsilon=-\alpha(\epsilon_0').$$

[1] Wilson (*op. cit.*) has shown that χ_2 is zero for perfectly free electrons.

Hence, χ_3 may be placed in the form

$$\chi_3 = -\frac{1}{12\pi^2}\frac{\alpha^2}{V}\int_S\left(\frac{\partial^2\epsilon}{\partial k_x^2}\frac{\partial^2\epsilon}{\partial k_y^2} - \frac{\partial^2\epsilon}{\partial k_x \partial k_y}\right)\frac{2V}{|\text{grad}_k\ \epsilon|}dS \tag{29}$$

where the integral extends over the surface of the filled region in wave-number space. This expression reduces to Landau's equation (15) of the previous section when the electrons are perfectly free, that is, when ϵ is equal to $h^2k^2/2m$.

The quantity in parentheses in Eq. (29) becomes large whenever the curvature of $\epsilon(\mathbf{k})$ is large at the edge of the filled region. Since this may occur near the boundary of a zone according to the zone theory, χ_3 should be largest for metals such as the alkaline earths and bismuth that have nearly filled zones. Jones[1] has postulated that the five valence electrons per atom in bismuth extend just beyond a prominent zone that has room

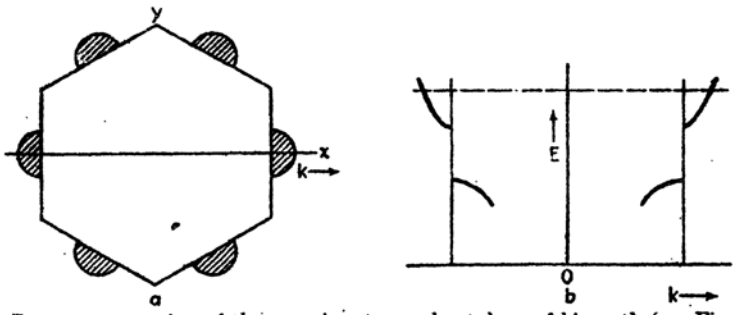

FIG. 7.—*a*, cross section of the prominent zone boundary of bismuth (see Fig. 6, Chap. XIII) normal to the preferred direction. The shaded regions are those in which it is believed the filled region extends into the outer zone. *b* represents schematically the behavior of the $\epsilon(\mathbf{k})$ curve for the line through the zone boundary shown in *a*. The dotted line in *b* is the top of the filled region. The curvature of the $\epsilon(\mathbf{k})$ curve is believed to be very large in the upper branch, so that the effective electron mass is small.

for five electrons per atom in several directions. In addition, he postulated that the behavior of the $\epsilon(\mathbf{k})$ curve near the zone is as in Fig. 7, so that the curvature is very great for the higher zone. The high diamagnetic susceptibility of this metal and of the alloys such as γ brass that have similarly filled zones may be understood in terms of this picture, for the integrand of Eq. (29) is large and positive for a part of the range of integration in all these substances.

In order to develop a semiquantitative theory of the diamagnetism of bismuth, Jones assumed that the energy contours are ellipsoids of revolution which are centered about the center points of the vertical plane faces of the zone in the six regions of Fig. 7 in which the filled region extends into the outer zones. Thus, if the z axis is parallel to the prin-

[1] H. JONES, *Proc. Roy. Soc.*, **144** 225 (1934); **147**, 396 (1934).

cipal axis of the crystal, the energy contours in any one of the six regions have the form

$$\epsilon(\mathbf{k}) = \frac{h^2}{2m}(\alpha_1 k_x^2 + \alpha_1 k_y^2 + \alpha_3 k_z^2) \tag{30}$$

where the origin is at the center point of the corresponding face. The constants α_1 and α_3 are, respectively, the ratios of the electron mass to the effective mass in the directions normal to the principal axis and along the principal axis. It follows from the symmetry of the prominent zone of bismuth that the ellipsoidal contours on opposite faces may be joined, six sets of completely ellipsoidal contours being thus produced.

If (30) is substituted in Eq. (29), it is found that the volume susceptibility in the z direction, expressed in cgs units, is

$$\chi = -0.122\sqrt{\epsilon_0'}\sqrt{\frac{\alpha_1^2}{\alpha_3}}10^{-6} \tag{31}$$

where ϵ_0' is the value of (30) at the top of the filled region expressed in ev. Thus, χ is largest in the direction in which α is smallest.

Now, the number of states per atom n_a within the ellipsoidal contour associated with ϵ_0' is

$$n_a = v_0\frac{8\pi}{3}\left(\frac{2m\epsilon_0'}{h^2}\right)^{\frac{3}{2}}\frac{1}{\sqrt{\alpha_1\alpha_1\alpha_3}}, \tag{32}$$

in which v_0 is the atomic volume. This result may be derived by computing the volume of the ellipsoid and using the fact that there are $2V$ states per unit volume of $\mathbf{k}$ space, if V is the volume of the crystal. Jones evaluated n_a by noting that the temperature coefficient of resistance of the tin-bismuth alloy system changes from positive to negative as tin is added to bismuth, the value zero occurring when about 0.13 atom per cent of tin is present. Each bismuth atom that is replaced by a tin atom presumably carries with it one of the electrons from the overlapping region, for the valence of tin is one unit less than that of bismuth. Thus, if it is assumed that the point at which the temperature coefficient of resistance changes sign is the same as that at which the boundary of the filled region extends just to the first zone, it follows that the number of electrons per atom outside the inner zone in pure bismuth is 0.0013, or there is 0.0002 electron per atom in each of the six shaded regions of Fig. 7. From this, ϵ_0' may be computed by the use of Eq. (32), and $\sqrt{\epsilon_0'}$ in Eq. (31) may then be given a value.

Jones finds that the observed room-temperature values of $\chi_\perp$ and $\chi_\parallel$, which are listed in Table VI, Chap. I, may be obtained from Eq. (34) by assuming

$$\alpha_1 \sim 40 \qquad \text{and} \qquad \alpha_3 \sim 1$$

The assumption that the α in the plane normal to the principal axis are equal is justified by the fact that the susceptibility is the same in all directions normal to the principal axis.

The most extensive theoretical treatment of the low-temperature susceptibility of bismuth has been given by Blackman,[1] whose work is based on an extension of Peierls's theory. As we pointed out in the last section, it is observed experimentally that the susceptibility fluctuates

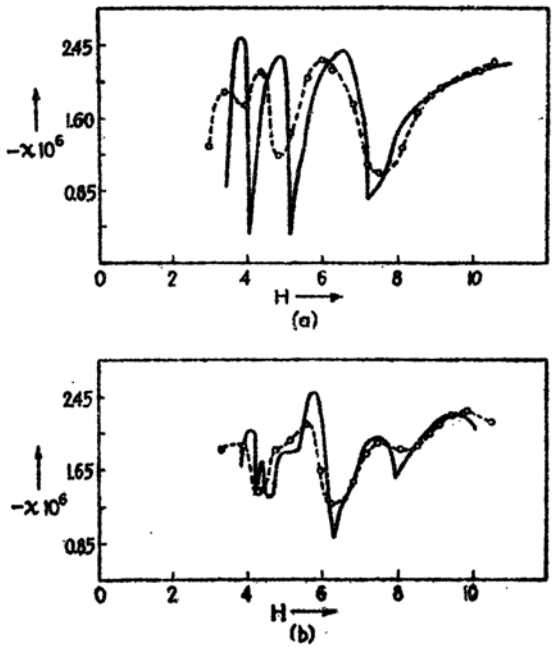

FIG. 8.—Comparison of the observed and calculated values of the low-temperature magnetic susceptibilities of bismuth in the plane normal to the principal axis. Curves a correspond to values along the x direction of Fig. 7, and curves b correspond to the y direction. The measured values, which are for 1.86°K, are represented by circles on the dotted curves.

with the field intensity in the neighborhood of absolute zero of temperature. For example, Figs. 8a and 8b show the variations[2] of $-\chi$ with field intensities at 1.86°K. The measurements a are for fields parallel to the x axis of Fig. 7, and the measurements b are for fields in the y direction. Thus, the effect is not the same in all directions normal to the principal axis. Fluctuations are not observed when the field is parallel to the principal axis. It may be mentioned that the curves of Fig. 8 for 1.86°K are closely similar to curves for 14.2°K in the region in which the abscissae

[1] M. BLACKMAN, *Proc. Roy. Soc.*, **166**, 1 (1938).

[2] W. J. DE HAAS and P. M. VAN ALPHEN, *Leiden Comm.*, 212 (1931); D. SHOENBERG and M. Z. UDDIN, *Proc. Roy. Soc.*, **156**, 687 (1936).

overlap. This suggests that the curves of Fig. 8 may safely be compared with theoretical curves computed for the absolute zero.

The fact that the susceptibility is not symmetrical about the principal axis in the low-temperature range indicates that the energy contours for the electrons which are responsible for the fluctuations cannot have the symmetry of the function (30), for this function is invariant under rotations about the z axis. Thus, Blackman was led to assume that the $\epsilon(\mathbf{k})$ function for these electrons is

$$\epsilon(\mathbf{k}) = \frac{h^2}{2m}(\alpha_1 k_x^2 + \alpha_2 k_y^2 + \alpha_3 k_z^2) \tag{33}$$

where α_1, α_2, and α_3 are different constants. At first sight, this appears to contradict Jones's results. Blackman points out, however, that the

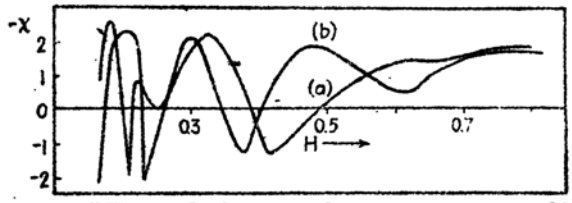

FIG. 9.—The susceptibility at absolute zero of temperature computed by assuming that there is only the type of electron corresponding to Eq. (33). The designations a and b have the same significance as in Fig. 8. The theoretical curves of Fig. 8 were derived by adding to the curves of this figure the susceptibility arising from the type of electron considered by Jones.

number of electrons responsible for the fluctuations probably is much smaller than the number determining the high-temperature susceptibility so that the two sets may occupy completely different parts of wave-number space and make independent contributions to the susceptibility In this connection, it should be emphasized that the zone shown in Fig. 7 and in Fig. 6, Chap. XIII, is not the first Brillouin zone but the fifth. Hence, it is very probable that there are regions in the outer zone other than those indicated in Fig. 7 in which the effective mass is very high. In support of this is the fact that the sign of χ fluctuates in the theoretical curves derived by Peierls (*cf.* Fig. 6) and Blackman (*cf.* Fig. 9) on the assumption of one type of electron, whereas the experimental susceptibility is always negative.

The susceptibility computed by Blackman for the absolute zero of temperature using (33) is shown in Fig. 9, which corresponds to the particular ratio $\alpha_1/\alpha_2 = 9.8$. The abscissa is the variable H/H_0, where H is the magnetic field intensity and H_0 is

$$H_0 = \frac{\epsilon_0'}{\beta(\alpha_1\alpha_2)^{\frac{1}{2}}}$$

in which ϵ_0' is the Fermi energy relative to the zero of (33). Blackman added a constant to his theoretical susceptibility in order to include Jones's type of diamagnetism and adjusted the parameters ϵ_0', α_1, α_2, and α_3 in order to fit the observed curves most reasonably. The results, which correspond to the parameters

$$\alpha_1 = 9.8, \qquad \alpha_2 = 1.0, \qquad \alpha_3 = 1.1 \cdot 10^3,$$
$$\epsilon_0' = 0.019 \text{ ev},$$

are shown in Fig. 8. The number of free electrons per atom in the part of the band responsible for the fluctuating susceptibility as computed from ϵ_0' is $1.2 \cdot 10^{-5}$, which is about 1 per cent of the number Jones found were responsible for the room-temperature susceptibility. As may be seen from Eq. (31), the large value of α_3 accounts for the absence of an observable fluctuating susceptibility in the z direction.

140. The Spin Paramagnetism of Valence Electrons*.—The origin of the paramagnetic behavior of many simple metals was first explained by Pauli in the elementary way described in Sec. 29. The value of the susceptibility obtained from this theory is

$$\chi = \frac{2\beta^2 g_s(\epsilon_0')}{V} \tag{1}$$

where β is the Bohr magneton, $g_s(\epsilon_0')$ is the density of energy levels of one spin at the top of the filled band, and V is the volume of the metal. Although this explanation, which involves the assumption that the two systems of energy states associated with opposite spins become displaced relative to one another in a field, is believed to be correct in principle, the simple computation requires modification for the following reasons:

a. The density function $g_s(\epsilon)$ is not necessarily the same as for free electrons.

b. The total energy of the solid cannot be expressed only as a function of one-electron energy terms, but also involves two-electron terms. Of these, the exchange and correlation energies are dependent upon the number of electrons having each kind of spin and affect the susceptibility in a way that cannot be included in the expression (1).

c. The orbital diamagnetism of inner closed shells and valence electrons, which was discussed in the previous sections, is comparable with the spin paramagnetism. These diamagnetic terms are so important in metals having newly filled d shells or nearly filled bands that they determine the sign of the susceptibility.

Let us assume that we have an electronic distribution, in which the first $(N + p)/2$ levels of electrons whose magnetic moments are parallel to the field are filled and in which the first $(N - p)/2$ levels of opposite spin are also filled. We shall designate the energy of the nth level from

the bottom in the absence of a field by $\epsilon(n)$. When there is a field, the total energy in the Bloch-Hartree approximation is

$$E(p) = \int_0^{\frac{(N-p)}{2}} \epsilon_s(n)dn + \int_0^{\frac{(N+p)}{2}} \epsilon_s(n)dn - p\beta\mathsf{H}_z. \tag{2}$$

If this is expanded in terms of p, it is necessary to retain only the first-order terms, since we shall be interested in the case in which p/N is small. The result is

$$E(p) \cong E(0) + \frac{p^2}{4}\left(\frac{d\epsilon}{dp}\right)_{p=\frac{N}{2}} - p\beta\mathsf{H}_z. \tag{3}$$

We shall elevate and add to (3) the electronic-interaction terms for the case of free electrons.

It may be recalled that the exchange interaction energy arises from the interaction between electrons of parallel spin. When electrons of both spins are present in equal numbers, the exchange energy per electron is (*cf.* Sec. 75)

$$\epsilon_e = -\frac{3^{\frac{1}{2}}e^2}{2\pi^{\frac{1}{2}}}n_0^{\frac{1}{3}} \tag{4}$$

where n_0 is the total electron density. This may be expressed in terms of the radius r_s of the equivalent sphere and is then

$$-0.458\frac{e^2}{r_s}. \tag{5}$$

If there are $(N + p)/2$ electrons of one spin and $(N - p)/2$ of opposite spin, the total exchange energy is

$$E_e(p) = -\left[\frac{(N-p)}{2}\left(\frac{N-p}{N}\right)^{\frac{1}{3}} + \frac{(N+p)}{2}\left(\frac{N+p}{N}\right)^{\frac{1}{3}}\right]\frac{0.458e^2}{r_s}, \tag{6}$$

which becomes

$$E_e(p) = -N\frac{0.458e^2}{r_s} - \frac{2}{9}\frac{p^2}{N}\frac{0.458e^2}{r_s} \tag{7}$$

when expanded in terms of p.

We shall assume that the correlation energy arises only from electrons of opposite spin, for reasons discussed in Sec. 76. The correlation energy as a function of p then is

$$\left.\begin{aligned} E_c(p) &= -e^2\left\{\frac{(N-p)}{2}f\left(\left(\frac{N}{N+p}\right)^{\frac{1}{3}}r_s\right) + \frac{(N+p)}{2}f\left(\left(\frac{N}{N-p}\right)^{\frac{1}{3}}r_s\right)\right\} \\ &\cong -e^2\left\{Nf(r_s) + f'(r_s)\frac{5r_s}{9}\frac{p^2}{N} + \frac{1}{18}f''(r_s)r_s^2\frac{p^2}{N}\right\} \end{aligned}\right\} \tag{8}$$

where

$$f = \frac{0.288}{r_s + 5.1a_h}.$$

The term in f' usually is at least ten times as large as the one in f''.

Combining Eqs. (3), (7), and (8), we obtain for the total energy

$$E_t(p) = E_t(0) + \alpha\frac{p^2}{N} - p\beta\mathsf{H}_z \tag{9}$$

where

$$\alpha = \frac{N}{4}\left(\frac{d\epsilon}{dp}\right)_{p=\frac{N}{2}} - \frac{2}{9}\frac{0.458}{r_s}e^2 - \frac{5}{9}f'(r_s)r_s e^2 - \frac{1}{18}f''(r_s)r_s^2 e^2. \tag{10}$$

The expression (9) is a minimum for the value of p satisfying the equation

$$2\alpha p = N\beta\mathsf{H}_z$$

or

$$p = N\frac{\beta\mathsf{H}_z}{2\alpha}. \tag{11}$$

If this is substituted in Eq. (9), we obtain

$$E_t(\mathsf{H}_z) = E_t(0) - N\frac{\beta^2\mathsf{H}_z^2}{4\alpha}. \tag{12}$$

Hence, the susceptibility is

$$\chi = n_0\frac{\beta^2}{2\alpha}. \tag{13}$$

This reduces to Eq. (1) when the exchange and correlation terms are neglected, since

$$g_s(\epsilon') = \left(\frac{dp}{d\epsilon}\right)_{p=\frac{N}{2}}.$$

The terms in α are given in Table LXXXI for sodium and lithium. Although the first term is largest the others[1] are not negligible. Values of the total susceptibility given by Eq. (13) appear in the same table. In addition, values of the free-electron diamagnetism and the inner-shell diamagnetism are listed. The former were obtained by the use of Eq. (29), page 595, and the relation $\epsilon = \hbar^2\mathbf{k}^2/2m^*$, the computed values of m being employed. The contribution to free-electron diamagnetism from exchange was not included since the corresponding term from correlations cannot be computed. The comparatively small ion-core terms were obtained from Van Vleck's book.

[1] Further details of this computation are to be published in the *Phys. Rev.*

The observed and calculated values of the susceptibility agree closely in the case of sodium, but the computed value for lithium is somewhat higher than the highest observed one. The agreement in the first case supports the general conclusion that the electrons in sodium are very nearly perfectly free, whereas the disagreement in the second case indicates that the relation $\epsilon = h^2\mathbf{k}^2/2m^*$ is not exact. The most reasonable source of the discrepancy would seem to be a comparatively small term in $\mathbf{k}^4$, which causes a lowering of the density of levels at the edge of the filled region and a corresponding decrease in paramagnetism.

TABLE LXXXI.—CONTRIBUTIONS TO α FROM THE TERMS IN EQ. (10) FOR LITHIUM AND SODIUM AND THE VALUE OF THE SUSCEPTIBILITIES GIVEN BY EQ. (13)
(The terms in the first row are expressed in electron volts; those in the second row in terms of 10^6 times the cgs unit of volume susceptibility.)

	$N(d\epsilon/dp)/4 = \epsilon_0'/3$	Exchange	Correlation	Total
Li	1.02	−0.86	0.19	0.35
Na	1.12	−0.70	0.19	0.61

	$\frac{n_0\beta^2}{2\alpha}$	Ion core	Diamagnetic	Total	Observed
Li	3.54	−0.05	−0.17	3.32	1.4–2.0
Na	1.11	−0.18	−0.23	0.70	0.63

It is interesting to note that the exchange energy is made more negative by increasing p [*cf.* Eq. (6)]. This shows that the exchange interaction of free electrons favors the alignment of spins. This tendency toward ferromagnetism ordinarily is more than compensated by the fact that both the Fermi energy and the correlation energy are raised when p increases. The change from paramagnetism to ferromagnetism can occur only when α becomes negative, for then Eq. (11) leads to a maximum rather than a minimum. Bloch[1] pointed out that the exchange term becomes larger than the Fermi term for sufficiently large values of r_s, since the first decreases as $1/r_s$ and the other as $1/r_s^2$. If we neglect the correlation terms, it follows from Eq. (10) that this occurs when

$$r_s > 6.03\frac{m}{m^*}a_h.$$

The limiting value of r_s for perfectly free electrons is about $6.0a_h$, which is larger than the value for any alkali metal. This fact and the fact

[1] F. BLOCH, *Z. Physik*, **57**, 545 (1929).

that the correlation term does not favor spin alignment make it safe to say[1] that the observed ferromagnetism of transition metals should not be associated with nearly free electrons.

141. Paramagnetic Salts.—The theory of the properties of the paramagnetic rare earth and iron group element salts has been highly developed in those cases in which the paramagnetic ions are so widely separated that the bands associated with their electrons are narrow and the atomic approximation is valid. We shall not discuss the details of this rather specialized topic here but refer the reader to other sources.[2]

142. Macroscopic and Local Field Corrections.—Suppose that the currents in an electromagnet are adjusted in such a way that the field at a given point in free space is H'. If the space is then occupied by a magnetic specimen, the orienting field that acts upon an atomic magnetic dipole is no longer H' because of the fields arising from the rest of the material. One part of the difference $\mathsf{H} - \mathsf{H}'$, namely, the demagnetization field, may be handled by classical methods. This contribution corresponds to the field of the effective surface distribution of magnetic charge that is induced on the specimen and is determined by the geometrical shape of the specimen. It usually varies from point to point, even when H' is constant; however, it is constant when the specimen has one of several possible shapes. In these cases, the correction takes the form

$$\Delta\mathsf{H}_d = D\mathsf{M} \tag{1}$$

where M is the intensity of magnetization and D is the *demagnetization constant*. D is -4π for a thin pillbox whose axis is parallel to the field and is $-4\pi/3$ for a sphere. Values for other cases have been listed by Stoner.[3] The correction (1) is negligible in substances having a small susceptibility since the fractional error made in neglecting it is of the order of χ.

Under certain conditions, it is convenient to discuss another type of correction field. Suppose, for example, that we are dealing with a dense paramagnetic gas of molecules having a molecular susceptibility χ_a. The magnetic moment per unit volume in this case is not simply

[1] *Cf.* E. WIGNER, *Phys. Rev.*, **46**, 1002 (1934); *Trans. Faraday Soc.*, **34**, 678 (1938).

[2] See the following books and articles: Van Vleck, *op. cit.;* W. G. Penney and R. Schlapp, *Phys. Rev.*, **41**, 194 (1932), **42**, 666 (1932); W. G. Penney, *Phys. Rev.*, **43**, 485 (1935); A. Frank, *Phys. Rev.*, **39**, 119 (1932), **48**, 765 (1935); J. H. Van Vleck, *Phys. Rev.*, **41**, 208 (1932); O. M. Jordahl, *Phys. Rev.*, **45**, 87 (1934); F. H. Spedding, *Jour. Chem. Phys.*, **5**, 316 (1937); A. Siegert, *Physica*, **3**, 85 (1936), **4**, 138 (1937). A survey of the topic has recently been given by J. H. Van Vleck, *Reports of The Strassbourg Conference* (1939); to be published in *Ann. Inst. Henri Poincaré.*

[3] E. C. STONER, *Magnetism and Atomic Structure* (E. P. Dutton & Co., Inc., New York, 1934).

$$\frac{N}{V}\chi_a \mathsf{H}, \tag{2}$$

where H is the demagnetically corrected field, but is different because of the interaction between the molecular magnets. If H_l is the average local magnetic field acting on a given molecule, the mean magnetic moment per molecule is $\chi_a \mathsf{H}_l$ and the intensity of magnetization is

$$\mathsf{M} = n_0 \chi_a \mathsf{H}_l \tag{3}$$

where $n_0 = N/V$. In order to use this, we must know the relationship between H and H_l. Lorentz[1] was the first person to derive a relationship of this kind. He obtained the equation

$$\mathsf{H}_l = \mathsf{H} + \frac{4\pi}{3}\mathsf{M} \tag{4}$$

on the basis of the following assumptions:

a. The arrangement of molecules is either isotropic or cubic.

b. The relative orientation of magnetic moments is statistically the same for both near and distant molecules.

Assumption *b* is analogous to the assumption made in the Bragg-Williams theory of order-disorder (Sec. 124). If Eq. (4) is placed in Eq. (3), we find

$$\mathsf{M} = \frac{n_0 \chi_a}{1 - (4\pi/3) n_0 \chi_a} \mathsf{H}. \tag{5}$$

Thus, the susceptibility per unit volume is

$$\chi = n_0 \frac{\chi_a}{1 - (4\pi/3) n_0 \chi_a}. \tag{6}$$

It should be noted that, from the standpoint of electronic approximations, this and the following discussions of the local field implicitly assume that the magnetic units may be described in an atomic or molecular approximation. Thus, these discussions have significance only when the bands are narrow.

Lorentz's treatment is not completely satisfactory for the same reason that the Bragg-Williams theory of order is not satisfactory, namely, it does not take into account the fact that near neighbors are aligned more often than distant neighbors. We shall discuss two attempts that have been made to improve the theory.

Onsager[2] modified Lorentz's method of computing χ in the following way. For mathematical purposes, Lorentz had circumscribed an imaginary sphere about a given molecule and derived the term $4\pi\mathsf{M}/3$ in

[1] H. A. LORENTZ, *The Theory of Electrons* (Teubner, Leipzig, 1906).

[2] L. ONSAGER, *Jour. Am. Chem. Soc.*, **58**, 1486 (1936).

Eq. (4) by considering the contributions to the field from the molecules inside and outside this sphere. In doing this, he assumed that the polarization is uniform. Onsager assumed that the sphere has physical reality as the volume within which the molecule is contained. In addition, he made the following two assumptions:

a. The polarization field in the magnetic medium outside the sphere is not uniform but is the same as the field about a hollow spherical cavity that contains a point dipole of magnitude $\mathbf{m}$. One part of the polarization field $\mathbf{M}_H$ is induced by the constant applied field $\mathbf{H}$ and is fixed; the rest arises from the dipole and varies when the dipole changes its direction.

b. The field $\mathbf{H}_l$ inside the cavity, exclusive of the dipole field of the molecule, is the orienting field that acts upon a molecule. $\mathbf{H}_l$ is the sum of the external field $\mathbf{H}$ (with depolarization correction) and the field arising from the polarization outside the sphere. The second part of $\mathbf{H}_l$ is analogous to the $4\pi\mathbf{M}/3$ term in the Lorentz equation (4).

In the case in which $\mathbf{m}$ is constant $\mathbf{H}_l$ may be determined as a simple solution of Laplace's equation and is

$$\mathbf{H}_l = \mathbf{H} + \frac{\mu - 1}{2\mu + 1}\mathbf{H} + \frac{2(\mu - 1)}{(2\mu + 1)a^3}\mathbf{m} \tag{7}$$

where μ is the permeability and a is the radius of the spherical cavity. The second term, which arises from the polarization of the external medium induced by the field $\mathbf{H}$, may be transformed to the form

$$\frac{4\pi\chi}{8\pi\chi + 3} \tag{8}$$

where χ is the macroscopic susceptibility $(1 - \mu)/4\pi$. This should be compared with the corresponding Lorentz term

$$\frac{4\pi\chi}{3}. \tag{9}$$

The third term in (7) is the reaction field of the dipole and is always parallel to $\mathbf{m}$. It does not exert an orienting force so that it is unimportant when $\mathbf{m}$ is constant and may be dropped. Thus,

$$\mathbf{H}_l = \left(1 + \frac{4\pi\chi}{8\pi\chi + 3}\right)\mathbf{H}. \tag{10}$$

It should be noted that this approaches a limiting value $3\mathbf{H}/2$ when the magnetic susceptibility becomes large, for the field then attempts to avoid the cavity. The same effect does not occur in Lorentz's approximation.

If this result is inserted into Eq. (3), the following implicit equation for χ is obtained:

$$\chi = \left(1 + \frac{4\pi\chi}{8\pi\chi + 3}\right) n_0\chi_a. \tag{11}$$

This equation has the solution

$$\chi = \frac{3}{16\pi}\left[-1 + 4\pi n_0\chi_a + \left(1 + \frac{8\pi}{3}n_0\chi_a + 16\pi^2 n_0^2\chi_a^2\right)^{\frac{1}{2}}\right]. \tag{12}$$

Equations (6) and (12) are identical with terms in $(n_0\chi_a)^2$ so that they do not give appreciably different results when $n_0\chi_a$ is much smaller than unity; however, they behave very differently in the region where $n_0\chi_a$ is near unity. Lorentz's expression (6) approaches infinity as $n_0 4\pi\chi_a/3$ approaches unity, whereas Onsager's expression remains finite, being equal to $3(1 + \sqrt{3})/8\pi$. This difference is very important when the atomic susceptibility satisfies the Curie law

$$\chi_a = \frac{C}{T}$$

for then χ_a becomes large at low temperatures. If Eq. (5) were correct, M would be finite even in the absence of a field when $n_0 4\pi\chi_a/3$ becomes unity. Since this effect implies ferromagnetism, Lorentz's theory implies that all substances obeying the Curie law should become ferromagnetic at sufficiently low temperatures. Onsager's equation, on the other hand, does not imply ferromagnetism since

$$\chi \sim \tfrac{3}{2}N\chi_a$$

for large values of χ_a. Simple calculations based on Lorentz's result show that the ferromagnetic Curie point should lie in the neighborhood of 0.1°K for most of the paramagnetic salts. Although several of these salts show ferromagnetic effects near this temperature, Van Vleck[1] believes that this ferromagnetism should be ascribed to the exchange coupling discussed in the next section. Hence, experimental evidence seems to support a modification of Lorentz's theory such as Onsager's.

Van Vleck has derived another relation that is valid at high temperatures and has a more rigorous foundation than either Lorentz's or Onsager's results. He included magnetic dipole-dipole interaction terms in the Hamiltonian function for a paramagnetic crystal of the type mentioned in the preceding section and computed the effect of these upon the partition function, using series expansion methods. If it is assumed that the atomic susceptibility χ_a satisfies the equation

$$\chi_a = \frac{\tau}{3T} \tag{13}$$

[1] J. H. VAN VLECK, *Jour. Chem. Phys.*, **5**, 320 (1937).

where

$$\tau = \frac{g^2\beta^2 J(J+1)}{k},$$

Van Vleck's equation for χ may be written in the form

$$\chi = \frac{\tau}{3T}\left[1 + \frac{4\pi\tau}{3k}\frac{1}{T} + \left(\frac{4\pi\tau}{9k}\right)^2 \frac{1}{T^2} - \frac{\delta}{T^2} + \cdots\right] \tag{14}$$

where

$$\delta = \frac{Q\tau^2}{9}\left(1 + \frac{3}{8}\frac{1}{J(J+1)}\right). \tag{15}$$

Here, Q is an integer of the order of magnitude 10 that depends upon the crystal structure. If Onsager's expression for χ is expanded and a value of Q appropriate to his model is placed in Eq. (14), the two expressions are identical with the terms shown in (14). Lorentz's expression, on the other hand, does not give the same value for the terms that vary as $1/T^2$. Thus, Onsager's result is more accurate when T/τ is larger than unity.

Since Eq. (14) cannot be used at low temperatures, it is not possible to check the validity of Onsager's relation in this region by direct computation of the partition function.

Van Vleck has extended Eq. (14) for the case in which the levels of the paramagnetic ions are split by crystalline fields. This work will not be discussed further here.

One of the most direct supports of the Onsager-Van Vleck theory of local fields arises from its application to polar liquids and molecular solids.[1] These substances contain molecules having permanent dipole moments, so that the preceding theory can be taken over with little modification for a discussion of their electrical properties. Since the relative magnitudes of electrical polarizabilities are of the order of one thousand times larger than those of magnetic polarizabilities at corresponding temperatures, the temperature at which the form of the local field is important is much higher in the electrical case. If Lorentz's equation were valid, these substances should show the electrical analogue of ferromagnetism in cases in which intermolecular aligning forces other than the dipole-dipole force are relatively small. Actually, this effect is not observed when it would be expected. For example, it can be estimated that the electrical Curie point should occur at about 260°K in the case of HCl, whereas no anomalies are observed until 100°K, at which point molecular reorientation stops (*cf.* Sec. 125).

143. Ferromagnetism.—The theory of ferromagnetism has developed in stages starting from two different points, namely, from the atomic

[1] *Ibid.*, p. 556.

approximation and from the band approximation. The treatment that starts from the atomic approximation has value primarily for understanding the spin aligning forces in ferromagnetic media, whereas the band treatment, which was discussed in Sec. 101, has qualitative value for discussing the relation between the conduction electrons and the *d*-shell electrons. The first three parts of this section will be devoted to the atomic approximation and the fourth to the connection between this and the band approximation.

There is a close analogy between the atomic theory of ferromagnetism and the theory of order and disorder in alloys that was presented in Chap. XIV. In fact, the theory of ferromagnetism, which was developed first, was used as a pattern for the other. It will be seen that the magnetized state, like the ordered state of alloys, has a lower entropy than other possible states, so that it can occur only when it is favored by a low energy.

a. The Weiss Theory.—It was seen in the previous section that a relationship between the external magnetic field H and the local field H_l, of the type derived by Lorentz, namely,

$$\mathsf{H}_l = \mathsf{H} + \frac{4\pi}{3}\mathsf{M}, \tag{1}$$

where M is the intensity of magnetization, can imply ferromagnetism if the atomic susceptibility χ_a becomes very large in a temperature range. Under this condition, the susceptibility χ, which is related to χ_a by the equation

$$\chi = n_0 \frac{\chi_a}{1 - 4\pi n_0 \chi_a/3} \tag{2}$$

where n_0 is the density of particles, becomes infinite when $4\pi n_0 \chi_a/3$ is unity so that the magnetic moment per unit volume may be finite, even in the absence of a field. χ_a satisfies this condition at sufficiently low temperatures if it obeys Curie's law

$$\chi_a = \frac{A}{T}. \tag{3}$$

Hence, Eqs. (1) and (3) are sufficient for ferromagnetism. Even if the Lorentz equation were accurate, however, which it is not for the reasons discussed in the last section, it could not explain the ferromagnetism of iron, cobalt, and nickel, for the reasonable values of A are too small. Thus, if we use the relation

$$A = \frac{\beta^2 g^2 J(J+1)}{3k} \tag{4}$$

discussed in connection with the theory of paramagnetism and give J and g ordinary atomic values, we should expect ferromagnetism only below 1°K.

Weiss[1] arbitrarily dismissed these difficulties and assumed that in ferromagnetic material

$$\mathsf{H}_i = \mathsf{H} + \alpha\mathsf{M} \tag{5}$$

where α is a large constant of the order of magnitude 10^4. In addition, he assumed that the scalar value of atomic moment $\mathbf{m}$ is related to H_i by Eq. (25), Sec. 137, namely,

$$m(\mathsf{H}) = \beta g J B_J\left(\frac{\mathsf{H}_i \beta g}{kT}\right), \tag{6}$$

which is the generalization of Eq. (3) for strong fields. Equations (5) and (6) lead to the following implicit equation for M:

$$\mathsf{M}(\mathsf{H}) = n_0 \beta g J B_J\left(\frac{\beta g(\mathsf{H} + \alpha\mathsf{M})}{kT}\right). \tag{7}$$

In his original work, Weiss actually used the classical analogue of the

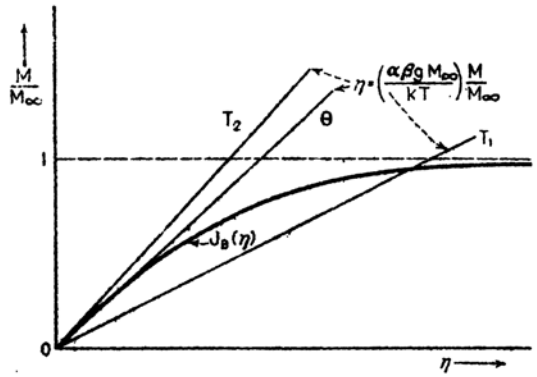

FIG. 10.—Schematic representation of a method of visualizing the roots of Eqs. (8*a*) and (8*b*). The lines correspond to (8*b*) for several temperatures, where $T_2 > T_1 > T_0$. The single curve represents (8*a*). It is assumed that H is zero, although the additive constant in (8*b*) usually cannot be shown on this scale anyway.

function B_J, which may be derived by allowing βg to approach zero and J to approach infinity in such a way that $\beta g J$ remains finite.

Equation (7) is equivalent to the two simultaneous equations

$$\frac{\mathsf{M}}{\mathsf{M}_\infty} = B_J(\eta), \tag{8a}$$

$$\eta = \frac{\beta g \mathsf{H}}{kT} + \left(\frac{\alpha\beta g \mathsf{M}_\infty}{kT}\right)\frac{\mathsf{M}}{\mathsf{M}_\infty}, \tag{8b}$$

[1] P. WEISS, *Jour. phys.*, **6**, 667 (1907). *Cf.* STONER, *op. cit.*

where M_∞ is the saturation value of M. The roots of these equations, which may be pictured by the graphical method shown in Fig. 10, are shown in Fig. 11. The decrease of M/M_∞ with increasing temperature follows a continuous curve, so that the melting of ferromagnetism is a transition of the second kind in Weiss's theory. The Curie temperature, at which M vanishes, is

$$\Theta = \frac{\alpha\beta g M_\infty}{k}\frac{J+1}{3}. \tag{9}$$

Since M_∞ is of the order of magnitude of 1,000 gauss for the common ferromagnetic metals, the value of Θ given by (9) is of the order of 0.1α. Thus, α must be of the order of magnitude 10^4, if Weiss's theory is to be adequate.

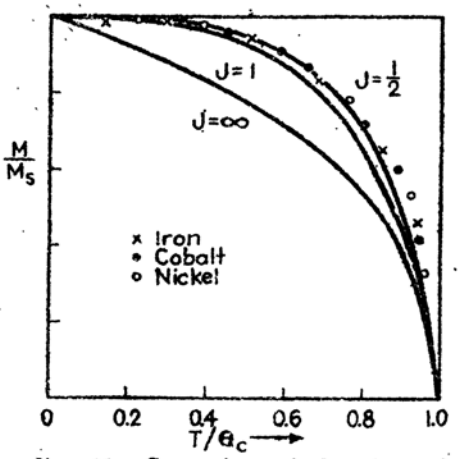

FIG. 11.—Comparison of the observed saturation magnetization curves of iron, cobalt, and nickel and the computed curves for several values of J. The theoretical curve for $J = \frac{1}{2}$ fits the measured ones best.

In Fig. 11, the observed values of M/M_∞ for iron, cobalt, and nickel as functions of T/Θ_c are compared with the computed functions for several values of J. It may be observed that the value $\frac{1}{2}$ fits the experimental work best, a fact suggesting that the magnetism arises almost entirely from spin. This is also supported by the fact that the gyromagnetic ratio is almost 2 (*cf.* Sec. 191).

The susceptibility above the Curie temperature may be found from the equation analogous to Eq. (2) of Lorentz's theory, namely,

$$\chi = n_0\frac{\chi_a}{1-\alpha n_0\chi_a}. \tag{10}$$

If the value of $n_0\chi_a$ that may be derived from Eq. (6), namely,

$$n_0\chi_a = \frac{1}{\alpha}\frac{\Theta}{T}, \tag{11}$$

is substituted in Eq. (10), it is found that

$$\chi = \frac{\Theta}{\alpha(T-\Theta)}, \tag{12}$$

which is known as the Curie-Weiss law. The susceptibilities in the

paramagnetic range have been investigated by Weiss[1] and coworkers. Figure 28, Chap. I, shows $1/\chi$ as a function of temperature for iron and nickel. If Eq. (12) were precisely valid, these curves should be straight lines; however, they are only approximately linear. In addition, the curve for iron shows a discontinuity because of the intrusion of the γ phase. Weiss and Foex have pointed out[2] that the curves for cobalt and nickel may be closely approximated by a series of straight lines in separate temperature regions. For this reason, it is suggested that the ferromagnetic metals have several magnetic allotropic phases above the Curie temperature and that a separate Curie-Weiss law is valid over the temperature range in which each phase is stable. A more reasonable interpretation is that the Curie-Weiss law is only a rough approximation to a more accurate equation. This is substantiated by more recent theoretical work which is discussed below.

It is possible to treat magnetocaloric effects on the basis of the Weiss theory.[3] Weiss postulated that the energy of magnetization E_m is related to the intensity of magnetization M by the equation

$$E_m = -\int_0^{\mathsf{M}} \mathsf{H}_l \cdot d\mathsf{M} \tag{13}$$

where H_l is the local field. It is implicitly assumed in this equation that the hypothetical local field H_l is an actual magnetic field. If we substitute the relation (5) in (13), we find

$$E_m = -\tfrac{1}{2}\alpha \mathsf{M}^2 \tag{14}$$

in the absence of an external field. Thus, the specific heat of magnetization is

$$c_m = -\frac{1}{2}\frac{\alpha}{\rho}\frac{d\mathsf{M}^2}{dT} \tag{15}$$

where ρ is the density. Since M varies most rapidly just below the Curie temperature and is zero above, the specific heat would rise to a peak at the Curie temperature and would then drop discontinuously to zero if Eq. (15) were valid. Although the areas under the experimental specific-heat curves are of the same order of magnitude as that of the theoretical curve, the forms of the two usually differ, inasmuch as a magnetic specific heat is observed above the Curie temperature. This fact is shown in Figs. 17 and 29 (Chap. I). The effect is largest in iron but is not negligible in the case of cobalt or nickel. It may be recalled that a similar discrepancy occurs between the specific heat predicted on

[1] P. WEISS, *Jour. phys.*, **5**, 129 (1924).
[2] *Ibid.*; G. FOEX, *Ann. phys.*, **16**, 304 (1921).
[3] *Cf.* STONER, *op. cit.*

the basis of the Bragg-Williams theory of order and disorder, and the observed specific heats. This discrepancy was removed in a qualitative way by taking into account short-distance order. We may conclude that a part of the error in the Weiss theory is related to the fact that it does not take into account the correlation of the magnetic moments of near-by atoms.

b. Heisenberg's Theory.—Heisenberg[1] first showed that the Weiss local field may be given a direct and simple explanation in the language of quantum theory. The principles involved in his work, which is based upon a Heitler-London approximation, may be demonstrated by the following simple problem.

Suppose that we have two atoms A and B that have one electron each[2] and are separated by a distance r_{ab}. We shall designate the atomic wave functions by ψ_a and ψ_b and the energies of the free atoms by ϵ. In addition, we shall assume that these states have no orbital angular momentum, so that all of the magnetic moment arises from spin. The possible antisymmetric wave functions of the complete system then are (*cf.* Secs. 48 and 56)

$$\left.\begin{aligned} \Psi_{\mathrm{I}} &= [\psi_a(1)\psi_b(2) + \psi_a(2)\psi_b(1)][\eta_1(1)\eta_2(-1) - \eta_1(-1)\eta_2(1)], \\ \Psi_{\mathrm{II}} &= [\psi_a(1)\psi_b(2) - \psi_a(2)\psi_b(1)]\begin{cases}[\eta_1(1)\eta_2(1)] \\ [\eta_1(1)\eta_2(-1) + \eta_1(-1)\eta_2(1)], \\ [\eta_1(-1)\eta_2(-1)]\end{cases}\end{aligned}\right\} \tag{16}$$

in an obvious notation. The first of these is the wave function of the singlet level, which has no spin moment, and the other three are the triplet functions, for which the spin quantum number S is unity. The second set of states evidently is the analogue of the set of ferromagnetic states of solids. We may assume that the interaction potential for the two atoms is

$$V_{ab} = \frac{e^2}{r_{ab}} + \frac{e^2}{r_{12}} - \frac{e^2}{r_{1b}} - \frac{e^2}{r_{2a}} \tag{17}$$

where r_{12} is the distance between the electrons, and r_{1b} and r_{2a} are the distances between a given nucleus and the electron on the other atom. The energies of the two types of state (16) are, respectively,

$$\left.\begin{aligned} E_{\mathrm{I}} &= E_c + J_c, \\ E_{\mathrm{II}} &= E_c - J_c, \end{aligned}\right\} \tag{18}$$

where

$$E_c = 2\epsilon + \int|\psi_a(1)|^2 V_{ab}|\psi_b(2)|^2 d\tau_{12} \tag{19}$$

[1] W. HEISENBERG, *Z. Physik*, **49**, 619 (1928).

[2] A treatment of this problem for the case in which each atom has more than one electron has been given by J. H. VAN VLECK, *Jour. Chem. Phys.*, **6**, 105 (1938).

is the sum of the atomic energy and the coulomb interaction energy and

$$J_e = \int \psi_a^*(1)\psi_b^*(2) V_{ab} \psi_a(2)\psi_b(1) d\tau_{12} \tag{20}$$

is the exchange integral. It should be noted that V_{ab} in the integrals in Eqs (19) and (20) could be replaced by e^2/r_{12} if the functions ψ_a and ψ_b were orthogonal. From Eq. (18), we see that the magnetic states Ψ_{II} are energetically stable relative to Ψ_I only if J is positive.

Equations (18) may be placed in a form that is significant for the theory of ferromagnetism. The square of the total spin operator

$$\mathbf{\Sigma}^2 = (\boldsymbol{\sigma}_1 + \boldsymbol{\sigma}_2)^2 \tag{21}$$

is a constant of motion in each of the states Ψ_I and Ψ_{II}, the eigenvalues having the form $\hbar^2 S(S+1)$, where S is 0 and 1, respectively. If (21) is expanded, it becomes

$$\boldsymbol{\sigma}_1^2 + \boldsymbol{\sigma}_2^2 + 2\boldsymbol{\sigma}_1 \cdot \boldsymbol{\sigma}_2. \tag{22}$$

Since the individual spin angular momenta $\boldsymbol{\sigma}_1^2$ and $\boldsymbol{\sigma}_2^2$ are also constants of motion that have the eigenvalue $3\hbar^2/4$, it follows that $\boldsymbol{\sigma}_1 \cdot \boldsymbol{\sigma}_2$ is also a constant of motion and has the eigenvalue $-3\hbar^2/4$ when S is zero and $\hbar^2/4$ when S is unity. Employing the operator (21), we may place Eqs. (18) in the operator form

$$E = E_c + J_e\left(1 - \frac{\mathbf{\Sigma}^2}{\hbar^2}\right) \tag{23}$$

or, using (22), in the form

$$E = E_c - \frac{J_e}{2} - J_e \frac{2\boldsymbol{\sigma}_1 \cdot \boldsymbol{\sigma}_2}{\hbar^2}. \tag{24}$$

If we now use the fact that the electronic magnetic moment $\boldsymbol{\mu}$ is $-2\beta\boldsymbol{\sigma}/\hbar$, the spin-dependent part of (24) may be written as

$$-\frac{J_e}{2\beta^2}\boldsymbol{\mu}_1 \cdot \boldsymbol{\mu}_2. \tag{25}$$

Thus, apart from the dependence of J_e on interatomic spacing, the energy is determined by the relative orientations of the electron spins. It should be emphasized that this interaction energy is fundamentally electrostatic. Spin enters primarily as a consequence of the Pauli principle.

Bethe[1] has made a simple qualitative analysis of the conditions under which J is most likely to have a given sign. Let us suppose that the functions ψ_a and ψ_b have no nodes in the region where they overlap appreciably, so that the product $\psi_a(1)\psi_b(1)$ may be assumed to be positive

[1] H. BETHE, *Handbuch der Physik*, XXIV/2.

everywhere. This condition is always satisfied if ψ_a and ψ_b are s functions that have nodes close to the nucleus but may also be satisfied in other cases if the nodal surfaces do not lie near the mid-point of the line connecting the centers of the two atoms. Under this condition, the essentially positive terms

$$\frac{e^2}{r_{12}} + \frac{e^2}{r_{ab}} \tag{26}$$

favor ferromagnetism, whereas the negative terms

$$-\frac{e^2}{r_{b1}} - \frac{e^2}{r_{a2}} . \tag{27}$$

do not. The variable term e^2/r_{12} in (26) is larger when the product $\psi_a\psi_b$ is very large in a small volume of space than when the product is small in a large volume. Moreover, the terms (27) are smallest when the overlapping region is as far from the nuclei as possible. Hence, J is most likely to be positive if (a) the distance r_{ab} is fairly large compared with the orbital radii and (b) the wave functions are comparatively small near the nuclei. In both these cases, the product $\psi_a\psi_b$ is small at the nuclei and large near the mid-point between the atoms. Condition (b) is most fully satisfied when the orbital angular quantum number l is high since the wave functions start as r^l. Hence, we should expect J to be positive for the interaction between unclosed shells of d or f electrons when the interatomic distance is large compared with the atomic radius. These conditions actually are satisfied by pairs of atoms in the metals of the iron group and rare earth type, in which the interatomic distances are determined primarily by the s-p valence electrons. We shall see below that this qualitative argument can be applied to these metals, since the interaction between the d shells may be expressed as a sum of interactions between pairs of atoms.

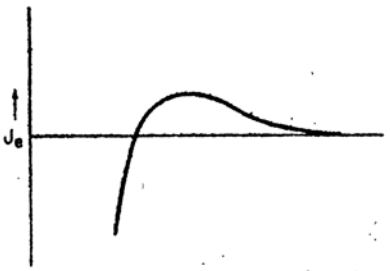

FIG. 12.—Behavior of J_e as a function of interatomic distance r.

It follows from the principles of the preceding discussion that the sign of J_e should depend upon the ratio x of the orbital radius and the interatomic distance in the manner shown in Fig. 12. If x is close to unity, J_e should be negative; if it is large, J_e may be positive. It is only fair to mention that Bethe's argument does not tell the entire story, for the diatomic molecules O_2 and NO, which have permanent magnetic moments, do not satisfy his conditions very well.

It may be shown[1] that in the Heitler London approximation the total energy of any number of electrons can be placed in the form

$$E = C - \frac{1}{2\hbar^2}\sum_{i,j}{}' J_{ij} 2\mathfrak{s}_i \cdot \mathfrak{s}_j, \tag{28}$$

which generalizes (24). Here C is a constant, J_{ij} is the exchange integral for the ith and jth electronic wave functions, and $\mathfrak{s}_i$ and $\mathfrak{s}_j$ are the spin operators of the ith and jth electrons. We shall be interested in the case in which each atom has one electron and in which J_e is appreciable only for nearest neighbors. Equation (12) then becomes

$$E = C - \frac{J_e}{\hbar^2}\sum_{\substack{\text{nearest}\\ \text{pairs}}} 2\mathfrak{s}_i \cdot \mathfrak{s}_j \tag{29}$$

where J_e is the exchange integral for neighboring atoms. The more general case in which there are several electrons per atom has also been considered, but we shall not treat it here since it does not lead to qualitatively different results.

Let us now discuss the number of states associated with different values of the z component of total magnetic moment. If there are N electrons, the largest value of the magnetic moment is βN, which occurs when all the spins are parallel and which can happen in only one way. The value $M\beta$, which occurs when there are $(N + M)/2$ moments parallel to the z axis and $(N - M)/2$ moments antiparallel to it, can happen in

$$n(M) = \frac{N!}{\left(\frac{N+M}{2}\right)!\left(\frac{N-M}{2}\right)!} \tag{30}$$

different ways. Thus, the state of maximum magnetic moment, which is energetically most stable when J_e is positive, has very low degeneracy, whereas the states of lower moment have larger values. Hence, we should expect the state of highest magnetization to occur only at low temperatures. The actual state at temperature T can be computed from the partition function; however, this computation is not easy to carry through directly because the $n(M)$ states (30) have different energies. Heisenberg assumed that the distribution of levels of given M may be approximated by the function

$$f_M(E) = \frac{n(M)}{(2\pi)^{\frac{1}{2}}\Delta_M} e^{-\frac{(E-\overline{E_M})^2}{\Delta_M^2}} \tag{31}$$

[1] *Cf.* J. H. VAN VLECK, *The Theory of Electric and Magnetic Susceptibilities* (Oxford University Press, New York, 1932).

where $\overline{E_M}$ is the mean value of the energy levels of given M and Δ_M^2 is the mean square deviation from this mean. These quantities were computed by an approximate method that is discussed in Van Vleck's book. With this assumption, Heisenberg computed the partition function in a straightforward way,[1] after adding an energy term

$$2\beta \sum_i \sigma_i \cdot \mathsf{H}$$

in order to include the effect of an external magnetic field. The magnetic equations obtained from this partition function are

$$\frac{\mathsf{M}}{\mathsf{M}_\infty} = \tanh \eta, \tag{32a}$$

in which

$$\eta = \frac{\beta \mathsf{H}}{kT} + \frac{1}{2}\left(\gamma - \frac{\gamma^2}{2}\right)\frac{\mathsf{M}}{\mathsf{M}_\infty} + \frac{\gamma^2}{4z}\left(\frac{\mathsf{M}}{\mathsf{M}_\infty}\right)^3 \tag{32b}$$

where z is the number of nearest neighboring atoms and

$$\gamma = \frac{zJ_e}{kT}.$$

Equations (32a) and (32b) are nearly the same as Weiss's equations (8a) and (8b) since $B_{\frac{1}{2}}(\eta)$ is equal to $\tanh \eta$. The only difference lies in the term in η containing $(\mathsf{M}/\mathsf{M}_\infty)^3$. If this is dropped and the correspondence

$$\frac{\alpha\beta g}{kT} \sim \frac{1}{2}\left(\gamma - \frac{\gamma^2}{2}\right) \tag{33}$$

is made, the two systems of equations are identical. The field parameter α defined by (33) is a constant only at high temperatures, in which case

$$\alpha \cong \frac{zJ_e}{2\beta g}. \tag{34}$$

The Curie temperature is not related to this value of α by Eq. (9) but is given instead by the equation

$$\Theta = \frac{2J}{k(1 - \sqrt{1 - 8/z})} \tag{35}$$

which is real only if z is at least 8 and is positive only if J is positive. Thus, Heisenberg's treatment leads to conventional ferromagnetic behavior only for the more close-packed lattices. This means not that

[1] Another method of evaluating the partition function has been used by J. H. Van Vleck, *Phys. Rev.*, 49, 232 (1936). This does not lead to qualitatively different results.

the crystal is not ferromagnetic at sufficiently low temperatures when z is less than 8 but only that the phase change is not of the second kind.[1]

Treatments of ferromagnetism using Heisenberg's model but employing distribution functions other than the Gaussian function (31) have been presented by several investigators.[2] By properly choosing this function, the difficulties associated with the imaginary behavior of (35) may be avoided.

The susceptibility above the Curie temperature does not conform to the Curie-Weiss law except when T is much greater than Θ. We shall not discuss the result since Heisenberg's model unquestionably is too simple to be applied quantitatively to actual ferromagnetic materials. It is important to know, however, that observed deviations from the law are not at variance with theory.

c. The Spin-Wave Treatment.—Heisenberg's treatment of ferromagnetism has the following weaknesses.

1. It is based upon a simple Heitler-London description in which the periodicity of the lattice is not taken into account.

2. An arbitrary approximation [*cf.* Eq. (31)] is used to obtain the distribution of levels. Since the thermal properties are strongly dependent upon this distribution, a more accurate description should be used for quantitative work.

Of the methods that have been employed to improve upon Heisenberg's work, we shall discuss that developed by Bloch[3] and extended more recently by Slater,[4] since it is the most fruitful. Although this treatment casts a new light upon the problem of ferromagnetism, its results are not radically different from those of Heisenberg's theory. For this reason, the older work can still be used for qualitative purposes.

It may be recalled that the Heitler-London approximation may be used to discuss the normal and lower excited states of insulators. When this is done, the lowest level is nondegenerate and the excited levels are very highly degenerate. Thus, if there are N atoms and the first excited one-electron state is g-fold degenerate, the first excited level is Ng-fold degenerate. A more accurate set of wave functions can be obtained by computing the matrix elements of the Hamiltonian connecting these Ng states and by diagonalizing the result. This problem, which was solved in Sec. 96 for a simple case in which the interatomic energy is

[1] This peculiar behavior of the Heisenberg model arises from the fact that the use of the Gaussian distribution is equivalent to assuming levels of arbitrarily low energy. Thus the $E(S)$ curve (Sec. 117) approaches the energy axis asymptotically with infinite slope, rather than with zero slope as it should.

[2] See, for example, F. Bitter, *Phys. Rev.*, **57**, 569 (1940).

[3] F. BLOCH, *Z. Physik*, **61**, 206 (1931).

[4] J. C. SLATER, *Phys. Rev.*, **52**, 198 (1937).

small, leads to the following results. The first excited wave functions Ψ_k are given by the equation

$$\Psi_k = a_k \sum_n e^{2\pi i \mathbf{k}\cdot\mathbf{r}(n)} \Psi_n \tag{36}$$

where Ψ_n is the determinantal eigenfunction that is formed from the lowest wave function Ψ_0 by replacing the normal wave function ψ_n for the nth atom by the excited wave function ψ'_n, and n is summed over all atoms. The Ψ_k, which evidently have wave characteristics, are called excitation waves. The energy associated with Ψ_k is

$$E_k = E_n + I \sum_\rho e^{2\pi i \mathbf{k}\cdot\rho} \tag{37}$$

where ρ ranges over the vectors joining an atom with its nearest neighbors, E_n is the energy of the Ψ_n, and I is composed of integrals involving pairs of neighboring atoms.

Bloch constructed a set of magnetic wave functions that bear the same relation to Heisenberg's atomic functions that the excitation waves do to the Ψ_n in (36). Let us consider a system of N atoms, each of which has one valence electron. We shall assume that the one-electron wave functions $\psi(\mathbf{r} - \bar{\mathbf{r}}(n)) = \psi_n$ are like atomic functions. For the basic nondegenerate wave function of the complete system, Bloch chose the state Φ_0 in which all electron spins are parallel. The energy E_0 of this state is

$$E_0 = N(\epsilon_0 + C - \tfrac{1}{2} J_e z) \tag{38}$$

where ϵ_0 is the energy of a free atom, NC is the coulomb interaction energy of the system, J_e is the Heisenberg exchange integral (2) involving the ψ_n for pairs of neighboring atoms, and z is the number of nearest neighbors. The states Φ_n analogous to the Ψ_n in Eq. (1) are determinants of functions that differ from Φ_0 in that the spin of the electron on the nth atom has been reversed. These N functions have the same energy and have a z component of magnetic moment equal to $(N - 2)\beta$. The *spin waves* Φ_k, analogous to the excitation waves Ψ_k, are

$$\Phi_k = a_k \sum_n e^{2\pi i \mathbf{k}\cdot\mathbf{r}(n)} \Phi_n \tag{39}$$

and have the energy

$$E_{k'} = E_0 + 2J_e \sum_\rho (1 - e^{2\pi i \mathbf{k}\cdot\rho}) \quad , \tag{40}$$

where ρ is summed over nearest neighbors as in Eq. (37). This function is shown schematically in Fig. 13.

It can be shown that, as long as the number of spin waves is small compared with N, the energy of the crystal in a state in which there are f spin waves of wave number $\mathbf{k}_1, \mathbf{k}_2, \ldots, \mathbf{k}_f$ is

$$E(\mathbf{k}_1, \cdots, \mathbf{k}_f) = E_0 + \sum_{r=1}^{f} \epsilon_s(\mathbf{k}_r) \tag{41}$$

where

$$\epsilon_s(\mathbf{k}_r) = E_{\mathbf{k}^r} - E_0. \tag{42}$$

Thus, the spin waves behave like elementary particles that are so nearly independent of one another that their energies are additive. It is evident that the z component of magnetic moment in the state having f spin waves is $\beta(N - 2f)$.

Under the restrictions for which Eq. (41) is valid, the necessary condition for ferromagnetism is that $E(\mathbf{k}) - E_0$ be positive, that is, that J_i be positive, for then Φ_0 is the lowest state of the system. This condition is identical with Heisenberg's.

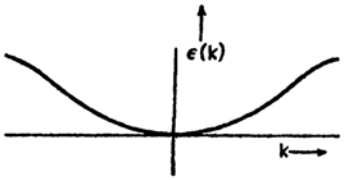

FIG. 13.—The schematic representation of the energy of Bloch's spin wave as a function of k in the ferromagnetic case. The curve is inverted in the nonferromagnetic one.

Bloch used Eq. (41) to compute the partition function for the system of electrons. There is no difficulty in determining the distribution of levels in this case, since one state is associated with each value of $\mathbf{k}$ in wave-number space. This partition function is

$$f = \sum_{f=0}^{\frac{N}{2}} e^{-\frac{E_0 - \beta H(N-2f)}{kT}} \sum_{\mathbf{k}_1, \ldots, \mathbf{k}_f} \prod_{r=1,\cdots,f} e^{-\frac{\epsilon_s(\mathbf{k}_r)}{kT}}, \tag{43}$$

in which $-\beta H(N - 2f)$ is the field interaction term. At low temperatures, when only the lowest levels are excited, $\epsilon_s(\mathbf{k})$ may be replaced by the value

$$\epsilon_s(\mathbf{k}) \cong J_s \sum_{\rho} (\rho \cdot \mathbf{k})^2. \tag{44}$$

Using this approximation, Bloch found that the magnetization M satisfies the equation

$$\frac{\mathsf{M}}{\mathsf{M}_\infty} = 1 - \alpha \frac{2.612}{2\pi^2} \left(\frac{kT}{J_s}\right)^{\frac{3}{2}} \tag{45}$$

where α depends upon the lattice and has the value $\frac{1}{4}$ for a face-centered lattice and $\frac{1}{8}$ for a body-centered lattice. This result may be placed in the form

$$\frac{M}{M_\infty} = 1 - \left(\frac{T}{\Theta}\right)^{\frac{3}{2}} \tag{46}$$

where Θ is the approximate Curie temperature, which for face-centered and body-centered lattices has the values

$$\Theta_{f.c.} = 9.7\frac{J_e}{k},$$

$$\Theta_{b.c.} = 6.1\frac{J_e}{k},$$

respectively.

Weiss[1] has made a careful experimental test of Bloch's $T^{\frac{3}{2}}$ law for iron and nickel. He found that a T^2 law holds above 70°K, but that the $T^{\frac{3}{2}}$ law applies in the range from 70° to 20°K. This verification of Bloch's result seems to be support for a spin-wave type of theory of ferromagnetism, although it must be admitted that Bloch's model, on which (46) was derived, is probably much too simple (see part *d*).

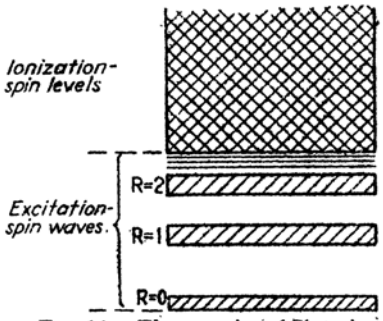

FIG. 14.—The energies of Slater's excitation-spin waves. The zero line represents the energy of the system when spins are parallel. The band $R = 0$ corresponds to Bloch's spin-wave curve (*cf.* Fig. 13) for which the electron having reversed spin remains on the same atom as the hole it leaves in the levels of opposite spin. The other discrete curves correspond to cases in which the electron having reversed spin is removed to an atom at distance R. The continuum represents the energy states of the electron and hole when they become completely free of one another.

Slater[2] extended Bloch's method of determining the magnetic wave functions by carrying the perturbation procedure several steps further. The important differences between the two procedures are as follows:

a. Slater added to Bloch's spin waves (39) the wave functions $\Phi_{\mathbf{k},R}$ that are defined by the equation

$$\Phi_{\mathbf{k},R} = \sum_n e^{2\pi i \mathbf{k}\cdot\mathbf{r}(n)}\Phi_{n,R} \tag{47}$$

where $\Phi_{n,R}$ is constructed from Φ_0 by taking an electron from the atom at $\mathbf{r}(n)$ to the atom at $\mathbf{r}(n) + \mathbf{R}$ and reversing its spin. The functions (39) evidently are the special set for which $\mathbf{R}$ is zero. These excitation-spin waves have energies that can be represented schematically for each value of $\mathbf{R}$ by discrete curves in a one-dimensional diagram (*cf.* Fig. 14). The curve for $\mathbf{R} = 0$ corresponds to the curve of Fig. 13.

b. The matrix components of the Hamiltonian were computed for the system of excitation-spin waves (47), and the perturbing effect on

[1] P. WEISS, *Compt. Rend.*, **198**, 1893 (1934).

[2] *Ibid.*

the Bloch states of the states for which **R** is not zero was estimated from these components.

c. Slater did not employ ordinary atomic functions but used instead an orthogonalized system χ_n that was obtained from Bloch type functions $\chi_k e^{2\pi i\mathbf{k}\cdot\mathbf{r}}$ of the ionization band approximation (*cf.* Chap. VIII) by means of the equation

$$\chi_n = \sum_{\mathbf{k}} \chi_{\mathbf{k}}(\mathbf{r}) e^{2\pi i\mathbf{k}\cdot[\mathbf{r}-\mathbf{r}(n)]}. \tag{48}$$

This procedure has two important consequences: (1) All terms in the exchange integral (20) except those arising from e^2/r_{12} vanish because of the orthogonality conditions. (2) Some of the quantities in the expression for the perturbed function can be expressed in terms of characteristic quantities of the band approximation.

Slater's result for the energy of Bloch's spin waves, in the higher approximation, is

$$\epsilon_s(\mathbf{k}) = A\sum_{\rho}(1 - e^{2\pi i\mathbf{k}\cdot\rho}). \tag{49}$$

Here,

$$A = J_s - \frac{2W^2}{I_1} \tag{50}$$

where J_s is the exchange integral for the χ_n, namely,

$$J_s = \int \chi_n^*(1)\chi_{n+1}^*(2)\frac{e^2}{r_{12}}\chi_n(2)\chi_{n+1}(1)d\tau_{12}, \tag{51}$$

W is the width of the ionization band, and I_1 is essentially the difference between E_0 and the center of energy of the excitation-spin waves for **R** greater than zero (*cf.* Fig. 14). In the case in which there are f spin waves, the total energy $E(\mathbf{k}_1, \ldots, \mathbf{k}_f)$ may be obtained by substituting (49) into Eq. (41). When the atoms are widely separated, J_s is positive, W is very small, and A is then positive. On the other hand, W becomes very large when the atoms are close together, so that we may expect A to change its sign. Thus, in this approximation we should expect ferromagnetism only for widely separated atoms just as in the Heisenberg theory.

The behavior of the lowest spin-wave energy curve as the ionization band widens is shown in Fig. 15*a* and *b*. The levels of the ionization band occur at the series limit of the discrete curves of the excitation-spin-wave system and are indicated by the striped region. In the first case, the ionization band is narrow and the energy curve of the lowest spin wave is above E_0. In the second, the ionization band is so wide that it depresses the spin-wave curve below E_0.

d. Critique of the Theories of Ferromagnetism.—The Heisenberg and spin-wave treatments of ferromagnetism are incomplete for metals because the valence and *d*-shell electrons are not considered simultaneously. Actual ferromagnetic metals are made of atoms whose total electronic states possess a mixture of *s-p* and *d*-electron characteristics. The *s-p* part of the atomic wave function is altered in such a way that the solid has metallic properties, such as high conductivity, and the *d* part produces ferromagnetism. Since the *g*-factor is ~ 2 and the observed atomic saturation moments are not integer multiples of the Bohr magneton, we know that there is not an integer amount of

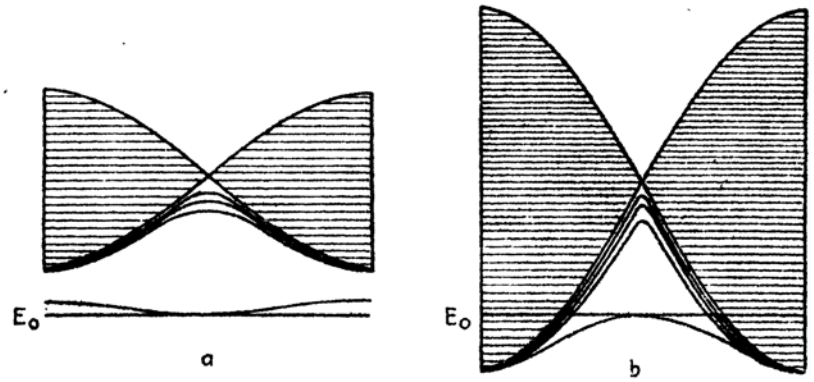

FIG. 15.—Schematic representation of the behavior of the spin-excitation levels as the ionisation band widens. In case *a* the ionization band is narrow and the system is ferromagnetic, whereas in case *b* the spin-wave curve is inverted so that the system is not ferromagnetic. In both of these diagrams the ordinate is energy and the abscissa is the difference of the wave-number vectors of the electron before and after excitation, which is the wave-number vector of the exciton. Hence the lowest discrete curve is analogous to that of Fig. 13. The shaded region represents the ionization-spin states, in which both the electron and hole are free. This has zero width at the midpoint, which corresponds to zero difference in wave number, because the $\epsilon(\mathbf{k})$ curve is the same for electrons of either spin. (*After Slater.*)

d property per atom. Thus, the two characteristics are intimately mixed, and in any complete theory of ferromagnetism they should be discussed simultaneously.

The band approximation, which is based on Bloch type one-electron functions, does an excellent job of picturing the balance between *s-p*- and *d*-electron character. Since it is found that the *d* and *s-p* bands in transition metals overlap, the relative number of electrons in each band is determined by the condition that the energy be stationary under the process of moving electrons from one band to the other, which means essentially that the bands are filled to the same level. Thus, there is no reason for expecting an integer number of *d* electrons per atom, for the positions of the bands are determined by many factors. As we have seen in Sec. 101, this picture can be used to correlate a large number

of the properties of transition metals that are related to *d*-electron character.

In order to explain ferromagnetism on the band theory, it unfortunately is necessary to assume arbitrarily that there are more electrons in the *d* band having one type of spin than the other. The excess in metals such as nickel and cobalt is so large that half the *d* band is completely filled, and the excess is slightly smaller in iron. If the band theory were accurate enough in the case of narrow bands to furnish a trustworthy explanation of this preponderance of electrons of one type of spin, the Heisenberg-Bloch-Slater type of treatment would be superfluous for most descriptive work. It is true that the exchange energy for Bloch functions, $\chi_k e^{2\pi i \mathbf{k}\cdot\mathbf{r}}$, favors ferromagnetism, but it is possible to show that for the narrow bands the correlation correction is just large enough to compensate for this effect in first approximation (*cf.* Sec. 75).

At first sight, it might seem possible to use the band scheme to determine the distribution of *s-p* and *d* electrons and to use the spin-wave scheme to handle the *d* electrons. This procedure cannot be carried out in a simple way, for wave functions that are more complicated than (47) would have to be employed, since there is not an integer number of *d* electrons per atom.

Thus, there does not seem to be a single, tractable, approximational scheme that can be used to develop satisfactory equations for all the properties of ferromagnetic metals. At present, we must use the spin-wave and band schemes in the separate domains in which they are individually most satisfactory.

It should be added that the Heisenberg and the spin-wave approximations are suited to discussions of ferromagnetism in ionic solids, such as magnetite and the rare earth salts, in which there is an integer number of magnetic electrons per atom.

144. Additional Application to Alloys.—We saw in Sec. 101 that many of the properties of ferromagnetic metals and alloys may be correlated on the basis of the band scheme. It is also possible to correlate other properties by the use of the Heisenberg type of theory in a way that will now be discussed.

Dehlinger[1] has attempted to construct semiquantitative exchange integral curves $J_e(r)$ of the type shown in Fig. 12 for the transition-metal atoms by the use of empirical information. Since the close-packed phases of both nickel and cobalt are ferromagnetic, it may be concluded that J_e is positive at the observed nearest-neighbor distance and that the complete curves have the forms shown in Fig. 16*e* in which the vertical dotted line represents the nearest-neighbor distance for the

[1] U. DEHLINGER, *Z. Metallkunde*, **28**, 116 (1936); **28**, 194 (1936); **92**, 388 (1937).

close-packed structures. The face-centered, or γ, phase of iron is not ferromagnetic; however, the body-centered, or α, phase, in which the interatomic distance is slightly larger, is ferromagnetic. Hence, the $J_e(r)$ curve for iron (Fig. 16*d*) is negative at the dotted line and crosses the axis at larger values of r.

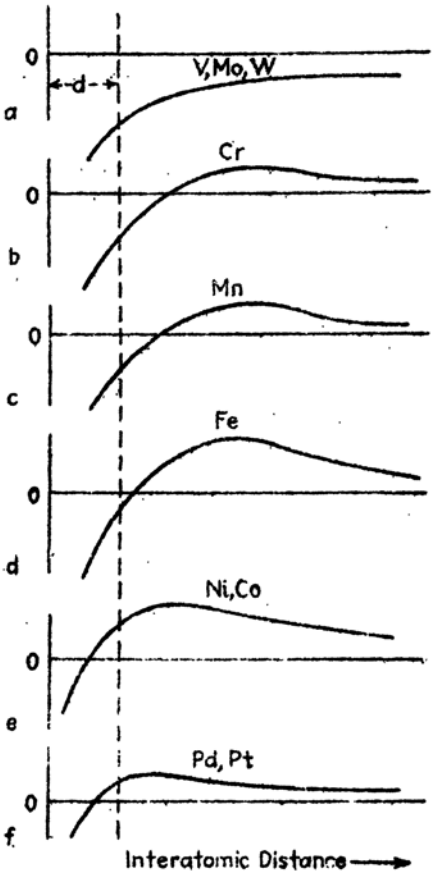

FIG. 16.—Hypothetical $J_e(r)$ curves for the magnetically important transition-metal atoms. Evidence discussed in the text indicates that the peak for nickel actually occurs to the left of the equilibrium spacing. (*After Dehlinger.*)

Dehlinger attempted to classify the $J_e(r)$ curves for the nonferromagnetic transition metals by studying their paramagnetism. He concluded that the corresponding J_e curve is nearly zero at the nearest-neighbor distance if the metals are strongly paramagnetic and if the paramagnetism increases with decreasing temperature. On the other hand, the crossing point is far away if the paramagnetism is weak or temperature-independent. It is possible, in the second case, that $J_e(r)$ is negative everywhere. Using considerations of this type, he arrived at the other curves of Fig. 16. It may be seen that in the cases of palladium and platinum he has concluded that the exchange integral is positive at the actual interatomic distances although the magnitude is small relative to that for the truly ferromagnetic metals.

Among the properties of ferromagnetic metals that are nicely explained in a qualitative way by Dehlinger's picture is the fact that their expansion coefficients change near the Curie point. Consider the case of iron, for example. It follows from the fact that the observed interatomic distance is on the left-hand side of the peaks of the $J_e(r)$ curves in this case that the additional interatomic force arising from exchange when the magnetic moments of two atoms are parallel instead of antiparallel tends to push them apart. The total force for the entire solid arising from this source is a maximum when all spins are parallel and decreases as the magnetization decreases, such as when the substance is heated, for then an increas-

ing number of atoms have opposite spin. Since the maximum change in magnetization occurs in the neighborhood of the Curie point, it may be expected that the greatest decrease in the interatomic repulsive force arising from ferromagnetism occurs in this region of temperature. This decrease, however, should compensate for at least a part of the internal pressure that causes the solid to expand when heated. Hence, it may be expected that the expansion coefficient would decrease near the Curie point. In some cases, such as in invar steel, which is an iron-nickel-carbon alloy, the two effects almost compensate for a range of temperature, and the expansion coefficient is nearly zero.

Shockley[1] has pointed out that the expansion coefficient of nickel *increases* near its Curie point, showing that in this case the actual interatomic spacing is to the *right* of the peak of the $J_e(r)$ curve, and is not as is shown in Fig. 16*d*. A similar conclusion has been drawn by Bozorth[2] from the fact that the Curie point of the iron-nickel system passes through a maximum as nickel is added to iron. It presumably is safe to conclude that the atomic spacing in cobalt, which lies between iron and nickel, corresponds to a point near the peak of the $J_e(r)$ curve.

TABLE LXXXII.—THE SIGNS OF THE EXCHANGE INTEGRALS FOR NEAREST NEIGHBORING ATOMS AND FOR FARTHER NEIGHBORS IN CLOSE-PACKED PHASES OF A NUMBER OF BINARY ALLOYS

	Pt	Pd	Ni	Co	Fe	Mn	Cr	Mo	W
Pt	++								
Pd	++	++							
Ni	....	++	++						
Co	++	++	++	++					
Fe	++	....	++	++	−+				
Mn	....	++	++	−+	−+	−+			
Cr	++	....	−+	−+	−+		−−		
Mo	....	....	−−	−−	−−	....	....	−−	
W	....	....	−−	−−	−−	....	....	−−	−−

Dehlinger extended this type of semiempirical work to substitutional alloys and predicted the rudimentary properties of the $J_e(r)$ curves for a number of unlike atoms. The results of this investigation, which is discussed in more detail below, are listed in Table LXXXII. The first of the two signs in a given square represents the sign of $J_e(r)$ for nearest neighbors in the binary alloy formed of the atoms associated with the row and column in which the square is situated. The other sign is the sign of $J_e(r)$ for all farther neighbors. Thus, according to this diagram, J_e is

[1] W. SHOCKLEY, *Tech. Pub. Bell Tel. System*, **18**, 645 (1939).
[2] R. M. BOZORTH, *Tech. Pub. Bell Tel. System*, **19**, 1 (1940).

positive for iron and nickel atoms that are separated by the nearest-neighbor distances of the iron-nickel alloys and is also positive for all larger distances. Similarly, J_e is negative for first neighbors in nickel and chromium atoms and is positive for others in the nickel-chromium alloy system. The data in the squares lying in the principal diagonal apply to the interaction of pairs of atoms of the same kind and express nothing that is not contained in the curves of Fig. 16. If the conclusions contained in this table are correct, we should expect an alloy to be ferromagnetic only if it contains platinum, palladium, nickel, cobalt, iron, manganese, or chromium.

The method of deriving this information may be demonstrated by giving several examples. It is found that the saturation moment of nickel is raised when nickel atoms are replaced by iron. Thus, it may be concluded that the exchange integral is positive, for otherwise the magnetic moment of iron would set itself antiparallel to that of the nickel atoms and the magnetization would decrease. By assumption, the $J_e(r)$ curve has the form of Fig. 12; hence, $J_e(r)$ must be positive for larger distances. If small amounts of tungsten or chromium are added to nickel, the saturation moment is decreased, a fact indicating that $J_e(r)$ is negative at least for the nearest neighboring nickel-tungsten and nickel-chromium atoms in the corresponding alloys. These two cases differ, however, inasmuch as the Curie temperature increases rapidly with increasing tungsten content in the nickel-tungsten system and remains practically constant in the nickel-chromium system. The reason the Curie temperature does not fall is not difficult to understand. In both these cases, the nickel atoms immediately surrounding tungsten or chromium atoms have parallel moments at absolute zero of temperature. In order to reverse its moment, one of these nickel atoms must do enough work to overcome not only the nickel-nickel exchange interaction but also the nickel-tungsten or nickel-chromium interaction. Hence, if the interaction for antiparallel moments is more than the nickel-nickel interaction for parallel moments, the Curie temperature should rise when tungsten is added, as is observed. It may be concluded from the behavior of the Curie temperature that the nickel-chromium exchange energy is less negative than the nickel-tungsten energy. Dehlinger also concludes from the differences of the two cases that the nickel-tungsten exchange energy is negative for both nearest and more distant neighbors, whereas the chromium-nickel interaction is negative for first neighbors and positive for others.

Dehlinger has used the results of this scheme to correlate a number of interesting and important properties of ternary ferromagnetic alloys such as the Heusler alloys.

145. Ferromagnetic Anisotropy.—A semiquantitative theory of the magnetic anisotropy of cubic ferromagnetic substances has been developed by Van Vleck using an atomic model.[1] This anisotropy, which is made evident by the fact that there are easy and hard directions of magnetization in cubic metals (see Sec. 2), cannot be explained on the basis of exchange coupling between the spins of electrons on different atoms if there is one or less than one magnetic electron per atom, as in the case of nickel, for it may be shown[2] that this type of interaction always leads to isotropic expressions for the energy as a function of magnetization direction. Van Vleck suggested that the anisotropy is due to a coupling between spin and orbital angular momentum not unlike that which gives rise to the inner multiplet splitting in Russell-Saunders coupling. This coupling would not lead to anisotropy if the electronic distribution in the d shells were isotropic, as in an S state of a perfectly free ion; however, the d-shell wave functions are appreciably distorted because of crystalline binding, as we have seen in Sec. 99, which means that the d-shell distribution is anisotropic. Since this anisotropy is fixed relative to the crystal axes, the electronic spin becomes conscious of its orientation relative to the crystal through the coupling with the orbital motion.

Van Vleck assumed that the Hamiltonian for a ferromagnetic solid contains magnetic terms of the type

$$-\sum_{i,j} J_{ij}\mathfrak{s}_i \cdot \mathfrak{s}_j + A\sum_j \mathfrak{m}_i \cdot \mathfrak{s}_j + \tfrac{1}{2}\sum_{i,j} f_{ij}(\mathbf{r}_{ij}, \mathfrak{m}_i \cdot \mathfrak{m}_j, \mathfrak{m}_i \cdot \mathbf{r}_{ij}, \mathfrak{m}_j \cdot \mathbf{r}_{ij}), \quad (1)$$

in which $\mathfrak{s}_i$ and $\mathfrak{m}_i$ are the spin and orbital angular momentum operators of the electrons on the ith atom, $\mathbf{r}_{ij}$ is the radius vector connecting the ith and jth atoms, J_{ij} is the exchange integral for the two atoms, A is the spin-orbit coupling constant, f_{ij} is a polynomial expression in the arguments indicated, and the sums extend over all atoms. The first term evidently is the Heisenberg exchange term, which is responsible for ferromagnetism. The second term describes the coupling between spin and orbital motion, whereas the third term leads to an anisotropic electronic distribution. Van Vleck showed that the observed magnitude for nickel of the constant K_1 in Eq. (2), Sec. 2, may be explained by use of the energy terms (1) with theoretically reasonable values of A and f_{ij}.

The saturation magnetic moment in iron and cobalt is larger than one Bohr magneton per atom, and in these cases, it is possible to explain the magnetic anisotropy by using only the first term of (1); however, it

[1] J. H. VAN VLECK, *Phys. Rev.*, **52**, 1178 (1937).

[2] R. BECKER, *Z. Physik*, **62**, 253 (1930); see also *ibid.* reference 36.

is likely that the higher terms also are important in determining the details of the anisotropy in these cases as well.

Brooks[1] has recently shown that this topic may also be approached on the basis of the band approximation.

The problem of magnetostriction is closely connected with the problem of anisotropy; however, we shall not discuss it here.[2]

[1] H. BROOKS, *Phys. Rev.*, **57**, 570 (1940).

[2] See J. H. Van Vleck, *Phys. Rev.*, **52**, 1178 (1937).

CHAPTER XVII

THE OPTICAL PROPERTIES OF SOLIDS

146. Introduction.—The classical theory of the optical properties of solids is based upon Maxwell's equations for an uncharged polarizable medium, namely,

$$\begin{aligned} &\operatorname{div}(\mathsf{E} + 4\pi\mathsf{P}) = 0, && \operatorname{div}(\mathsf{H} + 4\pi\mathsf{M}) = 0, \\ &\operatorname{curl}\mathsf{E} = -\frac{1}{c}\frac{\partial(\mathsf{H} + 4\pi\mathsf{M})}{\partial t}, && \operatorname{curl}\mathsf{H} = \frac{1}{c}\frac{\partial\mathsf{E}}{\partial t} + \frac{4\pi}{c}\frac{\partial\mathsf{P}}{\partial t} + \frac{4\pi\mathsf{J}}{c}, \end{aligned} \tag{1}$$

where P and M are the electric and magnetic polarization intensities and J is the current per unit area. We shall be interested only in the case in which M is small enough to be dropped. In practically all applications of these equations, it is found possible to assume that P and J are related to E by the equations

$$\left.\begin{aligned} \mathsf{P} &= \alpha \cdot \mathsf{E}, \\ \mathsf{J} &= \sigma \cdot \mathsf{E}, \end{aligned}\right\} \tag{2}$$

where α and σ are the polarizability and conductivity tensors of the system. Maxwell's theory does not give an explanation of the dependence of α and σ upon frequency; the derivation of these relationships is the purpose of the atomic theory of solids.

Maxwell's theory of radiation is subject to direct experimental test whenever α and σ may be measured without performing an optical experiment. Unfortunately, this includes only the long wave-length region of the spectrum that is employed in radio work. For shorter waves ($\lambda \ll 1$ cm), the results of Maxwell's theory must be employed to determine the constants, in lieu of values determined by use of atomic theory. Although this may seem to be only an experimental difficulty, it should be realized that the size of the electrical circuit which can resonate to radiation having frequency 10^{14} cycles per second is of the order of atomic dimensions. For this reason, it is necessary to have intimate knowledge of the theory of atomic systems before the results of optical experiments can be interpreted in a way that throws light upon the behavior of the charges in solids.

The classical theory of α and σ was developed farthest by Lorentz[1] although important contributions have been made by other workers.[2]

[1] H. A. Lorentz, *Theory of Electrons* (Teubner, Leipzig, 1906).

[2] P. Drude (see *ibid.*); C. Zener, *Nature*, **132**, 968 (1933); R. de L. Kronig, *Nature*, **133**, 211 (1934).

This work is still very useful since some of its most significant results have not been modified. The quantum treatment of the optical properties is in principle just one of the fields of application of the theory of radiation developed in Chap. V. From a purely formal standpoint, it should only be necessary to apply Dirac's theory in order to determine the optical behavior of any solid. This formal procedure actually has not been followed very closely, however, and the subject has developed unevenly. Individual contributions have been made in order to obtain reasonably correct equations in a simple way rather than to obtain a self-consistent description of all properties. The reason for this procedure is, of course, that the rigorous theory is difficult to apply.

147. Classical Theory.—We shall discuss the solutions of Maxwell's equations (1) for an isotropic or cubic medium in which the electrical polarizability and the conductivity are constants instead of tensors. The equations then are

$$\begin{aligned} \operatorname{div} \mathsf{E} &= 0, & \operatorname{div} \mathsf{H} &= 0, \\ \operatorname{curl} \mathsf{E} &= -\frac{1}{c}\frac{\partial \mathsf{H}}{\partial t}, & \operatorname{curl} \mathsf{H} &= \frac{\epsilon}{c}\frac{\partial \mathsf{E}}{\partial t} + \frac{4\pi\sigma}{c} \mathsf{d} \end{aligned} \tag{1}$$

where

$$\epsilon = 1 + 4\pi\alpha \tag{2}$$

is the dielectric constant. There is one important point that should be kept in mind for future reference. The quantity

$$\alpha \frac{\partial \mathsf{E}}{\partial t}, \tag{3}$$

which appears in the fourth of Eqs. (1) when ϵ is replaced by use of (2), has the nature of a current—the polarization current. Maxwell believed that this current could be distinguished from the current J by the fact that the latter arises from the motion of obvious charge, such as that in conductors, whereas the former arises from hidden charge. In adopting an atomic viewpoint, we are no longer able to distinguish between the two types unambiguously; hence, we must be careful not to include the same current twice.

Since we are interested in periodic solutions of Eqs. (1), we shall employ complex values of E and H of the form

$$\begin{aligned} \mathsf{E}(x,y,z,t) &= \mathsf{E}'(x,y,z)e^{2\pi i\nu t}, \\ \mathsf{H}(x,y,z,t) &= \mathsf{H}'(x,y,z)e^{2\pi i\nu t}, \end{aligned}$$

Only the real parts of these functions will be regarded as physically interesting. The phases of the true current J and the polarization current $\alpha\partial\mathsf{E}/\partial t$ evidently differ by 90 deg when α and α are real. For

this reason, we may, if we choose, eliminate the term in J in the fourth of Maxwell's equations by replacing α with the complex polarizability α_c,

$$\alpha_c = \alpha + \frac{\sigma}{2\pi i\nu}, \tag{4}$$

or we may eliminate the term $\alpha\partial\mathsf{E}/\partial t$ by replacing σ by the complex conductivity

$$\sigma_c = \sigma + 2\pi i\nu\alpha. \tag{5}$$

The current defined by the equation

$$\mathsf{J} = \sigma\mathsf{E}$$

where σ is real is always in phase with the electrostatic field; hence, it constantly takes energy from the field. The mean power per unit volume that is lost in this way is

$$P = \overline{\mathsf{J}\cdot\mathsf{E}} = \sigma\overline{\mathsf{E}^2} \tag{6}$$

where the line indicates the average value. This relation may be used to show that the absorption is proportional to σ. Now the absorption coefficient η is defined by the equation

$$\frac{\partial\bar{W}}{\partial x} = -\eta\bar{W}$$

where $\bar{W}$ is the mean energy density and $\partial\bar{W}/\partial x$ is the decrease due to absorption alone Since

$$\bar{W} = \frac{\overline{\mathsf{E}^2}}{4\pi}$$

and

$$P_l = \frac{\bar{W}}{l} = -c\frac{\partial\bar{W}}{\partial x} \tag{7}$$

for a unidirectional wave, it follows that

$$\eta = \frac{4\pi\sigma}{c}$$

The polarization current, on the other hand, is 90 deg out of phase with E and does not remove energy from the field.

The plane-wave solutions of Eqs. (1) in which we are interested may be taken in the form

$$\begin{aligned}\mathsf{E} &= \mathsf{E}_0 e^{2\pi i\nu\left(t-\frac{N}{c}\eta_0\cdot r\right)}\\ \mathsf{H} &= \mathsf{H}_0 e^{2\pi i\nu\left(t-\frac{N}{c}\eta_0\cdot r\right)}\end{aligned} \tag{8}$$

where E_0 and H_0 are constant vectors, $\mathbf{n}_0$ is a unit vector in the direction of propagation of the wave, and N is the complex index of refraction, which may be written

$$N = n - ik, \tag{9}$$

in which n is the ordinary index of refraction and k is the extinction coefficient.

The imaginary part of N evidently measures the damping of the wave. The equations connecting the quantities in (8), which may be derived by substituting for E and H in (1), are

$$\begin{gathered} \mathbf{n}_0 \cdot \mathsf{E}_0 = 0, \qquad \mathbf{n}_0 \cdot \mathsf{H}_0 = 0, \\ N\mathbf{n}_0 \times \mathsf{E}_0 = \mathsf{H}_0, \qquad N\mathbf{n}_0 \times \mathsf{H}_0 = -\left(\epsilon + \frac{4\pi\sigma}{2\pi i\nu}\right)\mathsf{E}_0. \end{gathered} \tag{10}$$

These relations show that E_0 and H_0 are orthogonal to $\mathbf{n}_0$ and to one another. For simplicity, we shall take $\mathbf{n}_0$, E_0, and H_0 to lie in the x, y, and z directions, respectively. The last two equations then become

$$N\mathsf{E}_y = \mathsf{H}_z, \qquad N\mathsf{H}_z = \left(\epsilon + \frac{2\sigma}{i\nu}\right)\mathsf{E}_y. \tag{11}$$

Hence,

$$N^2 = \left(\epsilon + \frac{2\sigma}{i\nu}\right), \tag{12}$$

or

$$\left.\begin{aligned} n^2 - k^2 &= \epsilon, \\ nk &= \frac{\sigma}{\nu}. \end{aligned}\right\} \tag{13}$$

The phase angle between E and H is arctan k/n, which may be expressed in terms of ϵ and σ by solving (13).

If σ is zero and ϵ is positive, it follows that

$$k = 0, \qquad n = \sqrt{\epsilon}.$$

Under these conditions, the wave is undamped, and E and H are in phase. This case evidently corresponds to the propagation of light through a perfectly transparent medium having index of refraction n. On the other hand, if ϵ is negative,

$$n = 0, \qquad k = \sqrt{-\epsilon},$$

and the wave is damped in the direction of propagation. This damping is not accompanied by absorption, however, for P in Eq (7) vanishes if

σ is zero. These conditions evidently can be satisfied only if the medium is totally reflecting, which is shown explicitly by the extension of the theory of light that takes into account the behavior of a plane wave that is incident upon a plane surface of a medium.[1] According to this work, the reflection coefficient for normal incidence is

$$R = \frac{(n-1)^2 + k^2}{(n+1)^2 + k^2}, \tag{14}$$

which is unity when n is zero.

If σ is not zero, the solutions of Eqs. (13) are

$$\left.\begin{aligned} n^2 &= \frac{\epsilon \pm \sqrt{\epsilon^2 + 4(\sigma/\nu)^2}}{2}, \\ k^2 &= \frac{-\epsilon \pm \sqrt{\epsilon^2 + 4(\sigma/\nu)^2}}{2}. \end{aligned}\right\} \tag{13a}$$

Thus, the medium is neither perfectly transparent nor perfectly reflecting. We shall discuss two cases of this type that are of particular interest.

a. Lorentz Treatment of Absorption and Dispersion in Insulators.—As early as 1880, Lorentz[2] showed that it is possible by use of a simple atomic model to account for the dispersive behavior of insulators near an absorption line. He postulated that insulating materials contain electrons that are bound to equilibrium positions by Hooke's law forces. We shall assume that these forces are isotropic and that the electrons are subject to a damping force proportional to the velocity. The equations of motion of an electron that is subject to a periodic electrostatic field directed along the y axis then is

$$m\frac{d^2y}{dt^2} + 2\pi m\gamma\frac{dy}{dt} + \kappa y = -e\mathsf{E}_0 e^{2\pi i\nu t} \tag{15}$$

where y is the displacement of the electron along the y axis, $2\pi m\gamma$ is the damping constant, κ is Hooke's constant, and E_0 is the amplitude of the electrostatic field. The solution of this equation is

$$\begin{aligned} y &= -\frac{e\mathsf{E}_0 e^{2\pi i\nu t}}{4\pi^2 m[(\nu_0^2 - \nu^2) + i\gamma\nu]} \\ &= -\frac{e}{4\pi^2 m}\frac{\mathsf{E}_0 e^{2\pi i\nu t} e^{-i\varphi}}{\sqrt{(\nu_0^2 - \nu^2)^2 + \gamma^2\nu^2}} \end{aligned} \tag{16}$$

where

$$\nu_0 = \sqrt{\frac{\kappa}{4\pi^2 m}}$$

[1] See, for example, P. Drude, *The Theory of Optics* (Longmans, Green & Company, New York, 1902).

[2] LORENTZ, *op. cit.*

s the natural frequency of the oscillator and

$$\varphi = \arctan \frac{\gamma\nu}{(\nu_0^2 - \nu^2)} \tag{17}$$

is the phase angle between the electronic motion and the field intensity. The current per unit area associated with this motion is

$$J = -n_0 e\dot{y} = \frac{n_0 e^2}{4\pi^2 m} \frac{2\pi\nu e^{i\left(-\varphi+\frac{\pi}{2}\right)}}{\sqrt{(\nu_0^2 - \nu^2)^2 + \gamma^2\nu^2}} E_0 e^{2\pi i\nu t} \tag{18}$$

where n_0 is the number of oscillators per unit volume. Since the complex conductivity σ_c is the coefficient of $E_0 e^{2\pi i\nu t}$ in this equation, we have

$$\alpha = \frac{n_0 e^2}{4\pi^2 m} \frac{2\pi\nu}{\sqrt{(\nu_0^2 - \nu^2)^2 + \gamma^2\nu^2}} \sin\varphi = \frac{n_0 e^2}{4\pi^2 m} \frac{2\pi\gamma\nu^2}{(\nu_0^2 - \nu^2)^2 + \gamma^2\nu^2}, \tag{19}$$

$$\alpha = \frac{n_0 e^2}{4\pi^2 m} \frac{1}{\sqrt{(\nu_0^2 - \nu^2)^2 + \gamma^2\nu^2}} \cos\varphi = \frac{n_0 e^2}{4\pi^2 m} \frac{(\nu_0^2 - \nu^2)}{(\nu_0^2 - \nu^2)^2 + \gamma^2\nu^2}. \tag{20}$$

It may be seen from Eq. (17) that φ is π or zero, depending upon the sign of $\nu - \nu_0$, whenever

$$|\nu - \nu_0| >> \gamma.$$

The phase angle varies between these limits in the manner shown in Fig. 1 as ν passes through the value ν_0, the width of the transition region being of the order of magnitude γ. Since σ is appreciably different from zero only in this transition region, this is the only region in which light may be absorbed. The absorption coefficient $4\pi\sigma/c$ is plotted in Fig. 1 and has

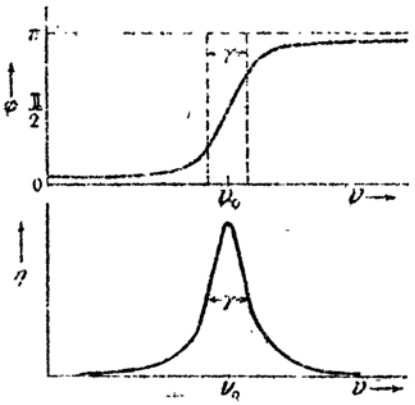

FIG. 1.—The phase angle φ and the absorption coefficient η of the assembly of oscillators as functions of frequency.

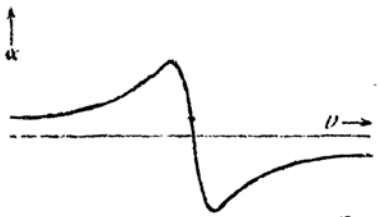

FIG. 2.—The polarizability of the system of oscillators

a peak of half width γ, centered about ν_0.

The polarizability α, given by Eq. (20), changes sign as we pass through the absorption maximum because cos φ changes from positive to negative values. Its absolute value increases as $1/|\nu_0 - \nu|$, as ν

approaches the absorption region, but does not go to infinity because of the term in γ in the denominator of (20). The characteristic behavior of α is shown in Fig. 2. The dielectric constant ϵ, which is of immediate interest for investigating the optical properties, is

$$\epsilon = 1 + 4\pi\alpha = 1 + \frac{n_0 e^2}{m\pi} \frac{(\nu_0^2 - \nu^2)}{(\nu_0^2 - \nu^2)^2 + \gamma^2\nu^2}. \tag{21}$$

Using these results and Eqs. (13), we may discuss the optical properties of the system of oscillators. In the region on the long wave-length side of ν_0 where $\nu_0 - \nu$ is much greater than γ, ϵ is positive and greater than unity, and σ is negligible. Hence, nk is zero, and $n^2 - k^2$ is positive. We may conclude that

$$k = 0, \qquad n^2 = \epsilon. \tag{22}$$

Thus, the system is transparent and has a refractive index greater than unity. This behavior is characteristic of most ionic and molecular crystals in the visible region of the spectrum. If we assume that n_0 is of the order of 10^{22} cm^{-3}, which is a normal atomic density, and that $\nu_0^2 - \nu^2$ is of the order of 10^{30} sec^{-2}, we find $\epsilon \sim 1.7$, or $n \sim 1.3$, which shows that this oscillator model can yield the correct magnitude for the optical quantities.

As we enter the absorption region, σ no longer is zero. ϵ is initially positive and passes through a maximum at

$$\nu = \nu_0 - \frac{\gamma}{2}.$$

It is readily found that

$$\sigma \sim 2\pi\nu\alpha$$

in the region of this maximum Equations (13) then become

$$n^2 - k^2 = 1 + 4\pi\alpha, \qquad nk = 2\pi\alpha. \tag{23}$$

The solutions of (23) show that n is larger than $\sqrt{\epsilon}$ in this part of the absorption region and that k is of the order of magnitude $\sqrt{\alpha}$ for large values of α and of the order of magnitude α for small values. It follows from Eq. (14) that the reflection coefficient approaches unity when α becomes large.

At the center of the absorption line, α is zero, whereas σ has the maximum value

$$\sigma_m = \frac{n_0 e^2}{2\pi m\gamma}$$

The values of n and k at this frequency are determined by the equations

$$n^2 = \frac{1 + \sqrt{1 + 4\sigma_m^2/\nu_0^2}}{2}, \qquad k^2 = \frac{-1 + \sqrt{1 + 4\sigma_m^2/\nu_0^2}}{2}.$$

As we pass to the other side of the absorption line, ϵ decreases and reaches a minimum value at

$$\nu = \nu_0 + \frac{\gamma}{2}.$$

Both n and k decrease as this occurs. If α reaches the value $-1/4\pi$, so that ϵ is zero, n and k are equal to

$$\sqrt{\frac{\sigma_m}{2\nu_0}}.$$

n is less than k in the region where ϵ is negative.

When $\nu - \nu_0$ is much greater than γ, σ is again zero and the medium no longer is absorbing. Whether it is perfectly reflecting or transparent here depends upon the sign of ϵ. Since α approaches zero as $-1/(\nu - \nu_0)$, ϵ is certainly positive for sufficiently high frequencies. The medium is transparent in this region although it is optically less dense than a vacuum. ϵ may be negative, however, in the non-absorbing region near the absorption line. When this happens, n is zero, k is finite, and the medium is totally reflecting (*cf.* Fig. 3). We shall see later that the optical properties of an ideal metal are similar to those of the system of oscillators on the high-frequency side of the center of the absorption line.

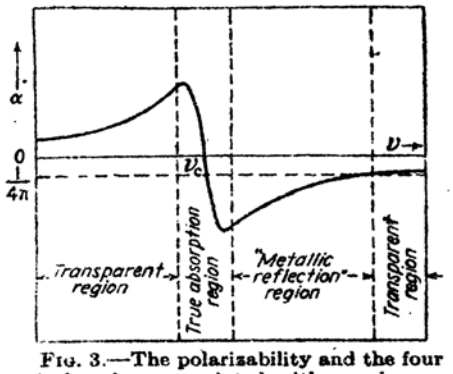

FIG. 3.—The polarizability and the four optical regions associated with an absorption line.

According to Eq. (19), the shape of an absorption line is determined by the function

$$\frac{\nu^2}{(\nu_0^2 - \nu^2)^2 + \nu^2\gamma^2}.$$

Since this is appreciable only in the region where ν_0 and ν are nearly equal, we may write

$$(\nu_0^2 - \nu^2)^2 = (\nu_0 - \nu)^2(\nu_0 + \nu)^2 = 4\nu^2(\nu_0 - \nu)^2.$$

We then obtain the relation

$$\frac{\nu^2}{(\nu_0^2 - \nu^2)^2 + \nu^2\gamma^2} \cong \frac{1}{4}\frac{1}{(\nu_0 - \nu)^2 + (\gamma/2)^2}, \tag{24}$$

which is the same as the form (7) of Sec. 45 determined by quantum theory.

It is not possible to make more than an order-of-magnitude estimate of the breadth γ of the absorption line by means of classical theory. A lower limit is determined by radiation damping. According to classical theory,[1] an oscillating charge radiates energy at the rate

$$\frac{2}{3c^3}\overline{\ddot{p}^2}$$

where p is the dipole moment, which is ey in the present case. For strictly periodic motion, this may be replaced by

$$\frac{2}{3}\frac{e^2}{c^3}\overline{\ddot{y}\dot{y}},$$

which is equivalent to assuming a damping force

$$\frac{2}{3}\frac{e^2}{c^3}\ddot{y} = -\frac{8\pi^2\nu^2}{3}\frac{e^2}{c^3}\dot{y}.$$

Thus, the damping frequency is

$$\gamma = \frac{4\pi\nu^2e^2}{3mc^3}.$$

As we remarked in Sec. 45, this is of the order of magnitude 10^8 sec^{-1} for optical frequencies and is usually masked by the damping due to other sources, such as collisions.

Before leaving this topic, we should mention that the local field[2] correction has been neglected in deriving the equations for the optical properties of the assembly of oscillators. This correction may be included by use of Lorentz's theory when α is not too large. The macroscopic polarizability is related to the polarizability α_a of a single oscillator by the equation

$$\alpha = \frac{n_0\alpha_a}{1 - \frac{4\pi}{3}n_0\alpha_a} \tag{25}$$

[1] See, for example, M. Abraham and R. Becker, *The Classical Theory of Electricity and Magnetism* (Blackie & Son, Ltd., London, 1932).

[2] See Sec. 142.

When the medium does not absorb,

$$n^2 = \epsilon = 1 + 4\pi\alpha,$$

or

$$\alpha = \frac{n^2 - 1}{4\pi}.$$

Thus, Eq. (25) may be transformed to

$$\frac{n^2 - 1}{n^2 + 2} = \frac{4\pi}{3} n_0 \alpha_a. \tag{26}$$

In the absorbing case, we may write Eq. (12) in the form

$$N^2 - 1 = 4\pi\alpha_c$$

where α_c is the complex polarizability. Equation (25) is then generalized to

$$\alpha_c = \frac{n_0 \alpha_{a,c}}{1 - \frac{4\pi}{3} n_0 \alpha_{a,c}} \tag{27}$$

where $\alpha_{a,c}$ is the complex polarizability of an oscillator. When these two equations are combined, the relation replacing (26) is

$$\frac{N^2 - 1}{N^2 + 2} = \frac{4\pi}{3} n_0 \alpha_{a,c}. \tag{28}$$

We shall discuss the application of these equations to particular cases below.

b. The Drude-Zener Treatment of Perfectly Free Electrons.—The classical treatment of the optical properties of metals that is based on the assumption of perfectly free electrons was developed by Drude,[1] Zener,[2] and Kronig.[3] The equation of motion for a free electron is

$$m\frac{d^2y}{dt^2} + 2\pi m\gamma\frac{dy}{dt} = -e\mathsf{E}_0 e^{2\pi i\nu t}, \tag{29}$$

which is identical with (15) except for the fact that κ is zero. Thus, we may anticipate that a system of free electrons behaves like a system of oscillators of frequency zero. In the present case, the damping term arises from the resistance of the metal, as we shall see more definitely below. The stationary solutions of Eq. (29) are

$$y = -\frac{e}{4\pi^2 m}\frac{\mathsf{E}_0 e^{2\pi i\nu t}}{-\nu^2 + i\gamma\nu},$$

[1] P. DRUDE, *op. cit.*
[2] C. ZENER, *op. cit.*
[3] R. DE L. KRONIG, *op. cit.*

om which we obtain

$$\sigma = n_0 \frac{e^2}{4\pi^2 m} \frac{2\pi\gamma}{\nu^2 + \gamma^2}, \tag{30}$$

$$\alpha = -n_0 \frac{e^2}{4\pi^2 m} \frac{1}{\nu^2 + \gamma^2}. \tag{31}$$

hen ν is zero, the first of these equations is

$$\sigma_0 = n_0 \frac{e^2}{2\pi m\gamma}. \tag{32}$$

omparing this with Eq. (6), Sec. 126, we see that

$$2\pi\gamma = \frac{v}{l} = \frac{1}{\tau}$$

here τ is the mean time between collisions, which is of the order of magnitude 10^{-13} sec at room temperature.

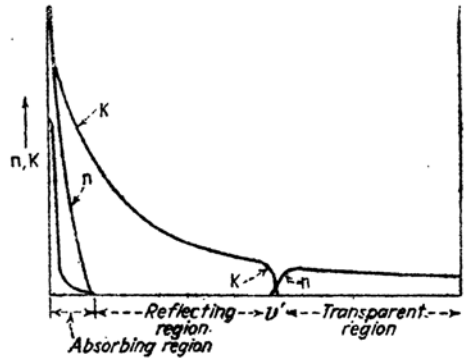

FIG. 4.—The quantities n and k as functions of frequency for a system of free electrons.

Since Eqs. (30) and (31) are identical with Eqs. (19) and (20) when ν_0 is zero, it follows that the optical properties of a system of free electrons should correspond closely to those of an insulator on the short wavelength side of the center of an absorption band. Thus, there should be an absorption region extending from zero frequency to $\nu \sim \gamma$, which in case n_0 is large enough should be followed by a nonabsorbing region in which ϵ is negative (*cf.* Fig. 4). Here, n is zero, and k is equal to $\sqrt{-\epsilon}$. ventually, ϵ should become positive, since $|\alpha|$ decreases as $1/\nu^2$ with creasing frequency, and the system should become transparent. nce, the system should be highly reflecting until α is $-1/4\pi$ and should en behave like an ordinary transparent insulator. The frequency ν' which this transition occurs is so much larger than γ for ordinary ensities of electrons that we may obtain it from Eq. (31) by setting ν

equal to zero. Thus,

$$\nu' = \sqrt{\frac{n_0 e^2}{\pi m}}. \tag{3}$$

We shall now discuss the three optical regions.

1. $\nu << \gamma$.—The optical relations corresponding to the absorbi region in which ν is much smaller than γ are

$$\left.\begin{aligned} n^2 &\cong \frac{n_0 e^2}{2\pi m}\frac{1}{\gamma^2}[-1 + \sqrt{1 + (\gamma/\nu)^2}] \cong \frac{n_0 e^2}{2\pi m \gamma \nu}, \\ k^2 &\cong \frac{n_0 e^2}{2\pi m}\frac{1}{\gamma^2}[1 + \sqrt{1 + (\gamma/\nu)^2}] \cong \frac{n_0 e^2}{2\pi m \gamma \nu} \end{aligned}\right\} \tag{34}$$

These may be simplified by use of Eq. (32), for they then reduce to

$$n = k = \left(\frac{\sigma_0}{\nu}\right)^{\frac{1}{2}} \tag{3}$$

If these values are substituted in Eq. (14) for R, we find

$$R = 1 - 2\left(\frac{\nu}{\sigma}\right). \tag{3}$$

This relation has been tested experimentally in the far infrared region b Hagen and Rubens.[1] According to (36), the value of $(1 - R)\nu$ should be equal to $36.5/\sqrt{\lambda}$ if λ is measured in microns. Table LXXXI shows the agreement between the observed and calculated values of th quantity for constantan.

TABLE LXXXIII.—VALUES FOR CONSTANTAN OF $(1 - R)\sqrt{\sigma}$

λ, microns	Observed	Calculated
4	19 4	18 25
8	13 0	12 90
12	11 0	10.54
25.5	7.36	7.23

2. $\nu \sim \nu'$.—In the region near ν', at which $4\pi\alpha$ becomes unity, ν is about one hundred times larger than γ so that σ/ν in Eqs. (13) is negligible in first approximation. These equations then are

$$\left.\begin{aligned} n^2 = k^2 &= 1 - \frac{n_0 e^2}{\pi m}\frac{1}{\nu^2}, \\ nk &= 0 \end{aligned}\right\} \tag{37}$$

[1] E. HAGEN and H. RUBENS, *Ann. Physik*, **14**, 936 (1904).

As we mentioned previously, n is zero and k is $\sqrt{-\epsilon}$ when ν is less than ν', and k is zero and n is $\sqrt{\epsilon}$ when ν is greater than ν'. Wood[1] has found that the alkali metals, in which the valence electrons are nearly free, satisfy these relations closely. Table LXXXIV contains the observed wave lengths at which the transition from the reflecting to the transmitting state occurs. These were determined by observations on thin films of the metals. The values calculated from Eq. (33) by the use of the true electronic mass and electron density are tabulated for comparison. In the cases of lithium and sodium, the values for the theoretical effective masses are also given.

TABLE LXXXIV

	Observed, Å	Calculated, Å	
		m	m^*
Li	1550	1500	1830
Na	2100	2090	2020
K	3150	2920	
Rb	3400	3220	
Cs	3800	3630	

3. $\nu' >> \nu >> \gamma$.—The theoretical and experimental results do not seem to agree very closely in the visible and near ultraviolet region where

$$\nu' >> \nu >> \gamma.$$

The values of σ and ϵ, given by Eqs. (30) and (31), in this region are

$$\sigma = \frac{n_0 e^2 \gamma}{2\pi m \nu^2} = \left(\frac{n_0 e^2}{2\pi m \nu}\right)^2 \frac{1}{\sigma_0}, \tag{38}$$

$$\epsilon = 1 - \frac{n_0 e^2}{\pi m \nu^2}. \tag{39}$$

Försterling and Freedericksz[2] obtained measurements of n and k for a number of metals, in the region from 1μ to 15μ, from which values of σ and ϵ may be determined by means of Eqs. (13). The observed values of ϵ usually agree with the theoretical ones determined from (39) to within about 10 per cent whereas the values of σ disagree by a comparatively large factor. It is found that the frequency dependence of the observed values is the same as that predicted by Eq. (38); however, the

[1] R. W. WOOD, *Phys. Rev.*, **44**, 353 (1933). See also R. W. WOOD and C. LUKENS, *Phys. Rev.*, **54**, 332 (1938).

[2] K. FÖRSTERLING and V. FREEDERICKSZ, *Ann. Physik*, **40**, 201 (1913).

value of σ_0 that is required to give the proper magnitude is much smaller than the actual static conductivity. The two values of σ_0 are listed in Table LXXXV. In addition, the value of the effective electron mass that gives the best fit between the observed and computed ϵ curves is given in the cases of copper, silver, and gold.

TABLE LXXXV

	Ag	Au	Cu	Pt	Ir
Value of σ_0 for best fit	1.4	2.5	1.0	0.12	0.13
Actual value	5.7	4.2	5.3	0.85	1.7
m^*/m	1.07	1.13	2.56		

It should be pointed out[1] that the optical properties in this spectral region are determined by a thin surface layer of the metal. The *penetration distance* δ, in which the light intensity drops to $1/e$th of its initial value, is

$$\delta = \frac{\lambda}{4\pi k}$$

where λ is the wave length. This is about 200Å at 1μ for silver, since k is 5.62. It is possible that the conductivity σ_0 of a sheath of this thickness is considerably lower than that of the bulk material because of surface contaminations.

148. Quantum Formulation of the Optical Properties*.—We shall now develop the equations for the optical properties of solids in three idealized cases, namely: (*a*) the case of a system of isolated atoms, (*b*) a case in which the excited state of the system may be described by exciton waves, and (*c*) a system in which the electronic wave functions are determinants of Bloch one-electron functions. The results for the first two cases evidently may be applied to insulators such as molecular and ionic crystals, whereas the results for the third should apply to metals. The effect of nuclear motion will be neglected for the present.

a. A System of Isolated Atoms.—When the atoms or molecules in a solid are very loosely bound, its optical properties may be obtained from the equations that were derived for free atoms in Sec. 43. We saw there that the effective atomic polarizability for dispersive scattering of quanta of frequency ν is the tensor

$$\alpha_a = \sum_k{}' \frac{\mathbf{M}_{0k}\mathbf{M}_{k0}}{h} \frac{2\nu_{k0}}{\nu_{k0}^2 - \nu^2} \tag{1}$$

[1] This suggestion apparently was made first by A. H. Wilson, *The Theory of Metals* (Cambridge University Press, 1936).

[*cf.* Eq. (33), Sec. 43]. Here, k is summed over all excited states,

$$\mathbf{M}_{0k} = -\int \Psi_0^*(\Sigma e\mathbf{r}_i)\Psi_k d\tau \tag{2}$$

is the matrix component of the atomic dipole moment, and

$$\nu_{k0} = \frac{E_k - E_0}{h}. \tag{3}$$

Similarly, the probability $P_j(t)$ that an atom jumps from a state Ψ_0 to a state Ψ_j, if the energy density as a function of frequency is ρ_ν, is

$$P_j(t,\nu) = \frac{8\pi^3}{h^2}|\mathbf{M}_{0j}\cdot\mathbf{n}|^2\rho_\nu t\delta\left(\frac{E_j - E_0}{h} - \nu\right) \tag{4}$$

in the δ-function approximation of Sec. 43, where $\mathbf{n}$ is the direction of polarization of the radiation. It should be possible to derive ϵ and σ from Eqs. (1) and (4).

Since it is convenient to treat cases in which ϵ and σ are constants instead of tensors, we shall usually consider examples in which (1) and (4) are independent of the direction. In the present case, this is true if the atoms are in S states (*cf.* Sec. 43).

The individual terms of Eq. (1) are very similar to those derived in the last section for the polarizability of an oscillator in a nonabsorbing region, namely,

$$\alpha_{k0} = \frac{e^2}{4\pi^2 m}\frac{1}{\nu_{k0}^2 - \nu^2} \tag{5}$$

[*cf.* Eq. (20) in the case in which γ is negligible] In fact, Eq. (1) may be written as

$$\alpha_c = \sum_k \mathbf{f}_{k0}\alpha_{k0} \tag{6}$$

where

$$\mathbf{f}_{k0} = \frac{8\pi^2 m}{he^2}\nu_{k0}\mathbf{M}_{0k}\mathbf{M}_{k0} \tag{7}$$

is the oscillator strength of the transition from Ψ_0 to Ψ_k which evidently is a tensor quantity. A theorem of the theory of atomic spectra states[1] that for free atoms the sum of all the $\mathbf{f}_{k0}$ connecting two levels is a multiple of the unit tensor. For example, in the case in which the ground state is a $^1S_0$ state, $\mathbf{f}_{k0}$ is nonvanishing only for a $^1P_1$ state when the Russell-Saunders coupling scheme is valid. If the three degenerate substates

[1] See, for example, E. U. Condon and G. H. Shortley, *The Theory of Atomic Spectra* (University Press, Cambridge, 1935); S. A. Korff and G. Breit, *Rev. Modern Phys.*, **4**, 471 (1932); G. Breit, *Rev. Modern Phys.*, **4**, 504 (1932).

are chosen to be eigenfunctions of the three components of orbital angul momentum, the sum of $\mathbf{f}_{k0}$ for the three states is

$$\sum_{k=1}^{3}\mathbf{f}_{k0} = \frac{8\pi^2 m}{3h}\nu_{k0}\sum_{k=1}^{3}\left[\left|\left(\sum_{i=1}^{n}x_i\right)_{k0}\right|^2 + \left|\left(\sum_{i=1}^{n}y_i\right)_{k0}\right|^2 + \left|\left(\sum_{i=1}^{n}z_i\right)_{k0}\right|^2\right]\mathbf{I}, \quad (8)$$

where **I** is the unit tensor. In the same case, the sum of the time derivatives of (4) for the transitions from the lowest state to the three degenerate P states is

$$\frac{dP_{l0}}{dt} = \frac{e^2\pi}{mh}\frac{f_{l0}}{\nu_{l0}}\rho_\nu\delta(\nu_{l0} - \nu), \quad (9)$$

in which ν_{l0} is the frequency ν_{k0} and f_{l0} is the coefficient of **I** in Eq. (8

The scalar coefficient of **I** in the equation corresponding to (8) fo any two levels l and m is usually designated by f_{lm} and is called the f factor or the line strength for the two levels. The reason for the second designation is that f_{lm} generally occurs in the equation analogous to (9) and thus measures the relative line intensity. It follows that the f_{lm} may be determined from absorption and emission measurements.

Another theorem of quantum mechanics[1] states that

$$\sum_l f_{lm} = n, \quad (10)$$

in which l is summed over all levels and n is the total number of electrons in the atom. Since the ν_{k0} in Eq. (7) are positive for the lowest state in the atom, it follows that the f factors for this level are all positive. Hence, in this case, (10) states that the sum of the f factors for *absorption* from the lowest state is equal to n. The same conclusion cannot be drawn for the absorption f factors of an excited atom, for there may be additional factors connecting this and lower levels. Since the emission factors are negative, it follows that the sum of the absorption line strengths of an excited atom usually is greater than n. This fact is of importance in discussing the absorption f factors in the cases of monovalent atoms, such as the lighter alkali metals, in which the valence electron wave functions can be derived from an effective ion-core field as we have seen in Sec. 78. In this case, there is a theorem analogous to (10) for the valence electron, namely,

$$\sum_l f'_{lm} = 1, \quad (11$$

[1] E. WIGNER, *Physik. Z.*, **32**, 450 (1932); H. A. KRAMERS, C. C. JONKER, and KOOPMANS, *Z. Physik*, **80**, 178 (1932).

where f'_{lm} refers to the levels of the ion-core field. In lithium, the lowest state is a $2s$ function, and there are no lower p functions; hence, the f_{lm} for the $2s$ state are all positive, and the sum of the absorption strengths of the valence electron should be unity. In sodium, on the other hand, the lowest state is $3s$. Thus, in this case there is a fictitious $2p$ state lying below the $3s$ for which there is a negative f factor. Hence, the sum of the absorption line strengths should be larger than unity. The same is true in any of the heavier alkali metal atoms whose levels may be obtained from an effective ion-core field.

In atomic lithium,[1] the strengths for the valence-electron transitions have the values given in Table LXXXVI.

TABLE LXXXVI

Transition from $2s$ to	f
$2p$	0.7500
$3p$	0.0055
$4p$	0.0047
$5p$	0.0026
Continuum	0.24
Sum	1.01

Thus, 75 per cent of the oscillator strength is associated with the first excited level, and the sum of the f is close to unity.

According to Eq. (26) of the preceding section, the index of refraction in a nonabsorbing region should be related to the atomic susceptibility (6) by the equation

$$\frac{n^2 - 1}{n^2 + 2} = \frac{n_0}{3} \sum_l \frac{e^2}{\pi m} \frac{f_{l0}}{\nu_{l0}^2 - \nu^2} \tag{12}$$

where l is summed over all excited levels. The f values of the rare gas atoms have been determined by expressing the observed index of refraction of the gas in a series of the type (12). It is found[2] in this way that the total f value associated with the transition from the lowest level to the levels of the $1s2p$ configuration is 1.12 for helium, which has two electrons. In the other rare gases, which have six p electrons in the outer shell, the corresponding numbers are as follows

Ne	2.37
Ar	4.58
Kr	4.90
Xe	5.61.

[1] [1] B. TRUMPY, *Z. Physik*, **61**, 54 (1929).

[2] See, for example, K. L. WOLFF and F. K. HERZFELD, *Handbuch der Physik*, Vol. XX.

The absorption coefficient in the absorbing region may be determined from Eq. (9). According to this, the energy loss per unit volume at a point where the energy density is ρ_ν is[1]

$$\frac{dW}{dt} = \sum n_c h\nu_l \frac{dP_l}{dt} = \frac{n_0}{m}\frac{\pi}{}\rho_\nu \sum_l f_l \delta(\nu_l - \nu)$$

where n_0 is the number of atoms per unit volume. Comparing this with Eq. (6) of the preceding section, we find

$$\sigma = \frac{n_0 e^2}{4m} \sum_l f_l \delta(\nu_l - \nu). \tag{13}$$

Hence, the absorption coefficient in this delta-function approximation is

$$\pi(\nu) = \frac{n_0 e^2 \pi}{mc} \sum_l f_l \delta(\nu_l - \nu) \tag{14}$$

according to which the absorption peaks should be infinitely narrow.

Combining Eqs. (6) and (13), we obtain for the complex atomic polarizability

$$\alpha_0 = \alpha_a + \frac{\sigma_a}{2\pi\nu i} = \frac{e^2}{4\pi^2 m} \sum_l \left[\frac{f_l}{\nu_l^2 - \nu^2} - \frac{i\pi f_l \delta(\nu - \nu_l)}{2\nu} \right]. \tag{15}$$

It was found in Sec. 45 that the shape of an abrerption line is given by the function

$$\frac{1}{(\nu_l - \nu)^2 + \Gamma^2} \tag{16}$$

instead of by a delta function. Hence, we should replace the delta function in Eqs. (13) and (15) by the function (16) multiplied by an appropriate normalization constant. Since the integral of (16) over all frequencies is π/Γ if ν_l is greater than Γ, the delta function should be replaced by

$$\frac{\Gamma/\pi}{(\nu_l - \nu)^2 + \Gamma^2}$$

or, if we use the approximation of Eq. (24) of the preceding section, by

$$\frac{2\gamma\nu^2/\pi}{(\nu_0^2 - \nu^2)^2 + \nu^2\gamma^2} \tag{17}$$

[1] Since the atoms are in their lowest state, we may drop the subscript zero in f, Γ and ν.

where $\gamma = 2\Gamma$. At the same time, the coefficient $1/(\nu_i^2 - \nu^2)$ of the real part of (15) should be replaced by

$$\frac{(\nu_i^2 - \nu^2)}{(\nu_i^2 - \nu^2)^2 + \gamma^2\nu^2}. \tag{18}$$

Thus, (15) becomes

$$\left.\begin{aligned} \alpha_c &= \frac{e^2}{4\pi^2 m}\sum_i f_i \frac{(\nu_i^2 - \nu^2) - i\gamma\nu}{(\nu_i^2 - \nu^2)^2 + \gamma^2\nu^2} \\ &= \frac{e^2}{4\pi^2 m}\sum_i \frac{f_i}{(\nu_i^2 - \nu^2) + i\gamma\nu} \end{aligned}\right\} \tag{19}$$

which is analogous to the result that is obtainable from the classical equation (16) of the preceding section.

b. The Case of Excitation Waves.—In treating the absorption and dispersion in a solid whose normal and lowest excited states are described by excitation waves, we must use the equations that were derived in Sec. 96 for extended atomic systems. We shall discuss a simple model in which there is only one electron per atom. According to the discussion of Sec. 96, the normal-state wave function then is $1/\sqrt{N!}$ times a determinant of normalized one-electron functions of the atomic type $\psi(\mathbf{r} - \mathbf{r}(n))$ that are centered about each of the atomic positions

$$\mathbf{r}(n) = n_1\tau_1 + n_2\tau_2 + n_3\tau_3. \tag{20}$$

The normalized excited states have the form

$$\Psi_{\mathbf{k},i} = \frac{1}{\sqrt{N}}\sum_n e^{2\pi i\mathbf{k}\cdot\mathbf{r}(n)}\Psi_{n,i} \tag{21}$$

where $\Psi_{n,i}$ is the wave function derived from Ψ_0 by replacing $\psi(\mathbf{r} - \mathbf{r}(n))$ by the excited atomic function $\psi_i(\mathbf{r} - \mathbf{r}(n))$, and $\mathbf{k}$ ranges over the points of a single zone. A band of levels of energy

$$E_i(\mathbf{k}) = E_i + I_i\sum_\rho' e^{2\pi i\mathbf{k}\cdot\rho} \tag{22}$$

is associated with each value of i where E_i is the unperturbed energy of the state $\Psi_{n,i}$ and I_i is an integral involving neighboring excited and normal atoms. We shall discuss a case in which the lowest atomic function is an S-state.

It was found in Sec. 96 that

$$\int \Psi_0 \operatorname{grad} \Psi_{\mathbf{k},i}\, d\tau = \frac{1}{\sqrt{N}}\left(\int \psi \operatorname{grad} \psi_i\, d\tau\right)\delta_{\mathbf{k},0} \tag{23}$$

where ψ is the normal atomic function and ψ_i is the excited function for the same atom [*cf.* Eqs. (17) to (20), Sec. 96]. We may conclude from this that the only allowed transitions take place between the excitation bands corresponding to atomic states between which transitions are allowed. The appearance of the factor $\delta_{k,0}$ in (23) implies that the excited states of the entire crystal must have the same wave number as the normal state in the reduced-zone sense, which is a generalization of the principle of conservation of momentum.

Now, the conductivity associated with these transitions is[1]

$$\sigma(\nu) = \frac{e^2h}{24\pi^2\nu m^2 V}\sum_{k,i}\left|N\int \Psi_{k,i}\,\mathrm{grad}\,\Psi_0 d\tau\right|^2 \delta(\nu_{0k,i} - \nu). \tag{24}$$

When the relation (23) is used, this becomes

$$\sigma(\nu) = \frac{n_0 e^2 h}{24\pi^2\nu m^2}\sum\left|\int \psi\,\mathrm{grad}\,\psi_i d\tau\right|^2 \delta(\nu_i - \nu) \tag{25}$$

where

$$\nu_i = \frac{E_i - E_0}{h},$$

in which E_i and E_0 are, respectively, the unperturbed energies of $\Psi_{n,i}$ and Ψ_0. Equation (25) is identical with the expression for the conductivity of a system possessing n_0 isolated atoms per unit volume. Thus, it may be transformed into Eq. (13) by use of Eq. (8) and the equation

$$\left|\int \psi\,\mathrm{grad}\,\psi_i d\tau\right| = \frac{2\pi m\nu_i}{h}\left|\int \psi r\psi_i d\tau\right| \tag{26}$$

[*cf.* Eq (24), Sec. 43].

[1] A detailed development of Eqs. (24) and (27) is omitted for brevity. These equations may be derived by the use of the semiclassical method by dividing the crystal into sections smaller than the wave length of light and larger than atomic dimensions and treating these sections both as specimens of the bulk solid and as molecular units to which the methods of Sec 43 are applicable. Perturbed wave functions may be computed for the case in which a radiation field is present; and, from these, the power loss P due to transitions and the mean value $\mathbf{J}$ of the current operator (see Sec. 44) may be evaluated The conductivity σ and the polarizability α are related to these quantities by the equations

$$P = \sigma E^2 \qquad \text{and} \qquad \bar{\mathbf{J}} = \alpha \cdot \mathbf{E}.$$

It follows from these remarks that Eqs (24) and (27) are valid only when the wave length of light is long compared with atomic dimensions. The second term in Eq. (27) arises from the part of Eq (8), p. 223, involving the vector potential.

If Eq. (23) is substituted in the equation for the polarizability,[1] namely,

$$\alpha = \left[\frac{e^2h}{24\pi^4m^2\nu^2V}\sum_{k,i}\frac{\nu_{k,i0}}{\nu_{k,i0}^2-\nu^2}\left(N\int\Psi_{k,i}\operatorname{grad}\Psi_0 d\tau\right)^2-\frac{e^2}{4\pi^2m\nu^2}n_0\right], \quad (27)$$

and Eq (26) is used to simplify the result, it is found that

$$\alpha(\nu) = \left(\frac{2n}{3h\nu^2}\sum_i \nu^3\frac{|\mathbf{M}_i|^2}{\nu_i^2-\nu^2}-\frac{n_0e^2}{4\pi^2m\nu^2}\right) \quad (28)$$

where

$$|\mathbf{M}_i|^2 = \frac{eh}{2\pi\nu_i m}\sum_{l=1}^{3}\left|\int\psi\operatorname{grad}\psi_i d\tau\right|^2 \quad (29)$$

is the dipole matrix component.

We may reduce this still further by use of the sum rule

$$\sum_l f_l = \sum\frac{8\pi^2m}{3he^2}\nu_i|\mathbf{M}_i|^2 = 1;$$

for if we subtract the equation

$$\frac{n_0e^2}{4\pi^2m\nu^2}\left(\sum_l f_l-1\right)=0$$

from Eq. (28), we obtain

$$\alpha = \frac{n_0e^2}{4\pi^2m}\sum_l\frac{f_l}{\nu_l^2-\nu^2} \quad (30)$$

which is equivalent to the expression for the polarizability of a system of isolated atoms.

We may conclude from the results of this part of the present section that the optical properties of a system that is described by means of excitation waves are the same as those of a system of free atoms. The absorption spectrum consists of discrete lines not because the energy levels do not form wide bands, but because the wave number of the exciton must be zero.

c. *The Case of Bloch Wave Functions.*—When the system may be described in the Bloch approximation, the lowest singlet wave function Ψ_0 is a determinant of functions

$$\psi_k = \chi_k e^{2\pi i k\cdot r}, \quad (31)$$

[1] See previous footnote.

in which each of $N/2$ ψ_k of lowest energy appear once with each spin. The excited singlet states are determinantal functions that are derived from Ψ_0 by replacing one or more of the ψ_k by excited functions $\psi_{k'}$. Since the matrix components in which we are interested are integrals of a one-electron operator, the interesting excited states differ from Ψ_0 by one Bloch function. If the state derived by replacing ψ_k with $\psi_{k'}$ is designated by $\Psi_{kk'}$, it follows from the discussion of Sec. 71 that

$$N\int\Psi_{kk'}^* \operatorname{grad}_1 \Psi_0 d\tau = (\int\chi_{k'}^* \operatorname{grad} \chi_k d\tau)\delta_{k',k+K}. \tag{32}$$

Thus, as was pointed out in Sec. 71, the allowed optical transitions correspond to "vertical" jumps in the reduced-zone scheme.

It should be noted that in the present case the electronic absorption spectra of the entire solid consist of broad bands instead of discrete lines, in contrast with the case of excitons. The reason for this is that in the transition from Ψ_0 to $\Psi_{kk'}$ the excited electron and the hole it leaves behind move independently of one another. Thus, the only restriction on electronic wave number is that the sum of the wave number $\mathbf{k}'$ of the excited electron and the wave number $-\mathbf{k}$ of the hole be equal to a principal vector $\mathbf{K}$ in the reciprocal lattice, which may be satisfied for any value of $\mathbf{k}'$.

The polarizability, which is given by Eq. (27), is

$$\alpha = \left[\frac{e^2h}{24\pi^4m^2\nu^2V}\sum_{k,K}\frac{\nu_{k,k+K}}{\nu^2_{k,k+K}-\nu^2}|\int\chi_{k+K}^* \operatorname{grad} \chi_k d\tau|^2 - \frac{e^2}{4\pi^2m\nu^2}n_0\right] \tag{33}$$

in the present case. The variable $\mathbf{k}$ extends over the occupied levels of the lowest state, once for each spin, and $\mathbf{K}$ is summed over all values of the principal wave-number vectors.

The sum rule for Bloch's one-electron functions[1] is

$$\frac{h}{6\pi^2m}\sum_{K\neq 0}\frac{|\int\chi_{k+K}^* \operatorname{grad} \chi_k d\tau|^2}{\nu_{k,k+K}} + \frac{m}{3h^2}\Delta_k\epsilon(k) = 1. \tag{34}$$

If this equation is multiplied by $e^2/4\pi^2m\nu^2$, summed over all values of $\mathbf{k}$, and is combined with (33), it is found that

$$\alpha = \left[\frac{e^2h}{24\pi^4m^2V}\sum_{k,K}\frac{|\int\chi_{k+K}^* \operatorname{grad} \chi_k d\tau|^2}{\nu_{k,k+K}(\nu^2_{k,k+K}-\nu^2)} - \sum_k\frac{e^2}{12\pi^2h^2\nu^2}\Delta_k\epsilon_k\right]. \tag{35}$$

The first part of this equation may be placed in the form

$$\frac{e^2}{4\pi^2mV}\sum_{k,K}\frac{f_{k,K}}{\nu^2_{k,k+K}-\nu^2} \tag{36}$$

[1] See, for example, Wilson, *op. cit.*

where

$$f_{\mathbf{k},\mathbf{K}} = \frac{h}{6\pi^2 m} \frac{|\int \chi_{\mathbf{k}+\mathbf{K}}^* \operatorname{grad} \chi_{\mathbf{k}} d\tau|^2}{\nu_{\mathbf{k},\mathbf{k}+\mathbf{K}}}. \tag{37}$$

Equation (36) is the counterpart of the polarizability of insulators since it is associated with transitions between the lowest zone and others. It approaches (30) in the limiting case of narrow bands in which the $\chi_{\mathbf{k}}$ become atomic functions. The last term in (35) may be transformed to

$$-\frac{n_0 e^2}{4\pi^2 m^* \nu^2} \tag{38}$$

by making use of the relation

$$\frac{1}{m^*} = \frac{1}{3h^2} \Delta_{\mathbf{k}} \epsilon(\mathbf{k}).$$

Comparing Eq. (38) with Eq. (31) of the preceding section, namely,

$$\alpha = -\frac{n_0 e^2}{4\pi^2 m} \frac{1}{\nu^2 + \gamma^2},$$

we see that they are identical in the case in which the resistance damping γ is neglected and m^* is equal to m. Hence, (38) corresponds to the polarizability of free electrons.

The expression (24) for the conductivity becomes

$$\sigma(\nu) = \frac{e^2 h}{24\pi^2 \nu m^2 V} \sum_{\mathbf{k},\mathbf{K}} \left| \int \chi_{\mathbf{k}+\mathbf{K}}^* \operatorname{grad} \chi_{\mathbf{k}} d\tau \right|^2 \delta(\nu_{\mathbf{k},\mathbf{k}+\mathbf{K}} - \nu), \tag{39}$$

which may be used to discuss the absorption associated with transitions between bands. This expression is not valid at zero frequency, for it does not allow for the fact that free electrons may be continuously accelerated in a static electrostatic field. In the present approximation in which damping is neglected, σ should have an infinite peak when ν is zero. This term is absent because the perturbation scheme used in Sec. 43 was not applied properly in the aperiodic case of zero frequency. We need not discuss this case here, since it was treated extensively in Chap. XV.

149. Application to Metals.—We shall now discuss the application of the preceding theoretical results to metals. If the theory were applied accurately to all cases, we should be able to test it by comparing observed and computed values of n and k for a wide range of frequencies. This actually can be done only for several of the alkali metals and then only semiquantitatively. In other cases, we must be satisfied with a rough comparison of the peaks and minima of the observed absorption curves with those which should be expected from estimated levels of the band approximation.

a. The Alkali Metals.—It was seen in Chap. X that the valence electrons in alkali metals are very nearly free, for the occupied electronic levels can be expressed in the free-electron form

$$\epsilon(\mathbf{k}) = \frac{\hbar^2}{2m^*}\mathbf{k}^2$$

where m^* is a constant. The computed values of m/m^* for lithium, sodium, and potassium are

Li	0.65
Na	1.07
K	~1.6

Using the sum rule

$$1 - \sum_{\mathbf{K}} f_{\mathbf{k},\mathbf{K}} \equiv 1 - \sum_{\mathbf{K}} \frac{\hbar}{2\pi^2 m} \frac{|\int \chi_{\mathbf{k}+\mathbf{K}}^* \operatorname{grad} \chi_{\mathbf{k}} d\tau|^2}{\nu_{\mathbf{k},\mathbf{k}+\mathbf{K}}} = \frac{m}{m^*}$$

[*cf.* Eq. (34) of the preceding section], we obtain a relation between m^* and the f factors that determine the absorption probability for transitions from one band to another. In sodium, m/m^* is very nearly unity so that $\sum_{\mathbf{K}} f_{\mathbf{k},\mathbf{K}}$ is very small. This means that the oscillator strengths for transitions from the lowest band to higher bands are small and that we should expect the Zener-Kronig theory for perfectly free electrons to apply closely for this metal. This actually turns out to be the case. Experimental and theoretical[1] curves, which are shown in Fig. 5, agree closely down to 1850Å except for the fact that the observed value of nk, although very small in the reflecting region, is several times larger than the value computed from resistance damping by using the observed static resistivity. Since nk is proportional to the absorption coefficient, this fact implies that the absorption is higher than we should expect from the free-electron theory. It is possible that the discrepancy has the same explanation as that proposed for the cases discussed under 3, part (*b*),

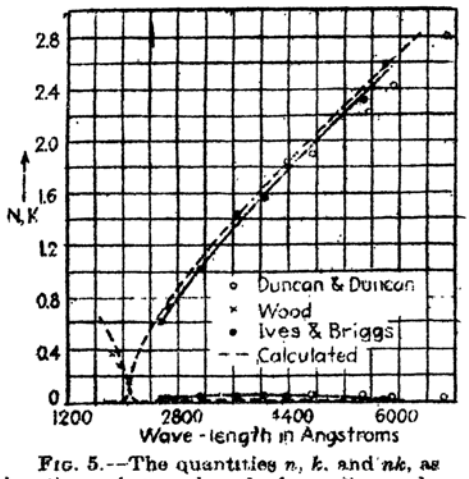

FIG. 5.—The quantities n, k, and nk, as functions of wave length, for sodium. In this case the agreement between observation and the simple theory is excellent. (*After Ives and Briggs*)

[1] H. E. IVES and H. B. BRIGGS, *Jour. Optical Soc. Am.*, **27**, 181 (1937)

Sec. 147, namely, that the surface conductivity is less than the volume conductivity. It is also possible, however, that the volume absorption due to interband transitions begins in the visible region of the spectrum, for the energy-level diagram of sodium discussed in Sec. 99 (*cf.* Fig. 1) indicates that the lowest transition should occur at about 2 ev. In contradiction to this explanation is the fact that the peaks for the volume photoelectric effect lie far in the ultraviolet for the lighter alkali metals.

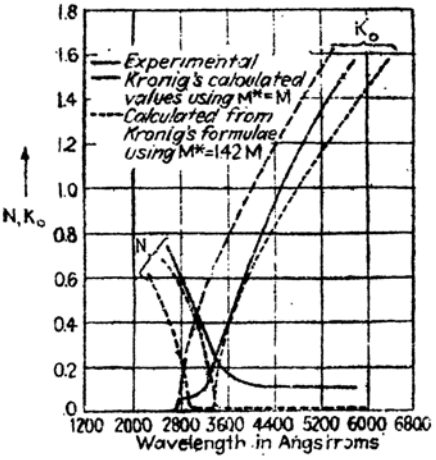

FIG. 6.—The quantities n, k, and nk for potassium. In this case the simple theory and experiment agree only if $m^* = 1.42m$ (see text). (*After Ives and Briggs.*)

The theoretical values of m/m^* are appreciably different from unity for lithium and potassium. Hence, we not only should expect the absorption coefficient to be greater for these metals but should also expect the frequency at which the dielectric constants become zero to be displaced relative to the value for perfectly free electrons. There do not seem to be available measurements on n and k for lithium; however, Ives and Briggs[1] have made very accurate observations on potassium. Figure 6 shows the observed values of n and k, which are compared with the theoretical curves obtained by use of $m^* = m$ and $m^* = 1.42m$. The second set of curves agrees with the experimental values much more closely than the first. Unfortunately, the corresponding value of m/m^* is less than unity rather than greater than unity, a fact suggesting that Gorin's estimate of m^* is not very accurate. As in the case of sodium, the observed value of nk is much larger than the theoretical one, although it is not possible to say whether or not the increase is due to internal absorption.

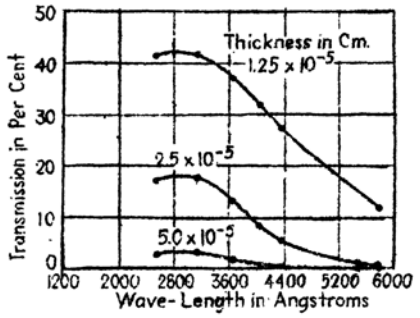

FIG. 7.—The transmission of several layers of cesium. The fall in transmission below 2800A presumably implies nonvanishing interband transition probabilities. (*After Ives and Briggs.*)

We should mention in passing that Ives and Briggs[2] have also examined the optical properties of cesium and rubidium. Transmission

[1] H. E. IVES and H. B. BRIGGS, *Jour. Optical Soc. Am.*, **26**, 238 (1936).

[2] H. E. IVES and H. B. BRIGGS, *Jour. Optical Soc. Am.*, **27**, 395 (1937).

curves obtained by these workers for three different layers of cesium are shown in Fig. 7. The rise in transmission on the long wave-length side of the figure undoubtedly is related to the change in reflectivity; however, the fall on the short wave-length side is presumably related to interband absorption.

b. Copper, Silver, and Gold.—The extent to which the optical properties of a metal specimen are sensitive to its previous history is shown by

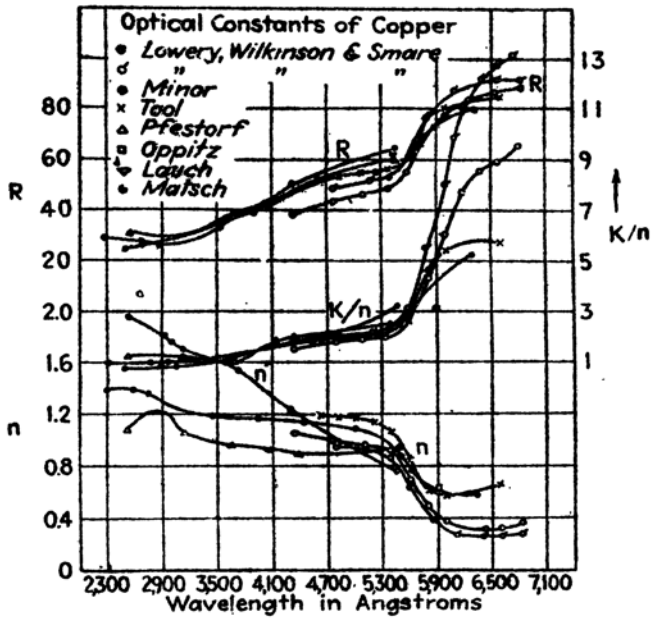

FIG. 8.—The quantities n, k/n, and R in per cent for copper as determined by various workers. (*After Nathanson.*)

the curves of Fig. 8, which contains a compilation of values of n and k/n for copper measured by several observers.[1] The shapes of the measured curves are the same, but the absolute values vary considerably from case to case. That the differences between the results for different cases are related to the treatment the surfaces of the specimens have received seems to be established beyond doubt. Lowery, Wilkinson, and Smare[2] have shown in the case of copper, for example, that k is increased and n is decreased when the metal surface is polished mechanically. Since nk increases during the polishing, it follows that the resistivity of the layer in which the light is reflected is increased. This effect can

[1] Taken from the review by J. B. Nathanson, *Jour. Optical Soc. Am.*, **28**, 300 (1938).

[2] H. LOWERY, H. WILKINSON, and D. L. SMARE, *Phil. Mag.*, **22**, 769 (1936).

be understood if the surface layer is made less perfectly crystalline as a result of polishing, for then the electronic mean free path is decreased. It is generally postulated,[1] at present, that the polished surface possesses a polycrystalline layer.

Typical nk curves for copper, silver, and gold are shown[2] in Fig. 9. The product nk is about ten times larger for these metals than for the alkalies, as measured by Ives and Briggs, a fact showing that the absorption is much larger in the former than in the latter. The peaks that occur near 2500Å and 4500Å in the case of copper are observed in almost all specimens, whereas the large rise that appears on the long wave-length side of 5700Å is very sensitive to surface treatment. For this reason, it is supposed that short wave-length peaks are related to volume absorp-

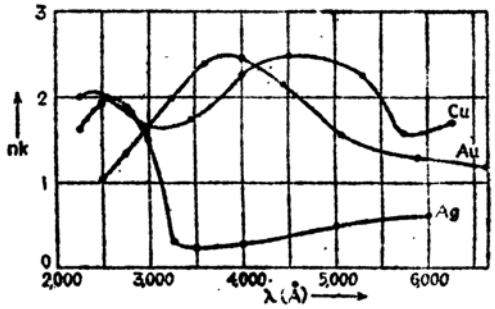

FIG. 9.—Typical nk curves for copper, silver, and gold (see text). (*After Minor and Meier.*)

tion which would occur in an ideal specimen, whereas the peak in the red is associated with the ordinary resistivity. Mott and Jones[3] suggest that the peak near 4500Å is due to transitions from the filled d band to the vacant s-p levels and that the peak at 2500Å is due to transitions from the occupied s-p levels to a higher valence-electron band. This interpretation, rather than the inverse one, is supported by the following two facts: (1) Silver, which has s-p bands similar to those of copper but which has different d bands, also has a peak at 2500Å. (2) The peak at 4500Å shifts toward the blue as zinc is added to copper, and the s-p band is filled higher.[4] Since gold and silver have similar valence-electron structures, it might also be expected that gold would have a peak at 2500Å if the preceding interpretation is correct; however, this peak apparently does not occur.

[1] See, for example, L. H. Germer, *Phys. Rev.*, **50**, 659 (1936).

[2] R. S. MINOR, *Ann. Physik*, **10**, 581 (1903); W. MEIER, *Ann. Physik*, **31**, 1017 (1910).

[3] N. F. MOTT and H. JONES, *The Theory of the Properties of Metals and Alloys* (Oxford University Press, New York, 1936).

[4] H. LOWERY, H. WILKINSON, and D. L. SMARE, *Proc. Phys. Soc.*, **49**, 345 (1937).

It seems natural to suppose that the large peak that is observed near 3700A in gold has the same origin as the peak in the visible region for copper, for the atomic $d^{10}s$ and d^9s^2 configurations lie very close together in both cases. In any event, the presence of these peaks accounts for the characteristic colors of these metals, whereas the absence of one in silver explains the normal metallic color of this metal.

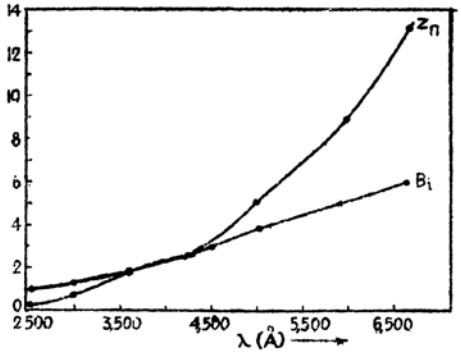

FIG. 10.—*nk* curves for zinc and bismuth. (*After Minor and Meier.*)

Kronig has applied the free-electron theory of Sec. 147 to Freedericksz's infrared optical measurements on copper, silver, and gold. The agreement was discussed under 3, part *b*, Sec. 147.

c. Divalent Metals.—Since the divalent metals have nearly filled overlapping bands the absorption regions that correspond to transitions between the bands of these metals should lie nearer the red end of the spectrum than the corresponding absorption regions in the monovalent metals. The *nk* curve[1] for zinc, which is shown in Fig. 10, seems to show that these regions actually extend into the infrared. This conclusion is not entirely safe, however, for it is also possible that the resistivity of the specimen of zinc on which the measurements of Fig 10 were made is high.

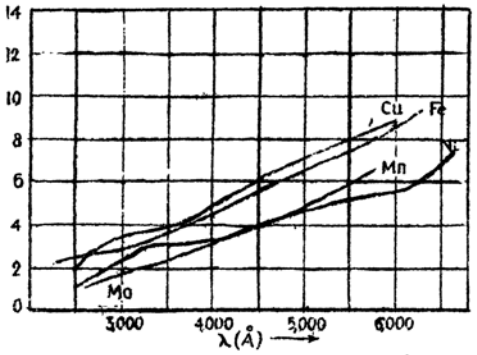

FIG. 11.—*nk* curves for several transition metals. (*After Minor and Meier.*)

d. Other Simple Metals.—Among the metals of higher valence with nearly filled bands, such as bismuth, antimony, white tin, and so forth, there apparently are available measurements only for bismuth. The *nk* curve for this metal, which is shown in Fig. 10, has a large rise in the

[1] See MINOR, *op. cit.*; MEIER, *op. cit.*

red, a fact suggesting that there is a peak in the infrared, as in the case of zinc.

It should be added that reflectivity measurements[1] indicate that aluminum is highly reflecting farther in the ultraviolet than most other metals. A reasonable explanation of this fact is given by the $n(\epsilon)$ curve for aluminum shown in Fig. 16, Chap. XIII, which indicates that all the valence electrons of aluminum are very nearly free. If we assume that they are free, the transition frequency ν' given by Eq. (33), Sec. 147, is near 800Å. Even if only one were free, however, the reflecting region would extend to about 1400Å.

e. Transition Metals. The *nk* curves for a number of transition metals are shown in Fig. 11. All these metals absorb strongly in the visible and near infrared, as might be expected from the fact that the unfilled *s-p* and *d* bands overlap.

150. Ionic Crystals.—The structure of the ultraviolet absorption bands of the alkali halides, which have been measured semiquantitatively by Hilsch and Pohl[2] and Schneider and O'Bryan,[3] are shown in Fig. 2, Sec. 95. At low temperatures, the regions of absorption consist of a number of narrow bands, each of which may be related to a transition between the lowest state and the state of wave-number zero in one of the excitation bands associated with the excited states of the halogen ion. According to the results of part *b*, Sec. 148, the absorption bands would consist of sharp lines if the transitions were purely electronic. As we have pointed out in Sec. 45, the observed width arises from the fact that lattice vibrations are stimulated during electron excitation.

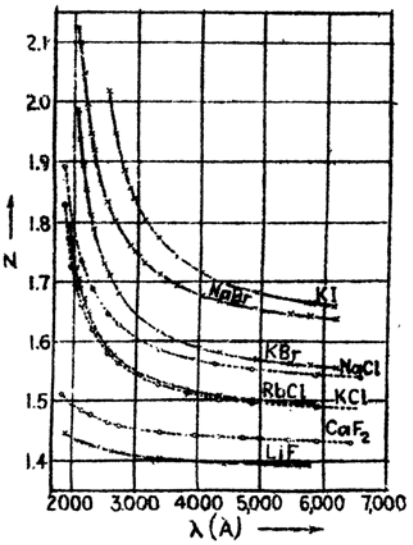

FIG. 12.—The refractive indices of a number of alkali halide crystals. (*After Gyulai.*)

The refractive indices of some of the alkali halides in the transmitting visible and ultraviolet regions of the spectrum as determined by Gyulai[4] are shown in Fig. 12. It may be observed that these curves exhibit the

[1] See, for example, the compilation of data in Landolt-Bornstein.

[2] R. HILSCH and R. W. POHL, *Z. Physik*, **44**, 421 (1927); **48**, 384 (1928); **64**, 606 (1930).

[3] E. G. SCHNEIDER and H. M. O'BRYAN, *Phys. Rev.*, **51**, 293 (1937).

[4] Z. GYULAI, *Z. Physik*, **46**, 80 (1928).

sharp rises which are to be expected on the long wave-length side of an absorption maximum.

Mayer[1] has attempted to correlate the measured absorption spectra and refractive indices of sodium chloride, potassium chloride, and potassium iodide by means of the theoretical results of Secs. 147 and 148. We have seen there that the atomic conductivity σ_a is related to the line strengths by the equation

$$\sigma_a(\nu) = \frac{e^2}{4m}\sum_l f_l \delta(\nu_l - \nu) \tag{1}$$

whereas the atomic polarizability in transparent regions is

$$\alpha_a = \frac{e^2}{4\pi^2 m}\sum_l \frac{f_l}{\nu_l^2 - \nu^2}. \tag{2}$$

The second quantity may be expressed in terms of the first by means of the equation

$$\alpha_a = \frac{1}{\pi^2}\int_0^\infty \frac{\sigma_a(\nu')}{\nu'^2 - \nu^2} d\nu', \tag{3}$$

which allows us to compute α_a from measured values of the absorption. The actual relationship between the index of refraction of a system of atoms and α_a is complicated by the local field correction. We have seen in Sec. 147 that in a transparent region

$$n^2(\nu) - 1 = \frac{4\pi}{3}\alpha(\nu) = \frac{4\pi n_0}{3}\frac{\alpha_a(\nu)}{1 - \frac{4\pi}{3}n_0\alpha_a} \tag{4}$$

if the Lorentz local field relations are employed [*cf.* Eq. (25)]. As we approach a single absorption frequency ν_0, α_a becomes

$$\alpha_a \sim \frac{e^2}{4\pi^2 m}\frac{f_0}{\nu_0^2 - \nu^2}$$

so that $\alpha(\nu)$ becomes

$$\alpha(\nu) \cong \frac{n_0 e^2}{4\pi^2 m}\frac{f_0}{\left(\nu_0^2 - \frac{e^2 n_0}{\pi m}f_0\right) - \nu^2}. \tag{5}$$

Hence, the effective absorption peak in the composite system occurs at

$$\nu_0' = \left(\nu_0^2 - \frac{e^2 n_0}{\pi m}f_0\right)^{\frac{1}{2}}. \tag{6}$$

[1] J. MAYER, *Jour. Chem. Phys.*, **1**, 270 (1933).

This displacement is not negligible in an ordinary solid, for $\sqrt{e^2n_0/\pi m}$ may be as large as 10^{15} sec^{-1} in an ordinary crystal. Since the measured absorption peaks occur at these displaced positions, it is not allowable to compute α_n from (3) by assuming that σ_n is proportional to the observed absorption. Instead, Mayer assumed that

$$\alpha = \frac{1}{\pi^2}\int_0^\infty \frac{\sigma(\nu')}{\nu'^2 - \nu^2}d\nu' \tag{7}$$

where $\sigma(\nu')$ is proportional to the observed absorption coefficient. Since only the relative absorption curves $\eta(\nu)$ are measured, we may place this equation in the form

$$n^2(\nu) - 1 = C\int_0^\infty \frac{\eta(\nu')}{\nu'^2 - \nu^2}d\nu' \tag{8}$$

where C is a constant that is determined by comparing the observed and calculated values of n at one frequency. Mayer fitted the observed Schumann-region $\eta(\nu)$ curves analytically with a system of parabolic segments and one narrow rectangular peak. The height of this peak h was taken as an adjustable parameter which was determined along with C by fitting observed and calculated values of n. The resulting $\eta(\nu')$ functions were then used to integrate Eq. (8) analytically. In the final determination of C and h, a small correction to the observed dispersion was made for the contribution arising from the absorption peaks of the alkali ions in the soft X-ray region. The two observed values of $n(\nu)$ used to fix these parameters were obtained from measurements in the visible and in the far ultraviolet regions, respectively. Table LXXXVII gives a comparison of the observed and calculated values of $(n^2 - 1)$ at an intermediate frequency.

TABLE LXXXVII

	NaCl	KCl	KI
$(n^2 - 1)$(obs.)	1.720 (2312 Å)	1.245 (2312 Å)	1.914 (3130 Å)
$(n^2 - 1)$(calc.)	1.708	1.258	1.910
f	3.25	3.24	4.00

If we assume that these Schumann-region bands are associated with the electrons of the halogen ions, we may obtain the total optical strength f per ion from the equation

$$f = \frac{4m}{n_0e^2}\int C\eta(\nu')d\nu' \tag{9}$$

where n_0 is the number of ions per cubic centimeter and $C\eta(\nu)$ is the final curve obtained by fitting (8). This equation is a consequence of Eqs. (5), (7), and (8). Calculated values of f are given in Table LXXXVII. It is interesting to note that the values for NaCl and KCl are closely alike, indicating that the optical strengths of the halogen ions are nearly the same in different compounds.

Mayer has used the functions $C\eta(\nu)$, determined by the preceding method, to evaluate the constants that appear in London's and Margenau's expressions for the van der Waals interaction of halogen ions. As we have mentioned in Sec. 12, this procedure leads to larger values of the interaction energy than are obtained by treating the halogens as though they had the same properties as neighboring rare gas atoms.

The fact that the optical strength of the halogen ions seems to be constant may be compared with the principle of additivity of refractivities, which has been evolved[1] from a study of the experimental refractive indices of ionic crystals. The molar refractivity of a crystal is defined by the equation

$$R = \frac{n^2 - 1}{n^2 + 2} V_M$$

where n is the refractive index and V_M is the molecular volume. It is evident from Eq. (26), Sec. 147, that R is a universal constant times the polarizability per molecule when the Lorentz equation for the local field is valid. Values of R, corresponding to the extrapolation of n to infinite wave length, are usually designated by R_∞. It is found experimentally that the values of R_∞ for a set of four simple ionic crystals AX, AY, BX, BY satisfy closely the additivity relations

$$R_{\infty,AX} - R_{\infty,AY} = R_{\infty,BX} - R_{\infty,BY},$$
$$R_{\infty,AX} - R_{\infty,BX} = R_{\infty,AY} - R_{\infty,BY}.$$

For example, the refractivities of several alkali halides satisfy the relations

$$\begin{aligned} R_{NaCl} - R_{NaBr} &= 3.13, \\ R_{RbCl} - R_{RbBr} &= 3.23, \\ R_{CsCl} - R_{CsBr} &= 3.21. \end{aligned} \tag{10}$$

This result suggests that we may speak with some significance of the refractivity of individual ions in the simpler ionic crystals. Using Eq. (6), Sec. 148, we obtain

$$R_\infty = \frac{N_1 e^2}{3\pi m} \sum_i \frac{f_i}{\nu_i^2}$$

[1] K. FAJANS and G. JOOS, *Z. Physik*, **23**, 1 (1923).

hence, if the absorption frequencies ν_i^2 lie sufficiently close to one another,

$$R_\infty = \frac{N_A e^2}{3\pi m \overline{\nu^2}} f \tag{11}$$

where f is the total optical strength per ion and $\overline{\nu^2}$ is the mean value of the $1/\nu_i^2$. Since the position of the Schumann-region absorption bands in those halides having the same halogen ion are nearly the same, it follows that the additivity of the refractivities implies that the f factors for separate ions are additive.

By choosing the value 0.50 for the refractivity of the sodium ion, for reasons which we shall not discuss here, Fajans and Joos[1] have obtained the ion refractivities given in Table LXXXVIII from observed differences

TABLE LXXXVIII.—THE REFRACTIVITIES OF IONS (AFTER FAJANS AND JOOS)

Ion	R	Ion	R	Ion	R
F^-	2.5	Li^+	0.2	Be^{++}	0.1
Cl^-	9.00	Na^+	0.5	Mg^{++}	0.3
Br^-	12.67	K^+	2.23	Ca^{++}	1.3
I^-	19.24	Cs	6.24	Ba^{++}	4.3

of the type (10). When the value 9.00 for Cl^- is substituted in Eq. (11) along with the value $\bar{\nu} = 2.4 \cdot 10^{15}$ sec $^{-1}$ for the approximate center of gravity of the absorption bands of the alkali chlorides, it leads to

$$f_{Cl} = 3.4,$$

which is to be compared with the value 3.25 derived by Mayer (*cf.* Table LXXXVII). The corresponding values for I^- agree to about the same degree of accuracy.

151. Semi-conductors.—It was pointed out in Sec. 6 that there are two types of semi-conductor, namely, monatomic crystals such as silicon and selenium that contain impurities, and ionic crystals that either are impure or contain a stoichiometric excess of one constituent. Most prominent among the semi-conductors of the second kind are alkali halides with F centers, phosphorescent zinc sulfide, and similar alkaline-earth oxides and sulfides. The impurity or stoichiometric-excess atoms in all these semi-conductors have their own characteristic absorption bands that lie in the visible or near ultraviolet part of the spectrum. In the case of natural semi-conductors, such as silicon and the natural sulfides, which may have as much as 1 per cent of impurity, this absorption band may show up as an appreciable peak in the nk curve determined from reflection, even though it may overlap the fundamental absorption

[1] *Ibid.*

band of the substance. For example, Fig. 13 shows the nk curves for silicon and natural stibnite,[1] MoS_2. The peaks that occur in the near ultraviolet are probably due to the impurities whose thermally or optically freed electrons make these substances semi-conductors. In most artificial semi-conductors, on the other hand, the number of impurity atoms is comparatively low so that they do not give rise to nk peaks of this magnitude. The absorption may be detected, however, by transmission measurements if the bands do not overlap the fundamental region.

The theory of dispersion has been applied to the F-center bands of the alkali halides by Smakula,[2] in order to determine the density of centers. It may be recalled that these bands probably arise from the excitation of electrons in vacant halogen sites in crystals containing an excess of alkali metal atoms, the absorption transition being analogous to the $1s$-$2p$ transition in atomic hydrogen (*cf.* Secs. 110 and 111). Since the electrons are coupled to the lattice, the observed absorption bands are much wider than the lines of free atoms at room temperature. The extinction coefficient of the bulk material is zero in the vicinity of the F-center bands, since these bands usually are far from the fundamental absorption region; moreover, the refractive index of the pure salt is usually constant in the vicinity of the F bands. We shall designate this constant by n'. For these reasons, Smakula assumed that the polarizability of the bulk material is given simply by the quantity

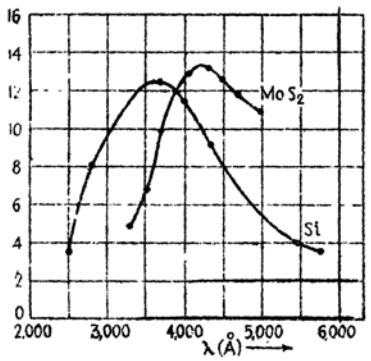

FIG. 13.—nk curves for silicon and natural MoS_2. (*After Meier.*)

$$\frac{3}{4\pi}\frac{n'^2-1}{n'^2+2}. \tag{1}$$

In addition, he assumed that the complex polarizability of the electrons in the F centers may be represented by the corresponding polarizability function for a single absorption line, namely,

$$\frac{n_0e^2}{4\pi^2m}\frac{f}{\nu_F^2-\nu^2+i\nu_d'\nu}. \tag{2}$$

Here, n_0 is the density of F centers, ν_F is the frequency at the center of the absorption band, ν_d' is the damping frequency which is of the order of magnitude of 10^{14} sec^{-1}, and f is the oscillator strength of the transi-

[1] MINOR, *op. cit.*; MEIER, *op. cit.*

[2] A. SMAKULA, *Z. Physik*, **59**, 603 (1930).

tion. Since only one absorption peak is observed, we may expect that practically all the optical strength of the stoichiometric-excess electrons is centered in this band and that f should be near to unity. Using Eq. (28), Sec. 147, for the relation between the complex index of refraction and the polarizability, we obtain

$$\frac{(n - ik)^2 - 1}{(n - ik)^2 + 2} = \frac{n'^2 - 1}{n'^2 + 2} + \frac{n_0 f e^2}{3\pi m} \frac{1}{(\nu_F^2 - \nu^2) + i\nu_d' \nu}. \tag{3}$$

If we now set

$$n = n' + \Delta n \qquad \text{and} \qquad \nu = \nu_F + \Delta\nu$$

where Δn is a small quantity, we obtain for the real and imaginary parts of (3)

$$\Delta n = \frac{n_0 f e^2}{18\pi m} \frac{(n'^2 + 2)^2}{n'} \frac{\Delta\nu(2\nu_F + \Delta\nu)}{\Delta\nu^2(2\nu_F + \Delta\nu)^2 + \nu'^2_d(\nu_F + \Delta\nu)^2}, \tag{3a}$$

$$k = \frac{n_0 f e^2}{18\pi m} \frac{(n'^2 + 2)^2}{n'} \frac{\nu_d'(\nu_F + \Delta\nu)}{\Delta\nu^2(2\nu_F + \Delta\nu)^2 + \nu'^2_d(\nu_F + \Delta\nu)^2} \tag{3b}$$

The observed k curves, which are measured directly by the extinction of transmitted radiation, may be fitted closely by a function of the form (3b), as is shown in Fig. 14.

ν_d' may be eliminated from (3b) by expressing this quantity in terms of the value $\Delta\nu_{\frac{1}{2}}$ of $\Delta\nu$ for which k is half its maximum value k_m. When the resulting equation is solved for $n_0 f$, it is found that

$$n_0 f = \frac{9k_m n' m \nu_F}{\pi(n' + 2)^2 e^2} \frac{\Delta\nu_{\frac{1}{2}}(2\nu_F + \Delta\nu_{\frac{1}{2}})}{(\nu_F + \Delta\nu_{\frac{1}{2}})^2}. \tag{4}$$

In making practical use of this equation, it is convenient to express the frequencies in electron volts and to express k in terms of the constant $\alpha(\nu)$ appearing in the equation

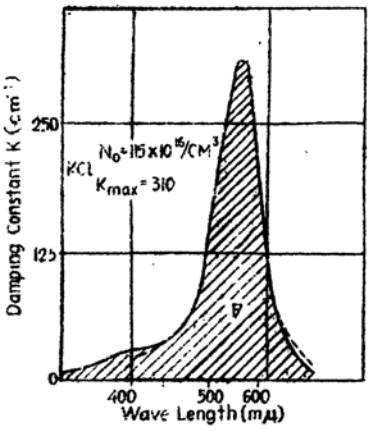

FIG. 14.—A comparison of the observed k curve for the F centers of KCl and the curve of the form (3b) that fits it most closely. (*After Smakula.*)

$$\frac{I}{I_0} = e^{-\alpha(\nu)d} \tag{5}$$

which expresses the decrease in intensity of light after it passes through a crystal of thickness d. The relation between k and α is

$$k = \frac{\alpha\lambda}{4\pi}. \tag{6}$$

When this is done, Eq. (4) becomes

$$n_0 f = 1.31 \cdot 10^{17} \frac{n'}{(n'^2 + 2)^2} \alpha_m \Delta\nu_{\frac{1}{2}} \frac{2\nu_F + \Delta\nu_{\frac{1}{2}}}{\nu_F + \Delta\nu_{\frac{1}{2}}} \tag{7}$$

where α_m, the value of α at the center of the absorption band, is expressed in inverse centimeters and the frequencies are expressed in electron volts.

If ν_F is much greater than $\nu_{\frac{1}{2}}$, as at low temperatures, we may simplify this equation to

$$n_0 f = 1.31 \cdot 10^{17} \frac{n'}{(n'^2 + 2)^2} \alpha_m W \tag{8}$$

where W is the width of the k curve at half maximum in electron volts.

Equation (7) has been used by Hilsch and Pohl[1] and their collaborators to determine the value of $n_0 f$ for F centers and for impurity

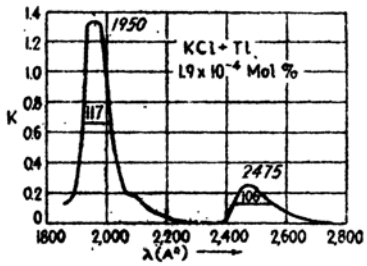

FIG. 15.—The impurity-induced k curve of a potassium chloride crystal containing thallium. (*After Koch.*)

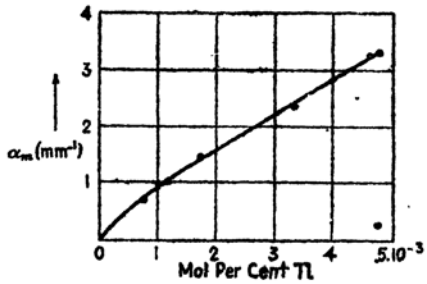

FIG. 16.—The curve obtained by plotting the optically determined values of α_m in crystals of KCl containing thallium as a function of the chemically determined number of impurity atoms.

atoms of other kinds. It has also been found possible to measure n_0 by direct chemical means in several of these crystals so that values of f may be determined by combining the results. Thus, in the case of F centers in KCl, Kleinschrod[2] has found that f is 0.81. The fact that this is not exactly unity indicates that the F-center electrons lose some optical strength because of interaction with the closed shells of the atoms present.

Koch[3] has combined optical and chemical measurements in a similar way to determine the f factors for the absorption bands of impurity thallium atoms in alkali halide crystals. It is found that small quantities of thallium halides may be dissolved in the alkali halides and that the resulting mixed crystals exhibit narrow absorption bands[4] in the ultra-

[1] See the survey by R. W. Pohl, *Physik. Z.*, **39**, 36 (1938).

[2] F. G. KLEINSCHROD, *Ann. Physik*, **27**, 97 (1936).

[3] W. KOCH, *Z. Physik*, **57**, 638 (1930).

[4] An interpretation of these peaks has been given by the writer, *Jour. Chem. Phys.*, **6**, 150 (1938).

violet below 3000 A. A typical absorption curve is shown in Fig. 15. In each case, there are two large peaks that seem to be closely related to the energy levels of free monovalent thallium ions. Figure 16 shows the α_m versus n_0 curve obtained by combining optical and chemical measurements. From the slope of these, Koch obtains $f \sim 0.1$ for the long wave-length band and $f \sim 0.6$ for the short wave-length band.

152. The Infrared Spectra of Ionic Crystals.—All polar compounds possess infrared absorption bands that are associated with the stimulation of oscillational motion of the atoms or ions. Although the interatomic forces in ionic crystals are comparable with electronic forces in atoms, the vibrational spectra lie in the infrared because ionic masses are of the order of magnitude 10^4 times larger than the electronic mass. This fact is made evident by the relation between the frequency ν and mass m of an oscillator having force constant κ, namely,

$$\nu = \frac{1}{2\pi}\sqrt{\frac{\kappa}{m}}. \tag{1}$$

In order to discuss the optical effects associated with the lattice vibrations, it is first necessary to obtain the expression for the dipole moment of the lattice as a function of ionic displacements. If we arbitrarily define the dipole moment as zero when all the ions are at their equilibrium positions $\mathbf{r}_\alpha(n)$, the dipole moment when the ions are at positions $\mathbf{R}_\alpha(n)$ relative to the equilibrium positions is

$$\mathbf{M} = \sum_{\alpha,n} e_\alpha \mathbf{R}_\alpha(n). \tag{2}$$

Here, α extends over the ions in the unit cell, n extends over the cells in the lattice, and e_α is the charge on the αth ion. The variables $\mathbf{R}_\alpha(n)$ may be expressed in terms of normal coordinates of the form

$$\mathbf{R}_\alpha(n) = \sum_{s=1}^{3n} \sum_{\mathfrak{d}} a_s(\mathfrak{d}) \frac{\xi_{\alpha,s}(\mathfrak{d})}{\sqrt{NM_\alpha}} e^{2\pi i \mathfrak{d}\cdot \mathbf{r}_\alpha(n)} \tag{3}$$

when the potential energy is a quadratic function of displacements (*cf.* Sec. 22). Here, $a_s(\mathfrak{d})$ is the amplitude of the normal mode of wave number $\mathfrak{d}$ in which the αth atom is polarized in the direction $\xi_{\alpha,s}(\mathfrak{d})$, and N is the total number of unit cells in the lattice. We shall employ the reduced-zone scheme so that $\mathfrak{d}$ extends over a single zone and s takes values from 1 to $3n$, where n is the number of atoms in the unit cell. When Eq. (3) is substituted in (2), it is found that

$$\mathbf{M} = \sqrt{N} \sum_\alpha e_\alpha \sum_s a_s(\mathfrak{d}) \xi_{\alpha,s}(\mathfrak{d}) \delta_{\mathfrak{d},0}. \tag{4}$$

Thus, only the modes of vibration associated with zero wave number in the reduced-zone scheme contribute to the dipole moment. The reason for this is that the contributions to **M** from different cells cancel one another in the other cases, since they have different phases.

Let us consider a cubic crystal such as sodium chloride that has two oppositely charged ions per unit cell. In this case, three of the normal modes associated with zero wave number are purely translational and, for this reason, do not contribute to the dipole moment. Hence, the dipole moment is determined by the remaining three modes, which correspond to the maximum frequency ν_m and represent oscillations in which the positive and negative ions move in opposite directions. Thus, the crystal is equivalent to a system of $3N$ diatomic oscillators of frequency ν_M. Since the polarizability of an oscillator is the same in quantum and in classical mechanics, it follows from the results of Sec. 147 that

$$\alpha_e = \frac{3n_0e_i^2}{4\pi^2\mu} \frac{1}{(\nu_m^2 - \nu^2) + i\gamma\nu} \tag{5}$$

where n_0 is the number of molecules per unit volume, μ is the reduced mass of the ions, e_i is the ionic charge, and γ is the damping frequency. As in the case considered in Sec. 147, this complex polarizability implies an absorption line of half-width γ at ν_m. Since an atomic mass rather than the electronic mass appears in the denominator of this equation, the polarizability arising from ionic oscillators is of the order of magnitude 10^{-4} times as large as the polarizability that would arise from an equal density of electronic oscillators of comparable frequency. For this reason, the index of refraction in the transparent visible and ultraviolet regions of most ionic crystals is determined almost entirely by the electronic absorption bands in the far ultraviolet.

In an ideal harmonic approximation, the damping frequency γ would be determined entirely by radiation damping and would have the value

$$\gamma = \frac{4\pi\nu_m^2}{3} \frac{e^2}{\mu c^3}$$

which is of the order of magnitude of 1 sec^{-1}, or about 10^{-14} ev for ordinary ionic crystals. The observed widths actually are far greater than this. For example, Fig. 17 shows observed[1] transmission curves for several specimens of sodium chloride at room temperature. It may be seen that the width of the peak is of the order of $5 \cdot 10^{12}$ sec^{-1}, or about 0.01 ev. It should also be observed that the transmission curves show more structure than should be expected from a single absorption

[1] R. B. BARNES, R. R. BRATTAIN, and F. SEITZ, *Phys. Rev.*, **48**, 582 (1935).

line. Even more complicated structure has been observed under higher dispersion in magnesium oxide, which has the same lattice structure as sodium chloride.

A qualitative interpretation of this large damping and the accompanying structure was first given by Born and Blackman[1] on the basis of classical mechanics. They related the structure to cubic terms in the expression for the potential energy of the ions that couple the optically active modes of vibration to other modes. Their work was later extended

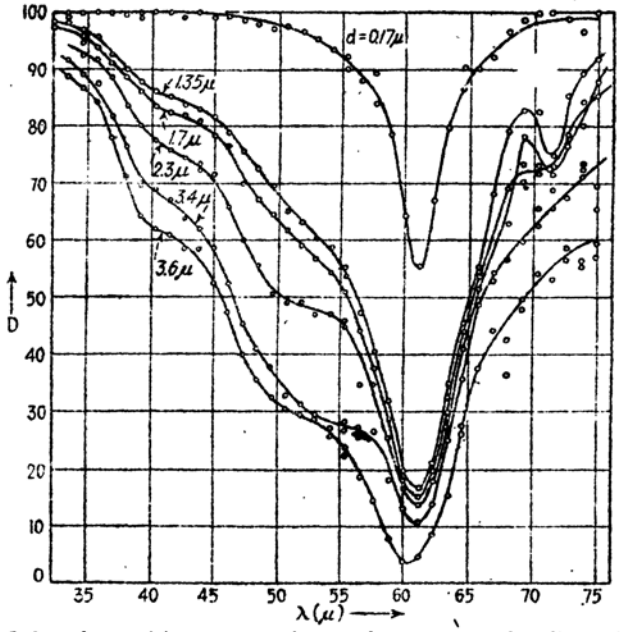

FIG. 17.—Infrared transition curves of several specimens of sodium chloride. The abscissa is the wave length in microns. The numbers accompanying the curves are the crystal thicknesses. (*After Barnes and Brattain.*)

by the use of quantum mechanics.[2] Although this work provides the machinery for a more complete theoretical investigation of the topic, a thorough experimental treatment of the transmission properties of a simple crystal over a range of temperatures is lacking at present. For this reason, it is not possible to say that the structure may be completely interpreted in terms of anharmonic potential terms. We shall present briefly the principles employed in this theory.

[1] M. BORN and M. BLACKMAN, *Z. Physik*, **82**, 551 (1933); M. BLACKMAN, *Z. Physik*, **86**, 421 (1933).

[2] BARNES, BRATTAIN, and SEITZ, *op. cit.*

In the quadratic approximation, the vibrational wave functions of the crystal have the form (*cf.* Sec. 118)

$$\Lambda_n(\cdots, \alpha_t(\mathfrak{d}), \cdots) = \prod_{t,\sigma} \lambda_{n_t(\sigma)}(\alpha_t(\mathfrak{d})) \tag{6}$$

where the $\lambda_{n_t(\sigma)}$ are harmonic oscillator wave functions and the $n_t(\mathfrak{d})$ are integers. The energy of this state has the same form as for an assembly of oscillators, namely,

$$E_n = \sum_{t,\sigma} \left(n_t(\mathfrak{d}) + \frac{1}{2}\right) h\nu_t(\mathfrak{d}). \tag{7}$$

During absorption, the system changes its state from Λ_n to the state Λ_{n+1} in which all quantum numbers are the same except for that of one of the optically active modes, which increases by unity. The energy difference between Λ_n and Λ_{n+1} is clearly $h\nu_m$.

The cubic perturbing potential has the form

$$V_c = \sum_{i,j,k} c_{ijk}\alpha_{t(i)}(\mathfrak{d}(i))\alpha_{t(j)}(\mathfrak{d}(j))\alpha_{t(k)}(\mathfrak{d}(k)) \tag{8}$$

where the c_{ijk} are constants. The limitations on the combinations of α that can occur in this series, which may be obtained from group theory, will not be discussed here.

In the perturbed scheme, the new wave functions Λ_n' have the form

$$\Lambda_n' = \Lambda_n + \sum_{n'} a_{n,n'}\Lambda_{n'} \tag{9}$$

where the $a_{n,n'}$ are given by the equations

$$a_{n,n'} = \frac{\int \Lambda_{n'} V_c \Lambda_n d\tau}{E_n - E_{n'}}, \tag{10}$$

in which the integration extends over the coordinate space of the variables $\alpha_t(\mathfrak{d})$. Since V_c is the sum of cubic terms and the $\Lambda_{n'}$ are products of one-dimensional oscillator functions, it follows that each state Λ_n is now coupled with states in which three quantum numbers differ from those of Λ_n by one unit. Thus, if the system is in the state Λ_n', it may make an optical transition not only to Λ_{n+1}' but to any other state in which a wave function Λ_{n+1} appears in the sum in Eq. (9). For this reason, the optical strength of the absorption process is distributed throughout many states, and the absorption band is broader than in the quadratic approximation. We may expect the width of this absorption band to increase with increasing temperature because the amplitudes $\alpha_t(\mathfrak{d})$ in (8) increase with increasing temperature. This effect has been observed qualitatively.

153. Special Topics.—There are a number of interesting topics concerning the optical properties of solids that limitations on space do not permit us to discuss in detail. For the benefit of readers who are interested, we shall outline several of these topics briefly and give the principal references.

a. The Photoelectric Effect in Metals.—In the interior of a metal, the only allowed optical transitions take place between bands in accordance with the selection rules discussed in the previous section, namely, that the transition must be vertical in the reduced-zone scheme. Tamm and Schubin[1] have pointed out that additional absorption may take place near the surface since the wave functions are not periodic in this region and the selection rules employed in Sec. 149 are not valid. Although the second type of absorption is relatively unimportant in a discussion of the optical properties of metals, since only about one quantum in five hundred is absorbed in this way in passing through the surface, it is extremely important for the photoelectric effect, for electrons that are excited near the surface are in an excellent position to get out of the metal. The first detailed treatment of the surface photoelectric effect was carried through by Mitchell[2] and has been extended by several workers.[3] We shall discuss a treatment given by Hill that is closely patterned after Mitchell's work and has been applied to the case of the alkali metals.

Hill assumed that the electronic potential is a constant $-W_a$ inside the metal and that the electrons are restrained from pouring out by a barrier at the surface. In the detailed computations, he considered two types of barrier, namely, a square barrier for which the potential jumps abruptly from $-W_a$ to zero, and an image-force barrier of the form

$$V(x) = \begin{cases} -\dfrac{e^2}{4x + e^2/W_a} & x \geq 0 \\ -W_a & x \leq 0 \end{cases}$$

(see Fig. 9, Chap. IV). Since the internal optical absorption is zero in this model, because the electrons are free, it can be used only for a discussion of the surface effect. Experimental work on the alkali metals seems to show that, even when the spectral peak for the volume photoelectric effect is appreciable, it lies so much farther in the ultraviolet than the peak for the surface effect that the two do not overlap. For this reason, the two effects can be discussed separately in these simple metals. In addition, we know from the work of preceding chapters that the properties of alkali metals usually conform closely to those of the

[1] I. TAMM and S. SCHUBIN, *Z. Physik*, **68**, 97 (1931).

[2] K. MITCHELL, *Proc. Roy. Soc.*, **146**, 442 (1934); **153**, 513 (1936); *Proc. Cambridge Phil. Soc.*, **31**, 416 (1935).

[3] R. D. MYERS, *Phys. Rev.*, **49**, 938 (1936); A. G. HILL, *Phys. Rev.*, **53**, 184 (1938).

simple free-electron model so that it should apply to them. Recent experimental work on the photoelectric effect in barium by Cashman and Bassoe[1] shows that the surface and volume peaks of this metal overlap. Thus, the two effects would have to be discussed simultaneously in this case; moreover, a more complicated model would have to be employed, for the electrons in divalent metals are not nearly free.

To begin with, Hill computed the energy distribution function of electrons that are emitted by light of a given frequency and compared the computed function with observed ones for the case of sodium. Although the two types of curve agree well at the high energy end, the agreement at low energies is poor, for the theoretical curves start out linearly whereas the observed curves start out nearly quadratically. The most reasonable explanation of these discrepancies is that the surface on which the measurements were made was sufficiently contaminated so that either the work function varied from point to point or the electronic transmission coefficient was different from the computed value. The way in which these quantities can affect emission was discussed in connection with thermionic emission at the end of Sec. 30.

In addition, Hill compared the observed and calculated spectral distribution functions, that is, the functions giving the dependence of the total current per unit light intensity on the frequency of the radiation. The observed curve possesses a peak that is much sharper than the peak of the theoretical curve, as may be seen from Fig. 18. A possible explanation of this discrepancy lies in the fact that the detailed optical properties of the metal were neglected in Hill's treatment. This possibility was first realized by Mitchell, but Schiff and Thomas[2] have furnished more direct evidence for its importance in a computation that is based on a semiclassical treatment of radiation. This topic has also been discussed, more recently, by Makinson.[3]

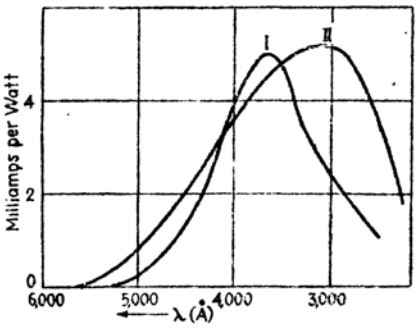

FIG. 18.—Comparison of the computed and observed spectral distribution curves for the photoelectric yield in sodium. I is the experimental curve and II is the theoretical curve. (*After Hill.*)

b. Breadth of Optical Absorption and Emission Bands.—If the atoms of an insulating crystal were held rigidly during a change in electronic

[1] R. J. CASHMAN and E. BASSOE, *Phys. Rev.*, **55**, 63 (1939).
[2] L. I. SCHIFF and L. H. THOMAS, *Phys. Rev.*, **47**, 860 (1935).
[3] R. E. B. MAKINSON, *Proc. Roy. Soc.*, **162**, 367 (1937).

state involving absorption and emission of radiation, the frequency distribution of absorbed or emitted light would have only the natural width (see Sec. 148, part *b*). The actual emission and absorption spectra of solids exhibit a broadening that increases with increasing temperature. The primary source of this breadth is the fact that the vibrational modes of the crystal also may be stimulated during an electronic transition. Since the amount of vibrational energy that may be involved has a finite range, the allowed optical emission or absorption frequencies also extend over a finite range.

A rudimentary treatment of the theory of broadening has been given by Peierls;[1] the salient points of his work are as follows. The elastic constants and the equilibrium atomic positions are usually different for the normal and excited electronic states of an insulator. For this reason, the systems of vibrational wave functions for the normal and excited states are not identical. If the difference between the atomic potential energies for the normal and excited states is designated by $\Delta E(\xi_1, \cdots, \zeta_f)$ where $\xi_1, \ldots, \zeta_f$ are the configurational coordinates of the atoms, the vibrational wave functions χ_n' for the excited electronic state may be expressed in terms of the vibrational wave functions χ_m for the normal state by means of the perturbation equation

$$\chi_n' = \chi_n + \sum_m \chi_m \frac{\int \chi_m^* \Delta E \chi_n d\tau}{E_n - E_m}. \tag{1}$$

The indices n and m correspond to sets of vibrational quantum numbers. Now, if χ_m is the vibrational wave function of the system before the transition, the final state may be any state χ_n' for which the integral

$$\int \chi_m^* \chi_n' d\tau \tag{2}$$

does not vanish, if we assume that the electronic transition is allowed. The integration in (2) takes place over the configurational coordinates. According to (1), the integral (2) is equal to

$$\frac{\int \chi_m^* \Delta E \chi_n d\tau}{E_n - E_m}.$$

An analysis of this integral that is based on a power series expansion of ΔE shows that at low temperatures the absorption or emission bands should consist of a sharp strong line which has a companion band on its long wave-length side whose shape is simply related to the vibrational frequency spectrum. At high temperatures, the structure is more complicated.[2]

[1] R. PEIERLS, *Ann. Physik*, **13**, 905 (1932).

[2] A treatment of this problem for the case of metals has been given by T. Muto, *Sci. Papers Inst. Phys. Chem. Res.*, **27**, 179 (1935).

c. The Fluorescence of Crystals.—Many simple crystals fluoresce when illuminated with ultraviolet light or bombarded with electrons. Although a large number of these *phosphors* have been prepared for commercial purposes, only a very few have been investigated with sufficient thoroughness to make a discussion of the mechanism of luminescence feasible.[1] Three substances in the second class are the zinc sulfide phosphors, willemite, which is a form of zinc silicate, and the alkali halide thallium phosphors, which are alkali halide crystals containing a small amount of thallium halide. We shall discuss briefly the properties of the first of these, which is typical of the set.[2]

The zinc sulfide phosphors are prepared most simply by heating zinc sulfide alone or with a small amount of another heavy metal sulfide, such as the sulfides of copper, silver, and manganese. The pure phosphor fluoresces with a light-blue color under near-ultraviolet light, whereas the other materials have different colors that depend upon the impurity atoms. The quantum efficiency of this luminescence usually is nearly unity at room temperature. The materials usually are strongly phosphorescent; that is, some of the light is emitted after excitation ceases. The length of time required for emission of this stored light increases as the temperature is lowered.

It is found that these fluorescent zinc sulfide materials are photoconducting and that the spectral sensitivity curve for stimulating photoconductivity extends over essentially the same region as the corresponding curve for stimulation of luminescence. On the basis of facts of this kind and a knowledge of the behavior of impurity atoms in semi-conductors (*cf.* Secs. 110 to 112), it has been concluded that the stimulating ultraviolet light liberates electrons from neutral interstitial atoms of the impurity metal, or of zinc in the pure phosphor, and that light is emitted when the electron and interstitial ion recombine, the color of the emitted light depending upon the kind of interstitial atom that does the emitting.

Since the freed electron may be trapped before returning, the crystal is phosphorescent. The decay of phosphorescence is temperature-dependent, since the trapped electrons must be freed thermally. On the basis of a detailed examination of this decay, Johnson[3] has concluded that there are at least two types of trapping center.

The zinc sulfide phosphors may be stimulated to a lesser extent by ultraviolet light that lies in the fundamental absorption band of zinc

[1] See the reviews by F. Seitz, *Trans. Faraday Soc.*, **35**, 74 (1939); H. W. Leverenz and F. Seitz, *Jour. Applied Phys.*, **10**, 479 (1939).

[2] This picture was presented independently by A. Schleede, *Angew. Chem.*, **50**, 908 (1937), and by the writer, *Jour. Chem. Phys.*, **6**, 454 (1938).

[3] R. P. JOHNSON, *Jour. Opt. Soc. Am.*, **29**, 387 (1939).

sulfide or by bombardment with athode rays. Although the energy efficiency of this type of excitation is of the order of one-tenth the efficiency of near-ultraviolet excitation, it is about one thousand times higher than it would be if only the centers that are ionized by direct absorption were responsible for the light. If the absorption of energy in the fundamental absorption band produces excitons, as in the case of the alkali halides, we may conclude that a fraction of the excitons eventually give their energy to the interstitial atoms by a process analogous to a collision of the second kind. It is possible in zinc sulfide, however, that absorption in the fundamental region produces free electrons instead of excitons and that these excite the interstitial atoms by a collision of the first kind.

The wave length of the emitted radiation is always longer than that of the exciting radiation; the reason for this is probably that given in Sec. 108. In addition, the emission band consists of a broad band at room temperature. This band becomes narrower as the temperature is lowered[1] and usually consists of a single sharp line and several weak satellites at very low temperatures. The explanation of the sharpening undoubtedly is that given in part *b* of this section; however, the fine structure has not yet been completely interpreted, although it probably is also connected with the stimulation of the vibrational modes of the crystal.[2]

Willemite resembles the sulfide phosphors closely, for photoconductivity[3] accompanies luminescence in this case as well. The alkali halide phosphors, however, belong in a different category, for they are not photoconductors.[4] A fuller discussion of these materials may be found in the articles listed in footnote 2, page 672.

d. The Photolysis of Crystals.—Many crystals become colored or decompose when they are irradiated with light of suitable wave length. In this connection, we have already discussed the discoloration produced in alkali halides by X rays (*cf.* Sec. 111), which is due to the transfer of electrons from inner shells to vacant negative-ion sites.

The most important and useful photolytic process occurring in a simple crystal is that responsible for the latent photographic image in silver halide crystals. If silver chloride or silver bromide crystals are exposed for a short time to light lying in the visible or near ultraviolet region of the spectrum, a visually imperceptible change is produced in them; however, when the crystals are placed in certain reducing agents,

[1] J. T. RANDALL, *Nature* **142**, 113 (1938); *Trans. Faraday Soc.*, **35**, 2 (1939).
[2] F. SEITZ, *Trans. Faraday Soc.*, **35**, 1 (1939).
[3] R. HOFSTADTER, *Phys. Rev.*, **54**, 864 (1938).
[4] See *Jour. Chem. Phys.*, **6**, 150 (1938).

known as "developers," the irradiated parts of the crystal proceed to decompose with the production of free silver and the corresponding halogen. The same decomposition may be produced by continuous irradiation without development—a process known as the "print-out effect."

The credit for unraveling the fundamental processes in the darkening of the silver halides belongs to a large number of workers whose contributions extend over many years of intensive work.[1] After it had been definitely established that the decomposition products of the print-out effect are free silver and halogen gas, Fajans suggested that the fundamental action of the light is to transfer an electron from a halogen ion to a silver ion, producing free silver in accordance with the reaction

$$Ag^+ + Br^- \rightarrow Ag^+ + Br + \text{electron} \rightarrow Ag + Br. \qquad (3)$$

This hypothesis was supported by the observation of Toy and Harrison (*cf.* Sec. 135) that photoconductivity accompanies the absorption of light in the region of wave lengths in which the latent image is produced. After the development of the zone theory of solids, Webb employed this scheme to describe the freeing of electrons and their subsequent trapping in the lattice. Although this work went a long way toward explaining the initial steps in the darkening process, it left unexplained the manner in which the silver ions migrate to a given point in order to form a clump of free silver. The final steps were developed by Gurney and Mott[2] who were able to give a fairly complete description of the darkening process. Briefly, the picture is as follows:

1. After being freed, the photoelectron wanders about through the crystal and ultimately becomes trapped at a point near the surface. It is believed that the most likely trapping center is a speck of silver sulfide, the reason for this being that extensive chemical work has shown that the gelatin of photographic emulsions must contain a small amount of a sulfur compound if the latent image is to be produced. Presumably, a small amount of this substance is used in the production of silver sulfide. Gurney and Mott suggest that the work function of silver sulfide is enough larger than the work functions of the silver halides so that a small speck of the former substance should be a good trapping center.

2. The trapped electron attracts the silver ions in its vicinity, and these ions migrate toward it by the ordinary process of ionic conductivity. One of the silver ions reaches the trapped electron and is neutralized, producing an atom of silver. This is the essential point in Gurney and

[1] See the survey by J. H. Webb, *Jour. App. Phys.*, **11**, 18 (1940).

[2] R. W. GURNEY and N. F. MOTT, *Proc. Roy. Soc.*, **164**, 151 (1938).

Mott's picture and is supported by the fact that the silver halides have an appreciable ionic conductivity at room temperature (*cf.* Fig. 66, Chap. I). It is assumed that there are only one or two trapping positions in the small crystals that occur in ordinary photographic emulsions, so that practically all the free electrons produced in a given crystal go to the same point. Thus, one atom of free silver is formed at the trapping center for each photoelectron released. It is believed that small specks of silver formed in this way represent the latent image.

3. It should be added that the free halogen atoms produced during the formation of the latent image presumably diffuse out of the crystal. The probability that they will run into the latent image and interact with it is small.

4. Gurney and Mott suggest that in the early stages of the formation of the latent image the trapped electrons have an appreciable chance of evaporating and returning to the halogen atoms from which they were originally released, thereby reversing the process. As the amount of free silver grows, however, the work function of the trapping centers should approach the value of about 4 ev for metallic silver, making it more and more difficult for reversal to occur. According to the most reliable measurements it requires between five and ten quanta per grain to form a stable latent image under the most favorable conditions. This fact indicates that the work function of a clump of five or ten silver atoms is sufficiently large to prevent reversal at ordinary temperatures.

5. Extensive experimental investigation by Webb and others has shown that the efficiency for producing the latent image decreases with decreasing light intensity at very weak intensities.[1] This fact is an immediate consequence of the possibility of the reversal discussed under 4, for if the light intensity is sufficiently weak each silver atom may dissociate thermally before another is formed. The efficiency for producing the latent image does not continually increase with increasing light intensity, however, for it is found to fall at high intensities. Limited ionic conductivity presumably is responsible for this effect. Unless the charges of the trapped electrons are neutralized as fast as they are trapped, some of the electrons will be repelled from the trapping center and will recombine with the holes. In this connection, Webb[2] has shown that the efficiency for production of the latent image attains a low value that is independent of light intensity at liquid-air temperature. Presumably, both the probability of thermal dissociation of the silver atoms and the ionic conductivity are vanishingly small at this temperature so that

[1] This type of change of efficiency with intensity is related to reciprocity-law failure of ordinary photographic plates for exposures with light.

[2] J. H. WEBB AND C. H. EVANS, *Jour. Optical Soc. Am.*, **28**, 249 (1938).

the light simply charges the centers to a point where all other electrons are repelled. When the crystal is warmed, enough silver ions migrate to the electrons to neutralize the charge, which happens to be sufficient to form a latent image. If it were not sufficient, no latent image would be formed as a result of low-temperature illumination.

6. If illumination is continued after the latent image has formed, the amount of free silver continues to grow and eventually an appreciable fraction of the crystal is decomposed corresponding to the results of the print-out effect.

7. Since the latent image is near the surface of the crystal, it comes in contact with the developer when the crystal is immersed. Apparently, the silver atoms of the latent image oxidize the developer molecules and thus obtain a negative charge which attracts silver ions and causes the amount of free silver to grow just as if illumination had been continued.

Another type of darkening process which has been studied extensively[1] is that occurring in zinc sulfide which has been suitably heated. Since zinc sulfide is most commonly used either as a paint pigment or as a luminescent material, this darkening usually is a disadvantage.

[1] This work is reviewed in a paper by N. T. Gordon, F. Seitz, and F. Quinlan, *Jour. Chem. Phys.*, 7, 4 (1938).

APPENDIX

DERIVATION OF HARTREE'S AND FOCK'S EQUATIONS

a. Hartree's Equations.—Hartree's equations are based upon an eigenfunction of the type

$$\Psi = \psi_1(\mathbf{r}_1)\psi_2(\mathbf{r}_2) \cdots \psi_n(\mathbf{r}_n), \tag{1}$$

in which it is assumed that the ψ_i satisfy the normalization condition

$$\int |\psi_i|^2 d\tau_i = 1 \tag{2}$$

but are not necessarily orthogonal.

From the variational theorem, we should expect the "best" ψ_i to be those for which

$$\delta \int \Psi^* H \Psi d\tau(x_1, \cdots, z_n, \zeta_1, \cdots, \zeta_n) = 0 \tag{3}$$

with the auxiliary condition (2). We shall write H in the form

$$H = \sum_i H_i + \frac{1}{2}\sum_{i,j}{}' \frac{e^2}{r_{ij}} \qquad (i, j = 1, \cdots, n) \tag{4}$$

where H_i depends only upon the variables $\mathbf{r}_i$ and is the same function of these as H_j is of $\mathbf{r}_j$. Equation (3) may then be written in the form

$$\sum_i \int \Big[\psi_1^*(\mathbf{r}_1) \cdots \psi_n^*(\mathbf{r}_n) \Big(\sum_j H_j + \frac{1}{2}\sum_{j,k}{}' \frac{e^2}{r_{jk}} \Big) \cdot \psi_1(\mathbf{r}_1) \cdots \psi_{i-1}(\mathbf{r}_{i-1}) \psi_{i+1}(\mathbf{r}_{i+1}) \cdots \psi_n(\mathbf{r}_n) \delta\psi_i(\mathbf{r}_i) \Big] d\tau' +$$

$$\sum_i \int \Big[\psi_1^*(\mathbf{r}_1) \cdots \psi_{i-1}^*(\mathbf{r}_{i-1}) \psi_{i+1}^*(\mathbf{r}_{i+1}) \cdots \psi_n^*(\mathbf{r}_n) \delta\psi_i^*(\mathbf{r}_i) \cdot \Big(\sum_j H_j + \frac{1}{2}\sum_{j,k}{}' \frac{e^2}{r_{jk}} \Big) \psi_1(\mathbf{r}_1) \cdots \psi_n(\mathbf{r}_n) \Big] d\tau' = 0. \tag{5}$$

When integrated, this reduces to

$$\sum_i \int \psi_i^* \Big[\sum_{k \neq i} \int \psi_k^* H_k \psi_k d\tau_k + \frac{1}{2}\sum_{j,k \neq i}{}' e^2 \int \frac{|\psi_j(\mathbf{r}_j)|^2 |\psi_k(\mathbf{r}_k)|^2}{r_{jk}} d\tau_{jk} +$$

$$H_i + \sum_j{}' e^2 \int \frac{|\psi_j|^2}{r_{ij}} d\tau_j \Big] \delta\psi_i + (\text{a symmetrical expression in } \delta\psi_i^*) = 0. \tag{6}$$

The variational equivalent of (2) is

$$\lambda_i(\int \psi_i^* \delta\psi_i d\tau + \int \delta\psi_i^* \psi_i d\tau) = 0. \tag{7}$$

The result of adding (7) to (6) with Lagrangian multipliers, λ_i, is

$$\sum_i \int \psi_i^* \Big[\sum_{j\neq i} \int \psi_j^* H_j \psi_j d\tau_j + \frac{1}{2} \sum_{j,k\neq i}{}' e^2 \int \frac{|\psi_j(\mathbf{r}_j)|^2 |\psi_k(\mathbf{r}_k)|^2}{r_{jk}} d\tau_j + H_i + \sum_j{}' e^2 \int \frac{|\psi_j|^2}{r_{ij}} d\tau_j + \lambda_i \Big] \delta\psi_i d\tau_i + (\text{a symmetrical expression in } \delta\psi_i^*) = 0. \tag{8}$$

If the condition that H is Hermitian is used, the position of $\delta\psi_i$ and ψ_i^* may be reversed in the written term of (8). Since $\delta\psi_i$ and $\delta\psi_i^*$ are independent variations and are independent of the variations of $\delta\psi_k$ and $\delta\psi_k^* (k \neq i)$, the necessary and sufficient condition that (8) be satisfied is that the coefficient of each $\delta\psi_i$ and each $\delta\psi_i^*$ be zero. These conditions are

$$H_i\psi_i + \Big(\sum_j{}' \int \frac{|\psi_j|^2}{r_{ij}} d\tau_j\Big)\psi_i + \Big(\sum_{j\neq i} \int \psi_j^* H \psi_j d\tau_j + \sum_{j,k\neq i}{}' e^2 \int \frac{|\psi_j|^2 |\psi_k|^2}{r_{jk}} d\tau_{jk} + \lambda_i\Big)\psi_i = 0 \tag{9}$$

and

$$H_i\psi_i^* + \Big(\sum_j{}' \int \frac{|\psi_j|^2}{r_{ij}} d\tau_j\Big)\psi_i^* + \Big(\sum_{j\neq i} \int \psi_j^* H \psi_j d\tau_j + \sum_{j,k\neq i}{}' e^2 \int \frac{|\psi_j|^2 |\psi_k|^2}{r_{jk}} d\tau_{jk} + \lambda_i\Big)\psi_i^* = 0.$$

Obviously, only one of these need be considered since the two equations are complex conjugates. We obtain Hartree's equations

$$H_i\psi_i + \Big(\sum_{j\neq i} \int \frac{|\psi_j|^2}{r_{ij}} d\tau_j\Big)\psi_i + \epsilon_i\psi_i = 0 \tag{10}$$

by setting

$$\Big(\sum_{i\neq j} \int \psi_j^* H \psi_j d\tau_j + \sum_{j,k\neq i}{}' e^2 \int \frac{|\psi_j|^2 |\psi_k|^2}{r_{jk}} d\tau_{jk} + \lambda_i\Big) = \epsilon_i. \tag{11}$$

If we require, in addition to (2), that

$$\int \psi_i^* \psi_j d\tau = \delta_{ij} \tag{12}$$

and if we add the variational equivalent of this to (8), we find that a term $\sum_{j\neq i}\lambda_{ij}\psi_j$ is added to (11).

b. Fock's Equations.—The derivation of Fock's equations may proceed along exactly the same lines as those employed in part *a* with the exception that the basic wave function is

$$\Psi = \frac{1}{\sqrt{n!}}\sum_{P_\nu}(-1)^{p_\nu}P_\nu[\psi_1(\mathbf{r}_1)\cdots\psi_n(\mathbf{r}_n)\eta_1(\zeta_1')\cdots\eta_n(\zeta_n')] \quad (13)$$

where

$$\psi_1 = \psi_2, \qquad \psi_3 = \psi_4, \cdots, \qquad \psi_{n-1} = \psi_n$$

and the spin functions η are opposite for the members of each of these pairs of equal functions. In this case, we have

$$\delta\Psi = \frac{1}{\sqrt{n!}}\sum_{P_\nu}(-1)^{p_\nu}P_\nu\Big[\sum_i \psi_1(\mathbf{r}_1)\cdot \psi_{i-1}(\mathbf{r}_{i-1})\psi_{i+1}(\mathbf{r}_{i+1})\cdots\psi_n(\mathbf{r}_n)\delta\psi_i(\mathbf{r}_i)\eta_i(\zeta_i')\cdots\eta_n(\zeta_n')\Big]. \quad (14)$$

We shall substitute this in the equation

$$\delta\int\Psi^*H\Psi d\tau = \int\Psi H\delta\Psi d\tau + \int\delta\Psi^*H\Psi d\tau = 0 \quad (15)$$

where H is given by (4). After integrating, summing over spin, and using the condition $\int\psi_i^*(\mathbf{r})\psi_j(\mathbf{r})d\tau = 0$, for $\psi_i \neq \psi_j$, and $\int|\psi_i|^2d\tau = 1$, we obtain

$$\sum_i\int\Big(\psi_i^*(\mathbf{r}_1)\Big[\sum_j\int\psi_j^*(\mathbf{r}_2)H_2\psi_j(\mathbf{r}_2)d\tau_2 + \frac{1}{2}\sum_{j,k}{}'e^2\int\frac{|\psi_j(\mathbf{r}_2)|^2|\psi_k(\mathbf{r}_3)|^2}{r_{23}}d\tau_{23} - \frac{1}{2}\sum_{\substack{j,k\\ \|\text{ spins}}}{}'e^2\int\frac{\psi_j^*(\mathbf{r}_2)\psi_k^*(\mathbf{r}_3)\psi_j(\mathbf{r}_3)\psi_k(\mathbf{r}_2)}{r_{23}}d\tau_{23} + H_i + e^2\sum_j\frac{|\psi_j(\mathbf{r}_2)|^2}{r_{12}}d\tau_2 + \lambda_{12}'\Big] - \Big\{\sum_{\substack{j\\ \|\text{ spins}}}{}'\psi_j^*(\mathbf{r}_1)\Big[e^2\int\frac{\psi_i^*(\mathbf{r}_2)\psi_j(\mathbf{r}_2)}{r_{12}}d\tau_2 + \int\psi_i^*(\mathbf{r}_2)H_2\psi_j(\mathbf{r}_2) + \lambda_{ji}'\Big]\Big\}\Big)\delta\psi_i(\mathbf{r}_1)d\tau_1 + [\text{a symmetrical expression in } \delta\psi_i^*(\mathbf{r}_1)] = 0. \quad (16)$$

The λ'_{ii} are the Lagrangian multipliers for the orthogonality and normalization conditions. We shall set

$$\lambda_{ii} = \lambda'_{ii} + \sum_j \int \psi_j^*(\mathbf{r}_2) H_2 \psi_j(\mathbf{r}_2) d\tau_2 + \frac{1}{2}{\sum_{j,k}}' e^2 \int \frac{|\psi_j(\mathbf{r}_2)|^2 |\psi_k(\mathbf{r}_3)|^2}{r_{23}} d\tau_{23} - \frac{1}{2} \sum_{\substack{j,k \\ \| \text{ spins}}} e^2 \int \frac{\psi_j^*(\mathbf{r}_2)\psi_k^*(\mathbf{r}_3)\psi_j(\mathbf{r}_3)\psi_k(\mathbf{r}_2)}{r_{23}} d\tau_{23} \quad (17)$$

and

$$\lambda_{ij} = \lambda'_{ij} + \sum_j \int \psi_i^*(\mathbf{r}_2) H_2 \psi_j(\mathbf{r}_2) d\tau_2. \quad (18)$$

We find, upon equating the coefficient of $\delta\psi_i(\mathbf{r}_1)$ to zero, as before, that

$$\left[H_1 + \sum_j e^2 \int \frac{|\psi_j(\mathbf{r}_2)|^2}{r_{12}} d\tau_2 + \lambda_{ii} \right] \psi_i(\mathbf{r}_1) - {\sum_{\substack{j \\ \| \text{ spins}}}}' \left[e^2 \int \frac{\psi_j^*(\mathbf{r}_2)\psi_i(\mathbf{r}_2)}{r_{12}} d\tau_2 + \lambda_{ij} \right] \psi_j = 0. \quad (19)$$

Equation (19) is valid only for those states of zero multiplicity which correspond to a complete set of paired ψ_i. In other cases, these equations will be modified in a way that depends upon the type of wave function. We shall not discuss these cases since the one leading to (19) is sufficiently general for our needs.

NAME INDEX

A

Abraham, M., 211, 213, 637
Ahlberg, J. E., 114*ff.*
Akulov, N. S., 22*ff.*
Allen, J. F., 485
Allison, S. K., 288, 475
Anderson, C. T., 13, 58
Andrews, D. H., 114*ff.*
Austin, J. B., 15

B

Baber, W. G., 540
Baedeker, K., 69, 70
Balamuth, L., 95
Banks, F., 495
Bardeen, J., 340, 348, 352, 354, 374, 381*ff.*, 395, 397*ff.*, 400, 421*ff.*, 520*ff.*, 530*ff.*
Barkhausen, H., 21
Barnes, R. B., 95, 125, 666, 667
Barnett, S. J., 426
Barrer, R. M., 494
Bartlett, J. H., 251
Bassoe, E., 670
Baumbach, H. H. v., 71
Bearden, J. H., 440
Becker, G., 45*ff.*
Becker, J. A., 146, 162, 168, 404
Becker, R., 20, 211, 213, 627, 637
Beeman, W. W., 440
Bethe, H., 92, 140, 141, 147, 166, 185, 233, 314, 505, 507, 511, 520, 613*ff.*
Beyer, J., 556
Bichowsky, F. R., 3, 46, 72
Biltz, W., 38
Birtwistle, G., 137
Bitter, F., 18, 617
Black, M. M., 250, 251
Blackman, M., 100, 116, 117, 120, 133*ff.*, 597*ff.*, 667
Bleick, W. E., 89, 265, 269, 383, 393, 493
Bloch, F., 140, 251, 301*ff.*, 303*ff.*, 314*ff.*, 319, 516, 518, 520, 530, 531*ff.*, 602, 617*ff.*, 642, 649*ff.*
Boas, W., 98
Bohr, N., 235, 237
Boltzmann, L., 139, 143, 169, 319, 479, 516*ff.*, 585*ff.*
Borelius, G., 41
Born, M., 76, 79, 82*ff.*, 85*ff.*, 91, 97, 99*ff.*, 111, 112*ff.*, 117, 118, 124*ff.*, 138, 265, 271, 272, 470, 493, 553, 667
Bose, 239
Bottema, J. A., 39
Bouckaert, L. P., 275
Bozorth, R., 21, 23, 625
Bragg, W. L., 505, 507, 509, 513, 544, 604, 612
Brattain, R. R., 95, 125, 666, 667
Brattain, W. H., 168, 404
Breit, G., 210, 643
Bridgman, P. W., 5, 137, 180, 374, 381*ff.*
Briggs, H. B., 652, 653*ff.*
Brillouin, L., 100, 141, 209, 234, 272, 283*ff.*, 384, 520, 581
Brody, E., 138
Brönsted, J. N., 483, 484
Brooks, H., 426, 628
Brown, F. W., 246, 251, 265
Brown, W. F., 20
Brüch-Willstäter, M., 393*ff.*
Buehl, R. C., 562, 563
Burrau, O., 255*ff.*
Burton, E. F., 485

C

Campbell, L. L., 68
Carrard, A., 58
Cashman, R. J., 401, 670
Channel-Evans, K. M., 28, 32
Chodorow, M. I., 275, 430*ff.*
Clark, A. R., 485
Clark, C. W., 15*ff.*, 57, 114, 117, 136, 157
Clusius, K., 13, 74, 485

Cohen, E., 8, 483*ff.*
Collet, P., 19
Compton, A. H., 288, 475
Condon, E. U., 210, 234, 246, 247, 450, 458, 559, 578, 643
Coolidge, A. S., 258*ff.*, 262
Courant, R., 238
Cristescu, S., 14
Curie, P., 23*ff.*, 36*ff.*, 58, 606*ff.*, 610*ff.*

D

Dannöhl, W., 187*ff.*
Davis, L., 185*ff.*
Davisson, C., 196
Day, H., 495
de Boer, J. H., 162, 540
de Broglie, M., 561
Debye, P., 14, 57, 86, 99*ff.*, 103, 104*ff.*, 117, 480*ff.*, 533*ff.*
de Haas, W. J., 13, 540, 597
Dehlinger, U., 623*ff.*
Deitz, V., 393
Dillinger, J., 21
Dirac, P. A. M., 139*ff.*, 144*ff.*, 195, 203*ff.*, 215, 245, 340, 384*ff.*, 517*ff.*, 586, 630
Döring, W., 20
Drude, P., 139*ff.*, 629, 633, 638
DuBridge, L. A., 146, 401
Dünwald, H., 71
Dunn, C. G., 251
Dushman, S., 162, 165*ff.*, 195, 402, 495

E

Einstein, A., 99*ff.*, 103–117, 209, 220, 480*ff.*
Eisenschitz, R., 268
Elam, C. F., 98
Endô, H., 42*ff.*
Epstein, P. S., 403
Eucken, A., 13, 74*ff.*, 111, 137*ff.*
Evans, C. H., 675
Evans, J., 563
Ewald, P. P., 77
Ewell, R. H., 489
Ewing, D. H., 443*ff.*
Eyring, H., 210, 470, 474, 489

F

Fajans, K., 660, 661, 674
Farineau, J., 437*ff.*
Farkas, L., 470
Ferguson, J. N., 413
Fermi, E., 139, 141*ff.*, 144*ff.*, 209, 370, 375, 379*ff.*, 384, 517*ff.*, 586*ff.*
Fleischmann, R., 401
Fock, V., 227, 242, 243*ff.*, 246*ff.*, 251*ff.*, 254, 365, 385, 386, 677, 679
Foëx, G., 19, 611
Försterling, K., 113*ff.*, 641
Forrer, R., 45
Fowler, R. H., 323, 457, 482, 509, 512, 513*ff.*, 586
Franck, J., 450, 458, 559
Frank, A., 603
Frank, N. H., 140, 179, 185
Franz, W., 177, 178, 562
Freedericksz, V., 641, 656
Frenkel, J., 395, 413, 414, 418, 460, 511*ff.*, 547
Friedman, H., 440
Fritsch, O., 192
Fröhlich, H., 315, 486, 559, 562
Fuchs, K., 116, 367*ff.*, 375*ff.*, 427

G

Gans, R., 23, 173
Germer, L. H., 196, 655
Giauque, W. F., 74*ff.*
Gibbs, J. W., 127, 483
Glaser, G., 566, 567
Goens, E., 111, 120
Goldschmidt, V. M., 83, 92*ff.*
Gombas, P., 385
Gordon, N. T., 676
Gordon, W., 215
Gorin, K. E., 348*ff.*, 356, 369*ff.*, 653
Gorsky, W., 507*ff.*, 515
Goudsmit, S., 203
Grew, K. E., 43*ff.*
Griffith, A. A., 98
Grüneisen, E., 13, 111, 120, 138, 379*ff.* 533, 540
Gudden, B., 63, 64, 70, 456, 568, 571
Guillery, P., 64
Gurney, R. W., 489, 674*ff.*
Gwinner, E., 440
Gyulai, Z., 566, 568, 657

H

Hägg, G., 35
Hagen, E., 640

Hall, E. H., 68, 181*ff.*, 191*ff.*
Hansen, M., 30
Hargreaves, J., 251
Harrison, G. B., 574, 674
Hartree, D. R., 227, 235*ff.*, 245, 246, 247, 250, 251*ff.*, 254, 333, 385, 386, 424, 443, 677*ff.*
Hartree, W., 247, 251, 386
Heisenberg, W., 318, 612*ff.*
Heitler, W., 210, 301*ff.*, 408*ff.*, 454*ff.*, 612*ff.*
Helmholz, L., 46, 49, 483
Hendricks, S. B., 8
Herring, C., 275, 332*f.*, 366, 371, 372, 400
Herzberg, G., 578
Herzfeld, K. F., 125, 405, 488, 492, 645
Hilbert, D., 238
Hill, A. G., 332*ff.*, 371, 372, 400, 669*ff.*
Hilsch, R., 71, 410, 459, 564, 566, 568, 571*ff.*, 574, 657, 664
Hirschfelder, J. O., 470, 489
Hofstadter, R., 673
Honda, K., 18, 21, 22
Hopf, L., 111
Houston, W. V., 140, 318*ff.*, 436, 438, 516, 518, 535
Huggins, M. L., 93
Hughes, A. L., 146, 401
Hume-Rothery, W., 5, 9, 11, 28*ff.*, 31, 32*ff.*, 432*ff.*
Hund, F., 251*ff.*, 453
Huntington, H. B., 366, 497
Hylleraas, E., 92, 233*ff.*, 254, 258, 261, 385, 390*ff.*

I

Inglis, D. R., 60
Ives, H. E., 652, 653*ff.*

J

Jacobs, R. B., 49, 91
Jaeger, F. M., 39
James, H. M., 258*ff.*, 262, 447
Jefferson, M. E., 8
Jensen, H., 384*ff.*
Johansson, C. H., 41
Johnson, R. P., 167, 428, 572, 573, 672
Johnson, V. A., 447
Jones, F. W., 35
Jones, H., 161, 185, 296, 307, 314, 425, 432*ff.*, 436, 438, 500*ff.*, 531*ff.*, 535, 595*ff.*, 655
Jonker, C. C., 644
Joos, G., 106, 141, 660, 661
Jordahl, O. M., 603
Jost, W., 551, 553, 555*ff.*, 575

K

Kane, Brother Gabriel, 492*ff.*
Kapitza, P., 185
Karwat, C., 74*ff.*
Kaya, S., 20*ff.*, 22, 45
Keesom, H. P., 485
Keesom, W. H., 15*ff.*, 57, 114, 117, 136, 152, 157, 158, 485
Keil, A., 494, 495
Kemble, E. C., 195, 199, 203
Kennard, E. H., 100
Ketelaar, J. A. A., 503*ff.*
Kimball, G. E., 210, 453*ff.*
Kirkwood, J. G., 268, 269, 486
Klein, O., 215, 221
Kleinschrod, F. G., 664
Koch, E., 556*ff.*
Koch, W., 664*ff.*
Kok, J. A., 152, 158
Koopmans, T., 313*ff.*, 396, 408, 644
Kopp, 38*ff.*
Korff, S. A., 643
Kramers, H. A., 278*ff.*, 320, 644
Kretschmann, E., 534
Kronig, R. de L., 272, 281*ff.*, 321*ff.*, 629, 638, 652, 656
Krüger, F., 406
Krutter, H. M., 385, 423, 424, 427*ff.*, 440, 442
Kubaschewski, O., 38
Kurrelmeyer, B., 158
Kussmann, A., 45

L

Landau, L., 583*ff.*, 595
Landshoff, R., 385*ff.*, 391
Lange, F., 483
Langevin, P., 582
Langmuir, I., 495
Lapp, E., 16
Laue, M. v., 288, 293, 296, 518*ff.*
Lawson, A., 58, 511*ff.*

Lechner, G., 111
Lehfeldt, W., 55, 460, 552, 554*ff.*, 566, 574*ff.*
Lennard-Jones, J. E., 81, 84, 269, 489
Lenz, W., 384*ff.*
Leverenz, H. W., 672
Levy, R. B., 89
Linde, J. O., 39, 40, 41
Littleton, M. J., 553
London, F., 84*ff.*, 265*ff.*, 268, 301*ff.*, 392*ff.*, 408*ff.*, 454*ff.*, 486*ff.*, 545*ff.*, 612*ff.*, 660
Lord, R. C., 114*ff.*, 116
Lorentz, H. A., 139*ff.*, 168, 170*ff.*, 190, 214, 516*ff.*, 549, 604*ff.*, 608*ff.*, 629, 633, 637, 658*ff.*
Lowery, H., 651, 655
Lozier, W. W., 448
Lukens, C., 641
Lyddane, R. R., 125

M

Mabbott, G. W., 28, 32
McDougall, J., 251
McKay, H. A. C., 495
Madelung, E., 76, 78, 97, 271
Maier, C. G., 13
Makinson, R. E. B., 670
Maltbie, M. McC., 88
Manning, M. F., 251, 275, 424, 430*ff.*, 535
Margenau, H., 86, 262, 268, 269, 393*ff.*, 660
Maxwell, J. C., 139, 143, 211*ff.*, 517*ff.*, 629*ff.*
May, A., 91
Mayer, J. E., 46, 49, 82*ff.*, 85*ff.*, 88, 89*ff.*, 93, 265, 268*ff.*, 383, 393, 493, 658*ff.*
Mayer, M. G., 82, 492
Mehl, R. F., 27, 494*ff.*
Meier, W., 655, 656, 662
Meissner, W., 178
Meyer, W., 65
Mie, G., 379
Miller, P., 495
Millman, J., 251, 422
Minor, R. S., 655, 656, 662
Misener, A. D., 485
Mitchell, K., 669*ff.*
Mitscherlich, 484
Morse, P. M., 272
Moser, H., 25, 36*ff.*
Mott, N. F., 151*ff.*, 153, 161, 296, 307, 378, 401, 425, 426*ff.*, 432, 436, 438, 489, 490*ff.*, 531*ff.*, 536, 544*ff.*, 552, 559, 566, 575, 655, 674*ff.*
Mulliken, R. S., 251*ff.*
Muto, T., 544, 671
Myers, R. D., 669

N

Nagel, K., 72
Nathanson, J. B., 654
Nehlep, G., 553, 556, 575
Nernst, W., 483, 484
Neumann, J., 38*ff.*
Nix, F. C., 495, 503, 571
Nordheim, L. W., 166, 520, 530*ff.*, 541*ff.*
Nottingham, W. A., 167

O

O'Bryan, H. M., 410, 437, 440, 657
Onsager, L., 604*ff.*
Oppenheimer, J. R., 470

P

Pauli, W., 139, 159, 204*ff.*, 208*ff.*, 599
Pauling, L., 81, 429, 434*ff.*, 441, 455*ff.*, 511, 512*ff.*
Peierls, R., 272, 414, 485, 523, 533, 534, 588, 589, 590*ff.*, 671
Pelzer, H., 470, 473
Penney, W. G., 272, 281*ff.*, 321*ff.*, 603
Perlick, A., 74
Peterson, E. L., 530*ff.*
Petrashen, Mary, 251, 386
Piccard, A., 58
Pickard, G. L., 158
Pohl, R. W., 71, 410, 459*ff.*, 563*ff.*, 566*ff.*, 568, 571*ff.*, 574, 657, 664
Polanyi, M., 98
Pollard, W. G., 323
Prokofjew, W., 349

Q

Quimby, S. L., 95, 116, 378
Quinlan, F., 676

R

Rabi, I., 196
Randall, J. T., 673
Reimann, A. L., 162, 572, 573
Rice, O. K., 381
Richardson, O. W., 165*ff*., 402
Rojansky, V., 195, 203, 281
Rollin, B. V., 485
Rose, F. C., 95
Rossini, F. D., 3, 46, 72
Roth, 484
Rubens, H., 640
Ruhemann, M., 57
Rumer, G., 210
Rupp, E., 196
Russell, H. N., 578*ff*., 627, 643

S

Sadron, C., 44
Sagrubskij, A., 495
Sampson, H. B., 563
Saunders, F. A., 578*ff*., 627, 643
Saur, E., 440
Scharnow, B., 45
Schiff, L. I., 670
Schlapp, R., 603
Schleede, A., 672
Schmid, E., 98
Schmidt, 238
Schneider, E. G., 410, 657
Schottky, W., 69*ff*., 161*ff*., 456, 547*ff*.
Schrödinger, E., 111, 197, 215
Schubin, S., 669
Schulze, A., 45
Schumann, W., 659*ff*.
Seeger, R. J., 559*ff*., 562*ff*.
Seith, W., 38, 494, 495, 557
Shaw, C. H., 440
Sherman, A., 210, 261, 270
Sherman, J., 81*ff*., 87*ff*.
Shimizu, Y., 18, 42
Shockley, W., 167, 323*ff*., 332, 414, 421, 442*ff*., 495, 503, 625
Shoenberg, D., 597
Shortley, G. H., 210, 234, 246, 247, 249, 578, 648
Shultz, J. F., 8
Siegel, S., 116, 378, 508
Siegert, A., 603
Simon, F., 14, 57, 484
Simson, O. v., 57
Skinner, H. W. B., 436, 437, 438*ff*.
Slater, J. C., 80, 137, 153, 227, 242*ff*., 264, 268, 269, 331, 332, 379, 385, 414, 420, 421, 426*ff*., 435, 455, 486, 546*ff*., 617, 620*ff*.
Smakula, A., 662*ff*.
Smare, D. L., 654, 655
Smith, L. P., 413
Smoluchowski, R., 275
Sommerfeld, A., 140, 141, 147, 166, 174, 179, 185, 314, 395, 516*ff*.
Spedding, F. H., 603
Sponer, H., 393*ff*.
Stabenow, G., 406
Steigman, J., 495
Stern, O., 97
Stoner, E. C., 24, 151, 426, 488, 603, 611
Strutt, M. J. O., 272
Sutton, P. P., 46, 49
Sykes, C., 35

T

Tamm, I., 281, 320*ff*., 669
Tammann, G., 27, 35
Taylor, G. I., 98
Teller, E., 255*ff*., 559*ff*., 562*ff*.
Thiele, W., 568
Thomas, L. H., 370, 379, 384*ff*., 670
Thomson, G. P., 196
Thomson, W., 179
Tibbs, S. R., 424, 443
Torrance, C. C., 246*ff*., 249, 454
Toy, F. C., 574, 674
Trombe, F., 25
Trouton, 3
Trumpy, B., 645
Tubandt, C., 56, 63, 66*ff*., 554*ff*.
Tyler, F., 24

U

Uddin, M. Z., 485, 597
Ufford, C. W., 249
Uhlenbeck, G. E., 203
Urbain, G., 25

V

Valasek, J., 413
Valentiner, S., 45*ff*.

van Alphen, P. M., 597
van den Berg, G. J., 13
van der Waals, 82, 84*ff.*, 262, 265*ff.*, 391*ff.*, 492, 553
van Eijk, C., 8, 483, 484
Van Vleck, J. H., 210, 261, 270, 583, 601, 603, 606, 607, 612, 615, 616, 627, 628
Vogel, R., 27
Vogt, W., 65
Voigt, W., 94, 106
Völkl, A., 64
von Hevesy, G., 494, 557
von Hippel, A., 411, 413, 450, 562, 563
von Kármán, Th., 99*ff.*, 111, 118, 272

W

Wagner, C., 67, 71, 72, 456, 547*ff.*, 556*ff.*
Waibel, F., 69
Wallasch, 484
Wang, S. C., 261
Wannier, G. H., 332, 419, 454
Warren, B. E., 74
Wasastjernas, J., 92
Watson, G. N., 279
Webb, J. H., 674, 675
Weiss, P., 20, 25, 45, 58, 60, 608, 609*ff.*, 611*ff.*, 620
Weisskopf, V., 223
White, H. E., 2, 220
Whittaker, E. T., 279
Wiebe, R., 74*ff.*
Wiedemann, 177, 178
Wigner, E. P., 204, 237, 241, 275, 290, 292, 329, 331, 340, 342*f.*, 348, 366, 395, 397*ff.*, 405*ff.*, 421, 422, 470, 473, 603, 644
Wilhelm, J. O., 485
Wilkinson, H., 654, 655
Williams, E. J., 507, 509, 513, 544, 604, 612
Wilson, A. H., 186, 457, 536*ff.*, 590, 594, 642, 650
Wolff, K. L., 645
Woltinek, H., 13
Wood, R. W., 641
Wulff, G., 97*ff.*

Y

Yamada, M., 97*ff.*

Z

Zeeman, P., 577
Zener, C., 185, 315, 319, 629, 638, 652
Ziegler, M., 60
Zwicky, F., 98

SUBJECT INDEX

A

Absorption coefficient, 631*ff*., 635, 646*ff*.
  alkali metals, 652
  semi-conductors, 662
  transition metals, 656
Absorption spectra, alkali halides, 410, 446, 657*ff*.
  F centers, 662
  infrared, 665
  ionic crystals, 408*ff*.
  metals, 651*ff*.
  semi-conductors, 661*ff*.
Acceleration in band scheme, 315*ff*.
Accidental degeneracy, 290
Activation energy, reactions in solids, 474, 550
  semi-conductors, 459*ff*.
Additivity, atomic heats, 38
  ionic radii, 51
  ionic susceptibilities, 59
  refractivities, 660
Adiabatic approximation, 470*ff*.
Alkali halides, absorption spectra, 408*ff*., 446
  bands, 441
  charge distribution, 444
  cohesion, 80*ff*.
  conduction levels, 446
  discoloration, 460
  F centers, 457
  Hall effect, 563
  ionic conductivity, 55, 385*ff*.
  lattice defects, 548*ff*.
  Madelung constants, 78
  optical properties, 657*ff*.
  photoconductivity, 413, 446, 459, 563
  semi-conductors, 457
  vacancies, 458*ff*.
Alkali metals, Bloch functions, 350*ff*.
  cohesion, 348*ff*., 366
  correlation energy, 366
  coulomb field, 349
  effective mass, 353
Alkali metals, elastic constants, 116
  electronic structure 420*ff*.
  exchange energy, 359, 421
  ion-core field, 348
  level density, 366
  optical properties, 423, 652
  paramagnetism, 599
  simple treatment, 382
  specific heat, 116, 421
  total wave function, 308*ff*.
  work function, 399
Alkaline earth metals, bands, 424*ff*.
  level density, 424
Alkaline earth salts, absorption spectra, 408*ff*.
  cohesion, 81*ff*.
  excitation states, 413*ff*.
  Hall coefficient, 467
  photoconductivity, 413
Allotropy, carbon, 484
  cobalt, 8, 487
  helium, 485
  ionic crystals, 89*ff*.
  iron, 8, 487
  metals, 2
  sulfur, 484
  theory, 473*ff*., 478*ff*.
  tin, 8, 483
Alloys, 25*ff*., conductivity, 541*ff*.
  Curie point, 45, 624
  diamagnetism, 595
  diffusion, 495
  equilibrium conditions, 500
  exchange integral, 624
  ferromagnetism, 45, 623*ff*.
  filling of levels, 434, 501
  heat of formation, 38
  Hume-Rothery rules, 28, 30*ff*.
  interstitial, 25*ff*.
  magnetic susceptibilities, 42*ff*., 595
  ordered, 37, 502
  phase boundaries, 499
  phase changes, 500
  quenching of magnetization, 44*ff*.

Alloys, resistivity, 39*ff*., 43*ff*.
substitutional, 25*ff*.
thermal properties, 37
Angular momentum, orbital, 426, 578
spin, 206*ff*., 232, 426, 577
Anisotropy, 21, 627*ff*.
Antisymmetric states, 209, 236, 243
molecular helium, 264
two electrons, 232, 260
Approximate methods, 329*ff*.
Atomic dipole moment, 218
Atomic heat (*see* Specific heat)

B

Band scheme, 251, 271*ff*.
alkali halides, 441
alkali metals, 348, 420*ff*.
anisotropy, 628
Boltzmann's equation, 319
conductivity, 274
connection with Heitler-London scheme, 337
diamond, 452
excited states, 407, 408
ferromagnetism, 339
holes, 317
ionic crystals, 441
level density, 307*ff*.
metals, 420*ff*.
narrow bands, 303*ff*.
overlapping, 296
rules concerning, 274*ff*., 295*ff*.
transition metals, 426*ff*., 468
Barkhausen effect, 25
Beryllium, 371*ff*.
level density, 371, 437
work function, 400
Beryllium atom, 247*ff*.
energy, 248
Beta brass, 35*ff*., 506
specific heat, 37
Bismuth, 425
diamagnetism, 595
effective mass, 596*ff*., 599
optical properties, 656
Bloch functions, 272*ff*.
accuracy, 312
alkali metals, 348, 350*ff*.
approximate, 273, 294, 303*ff*., 331*ff*.
excitation waves, 647*ff*.
free electrons, 272
Bloch functions, narrow bands (*see* Approximate methods)
symmetry, 275
Bloch scheme (*see* Band scheme)
Boltzmann's equation of state, 168*ff*., 173*
in band scheme, 319 516*ff*., 526
Boltzmann's theorem, 99
entire solid, 479
Bond functions, 210
Born-Mayer equation, 87, 96
justification, 445
Born-Oppenheimer equation, 470
Born-von Kármán boundary conditions, 118, 121, 126, 272
Bound electrons, 274
Brass system, 30, 43
Breaking strengths, 98
Brillouin functions, 581
Brillouin zones, 284, 287*ff*., 294*ff*., 298

$C_p - C_v$ correction, 136*ff*.
Carbon atom, 249
Carbon dioxide, 394
Carborundum, 2, 61, 63
Cauchy-Poisson relations, 94, 376
Cellular method, 329
alkali metals, 349
empty-lattice test, 332
Cellular polyhedron, 330*ff*., 352
Characteristic temperature, ionic crystals, 57, 114, 134*ff*.
metals, 108, 109*ff*.
Chemical constant, 403
Chemical reactions, 470
Closed shells, 228, 247, 262*ff*., 302*ff*., 310, 346
copper, 367
diamagnetism, 582
ionic crystals, 388
rare gases, 393
Closed-shell interaction, 262*ff*.
alkali metals, 360
metals, 376
Cobalt, allotropy, 8, 487
Coherent scattering, 542
Cohesion, 345*ff*.
alkaline earth salts, 81*ff*.
alkali metals, 348, 366
alloys, 38, 271*ff*., 378
carbon dioxide, 393

Cohesion, copper, 367
Fock approximation, 368
ionic crystals, 46*ff*., 78, 80*ff*., 88*ff*., 271, 385*ff*.
lithium hydride, 390*ff*.
metallic hydrogen, 367
metals, 3, 271*ff*., 367*ff*.
molecular solids, 73, 391*ff*.
molecules, 254*ff*.
solids, 271*ff*.
transition metals, 427*ff*.
valence crystals, 61, 271*ff*.
Collision terms, 169, 525, 538
Competition of energy terms, 230
Compressibility, 76, 138
ionic crystals, 391
theory, 373*ff*.
Conductivity, alkali halides, 55, 64
alloys, 544
band theory, 274, 297*ff*.
change with melting, 491
change with order, 41, 504
classical theory, 190
critique of theory, 534
cuprous oxide, 65
dependence on vapor pressure, 70, 461
excitation waves, 416
ionic solids, 55*ff*.
low temperature, 531
magnetic field, 184*ff*.
metals, 9, 170*ff*., 174*ff*., 190, 425, 516*ff*.
optical region, 631*ff*., 635*ff*., 648
semi-conductors, 63, 189*ff*., 457, 461, 465
simple metals, 535*ff*.
surface, 642
transition metals, 535
Copper, bands, 367, 423*ff*.
cohesion, 367
optical properties, 424, 654
Copper-gold system, 33, 36, 503
Copper-silver system, 33
Correlation of electrons, 231
exchange, 240
free electrons, 242
hydrogen molecule, 259
metals, 420
narrow bands, 339
solids, 339
Correlation energy, 231, 234
alkali metals, 366
atoms, 247*ff*.
Correlation energy, beryllium, 373
free electrons, 342*ff*.
narrow bands, 339
Coulomb energy, 346, 357
alkali metals, 363
Cross section, alloys, 543*ff*.
angular dependence, 528*ff*.
electronic collisions, 169, 320, 526, 541*ff*., 545
ionic crystals, 554
low temperature, 531
Cuprous oxide, 2
conductivity, 65
levels, 467*ff*.
rectification, 575
vacancies, 467*ff*.
work function, 491
Curie law, 581, 606
Curie temperature, 23, 25
alloys, 45, 624
dielectric, 607
theory, 610, 616
Curie-Weiss law, 24
theory, 610
Current operator, 221*ff*., 417

D

Damping, lattice vibrations, 666*ff*.
radiation, 633, 637
Darkening, silver halides, 672
zinc sulfide, 672
Debye function, 109, 152
Debye's theory of specific heats, 104*ff*.
deviations, 117, 120, 134
modification, 112*ff*., 124
Degeneracy, 210
accidental, 290
diamond, 453
excited states, 411*ff*.
Fock's equations, 302
lattice vibrations, 479
magnetic field, 583*ff*., 617
orbital, 579
spin, 579
spin waves, 617
d electron band, 153*ff*.
copper, 423
filling, 156
holes, 155*ff*.
noble metals, 423*ff*.
Pauling's theory, 429

d-electron band, splitting, 429
transition metals, 426*ff.*
widths, 158
Demagnetisation factor, 603
Density of levels, 143, 153*ff.*
Density matrix, 244
Determinantal wave functions, 237
molecules, 263
solids, 302
Diamagnetism, alloys, 595
bismuth, 596
closed shells, 582
free electrons, 583*ff.*, 594
narrow bands, 590
Diamond, 2, 61
allotropy, 484
bands, 452*ff.*
Dielectric breakdown, 319, 562
Dielectric constant, 629, 635
Diffusion, 494*ff.*, 548*ff.*
alloys, 495
interstitial, 495*ff.*
ionic conduction, 548*ff.*, 557
jump frequency, 495, 548
Dipole-dipole interaction (*see* van der Waals interaction)
Dipole layer, 396
Dipole moment, atomic, 218
surface, 396
Dipole-quadrupole interaction, 86*ff.*
Dislocations, 92
Dispersion, 220, 633*ff.*
Displacement distance, 565
Displacement operator, 591
Domain theory, 20*ff.*
Drift terms, 169, 525
d shells, 2, 16, 420*ff.*
ferromagnetism, 614
Dulong and Petit's law, 14, 38, 103, 138, 487

E

Effective electron mass, 141, 153, 316
alkali metals, 354
bismuth, 596*ff.*, 599
ionic solids, 441, 445
negative, 316
optical, 653
theory, 350
transition metals, 158*ff.*, 536
Eigenfunction, 197
antisymmetric, 209
Einstein function, 103
Einstein's theory of specific heat, 39
Elastic constants, 94*ff.*
alkali metals, 116, 373
Cauchy-Poisson relations, 94, 376
change with ordering, 503
component parts, 375*ff.*
ionic crystals, 95, 391
isotropic media, 106, 377*ff.*
theory, 373*ff.*
Elastic waves, 129
Electric polarization, 607
Electromagnetic theory, 203, 210*ff.*
Electron affinities, 46
halogens, 49, 80*ff.*
negative ions, 80*ff.*, 414*ff.*, 448*ff.*
Electron-atom ratio rule, 30*ff.*
Electron coupling, 535
Electronic distribution, 231
alkali halides, 443
zinc oxide, 447
Electron-electron collisions, 535, 540
Electronic conductivity, 62
ionic crystals, 554
Electronic specific heat, alkali metals, 42
aluminum, 152
classical, 144
copper, 152
free electrons, 422
free energy, 487
iron, 158
nickel, 15
palladium, 158
platinum, 158
silver, 152*ff.*
zinc, 152*ff.*
Electron magnetic moment, 203
Electron mobility, 183
Electron spin, 203*ff.*, 232
Dirac theory, 203
magnetic moment, 207
Pauli theory, 204*ff.*
Electrostatic energy, 77
Electrothermal effects, 178*ff.*, 191
Emission probability, 218*ff.*
Entropy, ferromagnetism, 608
lattice vibrations, 481
mixing, 458, 499
ordering, 504*ff.*, 505
solid, 476
superconductors, 546
vacancies, 458, 461

Exchange correlation, 240
narrow bands, 334
Exchange energy, 240
alkali atoms, 350
alkali metals, 359, 421
beryllium, 371
copper, 367
Fermi-Thomas theory, 385
ferromagnetism, 612*ff*., 618, 623
free electrons, 339*ff*.
ionic crystals, 388
metals, 398
narrow bands, 334*ff*.
Exchange function, 340, 398
Exchange integral, 240
alloys, 624
ferromagnetism, 612*ff*., 618, 623
Excitation function, 561
Excitation spin waves, 620
Excitation waves, 413, 414*ff*., 617*ff*.
alkali halides, 413
conductivity, 413, 416
decomposition, 563,
insulators, 451
metals, 408
molecular solids, 468
narrow bands, 416
normalization, 415
optical properties, 647*ff*.
Excited states of solids, 407*ff*.
atomic arrangement, 451
band scheme, 407, 408*ff*.
ionic solids, 409
metals, 409*ff*.
semi-conductors, 414
Exciton (*see* Excitation waves)
Expansion coefficients, 380
ferromagnetism, 625
Extinction coefficient, 632*ff*.

F

F centers, 459, 565
absorption, 459
free energy, 458
levels, 463
optical properties, 565, 662
F' centers, 567
Fermi energy, 355
alkali metals, 355
copper, 369
Fermi-Dirac distribution, 145
Fermi-Thomas theory, 368, 376, 384*ff*.
Ferromagnetism, 156
alloys, 45, 434, 623
anisotropy, 22, 627
critique of theory, 622
domain theory, 20*ff*.
entropy, 615
free electrons, 602
gadolinium, 25
Heisenberg theory, 612
Heusler alloys, 45
ionic crystals, 60, 623
partition functions, 615
specific heat, 611
spin-wave theory, 617
Weiss theory, 608
factor, 643*ff*.
F centers, 662
ionic crystals, 658*ff*.
rare gases, 645
sum rules, 649
Filling of levels
alkaline earth metals, 424
alloys, 434*ff*., 501
magnetic field, 587
semi-conductors, 456*ff*.
transition metals, 429, 535
Fluctuations, 478
Fock operator, 245
Fock scheme, 227
Fock's equations, 242*ff*., 252, 677
connection with Hartree's, 335, 397.
molecular hydrogen, 260
solids, 302, 313, 335, 347
solutions, 246*ff*.
Forbidden region, 273*ff*.
Free electrons, correlation, 242
diamagnetism, 583, 594
ferromagnetism, 602
magnetic field, 584
metals, 139
optical properties, 638*ff*.
wave functions, 241, 272
Free energy, carbon, 484
electronic, 427
F centers, 458
lattice vibrations, 480
rare-gas solids, 492
semi-conductors, 466
solid, 479
vacancies, 458

Free rotation, 511
Fowler's theory, 513
Pauling's theory, 511
Fundamental absorption band, 411, 575

G

Gamma brass, 30*ff.*
zone boundaries, 433
Gibbs-Helmholtz equation, 483, 487
Glasses, 476
Goldschmidt radii, 92*ff.*
Graphite, 61, 455
allotropy, 484
Group theory, 275, 297
Grüneisen's function, 533, 540
Grüneisen's law, 138*ff.*
Grüneisen's theory of metals, 379
Gyromagnetic ratio, 496

H

Hägg's rules, 35
Hagen-Rubens relation, 640
Hall constant, metals, 181*ff.*, 318
photoconductors, 563
positive, 182, 183, 194, 318
semi-conductors, 68*ff.*, 192, 563
zinc oxide, 467
Halogen ions, electron affinity, 46, 80*ff.*, 414*ff.*
Hamiltonian operator, 197, 199, 202, 212*ff.*, 227, 245
complete, 470
crystals, 345*ff.*
hydrogen molecule, 258
hydrogen molecule ion, 254
ionic crystals, 387
magnetic field, 576
mean value, 229, 236
Hamilton's equations, 213
Hartree fields, 251, 333
Hartree functions, 234
Hartree's equations, 235, 677
connection with Fock's, 335
solids, 329*ff.*, 335, 347
solutions, 246*ff.*
Heat of formation (*see* Cohesion)
Heat of sublimation, 3
Heitler-London scheme, 251, 254*ff.*, 263
accuracy, 312
connection with band scheme, 337
Heitler-London scheme, connection with Hund-Mulliken scheme, 252, 263, 301
excited states, 408
ferromagnetism, 612
ionic crystals, 441*ff.*
metals, 348, 420*ff.*
Helium atom, 231*ff.*
Helium interaction, 264, 269
Hermitian matrix, 129, 199
Heusler alloys, 44
High pressure, 374, 382*ff.*
Holes
in bands, 155*ff.*, 317, 430
ionic crystals, 446
semi-conductors, 457
Hume-Rothery rules, atomic size, 28
electron-atom ratio, 30*ff.*, 434
solubility limits, 28
Hund-Mulliken scheme, 251, 254*ff.*, 263
connection with Heitler-London scheme, 252, 263, 301
Hydrogen interaction, 268
Hydrogen molecule, 258
Hydrogen-molecule ion, 254

I

Image-force barrier, 162
Impurity levels, 325, 456*ff.*
Inelastic collisions of electrons, 523
Infrared spectra, ionic crystals, 665
width, 666*ff.*
Inner shells, 272
diamagnetism, 601
Interstitial alloys, 25*ff.*
Hägg's rules, 35
Interstitial atoms, conductivity, 547*ff.*
diffusion, 495
Invar, 625
Ion-core field, 330, 383
Ionic conductivity, 64*ff.*
mean free path, 554
mechanism, 550*ff.*
theory, 547*ff.*
Ionic crystals, 1, 46*ff.*
absorption spectra, 408*ff.*
allotropy, 89*ff.*
characteristic temperature, 57, 114
cohesion, 46*ff.*, 78, 80*ff.*, 88*ff.*, 385*ff.*
conductivity, 55, 548*ff.*
effective mass, 441, 445

Ionic crystals, elastic constants, 95, 391
equilibrium arrangement, 451
exchange, 388
excited states, 409
Hamiltonian, 387
holes, 446
infrared spectra, 665
magnetic properties, 59*ff.*
mean free path in, 558
photoconductivity, 446
radii, 82, 91*ff.*
specific heats, 57*ff.*, 99*ff.*
structures, 49*ff.*
total wave function, 442
transport numbers, 56, 65
work function, 400*ff.*
Ionization levels, 413
Iron, allotropy, 9, 487
band scheme, 428*ff.*
expansion coefficient, 625
magnetization, 20*ff.*, 610
specific heat, 15, 158

J

Jump frequency, 495, 548

K

k space (*see* Wave-number space)
Kinetic energy, 229
Koopmans' theorem, 313*ff.*, 408
Kopp-Neumann law, 38
Kronecker delta function, 128
Kronig-Penney model, 282, 321

L

Lagrangian parameter, 202
Lambda point, 485
ammonium chloride, 511
crystals, 511*ff.*
specific heat, 512
Landé factor, 581
Latent image, 675
Lattice defects, density, 556
relative energy, 551
silver halides, 556
types, 551
Lattice vibrations, assembly of oscillators, 100*ff.*
Born-von Kármán boundary conditions, 133, 275*ff.*
change during ordering, 505
coupling, 667, 672
damping, 451
diatomic lattice, 121
free energy, 481
frequency distribution, 103*ff.*, 121, 135
general theory, 476
Hamiltonian, 131
kinetic and potential energy, 131
normal modes, 105*ff.*, 119, 127
optical properties, 665*ff.*
scattering by, 518*ff.*
velocity, 120, 123
wave functions, 477*ff.*, 521
Laue's conditions, 288
conductivity, 518
Level density, alkali metals, 366, 437
alkaline earth metals, 424
alloys, 433
anomalous, 439
bands, 307*ff.*
beryllium, 371, 437
complex metals, 425
from X rays, 436*ff.*
transition metals, 427, 440
Line breadth, 223*ff.*, 646*ff.*
natural width, 224
vibrational broadening, 226, 670
Liquid helium, 269, 485
lambda point, 485
specific heat, 485
Liquid state, 475*ff.*, 488*ff.*
helium, 485
supercooled, 475
Liquidus curve, 27
Lithium hydride, 390*ff.*
bands, 444
Lithium molecule, 262
Local field correction, 603*ff.*, 637*ff.*, 658
Long-distance order, 507
Lorentz force, 170, 213, 317
Lorentz theory of collisions, 170
Luminescence, 452, 573, 672

M

Madelung constant, 78
Madelung energy, 363

Madelung energy, alloys, 378
ionic crystals, 388
Magnesium-antimony system, 33
Magnetic anisotropy, 22
Magnetic moment, electronic, 208, 207, 426
Magnetic susceptibility, above Curie point, 617
additivity, 59
alloys, 42*ff*., 44*ff*.
atomic, 605
dependence on strain, 18
diamagnetic, 577
ionic crystals, 59*ff*.
metals, 16, 159*ff*.
theory, 159*ff*., 576*ff*.
Magnetization, 16
curves, 20*ff*.
quenching, 44*ff*.
saturation, 23*ff*.
temperature dependence, 19
theory, 576*ff*.
Many-body problem, 227*ff*.
Maxwell-Boltzmann statistics, 139
Maxwell's equations, 211, 629*ff*.
Mean energy of electrons, 144
Mean free path, 139
alloys, 541
electrons in ionic crystals, 558
high temperatures, 527
ionic crystals, 554*ff*.
low temperatures, 531
metals, 172, 184, 190, 518*ff*.
photoconductivity, 565*ff*., 568
semi-conductors, 190
theory, 516*ff*., 518*ff*., 526
Mean value, 198
Hamiltonian, 229
Melting, 475*ff*., 488*ff*.
conductivity change, 491
latent heat, 490
Mott theory, 490
rare-gas solids, 492
Metallic hydrogen, 367
Metals, allotropy, 5
alloys, 25*ff*.
atomic radii, 9
band theory, 272*ff*., 420*ff*.
cohesion, 3, 348*ff*.
conductivity, 9, 516*ff*., 532
elastic constants, 393*ff*.
electronic structure, 420*ff*.
Metals, excited states, 407*ff*.
Fermi-Thomas theory, 368
free-electron theory, 139*ff*.
high pressures, 374, 382
iron group, 427
magnetism, 16*ff*.
mean free path, 184, 190, 516, 526
optical properties, 638*ff*., 649
resistivity, 9
simple, 2
simplified theory, 379*ff*.
specific heats, 13*ff*.
structures, 4*ff*.
superconductivity, 12, 545
total wave function, 308*ff*.
transition, 2
work function, 395*ff*.
X-ray emission, 436*ff*.
Metastable states, 452
Miller indices, 20
Mobility, electronic, 68, 183, 565
Molecular binding, 254*ff*.
Molecular crystals, 1, 72*ff*.
cohesion, 391*ff*.
levels, 468*ff*.
Molecular notation, 254*ff*.
Molecular wave functions, 253, 254*ff*.
Multiplet, 579
Multiplicity, 210, 242

N

Neon interaction, 265, 393
Nickel, band scheme, 428*ff*.
electronic specific heat, 15, 157
expansion coefficient, 625
magnetization curve, 20*ff*.
optical properties, 656
Noble metals, monovalent, 367, 423*ff*.
optical properties, 655
Normal modes of vibration, 105*ff*., 121, 127, 275*ff*., 476
distribution, 135
energy, 131*ff*.
Hamiltonian, 131
Lagrangian, 131
optical properties, 665
Nuclear-motion, equations, 470*ff*.
Nucleation, 515

O

One-electron scheme, 227*ff*., 233, 272*ff*., 280

Operators, 195ff.
Hermitian, 199
Optical properties, alkali halides, 408ff., 446, 657ff.
alkali metals, 423, 652ff.
alkaline earth salts, 450
Bloch functions, 649
excitation waves, 647ff.
F centers, 459
free electrons, 638ff.
ionic crystals, 657ff.
metals, 633ff., 649, 651ff.
monovalent noble metals, 424, 649
quantum formulation, 642ff.
semi-conductors, 459, 661ff.
Order-disorder, 35ff., 41, 486, 502
amalgams, 503
beta brass, 35ff., 506
change in elastic constants, 503
conductivity, 35ff., 504
dependence on vibrational frequencies, 501
entropy change, 504ff.
magnetism, 608
specific heat, 37
theories, 508ff.
Order parameters, 36, 505ff.
Oscillator strength, 645ff.
(*See also f* factor)
Oxygen atoms, 250

P

Paramagnetic salts, 608
Paramagnetism, alkali metals, 599ff.
contribution from exchange and correlation, 600
above Curie temperature, 610, 617
free ion, 590ff.
valence electron, 599
Partition function, 101
ferromagnetism, 615
lattice vibrations, 482
magnetic field, 580, 586
spin waves, 618
Pauli principle, 141, 208ff., 231
Peltier effect, 179
Penetration distance, 642
Periodic boundary conditions (*see* Born-von Kármán boundary conditions)
Periodic wave functions, 272, 280ff.
Permeability, 17
Permutations, 208ff.
Perturbation methods, Bardeen's, 520
Herring and Hill's, 332
Schrödinger, 284, 289
semiclassical, 560ff.
time-dependent, 216, 521ff.
Phase changes, 470ff., 473ff.
Phase diagrams, 26ff.
brass, 30, 502
copper-aluminum, 31, 502
copper-gold, 33
copper-silver, 33
iron-cobalt, 34
magnesium-antimony, 33
Phase space, 143
Photoconductivity, 558ff.
alkali halides, 413, 446ff., 459, 563
darkening, 574
decrease at low temperatures, 566
displacement distance, 565
mean free path, 569, 572
quantum yield, 565ff.
silver halides, 574
Photoelectric effect, 153ff., 670
Photographic theory, 674ff.
Photolysis, 678
Plasticity, 98
Polarisability, 629, 634, 639
atomic, 267, 649ff.
complex, 631ff., 642
Polarization current, 570ff., 630ff.
Polarization energy, 463
lattice defects, 551
Polymorphism (*see* Allotropy)
Potassium chloride, anomalous specific heat, 57
Potential in metal, 140
Primary current, 565
Primitive translations, 15, 125
Principal lattice vectors, 285, 298

Q

Quantum mechanics, 195ff.
Quantum statistics, 209
Quantum yield, photoconductivity, 464, 565
Quenching, 27

R

Radiation field, Fourier resolution, 212ff.
Hamiltonian, 212ff.
Interaction with matter, 218

Radiation theory, absorption probability, 218*ff.*
damping, 224
Dirac theory, 215
dispersion, 220
emission probability, 218*ff.*
line breadth, 223*ff.*
natural width, 223
Schrödinger-Gordon-Klein theory, 215
selection rules, 225, 326, 418, 423
Radii, atomic, 9
ionic, 51, 82, 91*ff.*
Raman scattering, 221
Rare-gas solids, free energy, 492
melting, 492
Reaction rates, 470, 494, 497
Reciprocal lattice, 294, 327
Rectification, 575
Reduced mass, 232
Reduced-zone scheme, 122, 287, 292, 328
Reflection coefficient, electrons, 165*ff.*
light, 633, 640
Refractive index, 632*ff.*
alkali halides, 657
Refractivity, 660
Relativistic electronic theory, 203
Repulsive-potential, ionic crystals, 79*ff.*, 96
Residual resistance, 541
Resistivity, alloys, 39*ff.*, 43*ff.*
high temperature, 12
low temperature, 12
measurement, 64
metals, 9*ff.*
residual, 541
(*See also* Conductivity)
Resonance, 217
Richardson-Dushman equation, 165
Russell-Saunders coupling, 578

S

Saddle point, 474
Scalar potential, 211
Schottky effect, 162*ff.*
Schrödinger equation, 198*ff.*
Screening, 261
Secondary current, 562*ff.*
Seeback effect, metals, 180
semi-conductors, 192
Selection rules, band scheme, 326
electronic collisions, 521*ff.*
Selection rules, excitation waves, 418, 648*ff.*
X-ray emission, 438
Self-consistent fields (*see* Hartree fields)
Self-energy of charge, 361
Semi-conductors, 1, 62*ff.*
activation energy, 459*ff.*
conductivity, 63*ff.*, 189*ff.*, 457, 461, 465
dependence of conductivity on vapor pressure, 70, 192, 465
electronic transport, 62*ff.*
free electrons in, 188
Hall constant, 68*ff.*, 192, 456
holes in, 457
impurities in, 456
ionic transport, 64*ff.*
levels 414, 457
mean free path, 190
optical properties, 661*ff.*
theory, 186*ff.*
vacancies, 458
Short-distance order, 507
Silica, 456
Silver-gold system, 28, 40
Silver halides, ionic conductivity, 64
lattice defects, 556
photoconductivity, 574
Simple metals, 2
Sodium chloride, cohesion, 385*ff.*
effective mass, 441, 445
energy levels, 442*ff.*
infrared absorption, 666
work function, 400
Solid types, 1
electronic structure, 420*ff.*
transition between, 74
Solidus curve, 27, 32
Solubility limit, Hume-Rothery rule, 28
theory, 502
Specific heats, alkali metals, 116, 422
alloys, 38
aluminum, 152
anomalous, 57, 99, 100, 111, 116*ff.*, 173, 512
benzene, 115
Blackman's treatment, 99, 116, 120, 133*ff.*
Born-von Kármán theory, 99
$C_v - C_p$ correction, 136*ff.*
copper, 152
Debye's theory, 104*ff.*
diamond, 484

Specific heats, Dulong and Petit's law, 38, 103
Einstein's theory, 103
electronic, 15, 117, 144, 422, 487
Fermi-Dirac theory, 150*ff.*
ferromagnetism, 611
ionic crystals, 57*ff.*
iron, 15, 158
liquid helium, 485
metals, 13*ff.*, 432
nickel, 25, 157
ordered alloys, 37
palladium and platinum, 158
silver, 152*ff.*
sulfur, 484
theory, 99*ff.*
tin, 483
zinc, 152*ff.*
Sphere approximation, 349, 362*ff.*
Spherical harmonics, 330
Spin angular momentum, 205*ff.*, 426, 577
Spin matrices, 205
Spinor, 204*ff.*
Spin waves, 617
excitation, 620
partition function, 618
State function, 195*ff.*
Statistics, classical, 139, 141, 517
Einstein-Bose, 486
Fermi-Dirac, 141, 144*ff.*, 209
Maxwell-Boltzmann, 139, 141
tructures, ionic crystals, 49*ff.*
metals, 4*ff.*
molecular crystals, 72
valence crystals, 60*ff.*
bstitutional alloys, 25*ff.*, 502
ands, 432*ff.*
iffusion in, 495*ff.*
der-disorder, 502*ff.*
ir, allotropy, 484
ific heat, 484
ucture, 74
rules, atoms, 644, 649
loch functions, 650
f factors, 644
Superconductivity, 545
Surface energy, 96, 515
Surface properties, 395
rface resistivity, 642
ce states, 320*ff.*
ce tension, 98

T

T^3 law of specific heats, 99, 533
deviations, 120
Theory of conduction, critique, 53
Lorentz, 190*ff.*, 516
metals, 170*ff.*, 516*ff.*
Sommerfeld, 174, 517
Theory of radiation (*see* Radiation theory)
Thermal conduction, theory in metals, 174*ff.*
Thermionic emission, 161*ff.*, 402*ff.*
Thermodynamics, 80, 402
Clausius-Clapeyron equation, 402
equilibrium conditions, 476, 479, 500
Gibbs-Helmholtz equation, 483, 487
Thomson effect, 179
Tin, allotropy, 8, 483
disease, 483
gray, 61
specific heat, 483
Total electronic-wave function of solids, 308*ff.*
alkaline earth salts, 448
divalent metals, 312
excited states, 311, 407*ff.*
insulators, 309
ionic solids, 409*ff.*, 442
metals, 308*ff.*, 407*ff.*, 420*ff.*
semi-conductors, 407*ff.*, 414*ff.*
Transition between solid types, 74, 469
Transition metals, 2, 426
allotropy, 487
alloys of, 434*ff.*
atomic heat, 15
bands, 426*ff.*
cohesion, 427*ff.*
conductivity, 535*ff.*
electronic heat, 153, 155, 432
holes in, 430
level density, 427, 440
magnetic properties, 426*ff.*
optical properties, 656
Pauling's theory, 429, 441
tungsten, 426
Transparent region, 635
Transport numbers, 65*ff.*, 465
Trapping centers, 565
Tungsten, 426*ff.*

U

Unallowed region (*see* Forbidden region)
Uncertainty relation, 230
Unit cells, 15, 332

V

Vacancies, **458**, 461
  alkali halides, 460
  conductivity, 547*ff.*
  cuprous oxide, 467*ff.*
  density, 550
  diffusion, 495*ff.*, 547*ff.*
  entropy, 458
  free energy, 458
Valence binding, diamond, 455
  molecules, 270
  solids, 421
Valence crystals, 1, 60*ff.*
Valence forces, 270*ff.*
van der Waals interaction, 82, 84*ff.*, 262*ff.*
  ionic crystals, 388
  metals, 360
  molecular solids, 391*ff.*
  rare gases, 492
Variational theorem, 200*ff.*, 227, 242, 259, 262, 473
Vector potential, 211, 577
Velocity, band scheme, 315*ff.*
  excitation waves, 417
  group, 315, 417
  sound, 109, 123
Vibrational broadening, 226

W

Wave functions, antisymmetric, 209, 236
  Bloch, 251, 272
  determinantal, 237, 302
  excitation waves, 414*ff.*
  excited states, 311*ff.*, 412
  free electrons, 241, 272
  Heitler-London, 251
  Hund-Mulliken, 251
  hydrogen molecule, 258
  impurity levels, 325
  lattice vibrations, 477*ff.*, 518*ff.*, 521
  magnetic field, 584*ff.*, 591*ff.*
  molecular, 253, 254*ff.*
  one electron, 227, 233
  periodic, 272, 278*ff.*
Wave functions, surface, 320
  total of solid, 308*ff.*, 420*ff.*
  two electron, 232, 260
Wave packets, 315
Wave-number components, 107
Wave-number space, 273, 294
  density of points, 294
Wave-number vector, 107, 212
  electronic, 272*ff.*
  principal, 135, 298
Wiedemann-Franz law, 178
Work function, 145*ff.*, 166, 404
  alkali metals, 399
  beryllium, 400
  internal contribution, 397
  nonmetals, 400*ff.*
  sodium chloride, 400*ff.*
  surface contribution, 397
  temperature dependence, 402
  theory, 395*ff.*
Wronskian, 279
Wulff's theorem, 97

X

X-ray absorption, 407
X-ray diffraction, 288, 296
X-ray emission, 344, 407, 413
  bands in metals, 436*ff.*
  transition probabilities, 438

Z

Zero-point energy, 86
Zinc oxide, 2, 464
  conductivity, 70, 192, 549
  diffusion, 496
  Hall effect, 193
  impurity levels, 414, 447*ff.*
  Seebeck emf, 193
  Thomson effect, 193
Zone boundaries, 273, 595
Zone scheme, 122, 273
Zones, 273, 290
  bismuth, 425
  Brillouin, 284, 287*ff.*
  figures, 298*ff.*
  gamma brass, 433
  mapping, 288
  rules concerning, 274*ff.*, 295*ff.*
  X-ray diffraction, 288, 296